Technische Universität München
TUM School of Medicine and Health

Generation of multicistronic DNA- and mRNA-based therapeutic vaccines against chronic hepatitis B virus infection

Hélène Anne Kerth

Vollständiger Abdruck der von der TUM School of Medicine and Health der Technischen Universität München zur Erlangung einer

Doktorin der Medizin (Dr. med.)

genehmigten Dissertation.

Vorsitz: Prof. Dr. Marcus Makowski

Prüfende der Dissertation:

1. Prof. Dr. Ulrike Protzer
2. Prof. Dr. Percy A. Knolle

Die Dissertation wurde am 30.11.2023 bei der Technischen Universität München eingereicht und durch die TUM School of Medicine and Health am 13.03.2024 angenommen.

Table of content

Abbreviations **1**

Abstract **7**

Zusammenfassung **9**

1 Introduction **11**

1.1 Hepatitis B virus 11

1.1.1 HBV structure and genome organization 11

1.1.2 HBV replication cycle 15

1.2 Hepatitis B virus infection 18

1.2.1 Epidemiology 18

1.2.2 Means of transmission 21

1.2.3 Acute versus chronic HBV infection 22

1.2.4 Hepatitis B and hepatocellular carcinoma 24

1.2.5 Prophylactic vaccination 24

1.3 Treatment of HBV infection 25

1.3.1 Standard treatment options 25

1.3.2 Treatment limitations 28

1.3.3 Alternative treatments 28

1.4 Adaptive immunity in chronic hepatitis B 33

1.4.1 Antiviral functions of HBV-specific $CD8^+$ T cells 33

1.4.2 Antiviral functions of HBV-specific $CD4^+$ T cells 34

1.4.3 B cell-mediated immune response and antibodies in CHB 35

1.5 Vaccines 36

1.5.1 Protein vaccines 36

1.5.2 Viral vector vaccines 37

1.5.3 DNA vaccines 38

1.5.4 mRNA vaccines 39

2 Aims of the study 41

3 Results 42

3.1 DNA-based therapeutic hepatitis B vaccine: *DNA-HBVac* 42

3.1.1 Generation of *DNA-HBVac* for *TherVacB* priming 42

3.1.2 Evaluation of DNA prime – MVA boost immunogenicity in HBV-naïve mice 44

3.1.3 Evaluation of the immunogenicity of *DNA-HBVac* in HBV carrier mice 48

3.1.4 Evaluation of the immunogenicity of simultaneous DNA/HBsAg prime – MVA boost regimen in HBV carrier mice 56

3.1.5 Investigation of the efficacy of distinct injection sites for DNA and HBsAg prime in HBV naïve mice 59

3.1.6 Investigation of the immunogenicity of sequential DNA/HBsAg prime – MVA boost regimen in HBV carrier mice 63

3.2 mRNA-based therapeutic hepatitis B vaccine: *RNA-HBVac* 70

3.2.1 Generation of *RNA-HBVac* for *TherVacB* 70

3.2.2 Implementation of chemical modifications to enhance the stability and protein expression of *RNA-HBVac* mRNA 73

3.2.3 Immunogenicity of priming immunization with *RNA-HBVac* in HBV-naïve mice 75

3.2.4 Evaluation of the long-term immunogenicity of RNA prime – MVA boost in HBV carrier mice 83

4 Discussion 91

4.1 Impact of the vaccination scheme on *DNA-HBVac* vaccine efficacy 91

4.2 Advantages, disadvantages, and improvements of DNA vaccines over protein or viral vector vaccines 92

4.3 Determining the optimal immunization strategy of *DNA-HBVac* 94

4.4 High anti-HBs levels correlate with successful therapeutic vaccination 95

4.5 Exploring critical factors for strong *DNA-HBVac* induced immunogenicity in both HBV-naïve and AAV-HBV mice 97

4.6 Advantages and disadvantages of RNA vaccines over viral vector or DNA vaccines 99

4.7 Incorporation of additional modifications to further upgrade *in vivo* mRNA immunogenicity 100

4.8 Strategies for improvement of *in vivo* RNA vaccine delivery to enhance *RNA-HBVac* immunogenicity 101

4.9 Investigating critical factors for optimal mRNA priming of *TherVacB* 103

5 Materials and Methods 105

5.1 Materials 105

5.1.1 Cell lines/bacterial strains 105

5.1.2 Media 105

5.1.3 Plasmids 106

5.1.4 Primers 106

5.1.5 Enzymes 106

5.1.6 Kits 107

5.1.7 Vaccine components 107

5.1.8 Mouse models 108

5.1.9 Peptides 108

5.1.10 Multimers 109

5.1.11 Antibodies 109

5.1.12 Buffers and solutions 110

5.1.13 Chemicals and reagents 111

5.1.14 Laboratory devices 113

5.1.15 Consumables 114

5.1.16 Software 114

5.2 Methods 115

5.2.1 Cell culture 115

5.2.1.1 Passaging of cell lines 115

5.2.1.2 Cell counting 115

5.2.1.3 Transfection 116
5.2.1.4 Cell lysis 116
5.2.1.5 Western Blot analysis 116
5.2.1.6 Cryoconservation of cells 118
5.2.1.7 Modified Vaccinia Ankara (MVA) amplification and purification 118
5.2.2 Molecular biology techniques 119
5.2.2.1 Culture of competent stlb3 Escherichia coli 119
5.2.2.2 Transformation of competent stlb3 Escherichia coli 119
5.2.2.3 Amplification and isolation of plasmid DNA 120
5.2.3 Generation of *RNA-HBVac*: Molecular techniques and cloning 121
5.2.3.1 PCR 121
5.2.3.2 Gel electrophoresis for PCR product analysis 121
5.2.3.3 DNA extraction from agarose gel 121
5.2.3.4 Ligation 122
5.2.3.5 Transformation in chemically competent Escherichia coli 122
5.2.3.6 Restriction enzyme digestion of RNA-HBVac plasmid 123
5.2.3.7 Sequencing of the plasmid construct 123
5.2.3.8 RNA-synthesis 123
5.2.3.9 Quality control of the in vitro synthesized mRNA 125
5.2.4 In vivo studies in C57BL/6 mice 125
5.2.4.1 Anesthesia 125
5.2.4.2 Transduction of mice with AAV-HBV 126
5.2.4.3 Intravenous injection 126
5.2.4.4 Immunization 126
5.2.4.5 Bleeding 127
5.2.4.6 Analysis of HBV serum parameters 127
5.2.4.7 Termination of mouse experiments 127
5.2.4.8 Isolation of immune cells from the liver and spleen 128
5.2.4.9 Assessment of T-cell responses in liver-associated lymphocytes (LALs) and splenocytes 129
5.2.4.10 Histological analyses: Immunohistochemistry 131
5.2.5 Statistical analysis 131
6 List of tables 133
7 List of figures 134
8 References 137

Publications and Meetings **157**

Acknowledgments **159**

Abbreviations

°C	degree Celsius
m^5C	5-methylcytidine
φ	pseudo
aa	amino acids
AASLD	American Association for the Study of Liver Diseases
AAV	Adeno associated virus
AAV-HBV	Adeno-associated virus carrying replicon competent HBV genome
ACK	Ammonium-Chloride-Potassium
ADCC	Antibody-dependent cell-mediated cytotoxicity
ADCP	Antibody-dependent cellular phagocytosis
AIDS	Acquired immunodeficiency syndrome
ALT	Alanine-Aminotransferase
ANOVA	Analysis of variance
anti-HBc	antibodies against HBV core antigen
anti-HBs	antibodies against HBV surface antigen
APC	Antigen presenting cells
APS	Ammonium persulfate
ARCA	Anti-reverse cap analogue
AuAg	Australia antigen
BD	Becton Dickinson
BFA	Brefeldin A
bp	base pairs
BSA	Bovine serum albumin
BSEP	Bile salt export pump
CAR	Chimeric antigen receptor
cccDNA	covalently closed circular DNA
CD	Cluster of Differentiation
CEF	Chicken embryo fibroblast
CHB	Chronic Hepatitis B
CIN	Cervical intraepithelial neoplasia
CMV	Cytomegalovirus

CpAMs	Core protein Allosteric Modulators
CTL	CD8 Cytotoxic T lymphocyte
CTP	Cytidine triphosphate
Ctrl	Control
DC	Dendritic cell
DMEM	Dulbecco's modified eagle medium
DMSO	Dimethyl Sulfoxide
DNA	Deoxyribonucleic acid
dsRNA	double-stranded RNA
DZIF	Deutsches Zentrum für Infektionsforschung
EASL	European Association for the Study of the Liver
ECL	Enhanced chemiluminescence
EDTA	Ethylenediaminetetraacetic acid
ELISA	Enzyme-linked immunoassay
FACS	Fluorescence-activated cell sorting
FCS	Foetal Calf Serum
FELASA	Federation of European Laboratory Animal Science
FITC	Fluorescein isothiocyanate
FSC	Forward light scatter
fw	forward
GAPDH	Glyceraldehyde 3-phosphate dehydrogenase
GE	Genome equivalents
GLOBOCAN	Global Cancer Observatory
GPT	Glutamate-pyruvic transaminase
GV-SOLAS	German Society for Animal Laboratory Science
h	hour
HBcAg	HBV core antigen
HBeAg	HBV e antigen
HBsAg	HBV surface antigen
HBV	Hepatitis B virus
HBx	HBV X protein
HCC	Hepatocellular carcinoma
HCV	Hepatitis C virus
HDV	Hepatitis D virus
HE	Haematoxylin/eosin

HEK	Human embryonic kidney
HIV	Human immunodeficiency virus
HLA	Human leukocyte antigen
HMGU	Helmholtz Center Munich
HPLC	High performance liquid chromatography
HPV	Human papillomavirus
HRP	Horseradish peroxidase
HTLV	Human T-cell leukaemia-lymphoma virus
ICS	Intracellular cytokine staining
IFN	Interferon
IFU	Infectious units
Ig	Immunoglobulin
IL	Interleukin
i.m.	intramuscular injection
INSERM	French National Institute of Health and Medical Research
IRTG	International Research Training Group
IU/ml	International unit/millilitre
i.v.	intravenous injection
IVT	*in vitro*
L	Large
LAL	Liver associated lymphocytes
LB	Lysogeny broth
LMU	Ludwig Maximilian University of Munich
LNP	Lipid nanoparticle
M	Medium
MAPK	Mitogen-activated protein kinase
mg	milligram
MHC	Major Histocompatibility complex
min	minute
ml	millilitre
mM	millimolar
mo.	months
mRNA	messenger RNA
MVA	Modified Vaccinia Ankara
NEAA	Non-essential amino acids

NF	Nuclear Factor
NIH	National Institute of Health
NK	Natural killer
n.s.	not significant
NTCP	Sodium taurocholate co-transporting polypeptide
NTP	Nucleoside Triphosphate
NUC	Nucleos(t)ide analogues
ORF	Open reading frame
OVA	ovalbumin
PAA	Phenyl acetic acid
PAMPs	Pathogen Associated Molecular Patterns
PBS	Phosphate-buffered saline
PCR	Polymerase chain reaction
PD-1/PD-L1	Programmed death-1/Programmed death ligand-1
PE	Phycoerythrin
PEI	Paul Ehrlich Institute Units/Milliliter
PFA	Paraformaldehyde
pgRNA	Pregenomic RNA
PKR	Protein kinase R
Pol	Polymerase
PRR	Pathogen Recognition Receptor
P/S	Penicillin/Streptomycin
PVDF	PolyVinyliDene Fluoride
qRT-PCR	Real-Time quantitative Reverse Transcription PCR
RAF	Rapidly accelerated fibrosarcoma
rcDNA	relaxed circular DNA
rev	reverse
RIG	Retinoic acid-inducible gene
RIPA	Radio-Immunoprecipitation assay buffer
RKI	Robert-Koch Institute
RNA	Ribonucleic acid
ROB	Authorities of Upper Bavaria
RPMI	Roswell Park Memorial Institute Medium
RT	Reverse transcriptase
S	Small

s	seconds
SARS-Cov-2	Severe Acute Respiratory Syndrome coronavirus 2
s.c.	subcutaneous injection
S/CO	Signal to cut-off
scFv	single-chain variable Fragment
SDS	Sodium Dodecyl Sulfate
SEM	Standard Error of the Mean
shRNA	short hairpin RNA
siRNA	small interfering RNA
SOC	Superoptimal broth with Catabolite repression
SSC	Side light scatter
TAE	Tris-acetate-EDTA buffer
TBST	Tris-buffered saline (TBS) containing 1 % Tween-20
TCR	T-cell receptor
TEMED	Tetramethylethylenediamine
Tfh	follicular helper T cells
Th1	T helper 1
Th2	T helper 2
TherVacB	Therapeutic hepatitis B vaccine
TLR	Toll-like receptor
TNF	Tumor necrosis factor
TP	Terminal protein
Treg	regulatory T cells
TRIF	TIR domain containing adapter inducing interferon beta
TUM	Technical University of Munich
UF	Unformulated
U/L	Units/Liter
µg	microgram
µl	microliter
µM	micromolar
USA	United States of America
UTP	Uridine Triphosphate
UV	Ultraviolet
WB	Western Blot
WHO	World Health Organization

wk	week

Abstract

More than 296 million people around the globe are chronically infected with the hepatitis B virus. Hepatitis B represents the eighth most frequent cause of mortality worldwide, mostly from liver cirrhosis and hepatocellular carcinoma. Available treatment options for chronic hepatitis B (CHB) with interferon-α and/or nucleo(t)side analogs rarely lead to viral clearance. It is known that HBV-specific $CD4^+$ and $CD8^+$ T-cells determine the course of infection. In CHB effective virus-specific T-cell responses are scarce and dysfunctional and neutralizing HBV-specific antibodies are absent thus resulting in viral persistence. Therefore, new therapeutic approaches are urgently needed. Therapeutic vaccination represents a promising strategy to restore strong virus-specific effector T-cell responses and strong neutralizing antibody response (anti-HBs) expected to restore antiviral immunity. In our laboratory we have previously developed *TherVacB,* a therapeutic hepatitis B vaccine based on two protein prime immunizations consisting of recombinant surface and core antigens (HBsAg and HBcAg), followed by a Modified Vaccinia Virus Ankara (MVA) boost that expresses five HBV antigens including the reverse transcriptase. *TherVacB* stimulates robust HBV-specific humoral and cellular immune responses, which ultimately lead to the long-term control of HBV, highlighting the critical role of an appropriate priming for the effectiveness of therapeutic vaccination. Developing DNA or mRNA-based vaccines that encompass the most common HBV genotypes and serotypes to enhance and broaden both HBV-specific B-and T-cell responses compared to *TherVacB* regimen that relies on recombinant proteins restricted in their variability might be a promising approach to result in a more potent antiviral effect.

Therefore, the present study aimed to assess and compare the effectiveness of mRNA and plasmid DNA-based vaccines in comparison to the well-established recombinant protein-based vaccine components to broaden and improve HBV-specific immunity when used for priming in the *TherVacB* regimen.

To that end, in the first part of this study, we successfully generated *DNA-HBVac*, a DNA-based therapeutic hepatitis B vaccine and showed that it encodes for the envelope, core, and reverse transcriptase proteins of the most prevalent HBV genotypes and serotypes. Vaccination of HBV carrier and HBV-naïve mice with 100 µg *DNA-HBVac* for priming followed by MVA-HBVac boost successfully prompted strong HBV-specific $CD4^+$ and $CD8^+$ T-cell responses but resulted in low anti-HBs antibody titers. Incorporating adjuvanted recombinant HBsAg into the *DNA-HBVac* priming regimen significantly enhanced the anti-HBs response and reduced serum HBsAg levels. Interestingly, simultaneous immunization with *DNA-HBVac* and recombinant HBsAg as well as distinct injection sites for DNA and HBsAg for priming completely abrogated the plasmid-mediated immunity in HBV-naïve and HBV carrier mice. In contrast, a sequential approach for immunization initiated by *DNA-HBVac* followed by

adjuvanted recombinant HBsAg for priming and final MVA booster vaccination, generated robust multi-specific HBV-specific $CD8^+$ T-cell responses and high anti-HBs titters, leading to significant reduction in circulating HBeAg and HBsAg levels.

Next, we generated *RNA-HBVac*, an mRNA-based vaccine encoding the same HBVac insert as *DNA-HBVac*. *RNA-HBVac* was chemically modified to enhance stability and protein expression. N^1 Methyl φ-UTP modified, and lipid nanoparticle (LNP) formulated *RNA-HBVac* proved to be the most promising candidates. The LNP-formulated mRNA was used to titrate and explore the immunogenicity of *RNA-HBVac* in HBV naïve and AAV-HBV mice. The most encouraging strategy was identified in HBV-naïve mice primed twice with 25 µg LNP-formulated *RNA-HBVac* followed by MVA booster immunization. This vaccination strategy resulted in higher anti-HBs titers compared to DNA priming but comparable to that using adjuvanted mixed recombinant proteins for priming. Mice primed twice with 25 µg LNP-formulated *RNA-HBVac* showed the strongest HBV-specific B- and T-cell responses among RNA groups but lower than previously tested DNA and protein prime immunization strategies. AAV-HBV-infected mice primed with *RNA-HBVac* demonstrated only a minor antiviral effect no matter whether the *RNA-HBVac* was formulated into LNPs or left unformulated.

Taken together, these findings indicate that sequential immunization consisting of *DNA-HBVac* followed by recombinant HBsAg as well as LNP formulated and chemically modified *RNA-HBVac* in combination with a final MVA booster immunization may be a promising priming alternative to the classical recombinant protein priming in the *TherVacB* regimen. However, optimal mRNA delivery strategies need to be further evaluated.

Zusammenfassung

Mehr als 296 Millionen Menschen auf der ganzen Welt sind chronisch mit dem Hepatitis-B-Virus infiziert. Hepatitis B ist weltweit die achthäufigste Todesursache, vor allem aufgrund von Leberzirrhose und Leberzellkarzinom. Die verfügbaren Behandlungsmöglichkeiten für Patienten mit chronischer Hepatitis B (CHB) sind Interferon-α und/oder Nukleotidanaloga. Sie führen nur selten zu einer Beseitigung des Virus. Es ist bekannt, dass HBV-spezifische $CD4^+$ und $CD8^+$ T-Zellen den Verlauf der Infektion bestimmen. In einer CHB sind wirksame virusspezifische T-Zell-Antworten selten und dysfunktional, und neutralisierende HBV-spezifische Antikörper fehlen. Daher sind neue therapeutische Ansätze dringend erforderlich. Die therapeutische Impfung ist eine vielversprechende Strategie zur Wiederherstellung starker virusspezifischer Effektor-T-Zell-Reaktionen und starker neutralisierender Antikörper (anti-HBs), die zu einer selbstlimitierenden Infektion führen. In unserem Labor haben wir *TherVacB* entwickelt, einen therapeutischen Hepatitis-B-Impfstoff, der auf zwei Protein-Grundimmunisierungen basiert, die aus rekombinanten Hepatitis B Oberflächen- und Coreantigenen (HBsAg und HBcAg) bestehen, gefolgt von einem modifizierten Vaccinia-Virus-Ankara (MVA)-Boost, der fünf HBV-Antigene und die reverse Transkriptase exprimiert. *TherVacB* stimuliert eine robuste, HBV-spezifische humorale und zelluläre Immunantwort, die letztlich zu einer langfristigen Kontrolle von HBV führen, was die entscheidende Rolle eines geeigneten Primings für die Wirksamkeit einer therapeutischen Impfung unterstreicht. Die Entwicklung eines DNA- oder mRNA-basierten Impfstoffs, der die gängigsten HBV-Genotypen und -Serotypen umfasst, um sowohl HBV-spezifische B- als auch T-Zell-Antworten zu verstärken und zu erweitern, könnte ein vielversprechender Ansatz sein, um eine stärkere antivirale Wirkung zu erzielen als das *TherVacB*-Schema, das auf rekombinanten Proteinen mit eingeschränkter Variabilität beruht.

Ziel der vorliegenden Studie war es, die Wirksamkeit von mRNA- und Plasmid-DNA-basierten Impfstoffen im Vergleich zu den etablierten proteinbasierten Impfstoffkomponenten als Prime Vakzine zu bewerten und zu vergleichen. Hierdurch wollten wir die HBV-spezifische Immunität erweitern und das *TherVacB* Schema verbessern.

Zu diesem Zweck haben wir im ersten Teil dieser Studie *DNA-HBVac* hergestellt, einen therapeutischen Hepatitis-B-Impfstoff auf DNA-Basis, der für die Oberflächen-, Core- und Reverse-Transkriptase-Proteine der am weitesten verbreiteten HBV-Genotypen und -Serotypen kodiert. Die Impfung von HBV-naiven und AAV-HBV infizierten Mäusen mit 100 µg *DNA-HBVac* als Prime und anschliessendem MVA-HBVac-Boost induzierte starke HBV-spezifische $CD4^+$- und $CD8^+$-T-Zell Antworten, führte jedoch zu niedrigen anti-HBs-Antikörpertitern. Die Aufnahme von adjuvantiertem rekombinantem HBsAg in das *DNA-HBVac*-Priming-Schema verstärkte die anti-HBs-Antwort erheblich und reduzierte die HBsAg-

Spiegel im Serum. Interessanterweise hob die gleichzeitige Immunisierung mit *DNA-HBVac* und rekombinantem HBsAg sowie unterschiedliche Injektionsstellen für DNA und HBsAg für das Priming die durch das Plasmid vermittelte Immunität sowohl in HBV-Carrier-Mäuse als auch in HBV-naiven Mäusen vollständig auf. Im Gegensatz dazu erzeugte ein sequenzieller Ansatz für die Immunisierung – eingeleitet durch *DNA-HBVac*, gefolgt von adjuvantiertem rekombinantem HBsAg für das Priming und einer abschließenden MVA-Booster-Impfung – robuste multispezifische HBV-spezifische CD8+ T-Zell-Antworten und hohe anti-HBs-Titer, die zu einer signifikanten Verringerung der zirkulierenden HBeAg- und HBsAg-Spiegel führten.
Als Nächstes haben wir *RNA-HBVac* hergestellt, einen mRNA-basierten Impfstoff, der für das gleiche HBVac-Insert wie *DNA-HBVac* kodiert. *RNA-HBVac* wurde chemisch modifiziert, um die Stabilität und Proteinexpression zu verbessern. Eine mit N1-Methyl φ-UTP modifizierte und mit Lipid-Nanopartikeln (LNP) formulierte *RNA-HBVac*-mRNA erwies sich dabei als der vielversprechendster Kandidat. Dieses Konstrukt wurde zur Titration und Erforschung der Immunogenität von *RNA-HBVac* in HBV-naiven und HBV-Carrier-Mäusen verwendet. Als vielversprechendste Strategie wurde bei HBV-naiven Mäusen, die zweimalige Gabe von 25 µg LNP-formuliertem *RNA-HBVac* identifiziert, gefolgt von einer MVA-Booster-Immunisierung. Dies führte zu höheren anti-HBs-Titern im Vergleich zur DNA-Grundimmunisierung, aber vergleichbar mit denen, die durch eine Grundimmunisierung mit adjuvantierten gemischten rekombinanten Proteinen hervorgerufen wurden. 25 µg erzielte die stärksten HBV-spezifischen B- und T-Zell-Antworten unter den RNA-Gruppen, aber niedriger als bei zuvor getesteten Grundimmunisierungsstrategien. Bei HBV-Carrier-Mäusen, die mit *RNA-HBVac* grundimmunisiert wurden, zeigte sich nur eine geringe antivirale Wirkung, unabhängig davon, ob *RNA-HBVac* in LNPs formuliert oder unformuliert gelassen wurde.
Zusammengenommen deuten diese Ergebnisse darauf hin, dass eine sequenzielle Immunisierung, bestehend aus *DNA-HBVac*, gefolgt von rekombinantem HBsAg, sowie aus LNP-formuliertem und chemisch modifiziertem *RNA-HBVac* in Kombination mit einer abschließenden MVA-Booster-Immunisierung eine vielversprechende Alternative zum klassischen rekombinanten Protein-Priming für das *TherVacB*-Regime sein könnten. Die optimalen Strategien für die mRNA-Verabreichung müssen jedoch noch weiter untersucht werden.

1 Introduction

1.1 Hepatitis B virus

Chronic Hepatitis B virus (HBV) infection represents one of the most severe health burdens worldwide. According to the World Health Organization (WHO) 296 million people are chronically infected with HBV worldwide, leading to approximately 820 000 deaths per year, mostly due to liver cirrhosis or hepatocellular carcinoma (HCC) (WHO, 2023). Public health relevance of HBV strongly differs across the globe, showing high prevalence in sub-Saharan Africa, east Asia, and East and Central Europe where almost up to 5-10% of the population is chronically infected with HBV (Robert Koch Institute, 2016; WHO, 2020). Based on HBV genome diversity, nine different HBV genotypes are known (A-I), each of them having a different geographic distribution around the globe (Kramvis et al., 2005; Yu et al., 2010). Each genotype differs in 8.3-9.3% of nucleotides from each other (Okamoto et al., 1988; Schaefer, 2007).

HBV was first discovered in 1970 by Dane et al. in the sera of three Australia antigen (AuAg)-positive hepatitis patients and described as 'virus-like particles about 42 nm in diameter' (Dane et al., 1970). HBV belongs to the *Hepadnaviridae* family which can be further subdivided into *orthohepadnaviruses*, infecting only mammals and *avihepadnaviruses* which are a bird-specific genus (Valaydon & Locarnini, 2017). Since the HBV host range is known to be limited to human and evolutive high species (Nassal, 2015), it belongs to the *Orthohepadnaviridae* subfamily. HBV is a partially double-stranded hepatotropic deoxyribonucleic acid (DNA) virus that constantly replicates in infected hepatocytes, leading to permanent secretion of viral particles into the bloodstream (Seeger & Mason, 2000). Even though HBV is a DNA virus it belongs to the pararetrovirus subfamily as replication occurs through a ribonucleic acid (RNA)-intermediate via the HBV reverse transcriptase polymerase (Valaydon & Locarnini, 2017).

1.1.1 HBV structure and genome organization

HBV virions are spherical structures of about 42 nm in diameter which contain the HBV capsid and viral genome. The viral envelope contains three different surface proteins, named the small (S), medium (M), and large (L) proteins, which are integrated into the membrane. The icosahedral capsid, also called the core particle, is built out of 120 core protein dimers and contains the viral genome. The HBV genome itself is quite small and consists of an approximately 3.2 kb long relaxed partially double-stranded circular DNA (Summers et al., 1975). Each base triplet has a coding function in more than one open reading frame (ORF) (Nassal, 2015).

When infection occurs, HBV-replicating cells secrete three different types of HBV particles

which can be detected in the sera of infected patients. They are known as the virions, also called Dane particles, first described in 1970 by Dane et al., and the subviral lipoprotein particles which are named filaments and spheres (Figure 1.1). It is known that infected cells produce a consistently higher amount of subviral particles compared to infectious virions in a ratio up to 1000 :1 to 10,000 :1 (Ganem & Prince, 2004). Whereas spheres have a mean diameter of 22 nm, filaments have a width of 22 nm and a variable length. Both subviral particles consist mainly of the small hepatitis B surface protein S and various lipids but do not contain viral genomes and thereby are non-infectious (Liang, 2009). Virions and filaments contain more of the large (L) and medium (M) surface protein than spheres. These 'empty envelopes' can be detected in the blood of infected individuals as HBsAg. Infected hepatocytes release spheres via the secretory pathway, whereas it is unknown if filaments are released like virions or spheres. HBV virions are released via multivesicular bodies in an endosomal sorting complex-dependent manner which is required for the transport of the infectious particles (Jiang, 2015).

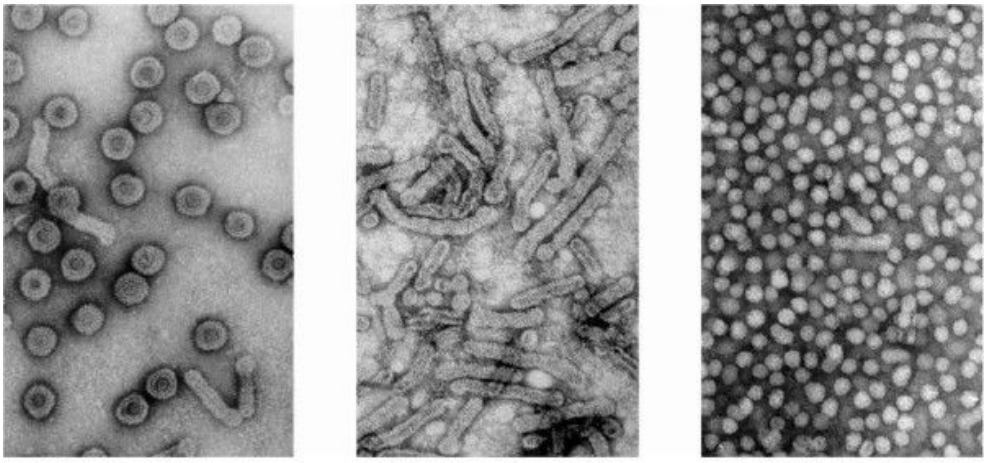

Figure 1.1 Electron microscopy images of HBV viral (Dane particles) and noninfectious subviral particles (filaments and spheres) detected in the serum of highly viremic chronic HBV carrier
Numbers indicate the abundance of each type of particle contained in 1 ml of serum (Gerlich et al., 2013).

Within a virion, an icosahedral capsid protects the HBV genome to which the HBV polymerase with its primase and reverse transcriptase domain is attached. The HBV capsids consist of 180 or 240 subunits of the HBV core protein that spontaneously assemble. In addition to the partially double-stranded HBV DNA and the viral polymerase, it contains host factors such as heat-shock proteins 60 (Figure 1.2 A).

The viral genome is efficiently organized in four, partially overlapping open reading frames (ORFs), which transcribe six major virus transcripts:

- the pre-core/core transcript encoding the core protein and the HBeAg and an almost identical pre-genomic RNA
- a longer and a shorter transcript encoding the L, M, and S surface proteins
- mRNAs encoding for the HBV polymerase and for the X protein, which is required for viral transcription and replication (Miller et al., 1989; Nassal, 2015; Zoulim et al., 1994).

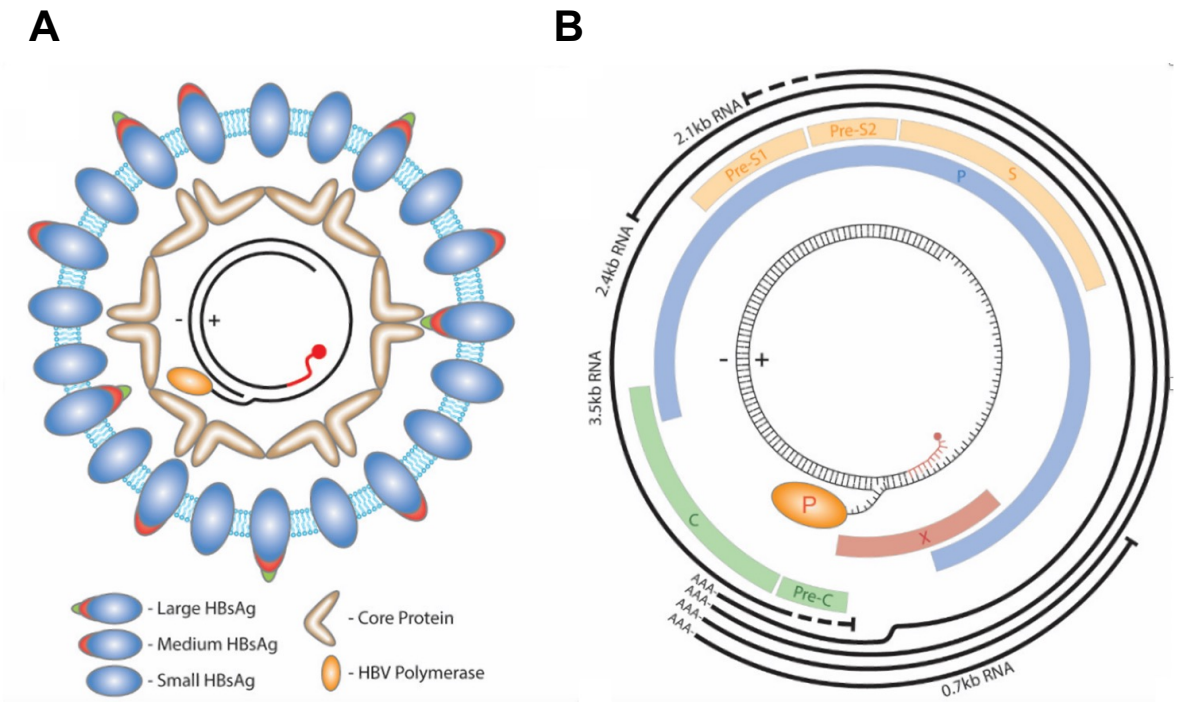

Figure 1.2 HBV virion structure and genome organization
A) HBV virion envelope consisting of the L, M and S surface proteins. Inside the virion's inner cavity is located the icosahedral capsid formed out of core protein. The capsid contains the rcDNA genome with the attached HBV polymerase (5' end, (-) strand)) and a capped RNA primer (red) (5' end, (+) strand). **(B)** Genomic organization of HBV; (Marchetti & Guo, 2020)

The first ORF region of the viral genome, also known as the preS-S region, can be subdivided into the preS1 (108-119 amino acids (aa) depending on the genotype), preS2 (55 aa) and S (HBV surface antigen, HBsAg, 226 aa) regions (Glebe & Urban, 2007) (Figure 1.2 B). The smallest viral surface protein of HBV whose translation initiation starts at the start codon of the S domain is also called the S protein. It is the most abundant surface protein of HBV. It has a molecular size of 24 kDa (Bruss & Ganem, 1991), and it can be detected as HBsAg in the sera of infected patients (Kaul, 2013). Initiation at the start codon of the preS2 domain yields the M protein (Stibbe & Gerlich, 1983). Compared to the S protein, the M protein is generated in smaller amounts and its function remains unknown until this date. The largest viral surface antigen of HBV is the L protein. Its initiation starts at the PreS1 domain (Heermann et al., 1984). It has been suggested that the L protein is essential for virion binding to hepatocytes and for virion assembly and release from infected liver cells. The viral surface proteins S and

M exist in glycosylated and non-glycosylated forms whereas the L protein is only present in a glycosylated form (Heermann et al., 1984; Stibbe & Gerlich, 1983; Tiollais et al., 1985). These viral proteins are integrated into the envelope of HBV virions.

The second ORF of the HBV genome encodes for core protein that forms the viral capsid. It can be subdivided into the preCore and the core region encoding for Hepatitis B core Antigen (HBcAg) and Hepatitis B envelope Antigen (HBeAg) (Figure 1.2 B). Upstream translation at the AUG initiation codon leads to the production of the preCore/Core protein. As it contains a secretory signal, the preCore/Core protein is addressed to the Golgi apparatus where it undergoes cleavage and thereafter leads to the formation of the HBe protein. The viral HBe protein is secreted into the bloodstream where it can be detected in the form of HBeAg and used as a diagnostic serological parameter. However, it is known from the literature that the e protein itself plays no significant role in viral replication nor virion assembly (Ganem & Prince, 2004).

The largest ORF of the viral genome encodes the HBV DNA polymerase, acting as a reverse transcriptase which consists of 4 catalytic domains: the terminal protein (TP), the spacer, the reverse transcriptase (RT) and finally the RNaseH (Clark & Hu, 2015) (Figure 1.2 B). The 5' end of the (-)-strand of the viral DNA is covalently linked to the terminal protein of the HBV polymerase, a characteristic feature of *Hepadnaviruses*, which is essential for priming of the DNA synthesis. Unlike the highly conserved HBV polymerase domains, the spacer domain shows genetic heterogenicity between different HBV genotypes. However, the genome region encoding the spacer domain overlaps with the PreS1 and PreS2 regions of the viral genome. As described above PreS1 and PreS2 are essential for the formation of the M and L surface proteins with L being the most important component in the interaction with the host cell. Therefore, a mutation in the spacer domain of the HBV polymerase may have crucial changes in the gene coding for the viral surface proteins.

The RT domain represents the main domain of HBV polymerase. The main task of viral polymerase is the transcription of the pre-genomic RNA into negative-stranded DNA (Nassal, 2008; Zoulim et al., 1994). Like all DNA polymerases, it consists of three subdomains entitled the palm, the thumb, and the fingers including several conserved regions called boxes, whose main task is to incorporate nucleotide or nucleos(t)ide analogs into the elongating strand mainly occurring in the palm region (Clark & Hu, 2015). Nowadays, the RT domain of the HBV polymerase is the best-known and used drug target against HBV as RT inhibitors have demonstrated high efficiency. Nevertheless, long-term use of RT inhibitors can lead to the emergence of drug-associated mutations, mostly located in the palm subdomain of the RT polymerase, and therefore can lead to drug resistance. Therefore, new treatment alternatives

need to be investigated. The last domain of the HBV polymerase located at the C-terminus is called the RNase H domain. This domain plays a key role in HBV replication as it deteriorates the pre-genomic RNA template from the RNA/DNA complex during reverse transcription and also takes part in RNA priming and DNA synthesis making it a possible candidate for drug development (Chen et al., 2013; Clark & Hu, 2015; Glebe et al., 2005; Meier et al., 2013; Radziwill et al., 1990).

Finally, the smallest ORF encodes for the 154 aa long HBx protein (Figure 1.2 B). As suggested by its name, the exact functions of HBx protein are yet not well understood. It has been shown that the X protein is not included in HBV virions but is only expressed within the host cell upon infection. It plays an important role in the replication cycle of HBV as it is required to establish and maintain viral replication in infected hepatocytes (Lucifora et al., 2011). Furthermore, the X protein transactivates promoters of cellular regulators and viral genes such as the RAS-RAF-Mitogen Activated Protein Kinase (MAPK) signaling pathway leading to the activation of transcription factors such as nuclear factor kappa-light-chain enhancer of activated B cells (NF-κB), and to the dysregulation of the cell cycle, which leads to increased cell proliferation and selection of genetically unstable cells. Therefore, HBx protein could act as an oncogene factor involved in the development of hepatocellular carcinoma (Benn & Schneider, 1995; Bouchard & Schneider, 2004).

1.1.2 HBV replication cycle

HBV infection initiates with an energy-dependent but reversible, low-specific binding of the virion to carbohydrate side chains of heparan sulfate proteoglycans on the cell surface of hepatocytes (Figure 1.3). For successful binding integrity of the preS domain from the large-surface protein is required (Schulze et al., 2007). Once attached to the cell surface, virions bind to the hepatocyte-specific receptor sodium taurocholate co-transporting polypeptide (NTCP). The NTCP receptor, encoded by the SLC10A1 gene and consisting of 349 aa in humans, is one of the major reasons for the liver specificity of HBV. Located on the sinusoidal side of the cell membrane of hepatocytes, NTCP is known to play key roles in the enterohepatic bile acid life cycle through the uptake of bile acid from the blood into hepatocytes in cotransport with Na^+, the viral entry of HBV and hepatitis Delta virus (HDV) and the transport of drugs, toxins and thyroid hormones (Döring et al., 2012; Hagenbuch & Meier, 1994; Stieger, 2011; Yan et al., 2015). NTCP is known to interact with aa 3-77 of the preS1 domain of the large surface protein (Yan et al., 2012). Moreover, approximately 50 aa and myristoylation of the N-terminal preS1 domain of L surface proteins are essential for infection (Nassal, 2015). Therefore, NTCP is a key determinant for viral entry and thus for enabling viral infection with HBV. As shown in cell culture with the HepRG cell line, effective infection depends not only on

the species' origin but also on the state of differentiation of the host cells as the infection rate increases with differentiation. Another hallmark of HBV infection is its natural host range, which is limited to chimpanzees and humans and mainly determined by an N-proximal region of the L protein (Glebe & Urban, 2007; Gripon et al., 2002).

Following the receptor binding, viral entry occurs most likely via fusion of the envelope of HBV virions with the endosome. This leads to the cytoplasmatic delivery of the nucleocapsid which contains the relaxed circular DNA genome (rcDNA) of HBV. However, for viral replication, the genome needs to reach the nucleus. Therefore, the HBV capsids are actively transported along the microtubules using a cellular transport mechanism. Upon reaching the nucleus, the viral genome is released directly into the nucleoplasm via the nuclear pore complex. The nuclear import of the viral genome is strongly regulated to exclusively import rcDNA into the nucleus to establish infection. To select only for replication-competent capsids, capsids are sorted out according to the expression level of the arginine-rich nuclear localization sequence in the C-terminal region of the HBV capsid protein (Eckhardt et al., 1991; Yeh et al., 1990). Moreover, further regulatory mechanisms imply that only a maturated viral genome is released from the capsid into the nucleus to achieve successful persistent infection of the host cell. The immature viral genome is trapped in the nuclear basket, a filamentous structure, which is located on the side of the nuclear pore complex facing the nucleus. Mature capsids disintegrate to leave the nuclear basket and release the relaxed circular partially double-stranded DNA bound to the HBV polymerase in the nucleoplasm for further DNA replication (Li et al., 2010; Rabe et al., 2006; Rabe et al., 2003; Schmitz et al., 2010). In the nucleoplasm, the conversion from rcDNA to covalently closed circular DNA (cccDNA) occurs, which serves as a template for the transcription of the subgenomic RNAs by a cellular RNA polymerase type II. cccDNA is the highly stable persistent form of HBV, which remains in the nucleus of infected hepatocytes and, therefore, represents a major hurdle for the development of any curative treatment of HBV. Viral RNAs (for surface proteins, HBx, pre-genomic RNA and pre-core RNA) are exported to the cytoplasm where translation of the viral proteins occurs (Figure 1.3).

The viral pregenomic RNA is packaged into newly assembled viral capsids and reverse transcription takes place leading to the formation of rcDNA. Next, mature capsids are addressed to the endoplasmic reticulum where envelopment with HBV surface proteins L, M, and S takes place. Once encapsidation and reverse transcription occur, mature virions are either enveloped in the endoplasmic reticulum or directly recycled back to the nucleus for further cccDNA establishment. Besides the assembly of Dane particles, the viral proteins encoding for the envelope proteins are addressed to the endoplasmic reticulum and released as capsid-free subviral particles consisting only of envelope proteins (filaments and spheres)

via the secretory pathway (Ko et al., 2017; Nassal, 2015) (Figure 1.3).

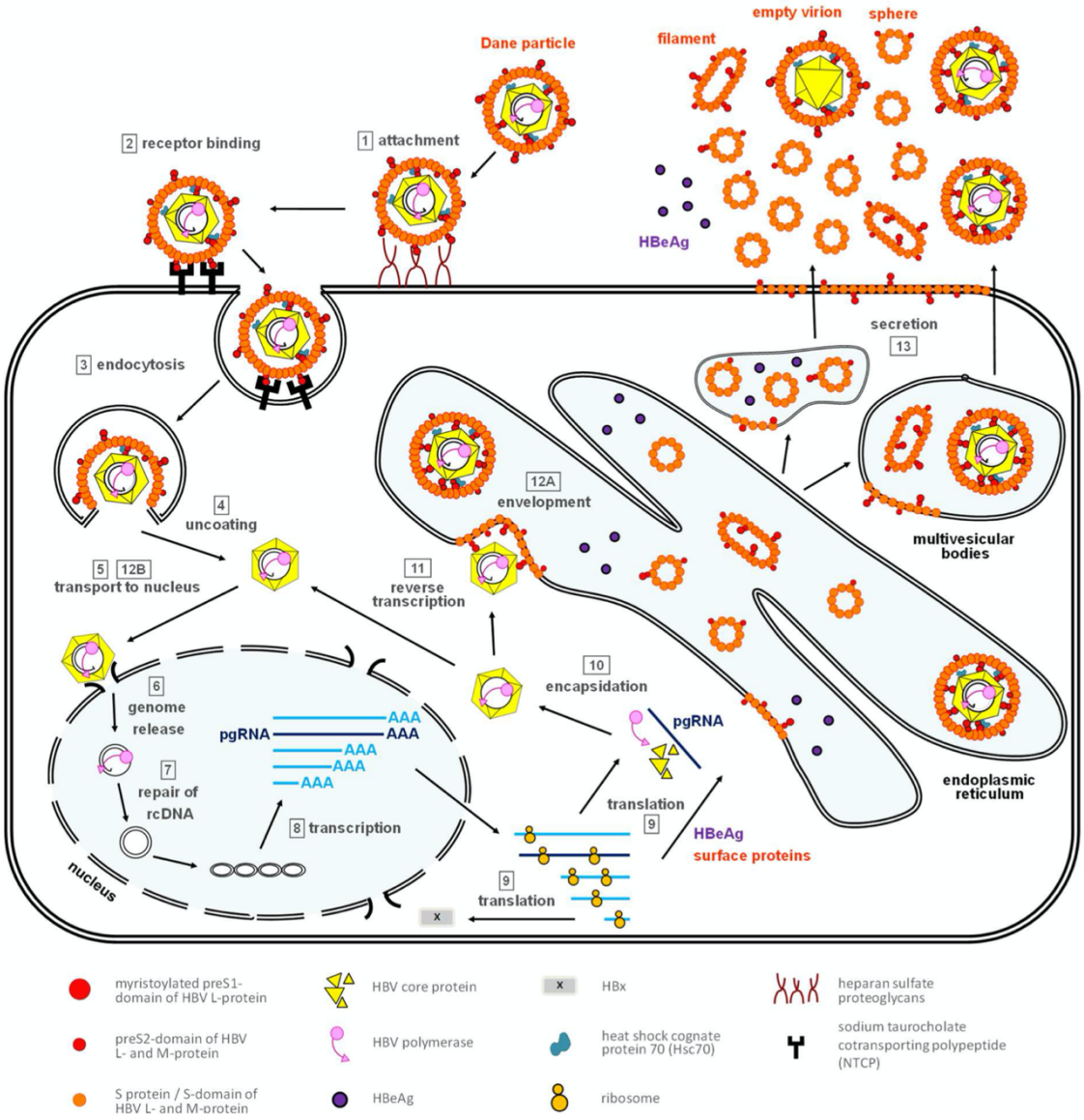

Figure 1.3 Schematic representation of the HBV life cycle
(1) unspecific and reversible attachment of HBV to heparin sulfate proteoglycans, (2) specific binding to NTCP, (3) endocytosis, (4) uncoating and (5) intracellular trafficking of the viral capsid, (6) release of the rcDNA genome into the nucleus, (7) conversion of rcDNA to the cccDNA persistence form, (8) transcription, (9) translation, (10) encapsidation and (11) reverse transcription of a pregenomic RNA, (12A) envelopment and (12B) recycling of mature capsid to the nucleus, (13) secretion of progeny virions. rcDNA = relaxed circular DNA, pg = pregenomic RNA (from (Ko et al., 2017).

1.2 Hepatitis B virus infection

1.2.1 Epidemiology

According to the WHO, approximately 4.0% of the world's population is chronically infected with hepatitis B virus (defined as HBsAg positive) (WHO, 2023). The epidemiology of hepatitis B in the world can be depicted according to the six regions defined by the WHO. In 2017, Africa (60 million people) and the Western Pacific regions (115 million people) accounted for 68% of the worldwide infected patients (WHO, 2017a). In the African region around 6.2% of the adult population is chronically infected with HBV whereas an estimated 3.2% of the Eastern Mediterranean Region, 2% of the South East Asia Region, 1.6% of the European Region, and 0.7% in the region of the Americas, respectively (WHO, 2020) (Figure 1.4). Around 45% of the world's population is considered to live in areas of high endemicity associated with a lifetime risk of infection with HBV of 60%. On the contrary, only around 12% of the world's population resides in areas with low endemicity such as the United States of America or Western Europe where the lifetime risk of infection with HBV represents less than 20% (Hwang & Cheung, 2011).

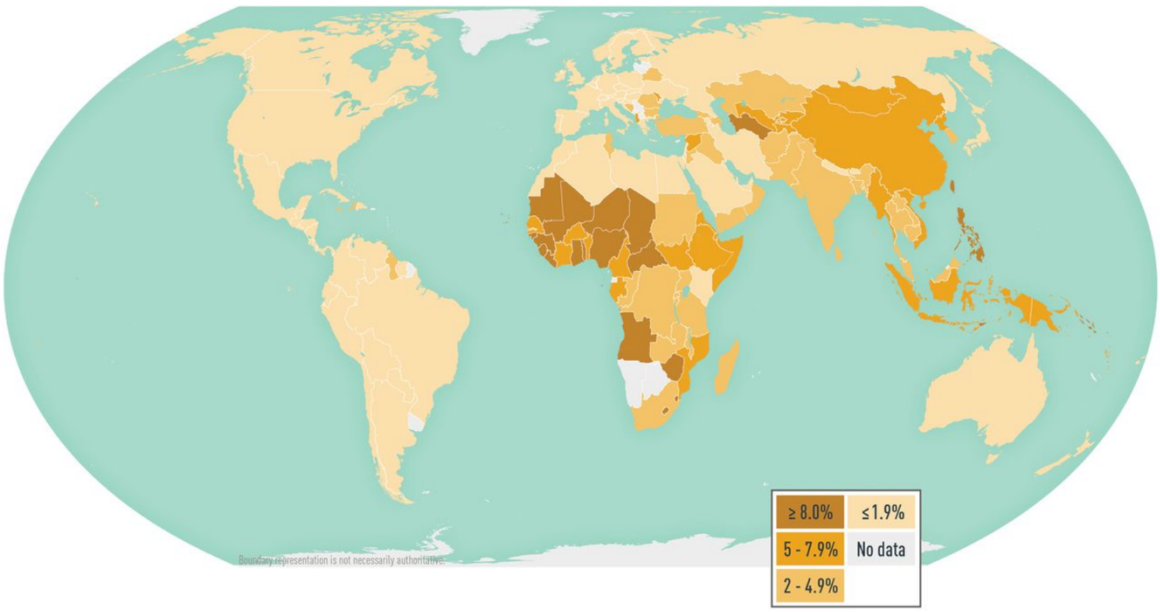

Figure 1.4 Prevalence of viral hepatitis B in the world (Harris, 2023).

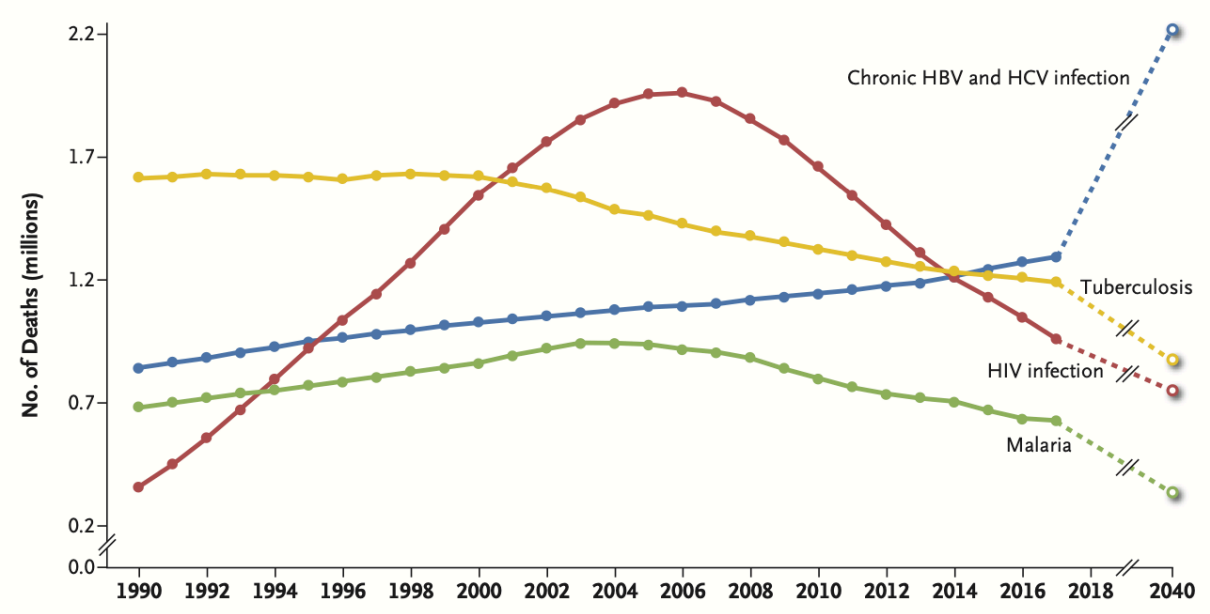

Figure 1.5 Worldwide annual mortality from chronic HBV and HCV infection as compared to mortality from tuberculosis, Human Immunodeficiency Virus infection, and malaria (Thomas, 2019).

The number of deaths due to viral hepatitis B significantly increased by 22% between 2010 and 2015. HBV-induced mortality, which is further increasing, is mostly due to a lack of an appropriate treatment. In 2015 viral hepatitis led to 1.34 million deaths of which 96% are related to late HBV (66%) or HCV (30%) related diseases. Among late HBV-related diseases liver cirrhosis (720 000 deaths) accounts for more deaths than hepatocellular carcinoma (470 000 deaths). Therefore, the number of deaths related to viral hepatitis is almost equal to those caused by tuberculosis (1.37 million deaths) and is higher than those related to HIV (1.06 million deaths) or malaria (0.44 million deaths) (Graber-Stiehl, 2018; WHO, 2017a) (Figure 1.5).

It is known that most of the patients currently infected with the hepatitis B virus were born in high-endemic countries before the introduction of prophylactic HBV vaccines. The first one of these was a plasma-derived HBV vaccine introduced in 1982 in the United States of America by Francis (FRANCIS et al., 1982). Therefore, this high endemic unvaccinated cohort was back then mainly represented by teenagers/young adults in Africa (Peto et al., 2014) or in Asia (Liang et al., 2013) who are now chronically infected with HBV and therefore at high risk to develop HBV related diseases such as liver cirrhosis or primary liver cancer.

The prevalence of HBV genotypes strongly differs among countries. Currently, nine HBV genotypes are known (A-I) (Yu et al., 2010). It is known that 96% of the world's chronic HBV infections are caused by 5 (A-E) of the 9 genotypes. Genotype C is the most common genotype (26% of chronic HBV infections), followed by genotype D (22% of chronic HBV infections), E

(18% of chronic HBV infections), A (17% of chronic HBV infections) and B (14% of chronic HBV infections) (Velkov et al., 2018) (Figure 1.6).

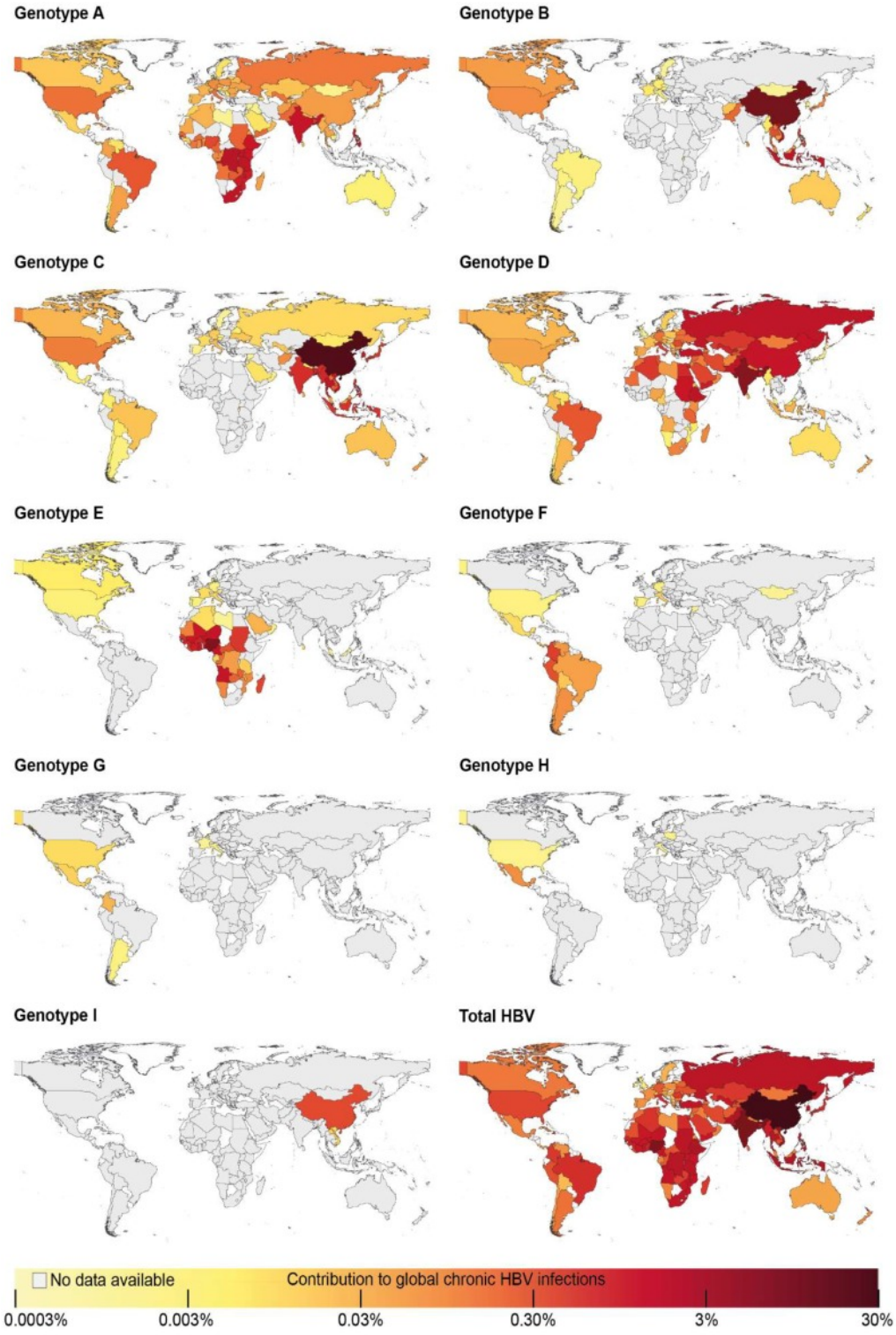

Figure 1.6 Contribution of genotypes to global chronic HBV infections
The number of infections with each genotype in a respective country is illustrated as a percentage of global chronic HBV infections (Velkov et al., 2018).

Each of them varies in prevalence and spread around the globe. The most common genotypes

in Europe and in the Middle East are genotypes A and D, A and E in Africa, genotype B and C in Asia and Southeast Asia, and finally genotype F in Latin America (Figure 1.7.) (Velkov et al., 2018) (Figure 1.7).

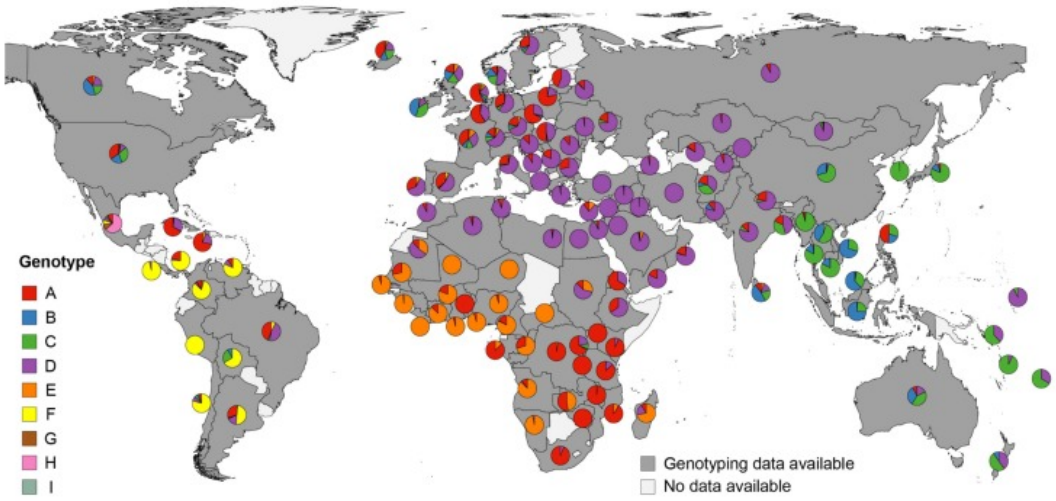

Figure 1.7 Distribution of HBV genotypes by country
Pie charts indicate proportional HBV genotype distributions in the respective countries. Genotype distributions within samples with successful genotyping are presented, excluding inter-genotype recombinant viruses, co-infections with more than one HBV genotype or undefined infections (Velkov et al., 2018).

Apart from the important epidemiological disparities in the repartition of HBV carriers or HBV genotypes around the world, knowledge about the global distribution of HBV genotypes is essential to combat the global burden of chronic HBV infections by designing novel optimized treatment strategies. Future innovations need to be able to efficiently target at least genotypes A-E to address the majority of global HBV infections.

1.2.2 Means of transmission

HBV can be transmitted via blood, saliva, seminal fluid, vaginal secretions, menstrual blood, sweat, tears, breast milk and urine (Boag, 1991). However, blood transmission remains the most common transmission route. In areas of high endemicity transmission mostly occurs vertically by perinatal infection from an infected mother to her child. The perinatal transmission rate is greater than 90%, depending on the HBsAg level of the mother (Margolis et al., 1991). In regions of low HBV endemicity such as Europe and North America transmission mainly occurs horizontally (Zuckerman, 1999). Most infections occur via sexual transmission and needle sharing amongst intravenous drug users, whereas blood contamination or organ transplantation only plays a minor role (Gust, 1996).

1.2.3 Acute versus chronic HBV infection

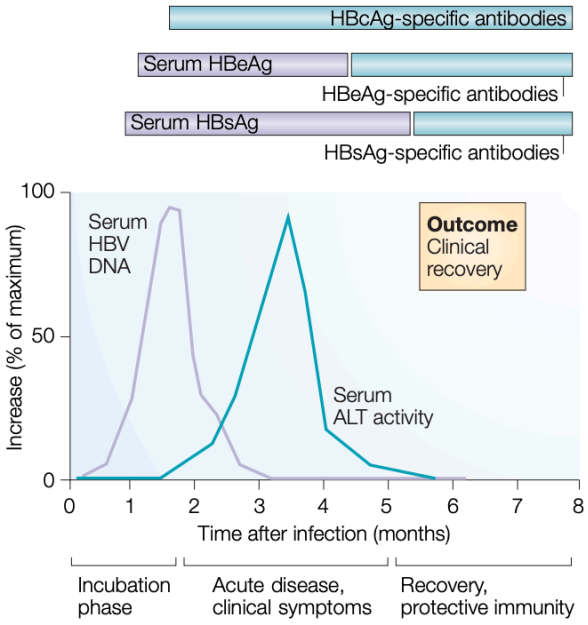

Figure 1.8 Clinical and virological course of acute infection with HBV
Schematic depiction of the immune response in acute HBV infection (horizontal transmission). After clinical recovery, the presence of HBsAg-specific antibodies and HBV-specific T cells leads to lifelong protective immunity (Rehermann & Nascimbeni, 2005).

The two main factors determining the course of infection are the patient's age at the onset of infection and their immunological status. In the majority of infections incubation phase lasts 60-110 days followed by prodromal viral symptoms, afebrile jaundice, and finally recovery and the establishment of a lifelong protective immunity (Juszczyk, 2000). Most hepatitis B cases undergo clinical recovery without the need for medical intervention; however, the clinical course of infection varies strongly between individuals. Acute HBV infection causes acute hepatitis which leads to liver cell necrosis and periportal inflammation. Liver failure due to fulminant hepatitis represents the most serious adverse event of acute HBV infection which occurs in less than 1% of the patients. Nevertheless, several studies demonstrated that 6.6% of Chinese patients develop fulminant hepatitis upon acute HBV infection (Du et al., 2017). Liver failure is a life-threatening diagnosis that requires supportive treatment and in most cases liver transplantation for survival. During acute HBV infection, serum HBV DNA as well as serum HBeAg and HBsAg levels become detectable 2-8 weeks before alanine aminotransferase (ALT) elevation. Anti-hepatitis B core (Anti-HBc) immunoglobulin type M (IgM) antibodies are detectable from the beginning of the clinical symptoms, followed by the detection of anti-HBc immunoglobulin type G (IgG) in the serum. Once HBeAg levels become undetectable, HBeAg-specific antibodies develop. Anti-hepatitis B surface (Anti-HBs) antibodies become detectable between 6 weeks and 6 months after the onset of HBV infection and lead in most cases to HBsAg clearance (Figure 1.8). If antigenemia remains detectable after 6 months, the patient

is considered a chronic carrier of hepatitis B (Juszczyk, 2000). Despite seroconversion from HBsAg to anti-HBs positive antibodies, low levels of cccDNA remain detectable in the liver of cured patients (Yotsuyanagi et al., 1998). Therefore, in the case of immunosuppression, HBV can reactivate.

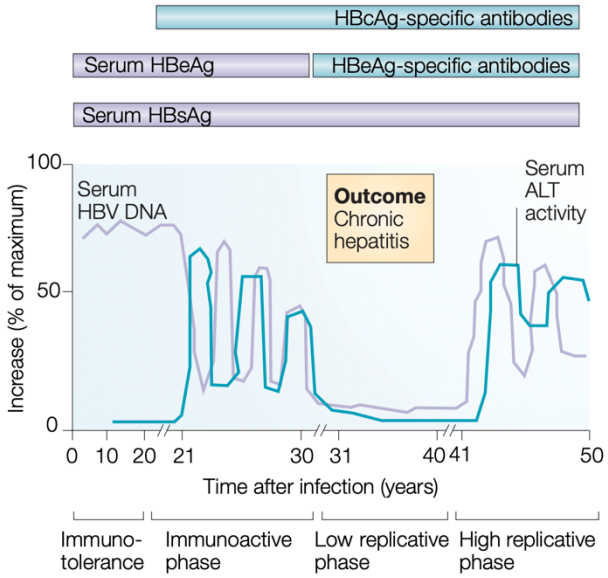

Figure 1.9 Clinical and virological course of chronic infection with HBV through vertical transmission from mother to neonate
For the details, see the main text. (Rehermann & Nascimbeni, 2005).

In most cases vertical transmission from mother to newborn results in chronically evolving hepatitis B (Beasley & Hwang, 1983; Stevens et al., 1975). The clinical and virological course of the disease can be divided into four phases (Figure 1.9). The first phase represents the immunotolerant phase, which can last for decades and is characterized by high levels of serum HBV DNA, HBeAg, HBsAg, and normal ALT values. The second phase is the immunoactive phase in which HBeAg and HBsAg levels decrease whereas ALT values increase due to increased liver damage by the immune system activation. During this phase, anti-HBc antibodies can be detected in the serum. The strong immune activation can result in liver cirrhosis. Alternatively, patients can enter a low replicative phase characterized by clearance of HBeAg and the formation of anti-HBe specific antibodies. ALT values normalize and HBV DNA reaches values under the detection limit of conventional assays. The clinical status of the patient improves as necroinflammatory liver disease reduces (Kao, 2008; Rehermann & Nascimbeni, 2005). This phase can be stable for life, but in patients who are immunosuppressed or have undergone immunosuppressive therapy virus replication can reach high levels again (Anastasiou et al., 2019).

1.2.4 Hepatitis B and hepatocellular carcinoma

HBV-related hepatocellular carcinoma (HCC) leads to approximately over 830,000 deaths/year worldwide and thus represents the third most prevalent cause of cancer-related death on Earth (Sung et al., 2021). Chronic infection with HBV represents a major risk for the development of HBV-related hepatocellular carcinoma. Approximately 50% of HCC cases worldwide can be attributed to HBV (El–Serag & Rudolph, 2007; Venook et al., 2010). It is known that chronic HBV carriers have a 10-25-fold greater lifetime risk of developing HCC compared to healthy individuals (Fattovich et al., 2004). Male gender and early-in-life infection with HBV resulting in longer exposure have also been described as significant risk factors for HCC (Sherman, 2009). Other factors such as alcohol consumption, tobacco smoking, combined exposure to HBV and aflatoxin B1, hemochromatosis, non-alcoholic fatty liver disease, and diabetes attribute to HCC development (Donato et al., 2002; El–Serag & Rudolph, 2007; Ming et al., 2002; Pollicino et al., 2013). Molecular driving forces in the development of HCC are, among others, chronic inflammation, DNA damage, DNA integration into the host's genome, chromosomal instability, epigenetic changes, neoangiogenesis, and genetic mutations. Several mechanisms have been proposed for the role of HBV in the molecular pathogenesis of HCC: (i) HBV DNA integration into the host genome, promoting clonal tumor cell expansion, genomic instability, and insertional mutagenesis (ii) epigenetic changes of tumor-suppressor genes (iii) extended expression of viral proteins (HBx and large surface protein) (Levrero & Zucman-Rossi, 2016; Ringehan et al., 2017).

1.2.5 Prophylactic vaccination

The first prophylactic vaccination attempts against HBV date back to the late 1960s (Blumberg, 2002). Baruch S. Blumberg and Harvey Halter discovered a small human serum protein initially called AuAg, later renamed HBsAg. Their finding could be clinically confirmed by Alfred Prince in patients with viral hepatitis (Gerlich, 2013). Patients having antibodies against HBsAg seemed to be protected against the disease. The first attempt at a prophylactic vaccine was launched by S. Blumberg in October 1969 and consisted of purified HBsAg from human plasma (Blumberg, 2002) (p. 137). Next, Robert Purcell and John Gerin (Purcell & Gerin, 1975) and Maurice Hilleman et al. (Buynak et al., 1976; Hilleman et al., 1975) isolated HBsAg from the serum of chronic HBV carriers, treated it to remove the residual infectivity, and immunized chimpanzees. Animals were then challenged with HBV and showed complete protection against the virus, thus confirming earlier findings. Those findings could also be confirmed in clinical trials and showed a 92.3% risk reduction of HBV infection in male homosexual vaccinees (Szmuness et al., 1980). Plasma-derived vaccines, so-called first-generation vaccines, were soon replaced by second-generation vaccines, namely recombinant vaccines.

In 1979, the molecular biologists Pierre Tiollais, Kenneth Murray, and William Rutter succeeded in cloning and sequencing the HBV DNA (Burrell et al., 1979; Charnay et al., 1979; Pasek et al., 1979). Mammalian cells were then transformed with the aa sequence encoding for HBsAg protein, thus enabling large-scale production of HBsAg particles (Dubois et al., 1980; Moriarty et al., 1981). As mammalian cell culture is costly and labor-intensive the extraction of HBsAg from genetically transformed yeast cells enabled a breakthrough in hepatitis B vaccine production (Harford et al., 1983; Valenzuela et al., 1982). The foremost yeast-derived recombinant HBV vaccines approved for clinical use consist of the small HBsAg protein subtype adw2 (Engerix-B®, Glaxo-Smith-Kline; Recombivax-HB®, Merck Sharp and Dome). The S protein is integrated into spherical particles thus enabling the presentation of the strongly immunogenic a-determinant of the S protein. In contrast to natural HBsAg particles yeast derived recombinant HBsAg lack the preS1 domain containing neutralizing epitopes and glycosylation. On the contrary, third-generation vaccines, produced in mammalian cells carry correctly folded HBsAg and the neutralizing epitopes of the preS domain, enabling more rapid antibody protection. Therefore, they represent an alternative for use in non-responders to second-generation vaccines and enable greater protection against perinatal mother-to-child-transmission (Gerlich, 2015). The WHO recommends hepatitis B vaccination for all children worldwide consisting of at least three doses of hepatitis B vaccine, each of them in an interval of at least four weeks. Since perinatal transmission represents the most common cause of chronic HBV infection worldwide, the WHO recommends for all children a hepatitis B vaccine dose within 24 hours post-birth. WHO also indicates hepatitis B vaccination for individuals at high risk of infection such as dialysis patients, diabetes patients, patients undergoing organ transplantation, or patients infected with the human immunodeficiency virus (WHO, 2017b). Major progress towards HBV eradication could be achieved with prophylactic vaccination against the hepatitis B virus. In 2015, more than 84% of the children worldwide received three doses of the hepatitis B vaccine leading to a decrease in chronically infected children (<5 years old) from 4.7% between the 1980s and 2000s to 1.3% in 2015 (WHO, 2017a).

1.3 Treatment of HBV infection

1.3.1 Standard treatment options

Treatment of chronic HBV infection aims to decrease the risk of liver disease progression and the development of HBV-associated complications. Patients chronically infected with HBV have a cumulative lifetime risk of around 40% to develop liver cirrhosis, of which 2-5%/year lead to HCC formation (Fattovich et al., 2004). Patients with an HBeAg negative chronic HBV infection represent the dominant form of disease among chronic HBV carriers. Treatment with

nucleos(t)ide analogs (NUC) or interferon (IFN)-α leads to the inhibition of HBV replication and so limits the disease progression (Hoofnagle et al., 2007; Lok & McMahon, 2009). Nevertheless, the hallmark of a durable and functional HBV cure is seroconversion, meaning HBsAg loss and generation of anti-HBs-specific antibodies (Boni et al., 2012). Treatment indication in adults is based on three criteria: i) serum HBV DNA levels, ii) liver disease severity, and iii) serum ALT levels (European Association For The Study Of The Liver (EASL), 2017) (Figure 1.10).

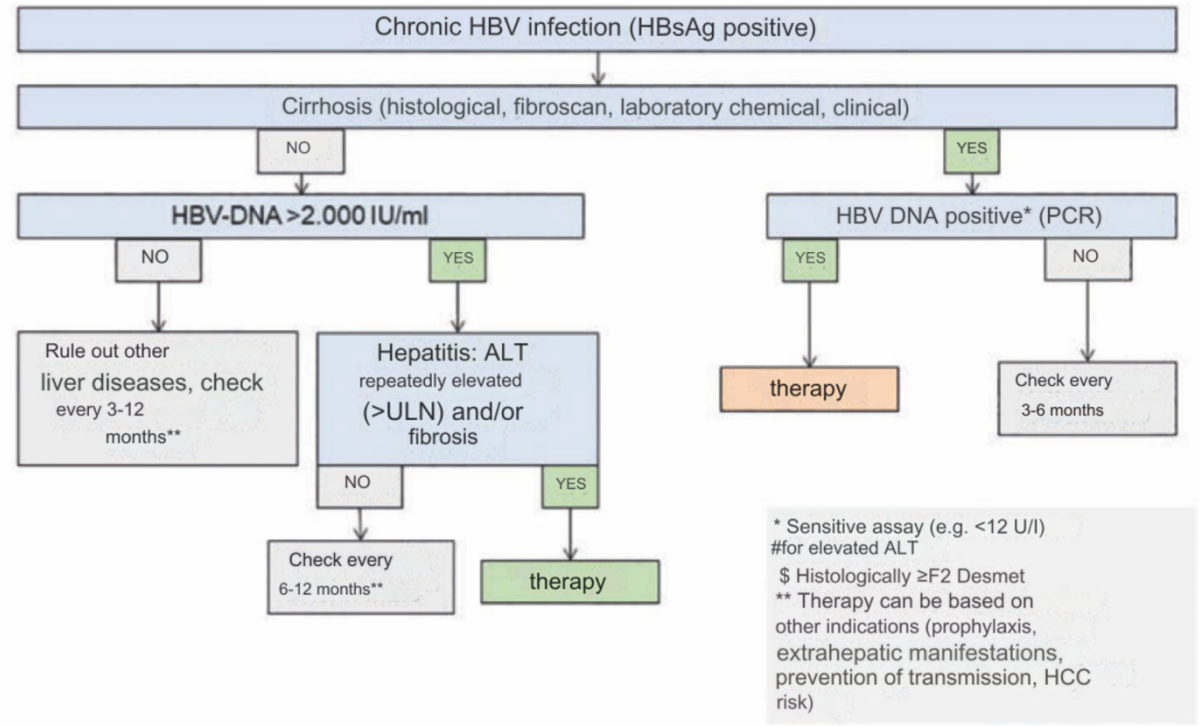

Figure 1.10 German guideline for chronic hepatitis B infection: algorithm for initiation of treatment (Cornberg et al., 2021)

As of today, seven drugs (Figure 1.11.) are approved by the regulatory authorities for the treatment of chronic HBV infection in Europe and the United States. However, even if nucleos(t)ide analogs successfully suppress HBV replication, long-term medication is needed to achieve sustained virological control. Alternatively, pegylated interferon can be administered short term. However, it is costly and associated with numerous side effects (Tang et al., 2014).

Antiviral agents	Immunomodulators			Nucleos(t)ide analogues				
	IFN-α	PEG-IFN-α	Thymosin	Lamivudine	Adefovir	Entecavir	Telbivudine	Tenofovir
Route	SC	SC	Oral	Oral	Oral	Oral	Oral	Oral
Dose	5-10 MIU *tiw*	180 μg *qw*	1.6 mg *biw*	100 mg *od*	10 mg *od*	0.5-1 mg *od*	600 mg *od*	300 mg *od*
Year approved	1992	2005	Asia only	1998	2002	2005	2006	2008
Antiviral effects								
HBV DNA	37	30	42	36-40	21	67	60	76
HBsAg clearance	++	++	N/A	-	-	+	-	-
HBeAg seroconversion	20-40	27	40	18-20	12	21	22	21
ALT normalization		39	42	62-77	48	68	77	68
Histological improvement		38	N/A	56-62	53	72	65	74
Side effects	Many	Many	Negligible	Negligible	Nephrotoxicity	Negligible	Negligible	Nephrotoxicity
Contraindications	Numerous	Numerous	Uncommon	Uncommon	Uncommon	Uncommon	Uncommon	Uncommon
Drug resistance (treatment-naïve patients)								
1 yr	None, but non-response			24	None	0	4	0
2 yr				38	3	0.2	25	0
> 5 yr				80	29	1	N/A	0
Drug resistance (LAM resistant patients)								
2 yr	None, but non-response			N/A	25	9	N/A	0
4 yr				N/A	N/A	39	N/A	0

PEG-IFN: Pegylated interferon; SC: Subcutaneous; *tiw*: Three times a week; *qw*: Once a week; *biw*: Twice a week; *od*: Once daily; ALT: Alanine transaminase; ETV: Entecavir; LAM: Lamivudine; ADV: Adefovir; TBV: Telbivudine; TDF: Tenofovir disoproxil fumarate; N/A: Not applicable.

Figure 1.11 Comparison of antiviral drugs for chronic hepatitis B (Tang et al., 2014)

Pegylated IFN-α, a type I IFN, is a cytokine used as a standard treatment in chronic hepatitis B virus infection, it inhibits HBV DNA synthesis and leads to an increased cellular immune response against infected liver cells (Tang et al., 2014). In a clinical study comparing the drug efficacy of lamivudine versus pegylated IFN-α, 32% of patients undergoing pegylated IFN-α therapy cleared HBeAg, developed anti-HBeAg, and reached HBV DNA levels under the detection limit of conventional assays (called inactive HBV carrier state) compared to 19% of patients in the lamivudine treated subgroup. HBsAg seroconversion was only observed in the group receiving pegylated IFN-α (Janssen et al., 2005; Lau et al., 2005). Despite their partial success, anti-HBV immune responses induced by pegylated IFN-α administration are rather low and the therapy is associated with several adverse events such as paraesthesia, myelosuppression, and flu-like symptoms (Tang et al., 2014).

Entecavir is a guanosine analog that inhibits the HBV DNA polymerase. Its efficacy in nucleos(t)ide naïve patients has been evaluated in two large double-blinded clinical studies including HBe positive and negative patients. Through 96 weeks, HBV DNA levels dropped under the detection limit and ALT value normalization could be achieved in 80 and 87% of patients when undergoing daily therapy with entecavir in a 0.5mg dose (Gish et al., 2007). Importantly, entecavir treatment in nucleos(t)ide naïve patients showed decreased risk of liver disease decompensation, HCC, and death in a 20-month median follow-up (Zoutendijk et al., 2013). Moreover, continuous entecavir therapy did not show any serious therapy-mediated side effects nor the development of drug resistance (Tenney et al., 2009). Therefore, according to meta-analyses nucleos(t)ide analogs like entecavir and the newest antiviral tenofovir prodrug tenofovir alafenamide represent the best, currently available antiviral therapies for treatment-naïve chronic HBV carriers (adults and adolescents) (Scott & Chan, 2017; Woo et

al., 2010).

1.3.2 Treatment limitations

Chronic hepatitis B (CHB) treatment needs to be adjusted individually. Several treatment limitations have to be taken into account when choosing between the available standard treatment options. Pegylated IFN-α therapy is finite whereas long-term medication is a prerequisite for successful nucleos(t)ide analogs therapy. According to the American Association for the Study of Liver Diseases (AASLD) guidelines from 2016, pegylated IFN-α is contraindicated in patients with autoimmune disease, psychiatric disease, cytopenia, severe cardiac disease, uncontrolled seizures and decompensated liver cirrhosis (Terrault et al., 2016). Moreover, the antiviral response to pegylated IFN-α is HBV genotype dependent. HBV genotypes A and B are more prone to HBeAg and HBsAg loss during treatment with IFN compared to other genotypes (Erhardt et al., 2005; Kao et al., 2000; Wai et al., 2002).

Contrary to IFN-based therapy, nucleos(t)ide analogs induce negligible side effects and show genotype-independent antiviral effects (Ahmed et al., 2000; Pichoud et al., 1999; Seignères et al., 2000; Westland et al., 2003). As nucleos(t)ide analogue treatment can be permanent in patients with low-level viremia it is essential for medical doctors to perform medical counseling about therapy adherence. Nucleos(t)ide analog dosage needs to be adjusted in patients with creatinine clearance <50ml/min (Pipili et al., 2014). Neither antiviral therapy with IFN nor with nucleos(t)ide analogs leads to the elimination of potential HCC formation thus stressing the need for continuous surveillance under therapy. Entecavir and tenofovir long-term medication may lead to kidney and bone injuries (Terrault et al., 2016). Although nucleos(t)ide analogs represent potent antiviral agents, their prolonged administration can lead to the establishment of drug resistances induced by resistant mutants. As the HBV polymerase naturally lacks a proof-reading function, nucleotides may be randomly exchanged and thus cause the emergence of resistant viral mutants (Park et al., 2003). As both IFN and nucleos(t)ide treatments do not target cccDNA (episomal HBV genome) formation in the nucleus of infected hepatocytes a risk of reactivation of HBV replication upon cessation of treatment remains. Therefore, the development of new curative therapeutic strategies which directly target cccDNA formation or HBV-infected cells is urgently needed to achieve functional cure of CHB.

1.3.3 Alternative treatments

Several alternative treatment options such as CpAMs (Core protein allosteric modulators),

siRNA, TLR-ligands, adoptive T-cell therapy, and therapeutic vaccination might have revolutionary potential in the treatment of CHB.

a. CpAMs

HBV core protein, which assembles into the capsid that contains the viral DNA has recently emerged as a protein of interest for the development of new drugs to treat CHB (Tang et al., 2017; Zlotnick et al., 2015). It has been shown that modulation of core protein dimer-dimer interactions by CpAMs inhibits nucleocapsid formation, and HBV DNA replication and prevents cccDNA establishment. CpAMs interfere with nucleocapsid formation by interacting with specific amino acids of the hydrophobic pocket located between two core protein dimers (Viswanathan et al., 2020). Through their mechanism of action, two classes of CpAMs can be distinguished. Type I CpAMs lead to the formation of aberrant capsids or non-capsid core protein polymers made out of core protein dimers which are then degraded in hepatocytes (Bourne et al., 2006; Kang et al., 2019; Stray et al., 2005; Stray & Zlotnick, 2006; Wu et al., 2013). Whereas type II CpAMs result in the assembly of capsids lacking pgRNA and Pol (Amblard et al., 2020; Corcuera et al., 2018; King et al., 1998; Wang et al., 2015; Yang et al., 2016). Therefore, CpAMs represent a new class of emerging, potent anti-HBV drugs which may interact with cccDNA metabolism and restore a functional immune response to achieve a finite HBV cure.

b. siRNA/ASOs

RNA interference-based therapies represent a potential antiviral treatment against CHB. RNA interference occurs post-transcriptionally, in the cytoplasm (Zeng & Cullen, 2002) by small interfering RNAs (siRNA) which bind to sequence-specific homologous regions of mRNA transcripts leading to their degradation and subsequent HBV inactivation (Fire et al., 1998). In eukaryotic cells, siRNA arises from the cleavage of long dsRNA constructs by RNase endonuclease III Dicer (Zhang et al., 2004). By specific and potent gene knockdown siRNA therapy may be a promising tool in HBV-specific antiviral therapy. However, several questions about siRNA stability, biodistribution, cellular uptake, side effects, and formulation optimization still need to be addressed to turn this new therapeutic strategy into an alternative treatment for hepatitis B (Chen et al., 2008). In addition, antisense oligonucleotide (ASO) treatment represents a promising approach to cure chronic HBV infection. Previous studies have shown that by targeting all HBV messenger RNA, ASOs can successfully reduce hepatitis B virus antigenemia and viremia (Billioud et al., 2016). Bepirovirsen, an ASOs showed promising results in patients with chronic hepatitis B (phase 2 randomized controlled trial) (Yuen et al., 2021)

c. TLR-ligands

Therapeutic activation of Toll-like receptors (TLRs) could be a promising strategy to activate HBV-specific immune responses which are downregulated in CHB patients. TLRs belong to the group of pattern recognition receptors. They are expressed in various cells such as hepatocytes as well as effector cells of the innate and adaptive immune system. TLRs represent an essential link between innate and adaptive immunity. They can be divided into two groups. TLR2, 4, 5, 6, 11, and 12 belong to group 1 and can be detected on the plasma membrane whereas group 2 includes TLR3, 7, 8, and 9 which are localized in different intracellular compartments of the cell (Akira et al., 2006; Kondo et al., 2011). After recognition of pathogen-associated molecular patterns (PAMPs) by TLRs, effector cells are immediately fully functional, thereby circumventing the initial proliferation in the lymph nodes which usually occurs before acquiring effector function. Recent studies imply the important role of TLRs in antiviral immune responses *in vivo* (Hoebe et al., 2003; Kurt-Jones et al., 2000; Lund et al., 2004). It has been shown that each TLR signal occurs through different but converging signaling pathways. For example, TLR4 signaling is mainly driven by a MyD88-independent, TRIF-dependent signaling pathway whereas TLR2, 5, and 9 signaling have mainly shown to be MyD88-dependent and TRIF-independent (Hoebe et al., 2003). To evaluate the antiviral efficacy of TLR signaling pathways in HBV, TLR-specific ligands were intravenously administered into HBV transgenic mice lineage 1.3.32 (Guidotti et al., 1995). 24 hours later, mice receiving 10 µg of TLR3, 4, 5, 7, and 9 ligands showed almost complete suppression of HBV replication. The antiviral effect was mainly noninflammatory and noncytopathic as the mice did not show ALT elevation or lymphocyte proliferation in the liver (Isogawa et al., 2005). Moreover, it has been shown that TLR-ligand-induced signaling triggers the production of intrahepatic cytokines (IFN-alpha, beta, and gamma) which inhibit HBV replication. Therefore, TLR activation by TLR ligands was considered as a promising immune therapeutic approach for/against persistent HBV infection. However clinical trials were somewhat disappointing.

d. Adoptive T-cell therapy

Adoptive T-cell therapy represents an encouraging therapeutic alternative for the treatment of CHB or HBV-induced HCC, schematically illustrated in Figure 1.12. In patients resolving acute hepatitis B a strong, polyclonal, and multifunctional T-cell response could be observed (Rehermann et al., 1995) whereas it is known that CHB virus infection is associated with a weak and oligoclonal T-cell response (Penna et al., 1991). Since current therapeutic treatment options do not target cccDNA, the viral replication template remains in the nuclei of infected hepatocytes. Viral replication can be reinitiated, often leading to hepatitis B relapse after cessation of therapy. Therefore, cccDNA eradication represents a prerequisite to achieving a complete sterile cure of hepatitis B (Wieland et al., 2004). Elimination of cccDNA can be

achieved by adoptive T cell transfer overcoming the inactivity of the host's immune system, which can be redirected to target the infected hepatocytes. This alternative therapeutic approach emerged from clinical observations in $HBsAg^+$ patients which received allogeneic hematopoietic stem cell transplantation from naturally HBV immune donors. In a long-term follow-up of those patients, 20 out of 31 recipients showed sustained HBsAg clearance in the serum after bone marrow transplantation (Hui et al., 2005). Adoptive T-cell transfer aims at redirecting the patient's T cells against HBV-infected or cancerous cells to eliminate them (June, 2007). For this, T cells are isolated from the peripheral blood, stimulated, and genetically modified to express either a natural T-cell receptor (TCR) or a chimeric antigen receptor (CAR) targeting certain proteins. After *ex-vivo* clonal expansion, quality control, and formulation of the genetically modified donor T cells, reinfusion into the patient occurs.

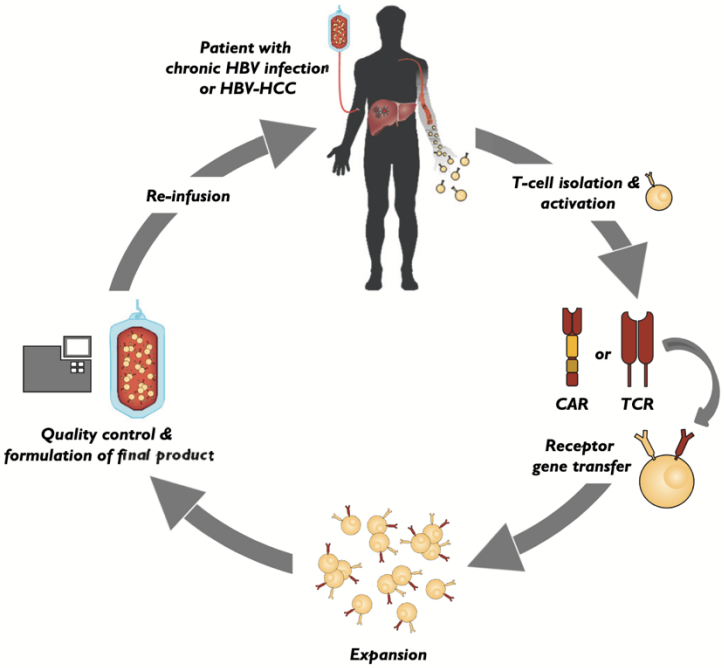

Figure 1.12 Adoptive T-cell therapy for patients with CHB or HBV-induced HCC
Adoptive T-cell therapy to treat CHB or HBV-induced HCC requires several steps: i) isolation and then activation of T cells from the peripheral blood of patients with CHB or HBV-HCC; ii) engraftment of T cells with a TCR or a CAR; iii) *ex-vivo* clonal expansion of genetically modified T cells; iv) quality control and formulation of final product; v) re-infusion of genetically modified donor T cells (Tan & Schreiber, 2020).

CARs are artificial receptor constructs that are highly antigen-specific thanks to a scFv (single chain variable fragment) obtained from an antibody. The use of a scFv allows a major histocompatibility complex (MHC) independent recognition of a native, unprocessed antigen on the surface of the cells (Gross et al., 1989). In addition to the scFv CARs consist of a spacer domain, a transmembrane domain, and intracellular signaling domain(s). The functionality of HBV-specific CAR T cells has already been analyzed both *in vitro and in vivo* (Bohne et al.,

2008; Krebs et al., 2013) in the context of CHB. Chimeric T-cell receptors directed against HBV surface proteins S and L were genetically engineered and engrafted onto primary human T cells. In this study, it has been shown that these, HBV small and large surface protein-specific, chimeric antigen receptor T cells were able to recognize HBsAg on the surface of infected hepatocytes, release antiviral cytokines and lyse HBV infected cells and thus effectively eliminate cccDNA (Bohne et al., 2008).

e. Therapeutic vaccination

Therapeutic vaccination against CHB represents a promising and broadly applicable immunotherapeutic strategy to cure the disease and reduce HBV-related disease burden. In contrast to a prophylactic vaccine which aims at preventing a disease, a therapeutic vaccine is meant to restore the patient's immune system to control or in optimal cases eliminate the viral pathogen to achieve cure. As described above, chronic HBV carriers lack a strong polyclonal and multifunctional immune response to fight the disease and achieve HBV clearance. Patients chronically infected with HBV have acquired an HBV antigen-specific immunotolerance which leads to HBV persistence. Immune tolerance can be established by antigen-specific T-cell depletion, absence of clonal T-cell expansion, and 'arming' of $CD8^+$ T cells as well as failure to establish a memory T-cell response (Protzer & Knolle, 2016). Therefore, strong immune tolerance needs to be overcome by therapeutic vaccination to achieve HBV clearance. Different approaches have been investigated to induce strong immunogenicity by therapeutic vaccination, but only suboptimal antiviral effects could be observed in clinical trials. Available prophylactic vaccines could reduce HBV replication *in vivo* (Rollier et al., 1999) but have failed to restore HBV-specific immunity in chronic HBV carriers (Pol et al., 2001; Vandepapelière et al., 2007). Although a DNA vaccine based on a DNA prime and a poxvirus-boost immunization encoding for HBV envelope proteins showed encouraging results in chimpanzees (Pancholi et al., 2001), it failed to induce broad and multispecific T- and B-cell responses in CHB patients (Cavenaugh et al., 2011). To break immune tolerance and boost functional HBV-specific immune responses it is essential to induce both humoral and cellular immune responses. It may be advantageous to add checkpoint inhibitors to the therapeutic strategy to defeat T-cell exhaustion. Moreover, more potent therapeutic vaccination strategies might require lowering of HBV antigen load (Kosinska et al., 2017; Michler et al., 2020). One promising approach for successful therapeutic vaccination is a heterologous prime-boost vaccination strategy. Recombinant viral vectors such as adenovirus- or Modified Vaccinia Virus Ankara (MVA)-based viral vectors, which can encode multiple HBV genes can boost previously elicited T-cell responses. Additional priming immunizations, with recombinant protein for instance, induce humoral responses against the viral proteins, increase the amount of HBV-specific effector cells and improve the boosting effect of

recombinant viral vectors (Gilbert et al., 2006; Webster et al., 2005) (Figure 1.13).

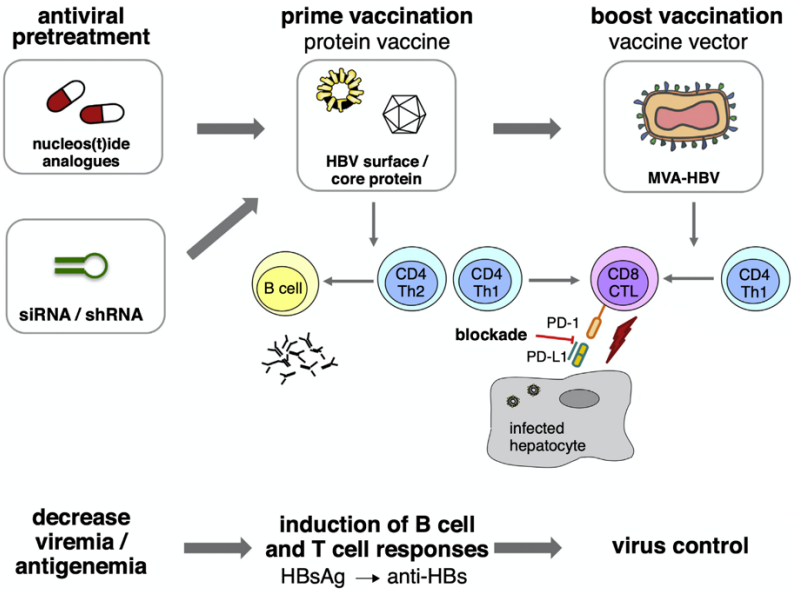

Figure 1.13 Optimized prime-boost vaccination strategy for therapeutic vaccination against CHB
Successful therapeutic vaccination to treat CHB requires i) antiviral pretreatment with nucleos(t)ide analogs to decrease viremia/antigenemia and liver inflammation or HBV-specific siRNA/short hairpin RNAs to suppress viremia/antigenemia; ii) protein priming with recombinant HBV antigens to induce HBV-specific antibodies and prime T-cell responses; iii) boost vaccination with a recombinant viral vector encoding HBV antigens (MVA-HBV); iv) optional: strategies to overcome T-cell exhaustion such as PD-1/PD-L1 blockade (modified from (Kosinska et al., 2017).

It has been shown that HBV-specific protein-prime/MVA vector-boost vaccination in high antigenemic HBV transgenic mice could overcome HBV-specific immune tolerance as it induced strong as well as potent humoral and cellular responses. Priming with recombinant HBsAg and HBcAg induced neutralizing antibodies (Buchmann et al., 2013) which complex circulating antigens and thus lead to decreased antigenemia. Accordingly, protein-primed virus-specific CD4 and CD8 T cells could then be expanded by recombinant MVA boost immunization expressing HBsAg and HBcAg. This study could show that an optimized prime-boost strategy is highly effective in inducing neutralizing anti-HBs antibodies in the serum as well as $CD4^+$ and $CD8^+$ T-cell responses in livers and spleens of HBV transgenic mice (Backes et al., 2016) (Figure 1.13).

1.4 Adaptive immunity in chronic hepatitis B

1.4.1 Antiviral functions of HBV-specific $CD8^+$ T cells

An adequate antiviral immune response to HBV is characterized by optimal coordination of both innate and adaptive immune responses. It has been shown that high frequencies of HBV-specific $CD8^+$ T cells can control viral spread in acute hepatitis B and thus lead to viral

clearance in patients (Maini et al., 1999). $CD8^+$ T cells show numerous defects in HBV-specific immunity. In CHB $CD8^+$ T cells circulate at extremely low frequencies due to Bim-mediated apoptosis, NK cell-mediated deletion, checkpoint inhibition (e.g., PD1), impaired effector function and metabolism, altered expansion, and inadequate $CD4^+$ T cell help (Bertoletti & Ferrari, 2016; Maini & Pallett, 2018; Shin et al., 2016; Suslov et al., 2018). Upon peptide recognition, $CD8^+$ T cells can mediate viral clearance through both cytolytic and non-cytolytic effector functions (Guidotti & Chisari, 2006; Guidotti et al., 2015; Thimme et al., 2003). HBV-specific $CD8^+$ T cells produce cytolytic mediators such as perforin and granzyme B, which lyse infected hepatocytes and thus eliminate cccDNA and integrated HBV DNA (Maini & Burton, 2019). The non-cytolytic $CD8^+$ T cell effector functions occur through the release of antiviral cytokines such as IFNγ and tumor necrosis factor (TNF). These cytokines act on hepatocytes, leading to the loss of viral parameters while simultaneously avoiding broad liver damage (Guidotti et al., 1996; Phillips et al., 2010). Through the activation of hepatocyte APOBEC3 deaminases IFNγ and TNF can eliminate viral intermediates and cccDNA but not integrated HBV DNA (Lucifora et al., 2014; Xia et al., 2016) (Figure 1.14).

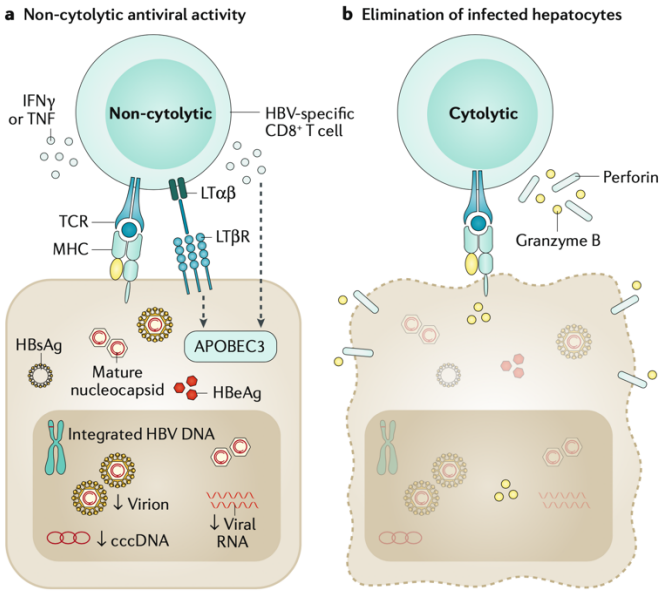

Figure 1.14 The dual mechanisms of action employed by HBV-specific $CD8^+$ T cells in eliminating HBV-infected hepatocytes
[a] The non-cytolytic effector function is depicted where HBV-specific $CD8^+$ T cells release antiviral cytokines (such as IFNγ and TNF) and induce APOBEC3 deaminases which degrade viral intermediates and cccDNA but not integrated HBV DNA. **[b]** The cytolytic elimination involves the use of molecules like granzyme B and perforin resulting in the eradication of all viral intermediates, cccDNA, and integrated HBV DNA (Maini & Burton, 2019).

1.4.2 Antiviral functions of HBV-specific $CD4^+$ T cells

$CD4^+$ T cells play a critical role in shaping the adaptive immune response. Naïve $CD4^+$ T-cell activation occurs in the T-cell areas of secondary lymphoid tissues where mature antigen-loaded dendritic cells (DCs) interact with naïve $CD4^+$ T cells. The specificity of the elicited immune response is determined by the peptide presented on MHC class II molecules on the surface of DCs. However, response subtype and width are controlled by costimulatory

molecules and cytokines from the activated DCs. Upon $CD4^+$ T cell activation, clonal expansion takes place. This step aims at increasing the number of $CD4^+$ T cells to help $CD8^+$ T cells and B cells (MacLeod et al., 2010). In addition, antigen-specific $CD4^+$ T cell proliferation is needed for differentiation into effector cells and migration to the site of infection. Following differentiation, activated $CD4^+$ T cells can be classified into 5 subsets: i) T helper (Th)1, Th2, and Th17 cells which are effector T cells directed against specific pathogens (Korn et al., 2007; Mosmann & Coffman, 1989; Romagnani, 1997); ii) regulatory T cells (Tregs) to preserve self-tolerance (Sakaguchi, 2005) and iii) follicular helper cells (Tfh) which help B cells for antibody production (Crotty, 2011). Each subset is defined by its specific cytokine production profile and/or subset-defining transcription factors (Geginat et al., 2014). Th1 effector cells are naïve T cells previously activated by IL-12-producing DCs and their effector cytokine is IFNγ (Nizzoli et al., 2013; Shortman & Heath, 2010). The Th1 cell subset confers increased cellular immunity against intracellular pathogens. In contrast, Th2 effector cells are naïve T cells primed with IL-4 which produces IL-4, IL-5, IL-10, and IL-13 (Geginat et al., 2014). Terminally differentiated Th2 effector cells are required to fight extracellular parasites. Furthermore, they are involved in allergies as it is known that they induce IgE production from B cells (Robinson et al., 1992). It has been shown that $CD4^+$ T-cell help is crucial for cytolytic $CD8^+$ T-cell activation (Zhang et al., 2009). It is also known that $CD4^+$ T cells are required for the generation of $CD8^+$ T-cell memory responses (Bourgeois & Tanchot, 2003).

In the context of CHB, it has been observed that patients who undergo clinical recovery have both strong $CD4^+$ and $CD8^+$ T-cell responses against the virus (Gehring & Protzer, 2019). Moreover, interactions between Tfh and B cells in the germinal center (Crotty, 2015) are essential for the selection, activation, antigen-specific differentiation, and regulation of B-cell function (Maini & Burton, 2019). The crosstalk between Tfh cells and B cells is crucial for the generation of high-affinity anti-HBs antibodies by B cells whereas anti-HBc antibodies can be generated in a T-cell dependent or T-cell independent fashion (Bertoletti & Ferrari, 2016; Milich & McLachlan, 1986). Therefore, anti-HBs antibody production may be impaired at some stages of CHB due to altered frequencies of HBV-specific $CD4^+$ T cells (Raziorrouh et al., 2014).

1.4.3 B cell-mediated immune response and antibodies in CHB

B cells play a central role in humoral adaptive immunity through antibody production such as neutralizing anti-HBs antibodies or non-neutralizing anti-HBc antibodies and auto-antibodies. It is known that Tfh cells help B cells to produce antibodies (Hu et al., 2014). The role of B cells has primarily been focused on neutralizing anti-HBs antibody secretion during CHB. However, B cells do not only play a positive role in the adaptive immune response to HBV as some B

cell subsets also promote persistent infection, immune tolerance, and liver damage. Three potential major functions of B cells in CHB have been described in the literature: i) antibody production, ii) antigen presentation, and iii) immune regulation (Cai & Yin, 2020). Antigen-neutralizing anti-HBs antibodies block HBV entry or replication which reduces HBV spread and confers lifelong protective immunity (Cerino et al., 2015). Therefore, impaired anti-HBs antibody secretion triggers the persistence of high HBsAg levels and hinders HBV cure. It is assumed that IgG anti-HBs antibodies bind HBsAg at the surface of infected hepatocytes and induce the release of cytolytic molecules such as granzyme B and perforin from natural killer (NK) cells which lyse HBV-infected hepatocytes (Chu & Liaw, 1987; Ray et al., 1976). On the cell surface, HBs serves as a therapeutic target (Zhao et al., 2021). Anti-HBs antibodies can also bind HBsAg to mediate phagocytosis by liver macrophages (Kupffer cells) and so promote HBV clearance (Lu et al., 2018). Moreover, anti-HBs antibodies can form immunocomplexes with HBsAg which bind to DCs to prime T cells (Yang et al., 2010). In addition to antibody production, B cells can act as professional antigen-presenting cells (APCs). Following exogenous peptide binding and recognition, B cells can present the Antigen-MHC-II complex to HBV-specific $CD4^+$ T cells to induce $CD4^+$ T-cell priming. Furthermore, B cells can cross-present HBcAg or HBsAg on MHC-I to HBV-specific $CD8^+$ T cells to induce antigen specific cytotoxic T-cell responses and hinder further immune tolerance (Barnaba et al., 1990; Lazdina et al., 2003). Finally, B cells can also regulate the adaptive immune response through antiviral cytokine secretion. B effector cells, a subset of B cells, induce pro-inflammatory cytokines such as IL-6, IFNγ, and TNF which trigger effector and memory $CD4^+$ T cells (Duddy et al., 2004; Shen & Fillatreau, 2015) and show non-cytolytic antiviral activity to eliminate HBV infected hepatocytes (Palumbo et al., 2015; Xia et al., 2016).

1.5 Vaccines

Vaccination represents a cost-effective and potent method to drastically and easily reduce the incidence of fatal diseases worldwide (Liljeqvist & Ståhl, 1999). Vaccines can be divided into the following subtypes: live attenuated, inactivated, subunit, DNA- and mRNA-based vaccines (Schiller & Lowy, 2015).

1.5.1 Protein vaccines

Protein vaccines are subunit vaccines that can be non-recombinant or recombinant. Non-recombinant subunit vaccines consist of bacterial polysaccharides or viral proteins of

pathogenic origin. These vaccines often need high-scale pathogen cultivation, and product purification and frequently require simultaneous adjuvants or conjugates to increase their immunogenicity (Liljeqvist & Ståhl, 1999). In contrast, recombinant subunit vaccines are produced in non-pathogenic organisms such as yeast. In 1986, the prophylactic Hepatitis B surface antigen vaccine (Valenzuela et al., 1982) produced in yeast was the first ever licensed recombinant subunit vaccine. In recombinant subunit vaccines, the gene of interest encoding the vaccine is first isolated from the pathogen and then transferred into a non-pathogenic organism for recombinant protein production. The advantages of protein vaccines are their defined and pathogen-free composition, safety, large-scale production in various hosts, easy administration, and their ability to induce strong humoral immunity with lifelong memory (Liljeqvist & Ståhl, 1999). The main disadvantages of recombinant subunit vaccines are low immunogenicity and high costs for protein purification. Low immunogenicity can be counteracted by repeated vaccinations and by using adjuvants (Felberbaum, 2015; Soema et al., 2015).

1.5.2 Viral vector vaccines

Viral vectors represent promising candidates for therapeutic vaccines as they are known to mediate antigen-specific cellular immune responses. For instance, MVA or adenovirus are intensively explored viral vector vaccines.

MVA is a highly attenuated viral vector derived from the vaccinia virus, which unmodified as a vaccine, has shown great success in smallpox eradication. Recombinant MVA is known to be safe and well-tolerated as it cannot replicate in human cells (Overton et al., 2015). MVA is highly immunogenic as it can induce both, strong cellular as well as humoral immune responses (Gilbert, 2013). It is often used in heterologous prime-boost vaccination regimens to boost the immune responses elicited by priming. Recombinant MVA is generated by intracellular homologous recombination of a vector plasmid expressing the desired antigens with an infectious wild-type MVA strain (Pavot et al., 2017). MVA efficacy as a vaccine candidate has been widely studied in clinical trials in the context of infectious diseases like tuberculosis or infections with human papillomavirus (HPV) (Corona Gutierrez et al., 2004; McShane et al., 2004) and even cancer (Harrop et al., 2006). Despite the induction of anti-vector immune responses, immunity can still be re-boosted after repeated recombinant MVA administration (Goepfert et al., 2011; Harrop et al., 2010).

Alternatively, adenoviruses also represent potent vaccine-delivery vehicles as they can elicit both innate and adaptive immune responses *in vivo*. Vector replication and vector-specific

mediated side effects can be hindered by the depletion of specific sequences of the viral genome. Adenoviruses represent attractive candidates for clinical use as they show broad tropism, and diverse application routes and are relatively thermostable. They are double-stranded, species-specific DNA viruses with a genome length of around 34-43 kb. Human adenovirus serotypes can be subdivided into six groups according to their sequence homology and ability to lyse erythrocytes (Tatsis & Ertl, 2004). It is assumed that adenoviruses activate the innate immune system via the expression of pathogen-associated molecular patterns (PAMPs) which bind to pathogen recognition receptors (PRRs) expressed on the surface of immature innate immune cells. Proinflammatory cytokines are being released and naïve antigen-presenting cells differentiate into professional antigen-presenting cells (Medzhitov & Janeway Jr, 2000). In the context of heterologous therapeutic vaccination for CHB, studies could show that adenoviruses were able to induce high-magnitude T-cell responses in mice both as a prime (Chinnakannan et al., 2020) or as a boost immunization (Chuai et al., 2013).

1.5.3 DNA vaccines

In 1990, Wolff et al. first demonstrated that the intramuscular injection of plasmid DNA resulted in significant expression of the encoded protein (Wolff et al., 1990). Several studies have shown that DNA plasmids can induce potent humoral (Tang et al., 1992) and cellular responses (Ulmer et al., 1993). DNA vaccines usually consist of plasmids encoding the antigens of interest and saline solution. For DNA vaccination first and new-generation DNA plasmids can be distinguished. First-generation plasmids carry prokaryotic elements such as a prokaryotic antibiotic resistance gene and a prokaryotic origin of replication for plasmid selection and replication after bacterial transformation (Faurez et al., 2010). Moreover, it is known that unmethylated CpG sequences, present on some DNA plasmids can lead to the activation of the innate immune system through TLR-9 signaling (Sato et al., 1996). This adjuvant effect may be beneficial in case of vaccination. However, prokaryotic sequences of DNA vaccines also have been shown to induce adverse effects both *in vitro* and *in vivo*. For instance, it has been reported that the expression of some antibiotic-resistance genes such as neomycin alters gene expression (Valera et al., 1994). Therefore, DNA plasmids lacking prokaryotic elements such as minicircles (Darquet et al., 1997) have been generated.

Intradermal and intramuscular delivery are the most common routes used for DNA plasmid immunization (Faurez et al., 2010). Intramuscular immunization with plasmid DNA primarily induces Th1 cells which stimulate cellular immune responses (Sin et al., 1999). However, within 90 minutes after intramuscular DNA injection, degradation of 95-99% of naked plasmid DNA by extracellular endonucleases could be observed in mice (Barry et al., 1999). Electroporation or high-pressure liquid injection may represent promising alternatives to

overcome this hurdle (Sheets et al., 2006; Widera et al., 2000). Next, naked plasmid DNA needs to overcome three obstacles to enable the expression of the genes of interest and so elicit an immune response. First, plasmid DNA needs to cross the plasma membrane, then the cytoplasm, and finally the nuclear barrier. Plasmid DNA can enter the nucleus in two possible ways: i) through nuclear membrane disassembly in dividing cells or ii) by crossing the intact nuclear barrier through passive diffusion via the nuclear pore complexes (Ludtke et al., 2002). Although DNA vaccines were safe, well-tolerated, and immunogenic, suboptimal efficacy has been shown in clinical trials (Kutzler & Weiner, 2008). Today, potential DNA integration into the host genome represents the major concern against broad plasmid DNA vaccine administration in humans (Faurez et al., 2010).

1.5.4 mRNA vaccines

Nucleic acid vaccines consisting of messenger RNA (mRNA) may represent a new era in vaccine technologies as they have the potential to overcome the limitations of viral-vector and DNA-based vaccines. mRNA vaccines can be subdivided into conventional mRNA vaccines and self-amplifying mRNA vaccines which derive from positive-strand RNA viruses (Zhang et al., 2019). In 1990, intramuscular mRNA injection in mice resulted for the first time in the production of the encoded protein and elicited immune responses against the encoded antigen (Martinon et al., 1993; Wolff et al., 1990). Nowadays mRNA can be produced synthetically through a cell-free enzymatic *in vitro* transcription reaction. Essential components for mRNA vaccine production are either a linearized plasmid DNA or polymerase chain reaction (PCR) derived template for mRNA transcription harboring a T7 or SP6 Promotor, a recombinant polymerase, and nucleoside triphosphates. Finally, a cap structure and a poly-A tail are enzymatically added to form a mature mRNA construct (Zhang et al., 2019). Various studies have demonstrated mRNA-induced antigen-specific immune responses followed by intramuscular (Wolff et al., 1990), intradermal (Granstein et al., 2000), subcutaneous, intravenous (Martinon et al., 1993), intranodal (Kreiter et al., 2010) injections and administration via gene gun (Qiu et al., 1996).

mRNA vaccines offer several advantages over DNA vaccines. First, in contrary to DNA vaccines, mRNA vaccines cannot integrate into the host's genome and therefore carry no risk of insertional mutagenesis. Second, mRNA vaccines do not need to cross the nuclear barrier as they are translated directly into the cytoplasm (Ulmer et al., 2012). Moreover, in contrast to DNA vaccines which show persistent antigen expression for a long period, antigen expression of mRNA vaccines peaks and declines rapidly after administration (Probst et al., 2007). Following injection, the mRNA is exposed to endonucleases, the tissue RNAses, which

degrade the vaccine and thus limit its uptake by cells (Probst et al., 2006). Moreover, aberrant RNA polymerase activities can lead to the production of double-stranded RNAs (dsRNAs) which inhibit translation and degrade mRNA thus decreasing protein expression and antigen presentation. Therefore, dsRNAs need to be removed to increase translation yield and vaccine potency (Kariko et al., 2011). mRNA uptake takes place via receptor-mediated endocytosis and involves membrane domains rich in caveolae and lipid rafts (Lorenz et al., 2011). Upon internalization, mRNA vaccines are translated into proteins in the cytoplasm of the cells. Next, the produced antigens are presented by MHC class I and II to APCs to induce T-cell responses (Ulmer et al., 2012). It is known that mRNA strongly stimulates the innate immune system through the engagement of pattern recognition receptors. This mechanism potentiates antigen-specific immune responses (Karikó et al., 2004). Although naked mRNA vaccines have been shown to elicit immune responses, the presence of RNAses hinders the internalization of large amounts of mRNA by cells. mRNA hydrolysis can be hindered by efficient encapsulation in liposomes (Martinon et al., 1993) or complexation with cationic polymers (Scheel et al., 2005). It has been shown that modified and encapsulated in lipid nanoparticles, mRNA can work as an adjuvant itself and induce potent Tfh cells and B cells producing high affinity neutralizing antibodies (Pardi, Hogan, Naradikian, et al., 2018). In addition, chemical modifications to the 5' cap structure, the untranslated regions, or to single codons can be implemented to increase the stability, integrity, and expression of the mRNA construct itself (Pascolo, 2008). Incorporation of nucleoside modifications such as pseudouridine (φ) or 5-methylcytidine (m^5C) prevents recognition from innate immune sensors thereby enhancing protein translation.

In addition, mRNA vaccines represent a potent therapeutic approach in times of a pandemic as they can be easily generated and produced at a large scale in a short period of time compared to conventional vaccines. For instance, mRNA vaccine technology has been extensively tested in patients with Covid-19 disease. Phase III clinical results showed 95% effectivity of the mRNA-based BioNTech/Pfizer (BNT162b2) vaccine against SARS-CoV-2 infection. The vaccine was shown to be safe and well-tolerated over time (Polack et al., 2020).

2 Aims of the study

Induction of a strong and functional HBV-specific B and T cell response by a therapeutic vaccine is a promising strategy to eliminate cccDNA and thereby achieve clearance of CHB in patients.

Our laboratory previously developed a therapeutic hepatitis B vaccine, termed *TherVacB*, which is based on two protein immunizations using adjuvanted, particulate, recombinant HBV S and core antigens (HBsAg, HBcAg) and a boost using the MVA-HBVac vector expressing the same HBV antigens plus the HBV L protein and the reverse transcriptase. The aim of this study was to improve the *TherVacB* regimen by using alternative vaccine components for priming to increase vaccine efficacy against a broad range of HBV genotypes and serotypes.

We wanted to compare genetically engineered DNA vaccines and mRNA-based vaccines producing the antigens of interest directly *in vivo*, circumventing the need for the time-consuming and expensive production and purification of the recombinant proteins *in vitro* and allowing the inclusion of several variants of vaccine antigens. Therefore, this study aimed to compare mRNA and plasmid DNA-based vaccines to the established recombinant protein-based vaccine components for priming in the *TherVacB* regimen.

The first part of this study aimed at generating *DNA-HBVac*, a DNA-based vaccine encoding the HBVac insert from the MVA-boost vector, which contained optimized sequences of HBV core, S, L, and RT proteins, thereby covering the most common HBV genotypes and serotypes. Next, we aimed to evaluate the immunogenicity of *DNA-HBVac* as a prime in wild-type and AAV-HBV transduced mice and establish the optimal immunization protocol for *DNA-HBVac*. Immune responses contributing to successful DNA immunization should be analyzed, such as the induction of neutralizing antibodies, the potency of $CD4^+$/$CD8^+$ T-cell responses, and the antiviral effect.

The second part of this study focused on the generation of *RNA-HBVac*, an mRNA-based vaccine encoding the identical HBVac insert as the *DNA-HBVac*. First, vaccine generation, stability, integrity, and implementation of chemical modifications to enhance protein expression should be established by generating different *RNA-HBVac* constructs and testing them *in vitro*. Since RNA vaccines are known to require adequate formulation to induce strong protein expression *in vivo*, safety and the optimal formulation should be evaluated in wild-type mice. Lipid nanoparticle (LNP) formulated *RNA-HBVac* should be titrated, and its efficacy *in vivo* needed to be determined. Finally, the therapeutic efficacy of the novel heterologous LNP-formulated or non-formulated naked *RNA-HBVac* prime combined with a recombinant *MVA-HBVac* booster immunization protocols should be tested in an HBV-carrier mouse model and compared to the *DNA-HBVac* prime using the well-established protein prime – MVA boost regimen (*TherVacB*).

3 Results

3.1 DNA-based therapeutic hepatitis B vaccine: *DNA-HBVac*

To optimize and broaden the efficacy of the *TherVacB* regimen for future clinical application, an optimal priming strategy is required. Therefore, the following studies aim at improving *TherVacB* prime immunizations by investigating the efficacy of a DNA or mRNA prime compared to a protein prime in wild-type as well as in a persistent HBV replication mouse model.

3.1.1 Generation of *DNA-HBVac* for *TherVacB* priming

Although immunization with plasmid DNA has been shown to elicit strong and potent humoral and cellular immune responses in animals (Donnelly et al., 1997), DNA vaccines induce only limited immunogenicity in various clinical trials up to date (MacGregor et al., 1998; Wang et al., 1998). Numerous approaches have been developed to enhance the immunogenicity of DNA vaccines. Several studies have shown that vaccine efficacy can be improved by employing a DNA prime and a viral vector boost vaccine regimen (Asbach et al., 2016). Priming with DNA before boost-immunization with a viral vector has repeatedly been shown to elicit stronger cellular and humoral immune responses than immunization with respective DNA or viral vector alone (Casimiro et al., 2003; Girard et al., 2011; Mascola et al., 2005). In addition, the optimization of regulatory elements present in the plasmid backbone represents a promising strategy to augment the immunogenicity of DNA vaccines (Barouch et al., 2005). Several studies in mice and monkeys indicate that cellular immune responses against viral antigens can be increased by adding the regulatory R region of the 5' long terminal repeat of the human T-cell leukemia virus type 1 (HTLV-1) to the cytomegalovirus (CMV) enhancer/promoter (Barouch et al., 2005). CMV enhancer/promoter is often used in vaccine development to induce high expression levels of a transgene in mammalian cells (Ulmer et al., 1993; Xu et al., 1998). HTLV-1 is known to be both a transcriptional and posttranscriptional enhancer (Takebe et al., 1988). This strategy results in increased gene expression and, as a consequence, better antigen expression which may facilitate antigen presentation *in vivo* leading to the induction of a more potent and polyfunctional immune response.

To test this hypothesis a novel DNA vaccine (*DNA-HBVac*) based on a DNA plasmid (pURVac, Prof. Ralf Wagner, Hospital Regensburg, Germany) encoding a HTLV-1 region between the CMV promoter and the HBVac insert was constructed in our laboratory by Dr. Martin Kächele. The HBVac insert was integrated into the multiple cloning site of the pURVac plasmid by cloning. For this purpose, pURHBVac was first enzymatically digested with the enzymes SalI and Eco72I and the digested plasmid was cleaned up via gel electrophoresis. Next, the HBVac insert was amplified via PCR from the original pURVac plasmid. The primers used for

amplification contained the necessary overlapping sequences for later Infusion cloning (Fw: 5‘-CGGTACCGTCGACACGTGGGCGCGCCAGATCTGAGC-3‘; Rev: 5‘-TCTAGATGATCACACGTGTTAATTAAAGATCTAAGCTTACGCG-3‘). The PCR product was purified by gel electrophoresis and then integrated into the digested plasmid by ligation. The successful insertion of HBVac into pURVac plasmid was analyzed by restriction digestion. The characteristic band of 4257 bp, corresponding to the HBVac insert could be observed on the agarose gel. Finally, the correct sequence of the HBVac insert was confirmed by Sanger sequencing. The HBVac expression cassette encodes for five HBV proteins (S(Small) serotype *adw*, genotype A2; C-terminally truncated $Core_{1-149}$ serotype *ayw*, genotype D; the consensus sequence of the RT domain of the viral polymerase RT(pol); L/S(Large) serotype *ayw*, genotype C and full-length $Core_{1-183}$ from genotype C). To allow equimolar expression, HBV proteins are linked via porcine teschovirus-1 2A (P2A) (Luke et al., 2008) and thosea asigna virus 2A (T2A) (Szymczak & Vignali, 2005) gene sequences. The protein sequences cover T-cell epitopes of genotype A-E and the serotypes *adw* and *ayw* to enable global application of the therapeutic vaccine (Fig. 3.1).

Figure 3.1 Gene expression cassette of the *HBVac* insert
Scheme of HBVac insert expressing HBV small (serotype *adw2*, genotype A2) and large (serotype *ayw*, genotype C) envelope proteins (S and L/S, respectively), truncated (serotype *ayw*, genotype D) and full-length (serotype *adw*, genotype C) HBV core ($Core_{1-149}$ and $Core_{1-183}$, respectively proteins as well as the consensus sequence of the RT domain of the HBV polymerase (RT(pol)) linked by P2A and T2A sequences.

To ensure the functionality of the generated *DNA-HBVac* plasmid, HepG2 (Human hepatoma cell line) cells were transfected with 1 µg *DNA-HBVac*. Untransfected HepG2 cells served as a control (Ctrl). The expression of HBV proteins was confirmed by Western blot (WB) analysis of cell lysate using S-, Core- or RT-specific antibodies (Fig. 3.2). HBs(S) and HBs(L) proteins were detected at 24 kDa and 42 kDa respectively in native and glycosylated forms. Truncated and full-length core proteins were detected at 19 kDa and 21 kDa, respectively. RT(pol) was detected at 37 kDa. None of the HBV proteins could be detected in the controls.

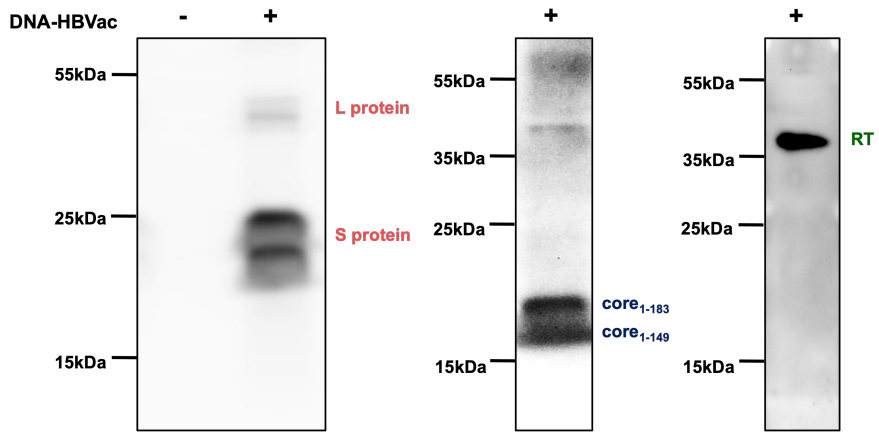

Figure 3.2 Expression of HBsAg, HBcAg, and RT(pol) in HepG2 cells 24h after transfection with *DNA-HBVac*
HepG2 cells were transfected with 1 µg of *DNA-HBVac* using Lipofectamine transfection reagent. Untransfected HepG2 cells served as a control. Cell lysates were separated and WB analysis was performed using HBsAg-, HBcAg-, and RT(pol)-specific antibodies. HBs(S) and HBs(L) proteins were detected around 24 kDa and 42 kDa respectively in naïve and glycosylated forms. Truncated and full-length core proteins were detected HBc at 19 kDa and 21 kDa, respectively. RT(pol) was detected at 37 kDa.

WB analysis confirmed that all encoded proteins of the HBVac insert are being correctly expressed by the new DNA vaccine, demonstrating the successful generation of *DNA-HBVac*.

3.1.2 Evaluation of DNA prime – MVA boost immunogenicity in HBV-naïve mice

To investigate whether immunization with *DNA-HBVac* can prime significant HBV-specific humoral and cellular immune responses, we evaluated the immunogenicity of *DNA-HBVac* in HBV-naïve mice. As depicted in Figure 3.3, C57BL/6 mice underwent two i.m. immunizations spaced two weeks apart, using 50 µg *DNA-HBVac* (D-50), 100 µg *DNA-HBVac* (D-100), or adjuvanted recombinant particulate antigens (comprising 10 µg HBsAg + 10 µg HBcAg + 15 µg CpG-1018 (P)). At week 4 a booster immunization with recombinant *MVA-HBVac* (3×10^7 IFU/mouse) was administered. Mice that received PBS injections were included as controls. At week 5, mice were sacrificed for the assessment of HBV-specific antibody and splenic T-cell responses.

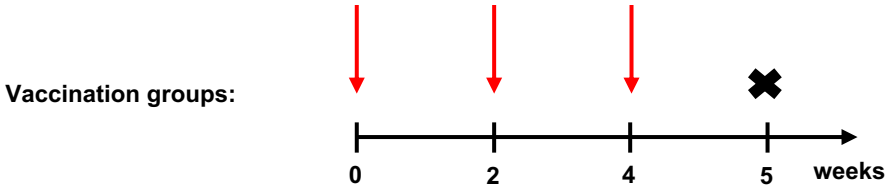

1)	**PBS**	PBS	PBS	PBS
2)	**HBsAg + HBcAg + CpG (P)**	P	P	*MVA-HBVac*
3)	**50 µg DNA-HBVac (D-50)**	D-50	D-50	*MVA-HBVac*
4)	**100 µg DNA-HBVac (D-100)**	D-100	D-100	*MVA-HBVac*

Figure 3.3 Immunogenicity of *DNA-HBVac* prime – MVA boost in HBV-naïve mice
Nine weeks old male C57BL/6 mice were i.m. immunized three times (red arrows) in a two-week interval (week 0, week 2, and week 4 respectively). All animals received two prime immunizations consisting of either 10 µg HBsAg + 10 µg HBcAg + 15 µg CpG-1018 (P) or *DNA-HBVac* in 50 µg or 100 µg dose (D-50 and D-100 respectively) followed by a final boost immunization with *MVA-HBVac* (3×10^7 IFU/mouse) at week 4. Mice receiving PBS served as controls. Splenectomy and final analysis were performed in week 5.

a. Evaluation of the humoral and CD4$^+$ T-cell response

The induction of HBV-specific antibodies as well as HBV-specific CD4$^+$ T-cell responses were evaluated. To assess the humoral response, anti-HBs and anti-HBc titers were detected by ELISA in the serum of mice at week 5. Immunization of mice from all three experimental groups induced anti-HBs titers. However, immunization of mice with adjuvanted protein antigens (P) resulted in significantly higher (*$p<0.05$) anti-HBs titers than those elicited by both *DNA-HBVac* groups. Comparison of the anti-HBs antibody levels between the groups of mice vaccinated with *DNA-HBVac* showed that a higher dose of *DNA-HBVac* was not able to induce stronger anti-HBs titers (Fig. 3.4 A). Evaluation of antibody responses in mice showed that immunization with *DNA-HBVac* (D-50 and D-100 groups) induced similar anti-HBc titers compared to immunization with HBsAg + HBcAg (Fig. 3.4 B). As predicted anti-HBc and anti-HBs titers from mice immunized with PBS as a control, remained at baseline levels.

Next, the induction of HBV-specific CD4$^+$ T-cell responses after immunization with *DNA-HBVac* was analyzed by intracellular IFNγ-staining of HBV-peptide stimulated splenocytes at the timepoint of sacrifice. As shown in Fig. 3.4 C, vaccination with a low dose of *DNA-HBVac* (D-50) led to a lower S-specific CD4$^+$ T-cell response compared to the protein antigen group (P). In contrast, a high dose of *DNA-HBVac* (D-100) resulted in a comparable S-specific CD4$^+$ T-cell response. All experimental groups elicited strong Core-specific CD4$^+$ T-cell responses. Immunization with *DNA-HBVac*, D-100 group displayed a trend of slightly stronger Core-specific CD4$^+$ T-cell response compared to the protein antigen group (Fig. 3.4 D). In addition, vaccination with *DNA-HBVac* (50 µg or 100 µg dose) led to a considerably higher (*$p<0.05$) percentage of IFNγ$^+$ RT(Pol)-specific CD4$^+$ T cells in the spleen, compared to those detected

in the protein antigen group (Fig. 3.4 E). As expected, mice immunized with PBS as a negative control did not show S-, Core- or RT-specific CD4$^+$ T-cell responses in the spleen.

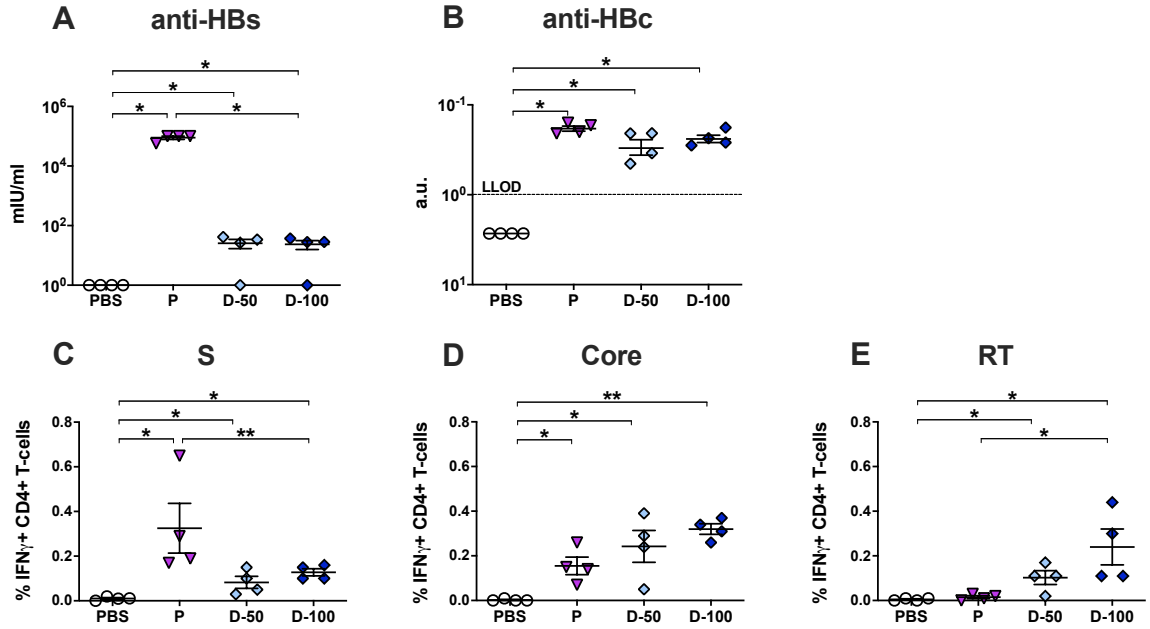

Figure 3.4 HBV-specific antibody and CD4$^+$ T-cell responses
Serum levels of (A) anti-HBs and (B) anti-HBc titers were detected at week 5. HBV S- (C), Core- (D), and RT (E)-specific IFNγ responses of *ex vivo* stimulated splenic CD4+ T cells determined by intracellular cytokine staining (ICS). Mean±SEM is shown. Statistical analysis was performed using nonparametric One-Way ANOVA. Symbols represent individual mice. Values of individual mice are shown. Asterisks indicate statistically significant differences (*p<0.05, **p<0.005). a.u.- arbitrary units; LLOD – lower limit of detection.

Taken together, these results indicate that immunization with *DNA-HBVac* elicits low anti-HBs and comparable anti-HBc titers compared to priming with protein antigens (HBsAg + HBcAg). The magnitude of core- and RT-specific CD4$^+$ T-cell responses were higher in mice receiving *DNA-HBVac* for prime immunization compared to the protein antigen group. An increase in the DNA dose for priming resulted in slightly higher HBV-specific CD4$^+$ T-cell responses.

b. Evaluation of HBV-specific CD8$^+$ T-cell response

Next, HBV-specific splenic CD8$^+$ T-cell responses elicited by DNA vaccination with *DNA-HBVac* were analysed by intracellular IFNγ-staining of *ex vivo* stimulated splenocytes one week after booster immunization. Splenocytes were stimulated *ex vivo* overnight with HBV S- and Core-specific peptide pools as well as with HBV-specific peptides S190, S208, and RT86. Splenocytes isolated from mice immunized with PBS served as negative controls. The magnitude of S-specific CD8$^+$ T cells detected in the spleens of mice vaccinated with protein antigens was comparable to *DNA-HBVac* groups. Immunization with a higher dose of *DNA-*

HBVac (D-100) did not result in a dose-dependent increase in the percentages of S-specific IFNγ^+ CD8$^+$ T cells in spleens (Fig. 3.5 A).

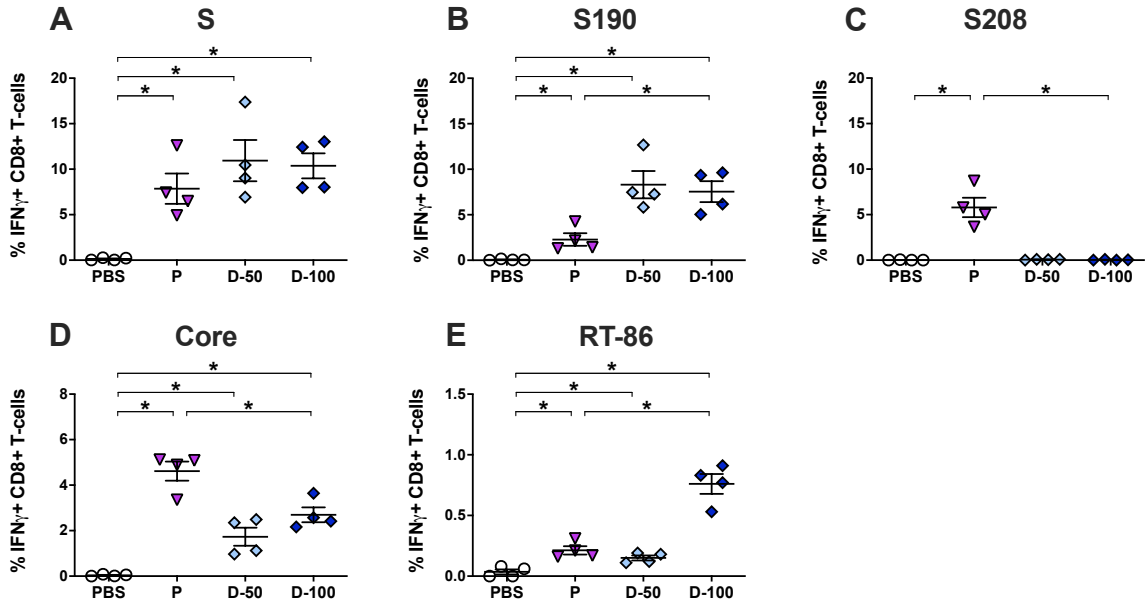

Figure 3.5 HBV-specific CD8$^+$ T-cell responses
(A) HBV S-specific IFNγ response of splenic CD8$^+$ T cells determined by ICS following *ex vivo* stimulation with overlapping HBV S-specific peptide pool and with HBV peptides (B) S190 and (C) S208. (D) Core-specific IFNγ responses of splenic CD8$^+$ T cells determined by ICS following *ex vivo* stimulation with HBV peptides. Flow-cytometry analysis of intracellular cytokine staining of CD8$^+$ T cells after *ex vivo* stimulation with HBV peptide (E) RT86. Mean±SEM is shown. Statistical analysis was performed using nonparametric One-Way ANOVA. Symbols represent individual mice. Asterisks indicate statistically significant differences (*p<0.05).

IFNγ responses after stimulation of splenic CD8$^+$ T cells with S-specific peptides S190 and S208 were further examined. It is described that S190 peptide is generated from endogenously expressed HBsAg whereas S208 peptide is generated from exogenously expressed HBsAg (Schirmbeck et al., 2003). As expected, immunization with 50 µg or 100 µg *DNA-HBVac* elicited robust and similar S190-specific CD8$^+$ T-cell responses compared to priming with HBsAg + HBcAg. This observation in the S190-specific CD8$^+$ T-cell response was statistically significant (*p<0.05) (Fig. 3.5 B). In addition, in contrast to S190-specific T cells, splenic S208-specific CD8$^+$ T-cell responses were mainly detected in mice immunized with protein antigens, implying that S-specific CD8$^+$ T-cell responses elicited by immunization with recombinant protein anitgens is mostly S208-specific (*p<0.05). Immunization with *DNA-HBVac*, however, resulted in baseline frequencies of S208-specific CD8$^+$ T-cell responses (Fig. 3.5 C). Priming with protein antigens elicited high percentages of Core-specific IFNγ^+ CD8$^+$ T cells in spleens (Median 4.990 %) compared to *DNA-HBVac* groups (Median 2.385 %) (**p<0.05). An increase of *DNA-HBVac* up to 100 µg showed a slight trend of the induction of stronger Core-specific CD8$^+$ T-cell response (Fig. 3.5 D). As expected, the frequencies of RT-specific IFNγ^+ CD8$^+$ T

cells in the spleens of mice vaccinated with *DNA-HBVac* were significantly higher compared to those elicited by protein antigens or PBS groups as these did not prime RT-specific immunity (Fig. 3.5 E). IFNγ response of splenocytes previously stimulated with RT86 peptide was significantly higher in the spleens of mice vaccinated with 100 µg *DNA-HBVac* compared to 50 µg *DNA-HBVac*. Stimulation of splenocytes isolated from mice receiving PBS immunization with S- and Core-specific peptide pools and with HBV peptides S190, S208, and RT86 did not elicit IFNγ responses.

These findings clearly demonstrate that prime immunization with *DNA-HBVac* effectlively primes S-, Core- and RT-specific $CD8^+$ T-cell responses. *DNA-HBVac* induced high frequencies of HBV S- and RT-specific $CD8^+$ T-cell responses in spleens of vaccinated mice compared to priming with recombinant HBsAg + HBcAg. For *DNA-HBVac* groups, HBV S-specific $CD8^+$ T-cell responses were mostly S190 peptide-specific. Moreover, *DNA-HBVac* dose of 100 µg showed to be crucial to induce a strong, significant, and functional RT-specific $CD8^+$ T-cell response. These observations highlight the importance of prime immunization to induce broad, strong, and polyfunctional $CD8^+$ T-cell responses against HBV peptides. Therefore 100 µg *DNA-HBVac* was considered as the optimal dose for further studies in persistent HBV replication mouse model (AAV-HBV).

3.1.3 Evaluation of the immunogenicity of *DNA-HBVac* in HBV carrier mice

Following immunogenicity and optimal dose evaluation of *DNA-HBVac* for priming in HBV-naïve mice, immune responses elicited by *DNA-HBVac* priming in a persistent infection mouse model (AAV-HBV) were assessed. As shown in Fig. 3.6 nine-week-old C57BL/6 mice were i.v. transduced with AAV-HBV to establish persistent HBV replication. Starting at week 0, mice underwent two rounds of prime immunizations, spaced two weeks apart. The immunizations included adjuvanted HBsAg (referred to as S), a mixture of adjuvanted recombinant particulate protein anitgens (HBsAg and HBcAg, (P)), or *DNA-HBVac* at doses of 50 µg (D-50) or 100 µg (D-100). A booster immunization with MVA-HBVac ($3x10^7$ IFU *MVA-HBVac*/mouse) was administered two weeks later, at week 4. Mice receiving PBS were included as the control group. Six weeks after the onset of the vaccination mice were sacrificed and analyzed.

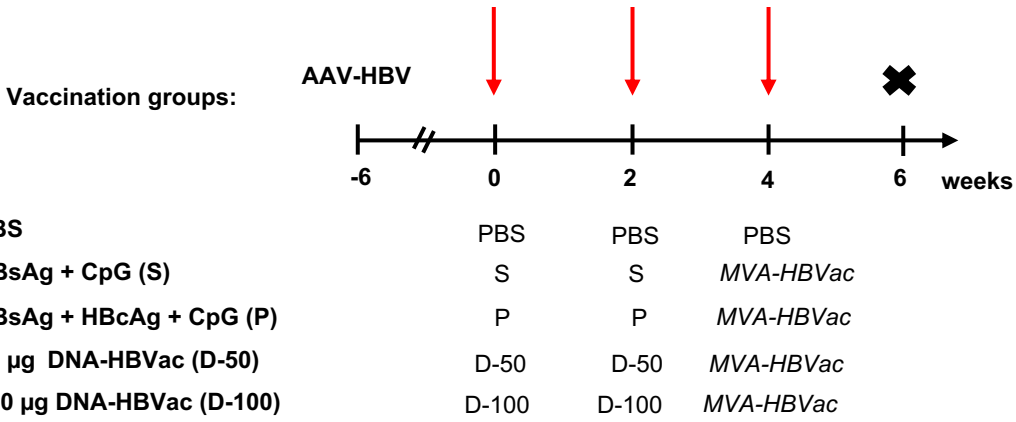

Figure 3.6 Immunogenicity of prime immunization with *DNA-HBVac* in AAV-HBV transduced mice
Nine weeks old C57BL/6 mice were i.v. transduced with AAV-HBV to establish persistent HBV replication. Six weeks later, mice were i.m. immunized three times (red arrows) in a two-week interval (week 0, week 2, and week 4 respectively). All animals received two prime immunizations consisting of either 10 µg HBsAg + 15 µg CpG (S), 10 µg HBsAg + 10 µg HBcAg + 15 µg CpG (P) or *DNA-HBVac* (50 µg or 100 µg) (D-50 and D-100 respectively) followed by a final booster immunization with *MVA-HBVac* (3×10^7 IFU/mouse) at week 6. Mice receiving PBS served as controls. The final analysis was performed in week 6.

a. Effects of prime immunization with *DNA-HBVac* on HBV-specific B-cell and CD4$^+$ T-cell responses in HBV carrier mice

To evaluate the effect of prime immunization with *DNA-HBVac* on HBsAg levels and anti-HBs antibody production in the sera of mice, HBsAg levels were monitored before and at the endpoint of the experiment, and anti-HBs antibody titers were assessed at week 6.

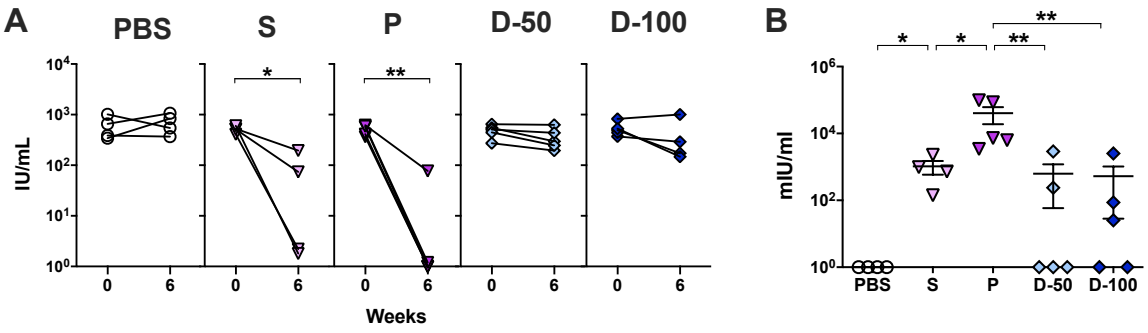

Figure 3.7 Serum HBsAg levels and anti-HBs titers induced by immunization with *DNA-HBVac* in HBV carrier mice
(A) Serum HBsAg levels before (week 0) and after (week 6) therapeutic vaccination. (B) Serum levels of anti-HBs titers at week 6. Mean±SEM is shown. Statistical analysis was performed using nonparametric One-Way ANOVA. Symbols represent individual mice. Values of individual mice are shown. Asterisks indicate statistically significant differences (*p<0.05, **p<0.005).

While a significant 3-log reduction in HBsAg levels could be observed in the sera of mice vaccinated with recombinant proteins (S and P groups), immunization with 100 µg *DNA-HBVac* resulted in a minor 1-log decrease in serum HBsAg levels. In D-50 group HBsAg levels

remained similar throughout the whole experiment similar to the control (Fig. 3.7 A). Next, the impact of priming with *DNA-HBVac* on anti-HBs production was assessed by detection of anti-HBs antibodies in the sera of mice at week 6. As depicted in Fig. 3.7 B, barely detectable anti-HBs titers could be detected in some animals primed with *DNA-HBVac*. In contrast, mice primed with recombinant proteins (S and P groups) showed more robust expression levels of anti-HBs titers in the sera of all mice, with 2-fold higher levels for the mixed protein antigen group (P) compared to DNA priming (*p<0.05). Immunization of control mice with PBS did not induce any anti-HBs antibodies. Taken together anti-HBs titers correlated with the minor drop in HBsAg levels observed in mice vaccinated with *DNA-HBVac*.

To evaluate $CD4^+$ T-cell responses elicited in livers and spleens by priming with *DNA-HBVac,* intracellular IFNγ staining of HBV peptide-stimulated splenocytes and liver-associated lymphocytes (LALs) was performed at week 6.

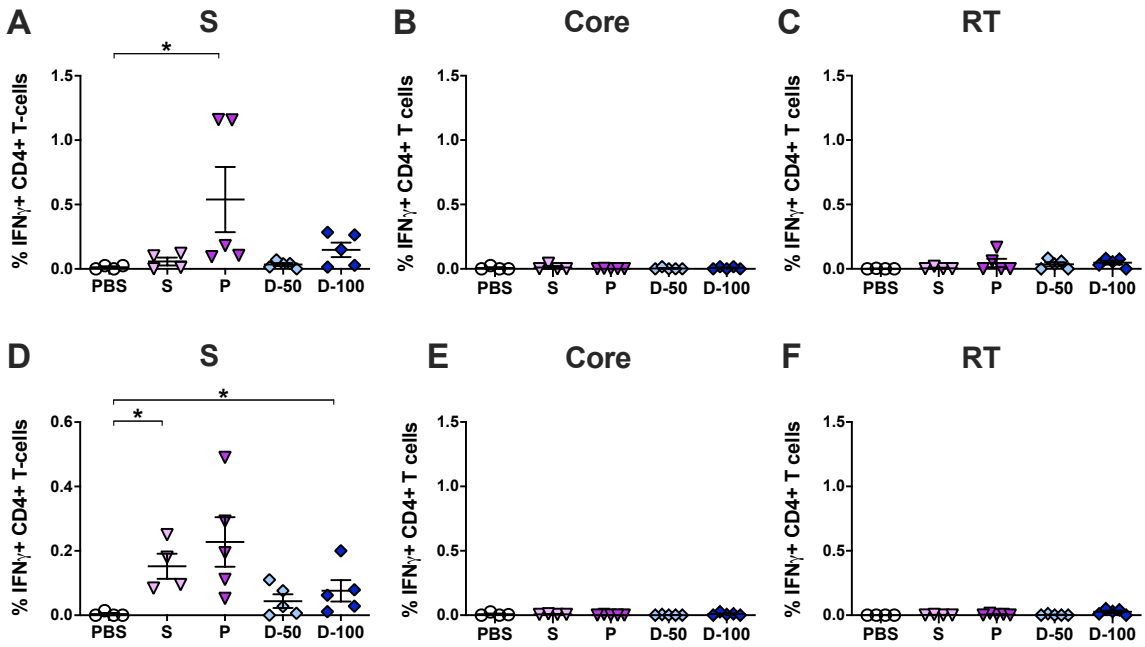

Figure 3.8 $CD4^+$ T-cell responses induced by immunization with *DNA-HBVac* in livers and spleens of HBV carrier mice
HBV-specific IFNγ responses of $CD4^+$ T cells determined by ICS following *ex vivo* stimulation with overlapping HBV S-, Core- and RT-specific peptide pools in livers (A-C) and spleens (D-F). Mean±SEM is shown. Statistical analysis was performed using nonparametric One-Way ANOVA. Symbols represent individual mice. Values of individual mice are shown. Asterisks indicate statistically significant differences (*p<0.05).

Priming with *DNA-HBVac* (D-50 and D-100 groups) elicited barely detectable but comparable S-specific $CD4^+$ T-cell responses in livers and spleens. In contrast, employing adjuvanted mixed HBsAg and HBcAg (P) for priming induced S-specific $CD4^+$ T-cell responses in livers

(Fig. 3.8 A) and spleens (Fig. 3.8 D) of immunized mice. In all experimental groups, no Core- (Fig. 3.8 B, E) and RT-specific (Fig. 3.8 C, F) $CD4^+$ T-cell responses could be detected in livers (Fig. 3.8 B, C) and spleens (Fig. 3.8 E, F). As expected, vaccination of control mice with PBS did not stimulate any S-, Core, or RT-specific $CD4^+$ T-cell responses.

The absence of significant anti-HBs generation resulted in a lack of decrease of serum HBsAg levels correlating with HBV-specific $CD4^+$ T-cell responses in livers and spleens.

b. Effects of prime immunization with *DNA-HBVac* on HBV-specific $CD8^+$ T-cell responses in HBV carrier mice

Studies have shown that vigorous $CD8^+$ T-cell responses are crucial to clear viral infection. Therefore, the magnitude of $CD8^+$ T-cell responses is essential to determine whether individuals will resolve acute HBV infection or progress toward CHB (Fisicaro et al., 2009; Phillips et al., 2010; Ye et al., 2015). To assess whether heterologous *DNA-HBVac* vaccination can break immune tolerance against HBV antigens, $CD8^+$ T-cell responses were analyzed at the endpoint. To evaluate antigen-specific $CD8^+$ T cells elicited by vaccination with *DNA-HBVac*, LALs, and splenocytes were stained *ex vivo* with S- and Core-specific multimers S190 and C93, respectively.

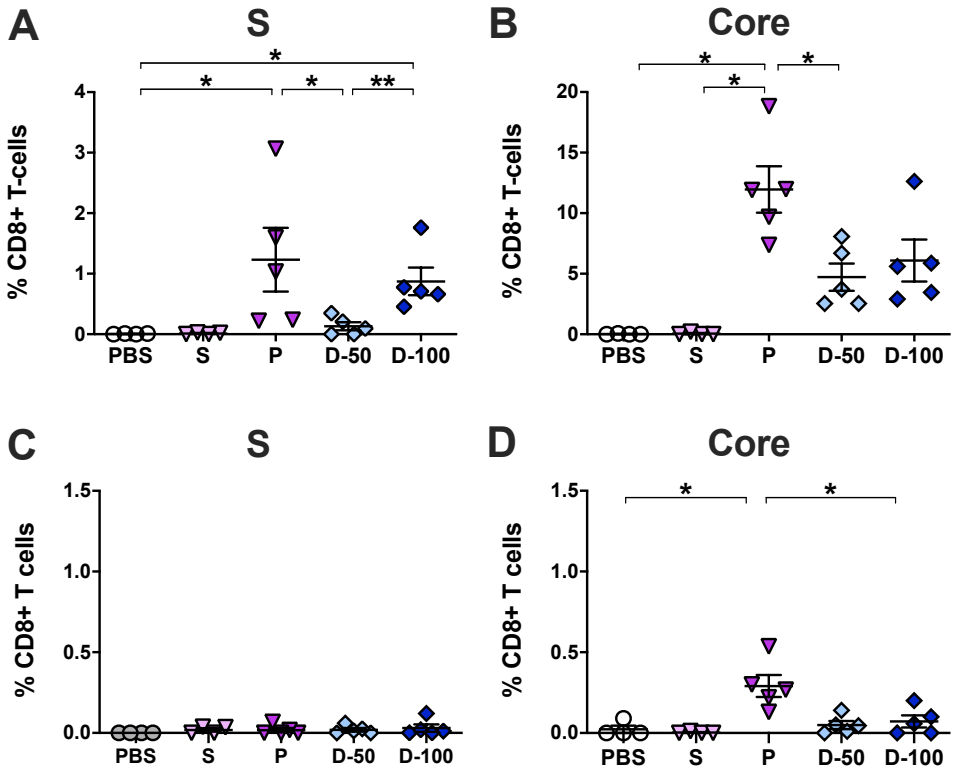

Figure 3.9 Induction of antigen-specific $CD8^+$ T cells by DNA-based therapeutic vaccination in HBV carrier mice

Frequencies of (A) S190- and (B) C93-antigen specific $CD8^+$ T cells in the liver determined by multimer staining of LALs. Frequencies of (C) S190- and (D) C93-antigen specific $CD8^+$ T cells in the spleen

determined by multimer staining of splenocytes. Mean±SEM is shown. Statistical analysis was performed using nonparametric One-Way ANOVA. Symbols represent individual mice. Values of individual mice are shown. Asterisks indicate statistically significant differences (*p<0.05, **p<0.005).

Immunization with 100 µg *DNA-HBVac* resulted in strong and similar S190-specific CD8$^+$ T-cell response in the liver compared to the mixed protein antigen (P) group. By contrast, priming with 50 µg *DNA-HBVac* induced barely detectable intrahepatic S190-specific CD8$^+$ T cells (Fig. 3.9 A). Immunization with *DNA-HBVac* (D-50 and D-100 groups) led to significant induction of intrahepatic C93-specific CD8$^+$ T cells ranging from 2.5 % to 12.6 % (mean 5.4 %) compared to 7.4 % to 18.9 % (mean 12.0 %) for mice immunized with adjuvanted mixed HBsAg and HBcAg (P). Unexpectedly, the magnitude of C93-specific CD8$^+$ T cells in the liver did not increase in the group of mice that received a higher dose of *DNA-HBVac* (D-100) (Fig. 3.9 B). In contrast to the high frequencies of antigen-specific CD8$^+$ T cells observed in the livers of mice immunized with *DNA-HBVac*, frequencies of splenic S190- (Fig. 3.9 C) and C93-specific (Fig. 3.9 D) CD8$^+$ T cells remained at baseline level. These observations indicate that antigen-specific CD8$^+$ T cells elicited by vaccination with *DNA-HBVac* predominantly remain in the liver to kill infected hepatocytes and control viral spread.

Next, functional analysis of S-, Core- and RT-specific CD8$^+$ T cells was performed by intracellular IFNγ staining of *ex vivo* stimulated LALs and splenocytes with overlapping HBV peptide pools as well as single HBV peptides.

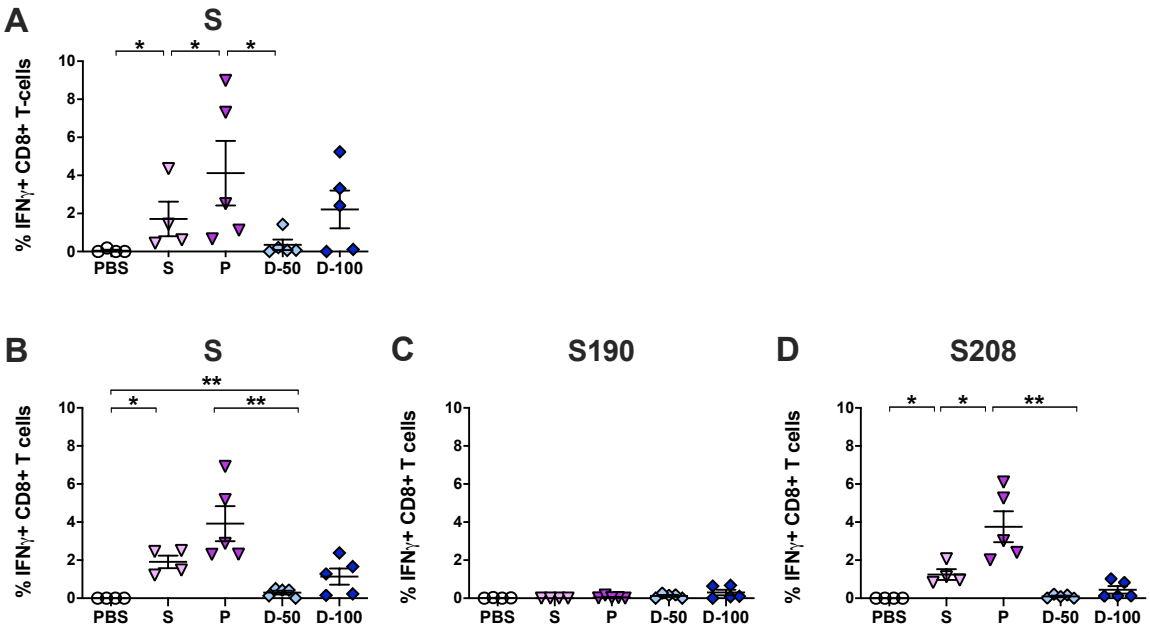

Figure 3.10 Functional analysis of S-specific CD8$^+$ T cells elicited by vaccination with *DNA-HBVac* in livers and spleens of HBV carrier mice
Percentages of (A) S-specific IFNγ^+ CD8$^+$ T cells in the liver determined by intracellular IFNγ staining following *ex vivo* stimulation with overlapping S-specific peptide pool. Percentages of (B) S-, (C) S190- and (D) S208-specific IFNγ^+ CD8$^+$ T cells in the spleen determined by intracellular IFNγ staining

following *ex vivo* stimulation with overlapping S-specific peptide pool and HBV peptides S190 and S208. Mean±SEM is shown. Statistical analysis was performed using nonparametric One-Way ANOVA. Symbols represent individual mice. Values of individual mice are shown. Asterisks indicate statistically significant differences (*p<0.05, **p<0.005).

As shown in Fig. 3.10 A and B, S-specific IFNγ^+ CD8$^+$ T cells were detectable in (A) livers and (B) spleens of mice immunized with recombinant protein antigens (S and P groups) as well as those receiving *DNA-HBVac* (D-50 and D-100 groups). Vaccination with 50 µg *DNA-HBVac* induced barely detectable S-specific IFNγ^+ CD8$^+$ T cells in livers (Fig. 3.10 A) and spleens (Fig. 3.10 B) compared to priming with 100 µg *DNA-HBVac*, implying that 100 µg *DNA-HBVac* are necessary to elicit strong and significant frequencies of S-specific IFNγ^+ CD8$^+$ T cells. Splenic S190-specific IFNγ^+ CD8$^+$ T cells remained at baseline level (Fig. 3.10 C). As anticipated, priming with recombinant proteins, especially with adjuvanted HBsAg + HBcAg, stimulated strong splenic S208-specific IFNγ^+ CD8$^+$ T cells compared to priming with *DNA-HBVac* (Fig. 3.10 D). As expected, in control mice no HBV peptide-specific IFNγ^+ CD8$^+$ T-cell responses were detected (Fig. 3.10 A-D).

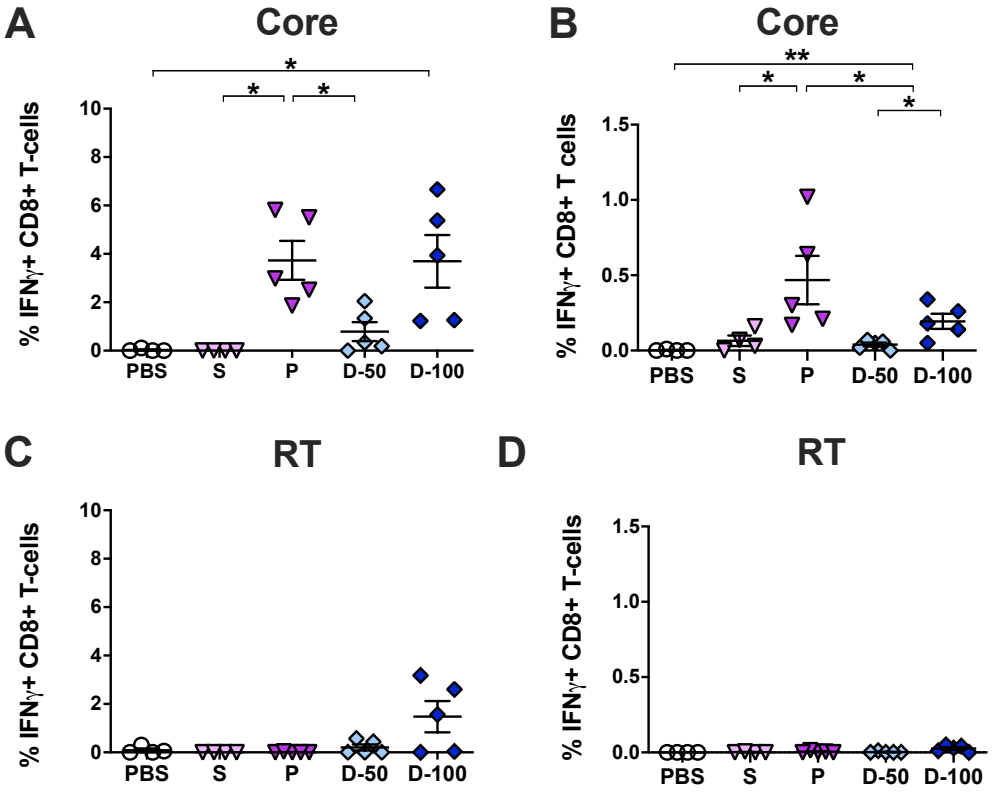

Figure 3.11 Functional analysis of Core- and RT-specific CD8$^+$ T cells elicited by immunization with *DNA-HBVac* in livers and spleens of HBV carrier mice
Percentages of Core-specific IFNγ^+ CD8$^+$ T cells in the (A) livers and in the (B) spleens determined by intracellular IFNγ staining of LALs following *ex vivo* stimulation with overlapping Core-specific peptide pool. Percentages of RT-specific IFNγ^+ CD8$^+$ T cells in the (C) livers and in the (D) spleens determined by intracellular IFNγ staining of splenocytes following *ex vivo* stimulation with overlapping RT-specific peptide pool. Mean±SEM is shown. Statistical analysis was performed using nonparametric One-Way

ANOVA. Symbols represent individual mice. Values of individual mice are shown. Asterisks indicate statistically significant differences (*p<0.05, **p<0.005).

The percentages of Core-specific IFNγ^+ CD8$^+$ T-cell responses determined in the livers and spleens of mice immunized with 100 µg *DNA-HBVac* for priming were considerably higher compared to those elicited by immunization with PBS. In D-100 group, the average percentages of IFNγ secretion following LALs and splenocyte stimulation with an overlapping Core-specific peptide pool were 3.7 % in the liver (Fig. 3.11 A) and less than 1.0 % in the spleen (Fig. 3.11 B), respectively). Again, immunization with 100 µg *DNA-HBVac* resulted in an increased and significantly improved IFNγ secretion in the liver (Fig. 3.11 A) and in the spleen (Fig. 3.11 B) compared to mice immunized with 50 µg *DNA-HBVac*. In addition, mice receiving recombinant protein antigens (S and P groups) or 50 µg *DNA-HBVac* (D-50) for prime immunization showed undetectable RT-specific IFNγ^+ CD8$^+$ T-cell responses in livers (Fig. 3.11 C) and spleens (Fig. 3.11 D) compared to D-100 group. By contrast high frequencies (mean 1.5 %) of RT-specific IFNγ^+ CD8$^+$ T-cell responses were detected in the livers (Fig. 3.11 C) of three mice immunized with 100 µg *DNA-HBVac* but not in the spleens (Fig. 3.11 D). Stimulation of LALs and splenocytes isolated from mice immunized with PBS did not induce any IFNγ responses (Fig. 3.11 A-D).
Taken together, these findings demonstrate that priming with 100 µg *DNA-HBVac* is necessary to induce strong and polyfunctional CD8$^+$ T-cell responses in AAV-HBV mice. The main advantage of priming with *DNA-HBVac* instead of recombinant protein immunization is that DNA immunization elicits an RT-specific CD8$^+$ T-cell response whereas protein immunization does not. These different immune responses resulting from different priming regimens lead to the conclusion that broad priming immunization is essential for successful therapeutic vaccination.

To examine the impact of *DNA-HBVac* vaccination on HBV replication in AAV-HBV transduced mice, HBeAg levels were monitored in the serum before the first immunization as well as at the time point of sacrifice. In addition, serum ALT levels were measured throughout the experiment. The quantification of HBeAg levels in the serum was performed by ELISA.

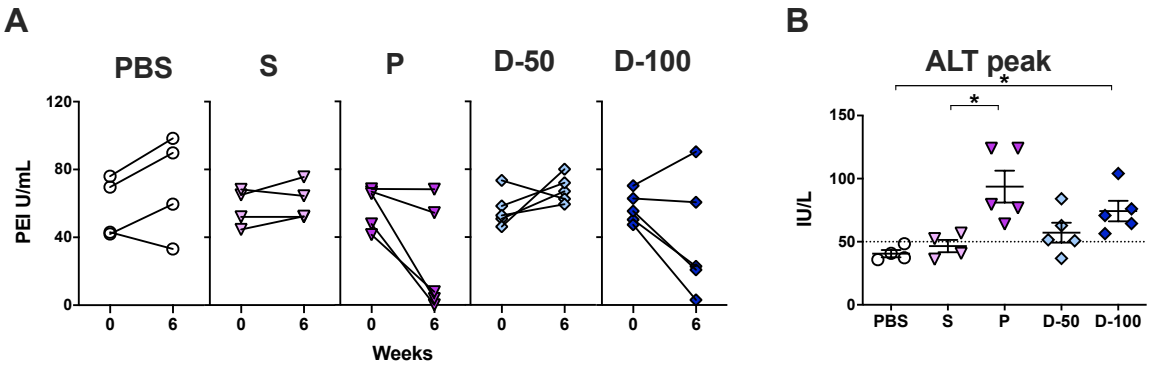

Figure 3.12 Evaluation of the antiviral effect induced by immunization with *DNA-HBVac* in the sera of HBV carrier mice
(A) HBeAg serum levels detected at onset and endpoint of analysis. (B) Serum ALT peak activity throughout the experiment. Mean±SEM is shown. Statistical analysis was performed using nonparametric One-Way ANOVA. Symbols represent individual mice. Values of individual mice are shown. Asterisks indicate statistically significant differences (*p<0.05).

As predicted, control mice injected with PBS mainly did not show any decrease in HBeAg levels throughout the experiment. In S and D-50 groups, an increase in serum HBeAg levels was observed at the end of the experiment compared to baseline. Compared to HBeAg levels at week 0, the strongest decrease in HBeAg levels was observed in the sera of mice immunized with adjuvanted HBsAg + HBcAg and *DNA-HBVac* 100 µg dose. In mice immunized with mixed protein antigens (P), nearly undetectable HBeAg levels were detected in the serum of three out of five mice (60 %) at the endpoint of the experiment. In the group of mice immunized with 100 µg *DNA-HBVac*, a strong and profound decrease in HBeAg levels in the serum could be measured in three out of five mice (60 %) at week 6, from which one had undetectable HBeAg levels (Fig. 3.12 A). As shown in Fig. 3.12 B, ALT peak values remained low and comparable in the groups of mice immunized with PBS, which served as a control as well as those primed with HBsAg. Immunization with 50 µg *DNA-HBVac* induced only a slight increase in ALT peak values. The most prominent ALT peak elevation was assessed in the sera of mice from mixed protein antigen group (P) followed by D-100 group (Fig. 3.12 B).

Data obtained in the AAV-HBV mouse model highlights that antiviral effects could only be observed in groups of mice primed with adjuvanted HBsAg + HBcAg (P) and 100 µg *DNA-HBVac* (D-100). In those groups, the antiviral effect seems to be very similar, involving apoptosis of HBV-infected hepatocytes and cytokine release. In addition, ALT peak elevation could only be measured in the sera of mice from mixed protein antigen group (P) and D-100 groups, implying liver damage induced by HBV-specific cytotoxic $CD8^+$ T cells due to therapeutic vaccination.

3.1.4 Evaluation of the immunogenicity of simultaneous DNA/HBsAg prime – MVA boost regimen in HBV carrier mice

Previous experiments demonstrated that prime immunization with 100 µg *DNA-HBVac* elicited strong and polyfunctional $CD8^+$ T-cell responses but low humoral immune responses compared to immunization of mice with adjuvanted recombinant proteins (HBsAg + HBcAg). Therefore, the immunization strategy was optimized to enable a strong B-and $CD4^+$ T-cell response when immunizing with 100 µg *DNA-HBVac*. To this extent, immunization with recombinant particulate HBsAg in combination with *DNA-HBVac* could be a prerequisite to achieve a strong B-cell response and high anti-HBs titers, which could have the additional effect of stopping viral spread. The following experiment aimed to determine whether simultaneous priming immunization with DNA and recombinant HBsAg could be an optimal strategy to induce both strong humoral and cellular immune responses.

As shown in Fig. 3.13, six weeks before the vaccination, nine-week-old C57BL/6 mice were subjected to AAV-HBV infection to establish persistent HBV replication. Beginning at week 0, mice underwent two rounds of i.m. priming immunizations, spaced four weeks apart. The immunizations consisted of a mixture of adjuvanted recombinant particulate HBsAg and HBcAg (referred to as P), a mixture of adjuvanted recombinant particulate HBsAg and *DNA-HBVac* at a dose of 100 µg (referred to as D/S/CpG), a mixture of *DNA-HBVac* at a dose of 100 µg and recombinant particulate HBsAg (referred to as D/S), or a mixture of adjuvanted *DNA-HBVac* at a dose of 100 µg (referred to as D/CpG). At week 10, a booster immunization with *MVA-HBVac* ($3x10^7$ IFU *MVA-HBVac*/mouse) was administered. The control mice received PBS. At week 10 animals were sacrificed and analyzed for the vaccination efficacy in serum, liver, and spleen.

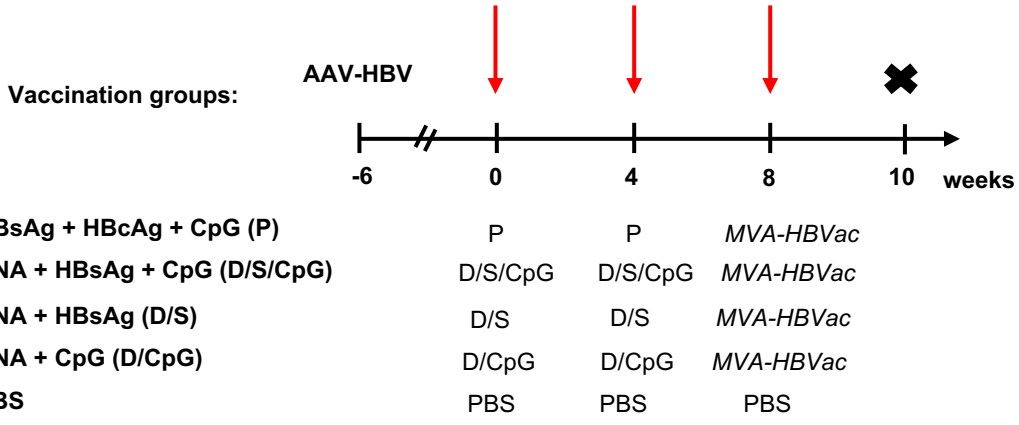

Figure 3.13 Vaccination scheme of simultaneous prime immunization with *DNA-HBVac* and recombinant HBsAg in HBV carrier mice
Nine-week-old C57BL/6 mice were transduced with AAV-HBV to establish persistent HBV replication. Six weeks after AAV-HBV infection mice received a prime-boost therapeutic vaccination. The priming vaccinations were initiated at week 0 and consisted of either only adjuvanted recombinant proteins (10 µg HBsAg + 10 µg HBcAg + 15 10 µg CpG, (P)), adjuvanted *DNA-HBVac* + HBsAg (100 10 µg DNA-

HBVac + 10 µg HBsAg + 15 µg CpG referred to as D/S/CpG), non-adjuvanted *DNA-HBVac* + 10 µg HBsAg (D/S) or adjuvanted *DNA-HBVac* only (100 µg *DNA-HBVac* + 15 µg CpG referred to as D/CpG). At week 8, mice were i.m. immunized with *MVA-HBVac* ($3x10^7$ IFU/mouse). Mice receiving three injections of PBS served as controls. Animals were sacrificed at week 10 and analyzed for the vaccination efficacy in serum, liver, and spleen.

Humoral immune responses were assessed by the detection of anti-HBs antibodies in the sera of mice at week 10.

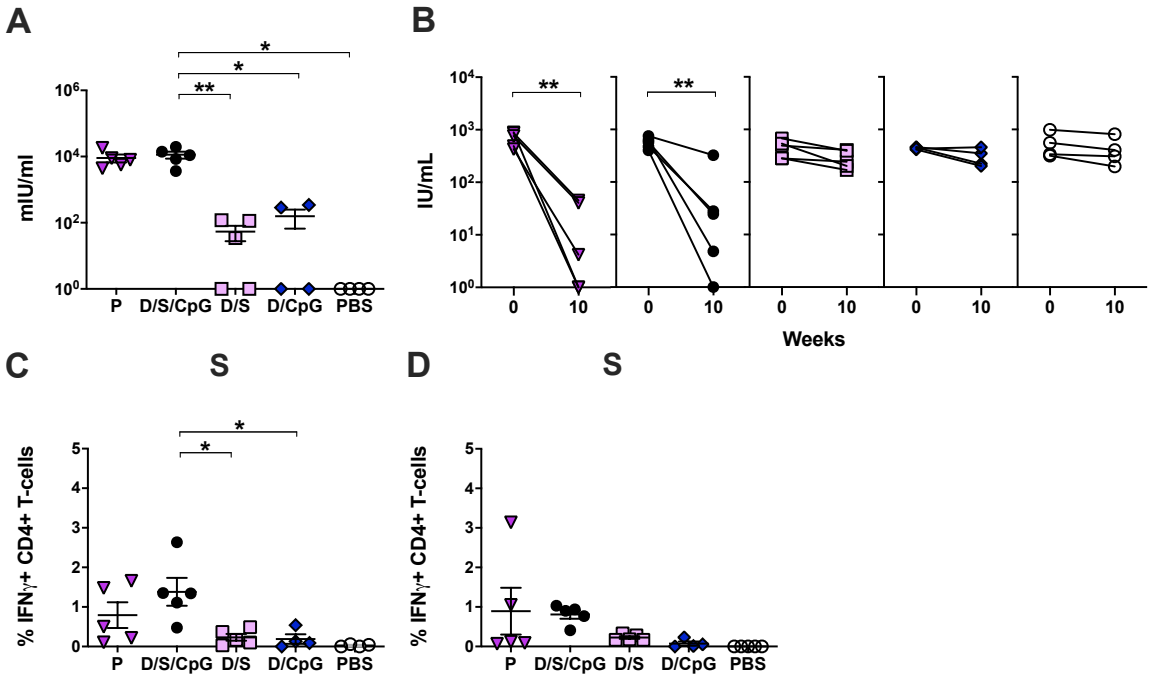

Figure 3.14 HBV-specific humoral and S-specific CD4 T-cell responses elicited by simultaneous DNA/HBsAg prime – MVA boost immunization in HBV carrier mice
(A) anti-HBs antibody levels detected in the sera of mice at the endpoint of analysis. (B) Serum HBsAg levels were measured at the onset and at the endpoint of the experiment. HBV S-specific IFNγ^+ $CD4^+$ T cells isolated from (C) liver and (D) spleen and analyzed by ICS following *ex vivo* stimulation with HBV S-specific overlapping peptide pool. Mean±SEM is shown. Statistical analysis was performed using nonparametric One-Way ANOVA. Symbols represent individual mice. Values of individual mice are shown. Asterisks indicate statistically significant differences (*p<0.05, **p<0.005).

As shown in Fig. 3.14 A, comparably high anti-HBs titers were generated in mice immunized with P and D/S/CpG groups (mean 10^4 mIU/ml). By contrast, priming with D/S or D/CpG resulted in 2-log lower anti-HBs titers. The differences observed were statistically significant (p<0.05). As anticipated immunization of control mice with PBS did not result in anti-HBs generation. These findings demonstrate that simultaneous immunization of HBsAg or CpG only, in combination with 100 µg *DNA-HBVac* is not sufficient to elicit adequate anti-HBs levels in the serum. Thus, it seems that immunizations with recombinant HBsAg in combination with CpG are necessary to induce satisfactory anti-HBs titers when priming with *DNA-HBVac*. Compared to baseline values at week 0, a profound and comparable decrease in HBsAg levels

was observed in the sera of mice primed with P and D/S/CpG ($p<0.005$). When looking closer at individual mice, remarkable decreases in HBsAg levels were detected in four out of five (80 %) mice immunized with D/S/CpG. Priming with D/S or D/CpG elicited only barely detectable HBsAg decrease, similar to the control group (Fig. 3.14 B).

At week 10, percentages of S-specific $CD4^+$ T-cell responses induced by various priming strategies were analyzed by intracellular IFNγ staining of *ex vivo*, overlapping S-specific peptide pool stimulated LALs and splenocytes. Mice receiving P or D/S/CpG as a prime showed similar high frequencies of S-specific $CD4^+$ T cells in livers and spleens (Fig. 3.14 C & D). By contrast immunization with D/S or D/CpG resulted in baseline percentages of S-specific $CD4^+$ T-cell responses both in livers and spleens. Control mice receiving PBS did not induce any $CD4^+$ T-cell responses (Fig. 3.14 C and D).

Next, S-, Core- and RT-specific $CD8^+$ T-cell responses elicited by the various heterologous prime-boost vaccination regimens were compared by intracellular IFNγ staining of LALs at week 10.

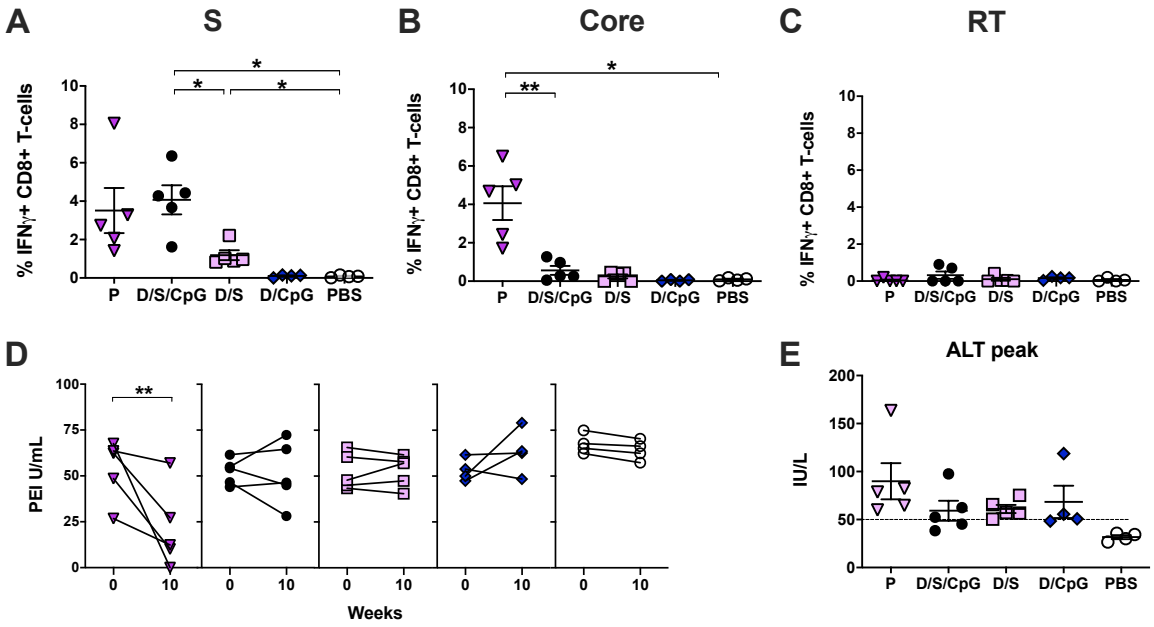

Figure 3.15 Hepatic HBV-specific effector T-cell responses induced by DNA/HBsAg prime – MVA boost regimen in HBV carrier mice
HBV (A) S-, (B) Core- and (C) RT-specific reactive, IFNγ^+ $CD8^+$ T cells isolated from the liver and analyzed by ICS after *ex vivo* stimulation with HBV S-, Core- and RT-specific overlapping peptide pools. (D) HBeAg serum levels were detected at the onset and endpoint of the analysis. (E) Serum ALT peak activity throughout the experiment. Mean±SEM is shown. Statistical analysis was performed using nonparametric One-Way ANOVA. Symbols represent individual mice. Values of individual mice are shown. Asterisks indicate statistically significant differences (*$p<0.05$, **$p<0.005$).

To this extent LALs were stimulated *ex-vivo* with S-, Core- and RT-specific overlapping peptide pools. The percentages of intrahepatic S-specific IFNγ^+ $CD8^+$ T cells determined in mice

vaccinated with D/S/CpG were high and similar to those elicited by priming with adjuvanted HBsAg + HBcAg (P). In the livers of mice vaccinated with D/S/CpG a three-fold increase in S-specific IFNγ^+ CD8$^+$ T cells was found compared to mice immunized with D/S only ($p<0.05$). Unexpectedly, the frequency of S-specific IFNγ^+ CD8$^+$ T cells measured in mice vaccinated with D/CpG remained at baseline level (Fig. 3.15 A). By contrast, Core-specific IFNγ^+ CD8$^+$ T cells remained barely detectable in mice immunized with D/S/CpG (mean 0.6 %) compared to those primed with P (mean 4.1 %) ($p<0.005$). LALs stimulated with an overlapping Core-specific peptide pool isolated from mice immunized with D/S and D/CpG did not show IFNγ responses (Fig. 3.15 B). In addition, priming with D/S/CpG resulted in low RT-specific IFNγ^+ CD8$^+$ T-cell responses whereas all other vaccination regimens did not elicit RT-specific IFNγ^+ CD8$^+$ T-cell responses (Fig. 3.15 C). No HBV-specific IFNγ^+ CD8$^+$ T-cell responses were observed in control mice immunized with PBS (Fig. 3.15 A-C).

Compared to baseline HBeAg levels at week 0, a significant drop in HBeAg levels was only observed in mice immunized with P at the endpoint of the experiment ($p<0.005$). In mice receiving D/S/CpG as a prime, slight decreases in HBeAg levels correlated with the previously described, low, Core-specific IFNγ^+ CD8$^+$ T-cell responses. As expected, no significant drop in HBeAg levels was observed in control mice (Fig. 3. 15 D). In addition, ALT levels remained stable throughout the experiment in all groups that received *DNA-HBVac* for priming. Elevated ALT peak values were only detectable in mice primed with P, implying cytotoxic CD8$^+$ T cell activity due to therapeutic vaccination (Fig. 3.15 E).

Taken together, those results indicate that priming with D/S/CpG results in strong anti-HBs titers, HBV S-specific CD4$^+$ and CD8$^+$ T-cell responses but in low HBeAg level drop as well as HBV Core- and RT-specific CD8$^+$ T-cell responses in the livers of AAV-HBV mice. Here it is of utmost importance to stress that Core- and RT-specific CD8$^+$ T-cell responses are induced solely by DNA vaccination, in contrary to S-specific CD8$^+$ T-cell responses which are induced simultaneously by recombinant HBsAg as well as *DNA-HBVac* administration.

3.1.5 Investigation of the efficacy of distinct injection sites for DNA and HBsAg prime in HBV naïve mice

Previous data (chapter 3.1.4) showed that simultaneous priming immunization with *DNA-HBVac* and adjuvanted recombinant HBsAg (D/S/CpG) induced strong anti-HBs titers, HBV S-specific CD4$^+$ and CD8$^+$ T-cell responses but only low reduction of HBeAg levels and scarce HBV Core- and RT-specific CD8$^+$ T-cell responses in the sera and livers of immunized AAV-HBV mice. Therefore, separating immunization sites of recombinant HBsAg and *DNA-HBVac* for priming could be a promising strategy to further optimize the immunogenicity elicited by a DNA prime. As shown in Fig. 3.16, nine weeks old C57BL/6 mice received two priming

immunizations in a two-week interval (week 0 and week 2) consisting of either 100 µg *DNA-HBVac* only (D), 100 µg *DNA-HBVac* in the left leg (L) and adjuvanted recombinant HBsAg in the right leg (R) or simultaneously 100 µg *DNA-HBVac* and adjuvanted recombinant HBsAg (D/S/CpG). At week 4, booster immunization consisting of $3x10^7$ IFU *MVA-HBVac*/mouse was administered. Mice receiving three injections of PBS served as controls. At week 5, mice were sacrificed and HBV-specific antibodies in serum as well as splenic T-cell responses were analysed.

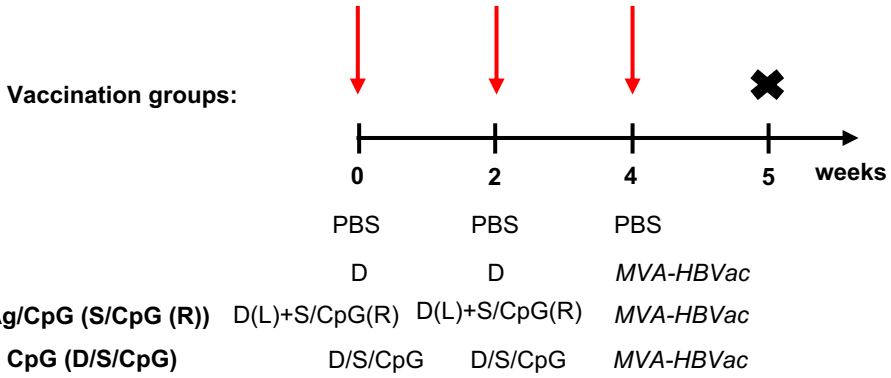

Figure 3.16 Vaccination scheme of distinct prime immunization sites for *DNA-HBVac* and recombinant HBsAg in wild-type mice
Nine weeks old HBV naïve C57BL/6 mice were immunized according to the prime-boost vaccination strategy. Mice receiving PBS served as controls. At weeks 0 and 2 mice were i.m. immunized with 100 µg *DNA-HBVac* only (D), 100 µg *DNA-HBVac* in the left leg (L), and adjuvanted recombinant HBsAg in the right leg (10 µg HBsAg + 15 µg CpG referred to as *R*) or simultaneously with 100 µg *DNA-HBVac* and adjuvanted recombinant HBsAg (10 µg HBsAg + 15 µg CpG) referred to as D/S/CpG. At week 4 mice received a boost with *MVA-HBVac* ($3x10^7$ IFU/mouse). At week 5, mice were sacrificed and analyzed to assess vaccination efficacy in serum and spleen.

To evaluate the amplitude of humoral immune responses elicited in this study, anti-HBs, and anti-HBc titers were determined in the sera of immunized mice at week 5.

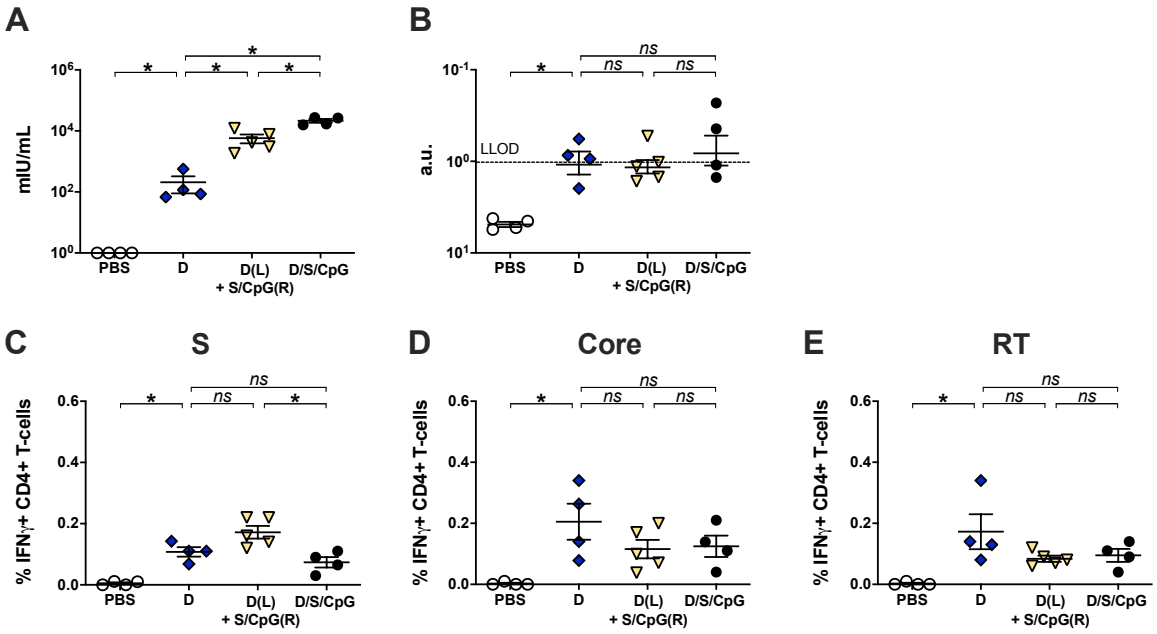

Figure 3.17 HBV-specific humoral and CD4⁺ T-cell responses elicited by distinct prime immunization sites for *DNA-HBVac* and recombinant HBsAg in HBV-naïve mice
(A) anti-HBs and (B) anti-HBc antibody levels detected in the sera of mice at week 5. HBV (C) S-, (D) Core- and (E) RT-specific reactive, IFNγ^+ CD4$^+$ T cells isolated from spleens and analyzed by ICS after *ex vivo* stimulation with HBV S-, Core- and RT-specific overlapping peptide pools. Mean±SEM is shown. Statistical analysis was performed using nonparametric One-Way ANOVA. Symbols represent individual mice. Values of individual mice are shown. Asterisks indicate statistically significant differences (*p<0.05, ns– not significant: p>0,05).

Mice from the groups that received HBsAg as a prime (D (L) + S/CpG (R) and D/S/CpG groups) showed high anti-HBs levels in the sera compared to baseline anti-HBs titers elicited by control immunization with PBS (p<0.05). In addition, priming with D (L) + S/CpG (R) resulted in higher anti-HBs antibody titers compared to priming with 100 µg *DNA-HBVac* only (D). However, the generated anti-HBs antibody levels remained lower than those induced by D/S/CpG immunizations (p<0.05) (Fig. 3.17 A). Despite using different regimens for priming, generated anti-HBc antibody titers were comparably high in all three experimental groups. As expected, anti-HBs and anti-HBc antibodies remained at baseline levels in control mice (Fig. 3. 17 B).
At week 5, HBV-specific CD4$^+$ T-cell responses elicited by the various immunization regimens were analyzed by intracellular IFNγ staining of *ex vivo* HBV-specific peptide pool stimulated splenocytes. As shown in Fig. 3.17 C, splenic S-specific CD4$^+$ T-cell responses were significantly stronger in mice vaccinated with D (L) + S/CpG (R) compared to mice immunized with 100 µg *DNA-HBVac* only (D) or D/S/CpG as a prime (p<0.05). The magnitudes of (Fig. 3.17 D) Core- and (Fig. 3.17 E) RT-specific CD4$^+$ T-cell responses were comparable in the spleens of mice from all three priming regimens. Mice immunized with PBS induced no IFNγ responses.

To evaluate whether priming immunization with D (L) + S/CpG (R) was able to induce higher frequencies of S-, Core- and RT-specific CD8$^+$ T cells compared to D only or D/S/CpG vaccination, intracellular IFNγ staining of HBV-specific peptide stimulated splenocytes was performed at week 5.

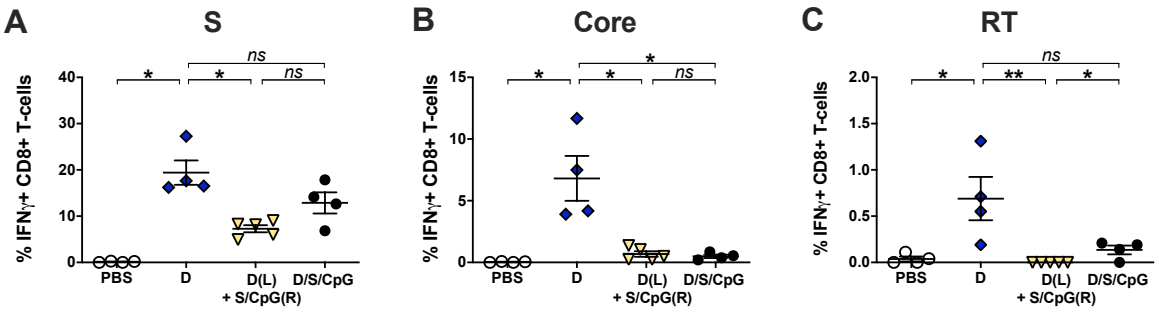

Figure 3.18 Splenic HBV-specific CD8$^+$ T-cell responses elicited by distinct prime immunization sites for *DNA-HBVac* and recombinant HBsAg in HBV-naïve mice
IFNγ^+ CD8$^+$ T cells from spleen detected after stimulation with HBV (A) S-, (B) Core- and (C) RT-specific overlapping peptide pools. Mean±SEM is shown. Statistical analysis was performed using nonparametric One-Way ANOVA. Symbols represent individual mice. Values of individual mice are shown. Asterisks indicate statistically significant differences (*p<0.05, **p<0.005, ns– not significant: p>0,05).

The magnitude of S-specific CD8$^+$ T cells induced by priming with D (L) + S/CpG (R) was comparable to mice primed with D/S/CpG but significantly lower to those immunized with 100 µg *DNA-HBVac* (D) (p<0.05). The most profound S-specific CD8$^+$ T-cell responses were observed in the mice primed with 100 µg *DNA-HBVac* only (Fig. 3.18 A). Immunization with D (L) + S/CpG (R) resulted in significantly lower frequencies of Core- (Fig. 3.18 B) as well as RT-specific (Fig. 3.18 C) CD8$^+$ T-cell responses compared to mice immunized with D only. Percentages of RT-specific CD8$^+$ T-cell responses were even lower in mice primed with D (L) + S/CpG (R) compared to those primed with D/S/CpG (p<0.05). IFNγ responses of control mice, injected with PBS remained at baseline level. Immunization of mice with D (L) + S/CpG (R), in general, showed weaker anti-HBs antibody titers as well as S-specific CD4$^+$ T-cell responses compared to simultaneous immunization (D/S/CpG group). In addition, separating injection sites of *DNA-HBVac* and HBsAg for prime immunizations resulted in barely detectable Core- and RT-specific CD8$^+$ T-cell responses.

Taken together, these findings demonstrated that distinct sites of vaccine administration for *DNA-HBVac* and recombinant HBsAg prime immunizations resulted in low neutralizing anti-HBs antibody titers as well as low frequencies of HBV-specific CD8$^+$ T-cell responses. All in all, the immunogenicity of D (L) + S/CpG (R) was even weaker than simultaneous prime immunization with *DNA-HBVac* and adjuvanted recombinant HBsAg.

3.1.6 Investigation of the immunogenicity of sequential DNA/HBsAg prime – MVA boost regimen in HBV carrier mice

Previous experiment (chapter 3.1.5) showed that simultaneous immunization of *DNA-HBVac* and adjuvanted recombinant HBsAg as well as injecting *DNA-HBVac* and adjuvanted recombinant HBsAg at different locations were not able to induce remarkable HBV-specific humoral and cellular immune responses. To fully investigate the potency of combined *DNA-HBVac* and adjuvanted recombinant HBsAg for priming to induce robust and polyfunctional B- and T-cell responses and break immune tolerance, sequential immunization was evaluated as a promising strategy to overcome this challenge. To test this hypothesis, the immunogenicity of sequential priming immunization with *DNA-HBVac* and recombinant HBsAg was assessed in AAV-HBV mice. As shown in Figure 3.19, six weeks before the onset of vaccination, mice were exposed to AAV-HBV to establish persistent HBV replication. Beginning at week 0, the mice were vaccinated sequentially, undergoing a total of four vaccinations, spaced two weeks apart. The vaccinations were organized into two groups. The first group received two initial vaccinations of *DNA-HBVac* at a 100 µg dose, followed by two additional vaccinations with CpG adjuvanted recombinant particulate HBsAg (DDSS). The second group received two initial vaccinations of CpG adjuvanted recombinant particulate HBsAg, followed by two additional vaccinations with *DNA-HBVac* at a 100 µg dose (SSDD). As reference groups, some mice were primed with two initial vaccinations, spaced four weeks apart. A group received a mixture of adjuvanted recombinant particulate HBsAg and HBcAg (PP). Another group was primed with *DNA-HBVac* at a 100 µg dose (DD). At week 8, all mice received a booster immunization consisting of MVA-HBVac ($3x10^7$ IFU/mouse). The control group received PBS injections. Ten weeks after the onset of the vaccination regimen, mice were sacrificed and subjected to analysis.

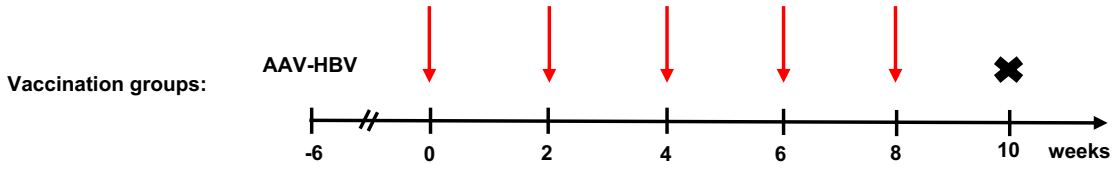

1)	**PBS**	PBS	PBS	PBS	PBS	PBS
2)	**HBsAg + HBcAg + CpG (PP)**	P	-	P	-	*MVA-HBVac*
3)	**DNA (DD)**	D	-	D	-	*MVA-HBVac*
4)	**DNA + HBsAg/CpG (DDSS)**	D	D	S	S	*MVA-HBVac*
5)	**HBsAg/CpG + DNA (SSDD)**	S	S	D	D	*MVA-HBVac*

Figure 3.19 Schedule of sequential prime immunization with *DNA-HBVac* and recombinant HBsAg in HBV carrier mice
Nine-week-old C57BL/6 mice were transduced with AAV-HBV to establish persistent HBV replication. Six weeks later, prime-boost vaccination was initiated at week 0. Mice were vaccinated sequentially, undergoing a total of four vaccinations, spaced two weeks apart. One group received two initial vaccinations of *DNA-HBVac* at a 100 µg dose, followed by two additional vaccinations with 15 µg CpG + 10 µg HBsAg (DDSS). The second group received two initial vaccinations of 15 µg CpG + 10 µg

HBsAg, followed by two additional vaccinations with *DNA-HBVac* at a 100 µg dose (SSDD). As reference groups, some mice were primed with two initial vaccinations, spaced four weeks apart. A group received a mixture of 10 µg HBsAg + 10 µg HBcAg + 15 µg CpG (PP). Another group was primed with *DNA-HBVac* at a 100 µg dose (DD). At week 8 all animals received an *MVA-HBVac* boost vaccination ($3x10^7$ IFU/mouse). Mice receiving five PBS injections every two weeks served as controls. Endpoint analysis was performed at week 10.

The humoral immune responses elicited by sequential immunization with *DNA-HBVac* and adjuvanted recombinant HBsAg were assessed by the detection of anti-HBs as well as anti-HBc titers in the sera of mice at week 10.

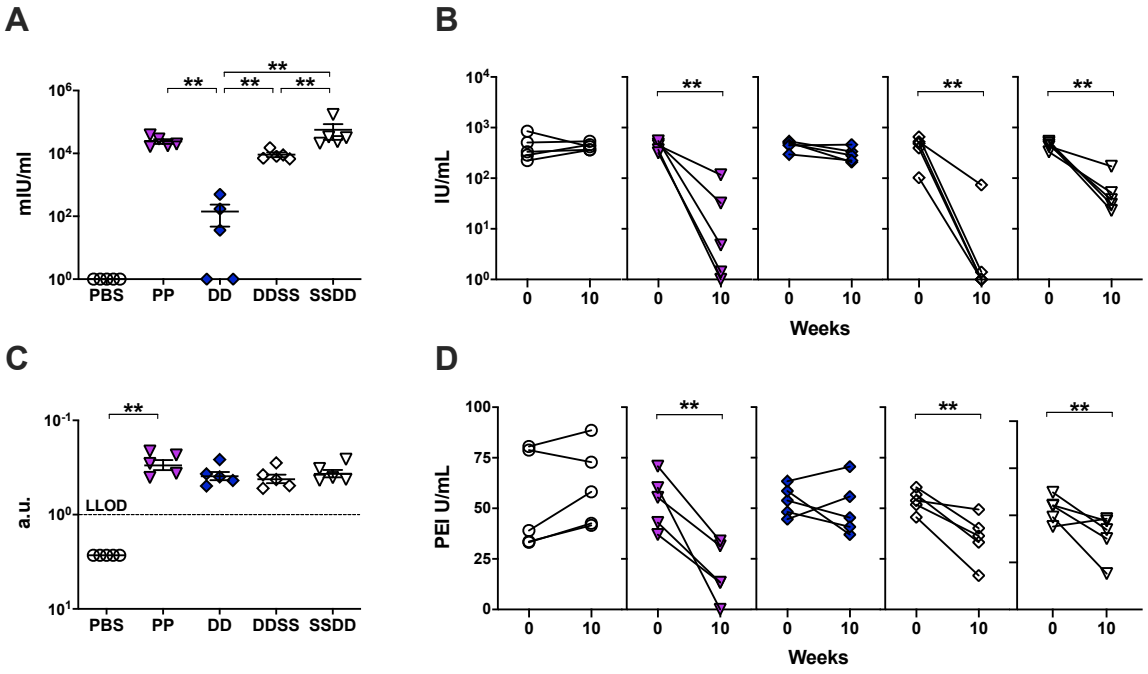

Figure 3.20 HBV-specific humoral responses and serum HBV antigen kinetics at experiment onset and endpoint in HBV carrier mice receiving sequential DNA/HBsAg prime – MVA boost regimen
Levels of (A) anti-HBs and (C) anti-HBc antibodies detected in the murine serum at the experimental endpoint. Levels of (B) HBsAg and (C) HBeAg determined in the sera of mice at the onset and endpoint of the experiment. Mean±SEM is shown. Statistical analysis was performed using nonparametric One-Way ANOVA. Symbols represent individual mice. Values of individual mice are shown. Asterisks indicate statistically significant differences (*p<0.05, **p<0.005, ns– not significant: p>0,05).

Mice primed sequentially with *DNA-HBVac* and recombinant HBsAg, especially the SSDD group, induced significantly higher levels of anti-HBs antibodies compared to the DD group (p<0.005). This result implies that additional prime immunizations separated in time and consisting of recombinant HBsAg could further enhance the anti-HBs antibody response. In addition, mice receiving sequential priming immunization starting with either *DNA-HBVac* (DDSS) or adjuvanted recombinant HBsAg administration (SSDD) showed similar anti-HBs antibody titers compared to those vaccinated twice with mixed adjuvanted protein antigens (PP). Interestingly, significantly higher anti-HBs titers could be detected in mice receiving

sequential immunization starting with *DNA-HBVac* (DDSS group) than those starting with recombinant HBsAg (SSDD group) ($p<0.005$) (Fig. 3.20 A). Substantial reductions in HBsAg levels were detected in all experimental groups immunized with recombinant HBsAg (PP, DDSS, and SSDD groups) ($p<0.005$). DDSS regimen led to the strongest decrease in HBsAg levels in the sera of immunized mice. At week 10, four out of five mice (80%) showed a 3-log reduction in HBsAg levels compared to baseline values at week 0. Consistent with the weak or absent anti-HBs titers, mice primed with *DNA-HBVac* only and PBS did not show any decline in HBsAg levels (Fig. 3.20 B). The levels of anti-HBc antibodies detected in the sera of all mice immunized with *DNA-HBVac* were significantly lower compared to those induced by vaccination with mixed adjuvanted protein antigens (PP) ($p<0.05$). Moreover, both sequential immunization groups showed similar and even lower anti-HBc levels than those detected in mice primed with *DNA-HBVac* only (Fig. 3.20 C). In addition, a decline in HBeAg levels was observed in all experimental groups primed with recombinant HBsAg (PP, DDSS, and SSDD groups) ($p<0.005$). However, the greatest decrease in serum HBeAg was noticeable in mice that received mixed adjuvanted protein antigens (PP) as a prime. Priming with *DNA-HBVac* only elicited barely detectable serum HBeAg decrease. As expected, no antiviral effect was observed in control mice (Fig. 3.20 D). The differences observed in HBeAg reduction might be caused by the lack of strong and polyfunctional HBV-specific T-cell responses.

Next, $CD4^+$ T-cell responses elicited by sequential immunization with *DNA-HBVac* and adjuvanted recombinant HBsAg were evaluated by ICS of *ex vivo* peptide-stimulated LALs and splenocytes.

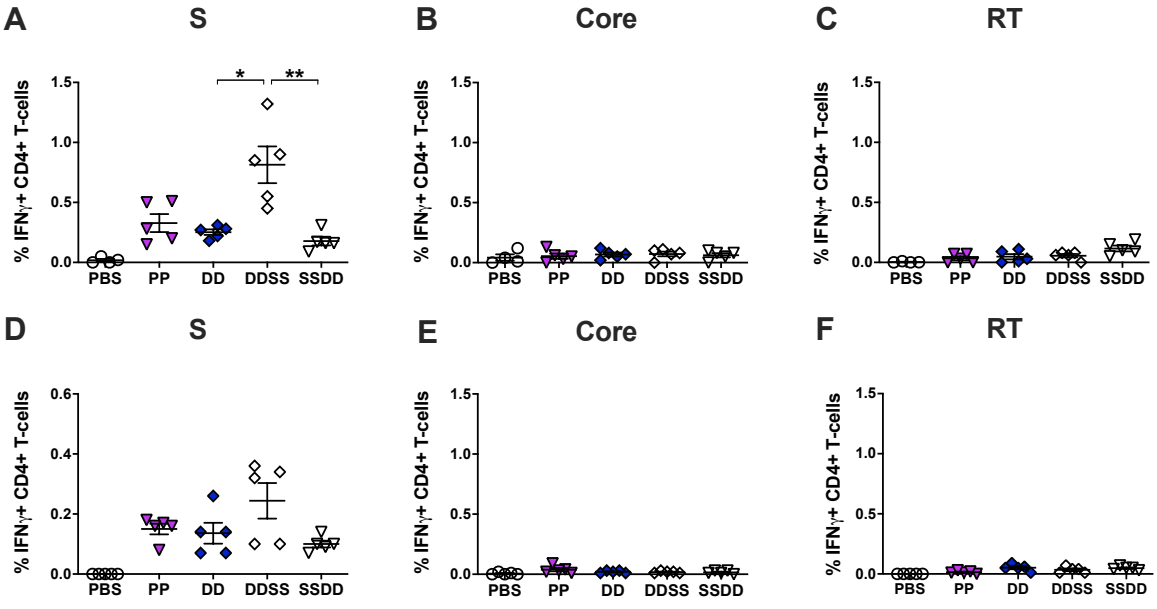

Figure 3.21 Hepatic and splenic HBV-specific CD4+ T cell responses in HBV carrier mice receiving sequential DNA/HBsAg prime – MVA boost regimen
Magnitudes of (A, D) S-, (B, E) Core- and (C, F) RT-specific IFNγ^+ CD4$^+$ T cells isolated from (A-C) liver and (D-F) spleen and analyzed by ICS following *ex vivo* stimulation with HBV S-, Core- and RT-specific overlapping peptide pools. Mean±SEM is shown. Statistical analysis was performed using nonparametric One-Way ANOVA. Symbols represent individual mice. Values of individual mice are shown. Asterisks indicate statistically significant differences (*p<0.05, **p<0.005, ns– not significant: p>0,05).

As shown in Fig. 3.21 (A and D), S-specific CD4$^+$ T-cell responses were detectable in the livers (Fig. 3.21 A) and spleens (Fig. 3.21 D) of all experimental groups. Mice sequentially immunized starting with DNA (DDSS) demonstrated the strongest magnitude of S-specific CD4$^+$ T cells in the liver compared to the responses elicited by all other vaccination regimens (p<0.05). Comparable results were obtained in the spleens of the immunized mice. No Core- (Fig. 3.21 B and E) and RT-specific (Fig. 3.21 C and F) CD4$^+$ T-cell responses were induced in the livers and spleens of all vaccine regimens. Taken together the strong S-specific CD4$^+$ T-cell responses observed in the livers and spleens of mice sequentially immunized starting with *DNA-HBVac* (DDSS) correlate with the observed drop in serum HBsAg levels (Fig. 3.20 B).

To investigate the effects of sequential immunization with *DNA-HBVac* and adjuvanted recombinant HBsAg on antigen-specific CD8$^+$ T cells induction in the livers and spleens of immunized mice, LALs, as well as splenocytes, were labeled *ex vivo* with S190- and C93-specific multimers and analyzed by flow cytometry.

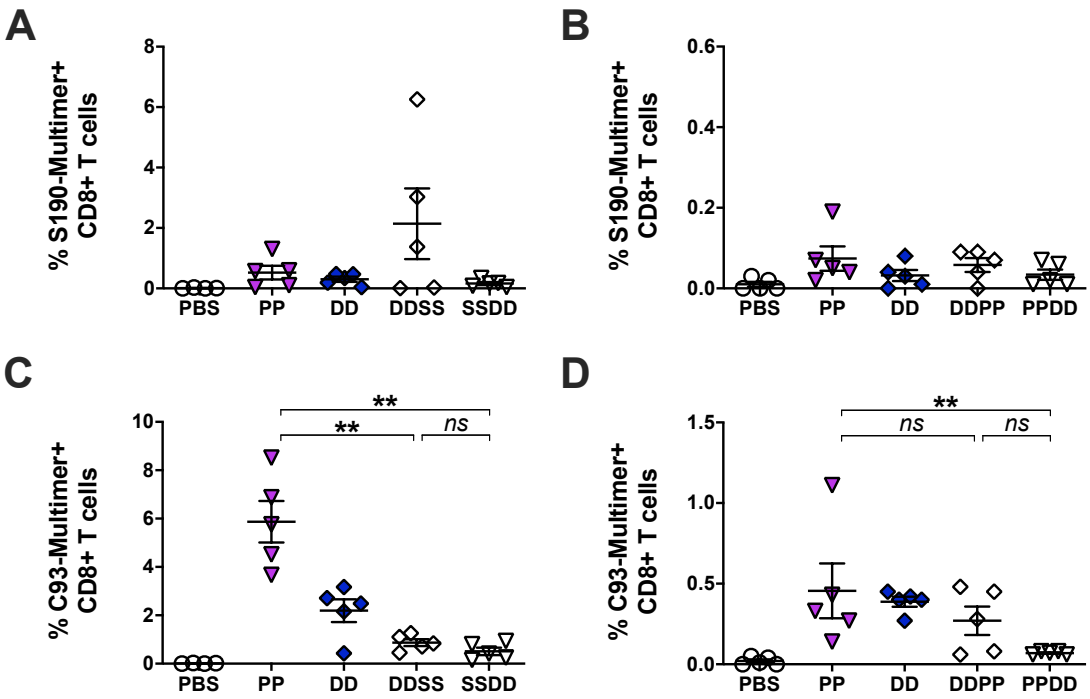

Figure 3.22 Hepatic and splenic HBV-specific effector T-cell responses induced by sequential immunization with DNA/HBsAg prime – MVA boost regimen in HBV carrier mice
Frequencies of (upper panel) S190- and (lower panel) C93-antigen specific CD8$^+$ T cells in the (A, C) livers and (B, D) spleens determined by multimer staining of LALs and splenocytes. Mean±SEM is shown. Statistical analysis was performed using nonparametric One-Way ANOVA. Symbols represent individual mice. Values of individual mice are shown. Asterisks indicate statistically significant differences (*p<0.05, **p<0.005, ns– not significant: p>0,05).

Remarkable percentages of S190-specific CD8$^+$ T cells were assessed in the livers of three out of five mice (60 %) vaccinated sequentially starting with DNA (DDSS) (Fig. 3.22 A). By contrast, S190-specific CD8$^+$ T cells remained at baseline levels in all other vaccination regimens. S190-specific CD8$^+$ T cells were barely detectable but comparable in the spleens of mice from all experimental groups (Fig. 3.22 B). By contrast, intrahepatic frequencies of C93-specific CD8$^+$ T cells remained at background levels (mean 0.5 %) in mice undergoing sequential immunization (DDSS and SSDD groups) compared to those elicited by prime immunization with mixed adjuvanted recombinant proteins (PP) (mean 6 %) (Fig. 3.22 C). Nevertheless, low, and comparable percentages of C93-specific CD8$^+$ T cells were detected in the spleens of mice primed with PP, DD as well as DDSS. Sequential immunization starting with the administration of recombinant HBsAg barely induced any C93-specific CD8$^+$ T cells in the spleens of mice (Fig. 3.22 D). As expected, no antigen-specific CD8$^+$ T cells were detected in control mice.

Next, the functionality of HBV-specific CD8$^+$ T cells elicited by the various immunization regimens were analyzed by intracellular IFNγ staining of *ex vivo* HBV-specific peptide-stimulated LALs and splenocytes.

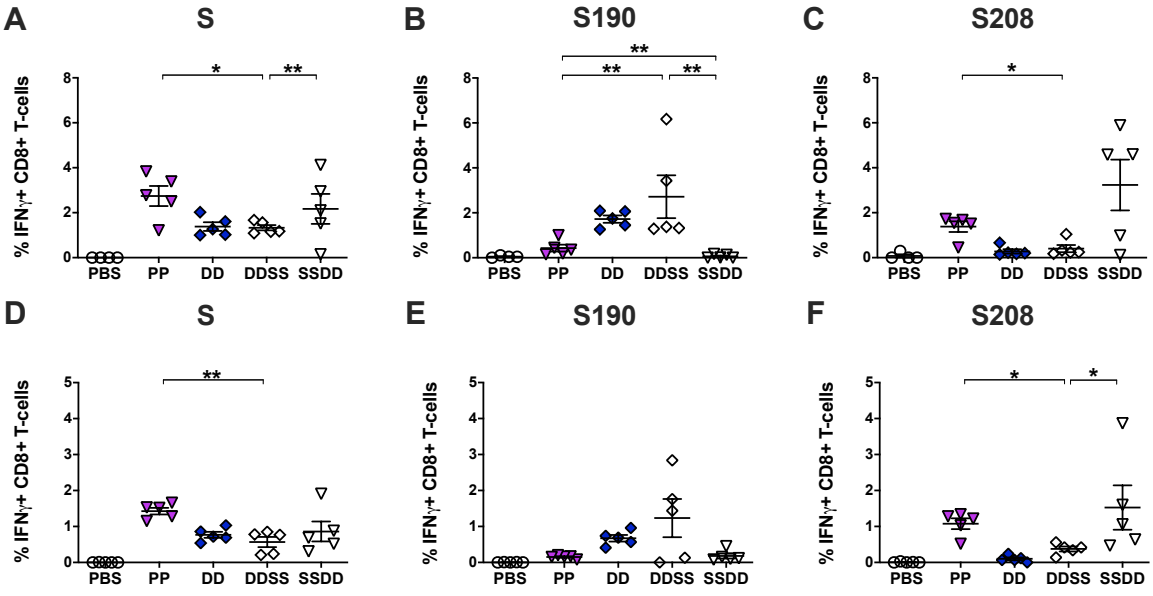

Figure 3.23 Functionality of HBV-specific CD8+ T cells isolated from livers and spleens of HBV carrier mice sequentially immunized with DNA and recombinant HBsAg

Percentages of (A, D) S-, (B, E) S190- and (C, F) S208-specific IFNγ^+ CD8$^+$ T cells determined by intracellular IFNγ staining of (A-C) LALs and (D-F) splenocytes previously *ex vivo* stimulated with overlapping S-specific peptide pool and HBV peptides S190 and S208. Mean±SEM is shown. Statistical analysis was performed using nonparametric One-Way ANOVA. Symbols represent individual mice. Values of individual mice are shown. Asterisks indicate statistically significant differences (*p<0.05, **p<0.005).

The percentages of S-specific IFNγ^+ CD8$^+$-T cell responses determined in the livers and spleens of mice immunized with adjuvanted mixed protein antigens (PP) were comparable to those induced by sequential vaccination starting with adjuvanted recombinant HBsAg (SSDD). Immunization with DD as well as with DDSS induced similar S-specific IFNγ^+ CD8$^+$ T-cell responses in livers (Fig. 3.23 A) and spleens (Fig. 3.23 D), however, the induction was significantly weaker than observed when using a protein prime ($p<0.05$). The most profound S190-specific IFNγ^+ CD8$^+$ T-cell responses in livers (Fig. 3.23 B) and spleens (Fig. 3.23 E) were observed in mice receiving DD or sequential immunization with DDSS as a prime. Sequential immunization initiated with *DNA-HBVac (*DDSS) elicited considerably stronger S190-specific IFNγ^+ CD8$^+$ T-cell responses in two out of five (40 %) mice in the liver and three out of five (60 %) mice in the spleen compared to the mice primed with *DNA-HBVac* only. By contrast, no S190-specific IFNγ^+ CD8$^+$ T-cell responses were detected in the spleens and livers of mice primed with mixed adjuvanted recombinant proteins (PP) nor in mice receiving sequential immunization starting with HBsAg (SSDD) ($p<0.005$) (Fig. 3.23 B and E). Of note, S208-specific IFNγ^+ CD8$^+$ T-cell responses were induced in all experimental groups receiving recombinant protein prime at the onset of the study (PP and SSDD groups), implying that initial protein priming seems a prerequisite to stimulate robust S208-specific IFNγ^+ CD8$^+$ T-cell responses in both liver (Fig. 3.23 C) and spleen (Fig. 3.23 F). Sequential immunization of mice initiated with recombinant HBsAg (SSDD) stimulated the most robust S208-specific IFNγ^+ CD8$^+$ T-cell responses, which were significantly higher in the livers of 3 out of 5 mice compared to those observed in mice primed with adjuvanted HBsAg + HBcAg (PP) (Fig. 3.23 C). No difference in percentages of S208-specific IFNγ^+ CD8$^+$ T-cell responses was assessed in the spleens of those mice (Fig. 3.23 F). S208-specific IFNγ^+ CD8$^+$ T-cell responses in livers (Fig. 3.23 C) and spleens (Fig. 3.23 F) of mice primed with DD or with sequential immunization starting with *DNA-HBVac* (DDSS) were barely detectable at week 10. As expected, control mice immunized with PBS did not show any S-, S190- or S208-specific IFNγ^+ CD8$^+$ T-cell responses in livers and spleens (Fig. 3.23 A-F).

Next, we further analyzed the impact of sequential immunization with *DNA-HBVac* and adjuvanted recombinant HBsAg on the generation of Core-and RT-specific IFNγ^+ CD8$^+$ T-cell responses by intracellular IFNγ-staining of LALs and splenocytes *ex-vivo* stimulated with overlapping Core- and RT-specific peptide pools.

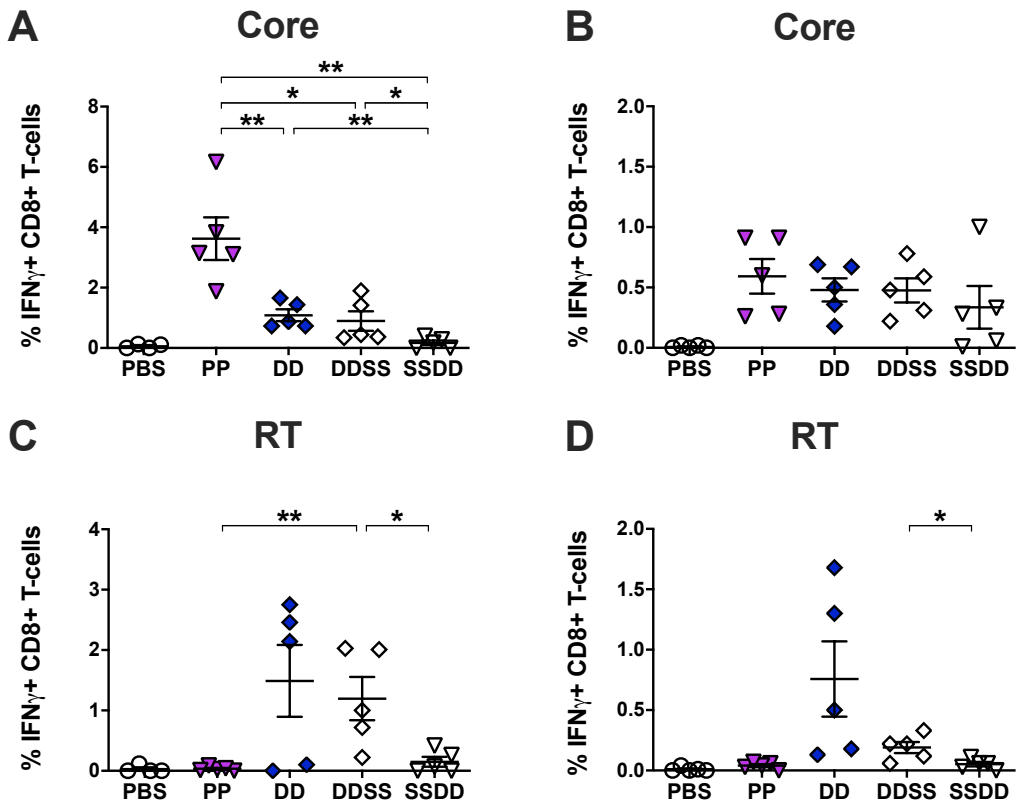

Figure 3.24 Core- and RT-specific CD8⁺ T-cell responses induced by sequential immunization with DNA/HBsAg prime – MVA boost regimen in HBV carrier mice
Percentages of (A-B) Core- and (C-D) RT-specific CD8⁺ T cells in the (A, C) livers and (B, D) spleens of vaccinated mice following intracellular IFN*γ* staining of LALs and splenocytes previously *ex vivo* stimulated with overlapping Core- and RT-specific peptide pools. Mean±SEM is shown. Statistical analysis was performed using nonparametric One-Way ANOVA. Symbols represent individual mice. Values of individual mice are shown. Asterisks indicate statistically significant differences (*p<0.05, **p<0.005, ns– not significant: p>0,05).

Immunization of mice with DD as well as sequential immunization starting with *DNA-HBVac* (DDSS) stimulated significantly lower intrahepatic Core-specific CD8⁺ T-cell responses than those detected in mice primed with mixed adjuvanted recombinant proteins (PP). Mice receiving sequential priming initiated with the immunization of HBsAg did not induce any Core-specific CD8⁺ T-cell responses in the liver (Fig. 3.24 A). All priming regimens elicited similar Core-specific CD8⁺ T-cell responses in the spleens of vaccinated mice (Fig. 3.24 B). Remarkably, RT-specific CD8⁺ T-cell responses were only observed in the livers of mice primed with DD as well as in mice receiving sequential immunization starting with *DNA-HBVac* (DDSS) ($p<0.05$) (Fig. 3.24 C). By contrast, sequential immunization starting with HBsAg (SSDD) resulted in lower and moderate RT-specific CD8⁺ T-cell responses in the spleen compared to those elicited by DD (Fig. 3.24 D). Control mice did not show any Core- and RT-specific CD8⁺ T-cell responses (Fig. 3.24 A-D).

Taken together, these results demonstrate that sequential priming initiated with DNA, followed by adjuvanted recombinant HBsAg and MVA-HBVac booster immunization generates not only strong HBV-specific cellular immunity but also induces robust anti-HBs responses, effectively reducing infection parameters in AAV-HBV mice. Therefore, to enhance HBV-specific humoral response, DNA-based vaccines can be combined with recombinant HBsAg to induce both strong antibody and $CD8^+$ T-cell responses.

In conclusion, this study showed that sequential immunization initiated with DNA, followed by adjuvanted recombinant HBsAg and MVA-HBVac proved to be the most suitable priming regimen for *TherVacB* to achieve strong humoral and cellular immune responses by DNA vaccination. However, a protein priming using a combination of adjuvanted HBsAg and HBcAg resulted in similar HBV-specific antibody titers and superior antiviral efficacy.

3.2 mRNA-based therapeutic hepatitis B vaccine: *RNA-HBVac*

The first review of successful administration of *in vitro* (IVT) synthesized mRNA dates back to 1990, when mice were immunized with reporter gene mRNAs and protein production was detected (Wolff et al., 1990). mRNA vaccines represent a new and promising approach in the field of therapeutic vaccination due to their ability to induce stronger antibody responses compared to DNA vaccines and their potential for rapid and low-cost large-scale manufacturing (Pardi, Hogan, et al., 2018a). To broaden and optimize the efficacy of *TherVacB* regimen, the following study aimed at evaluating the potency of mRNA vaccine for priming in wild-type mice as well as in HBV carrier mice.

3.2.1 Generation of *RNA-HBVac* for *TherVacB*

Nucleic acid-based vaccines represent promising alternatives to conventional, protein-based therapeutic vaccines. To evaluate the efficacy of mRNA vaccines in the context of persistent HBV replication we generated highly functional IVT mRNA termed *RNA-HBVac*. For this purpose, the original #1116 plasmid was first enzymatically digested with the restriction enzymes *NheI* and *EcoRI* and then cleaned up via gel electrophoresis. The HBVac insert was amplified from the original plasmid (#1116) via a Polymerase Chain Reaction (PCR) reaction. The PCR product was purified by gel electrophoresis and integrated into the digested *RNA-HBVac* plasmid by cloning. As described previously in Figure 3.1, the HBVac expression cassette encodes for five HBV proteins. In order to ensure equimolar expression, HBV proteins were linked via porcine teschovirus-1 2A (P2A) (Luke et al., 2008) and thosea asigna virus 2A

(T2A) (Szymczak & Vignali, 2005) gene sequences. The HBV protein sequences cover T-cell epitopes from genotypes A-E as well as the serotypes *adw* and *ayw* to enable global application of the therapeutic vaccine. Upstream of the HBVac insert, a T7 bacteriophage RNA polymerase-specific promoter was inserted. This RNA polymerase is promoter-specific and transcribes only double-stranded DNA downstream of the promoter to generate RNA transcripts (Rong et al., 1998). The successful insertion of the HBVac insert into the *RNA-HBVac* plasmid was verified by restriction digestion. Next, competent stbl3 *E.coli.* were transformed with *RNA-HBVac* plasmid. Several positive colonies were picked, and informative digestion was performed using restriction enzymes *EcoRI* and *SacI*. As depicted in Fig. 3.25, clone 5 showed a correct digestion profile as two fragments of 5.835 bp and 3.729 bp were generated. The correct sequence of the HBVac insert was confirmed by Sanger sequencing.

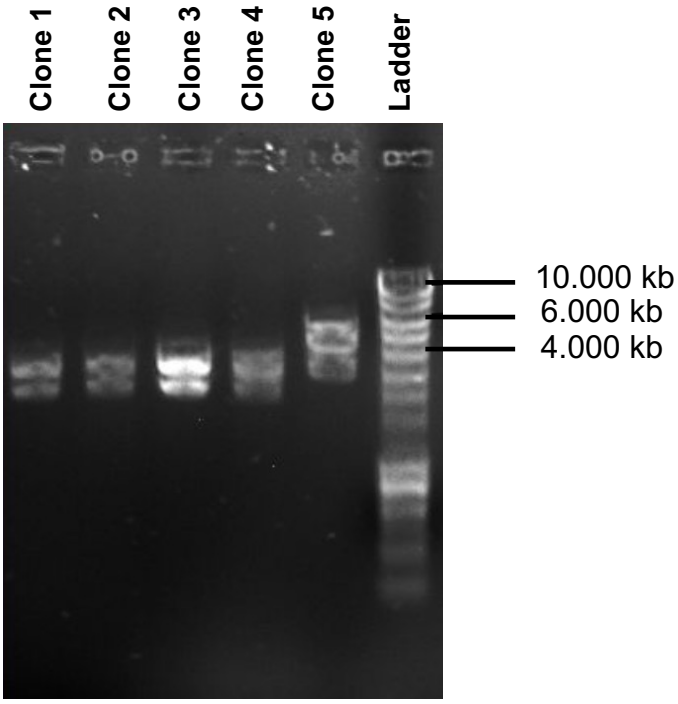

Figure 3.25 Digestion profile of *RNA-HBVac* plasmid
Agarose gel electrophoresis following digestion of *RNA-HBVac* plasmid using restriction enzymes *EcoRI* and *SacI.*

To ensure the functionality of the *RNA-HBVac* plasmid, HepG2 NTCP K7 cells (human hepatoma cell line expressing sodium taurocholate co-transporting polypeptide (NTCP)) were transfected with 0.75, 1.5 and 3.0 µg *RNA-HBVac.* Untransfected cells served as control (Ctrl). HBV-specific protein expression was confirmed by WB analysis of cell lysates 72h after transfection using S-specific- or Core-specific antibodies (Fig. 3.26 left and right respectively). S and L proteins were detected at 24 kDa and 42 kDa in naïve and glycosylated forms,

respectively. A single band of core protein was detected at 19 kDa. No HBV proteins were detected in the control cells.

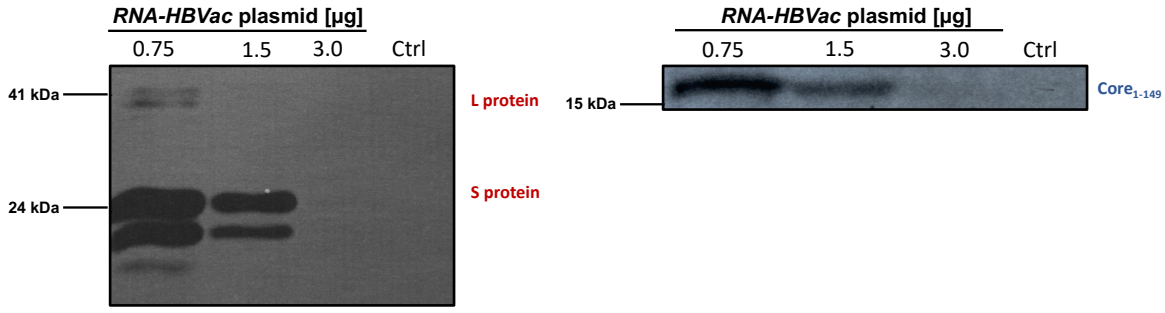

Figure 3.26 Expression of S and Core proteins 72h post-transfection with *RNA-HBVac* plasmid
HepG2 NTCP K7 cells were transfected with 0.75, 1.5, and 3.0 µg of *RNA-HBVac* using Lipofectamine transfection reagent. Untransfected cells served as a control. Cell lysates were separated, and WB analysis was performed using HBsAg- and HBcAg-specific antibodies. S and L proteins were detected around 24 kDa and 42 kDa in naïve and glycosylated forms respectively (left panel). A singular Core protein band was detected at 19 kDa (right panel).

Taken together, these data confirm the successful generation of the *RNA-HBVac* transcription template.

Next, the highly functional IVT mRNA *RNA-HBVac* was generated by T7 *in vitro* transcription using T7 RNA Polymerase for transcription. Transcription was performed as described in the methods section. To improve the functionality and stability of IVT mRNA, ARCA (anti-reverse cap analog) cap structure as well as polyA tail were attached to the mRNA. ARCA cap structure was implemented to strictly insert the cap in the correct orientation due to the 3'-O-methyl group of the ARCA cap. For quality control of IVT mRNA, gel electrophoresis was performed on 2 % agarose gel. Analysis showed a correct generation of untailed and tailed IVT mRNA. To validate IVT mRNA expression and compare it to *RNA-HBVac* plasmid expression, HEK293 (Human Embryonic 293) cells and HepG2 NTCP K7 cells were transfected with 0.5 µg and 1.0 µg *RNA-HBVac* plasmid or IVT mRNA. Untransfected cells served as controls. 96h later, the supernatant was collected for HBsAg and HBeAg measurement. In addition, cell lysates were separated, and WB analysis was performed using HBsAg- and HBcAg-specific antibodies. S and L proteins were detected at 24 kDa and 42 kDa respectively in HepG2 NTCP K7 as well as in HEK 293 cell lysates (data not shown). Core proteins remained undetectable by WB analysis (data not shown). Evaluation of antigen levels secreted in the supernatant of the transfected cells showed that transfection with 0.5 µg *RNA-HBVac* plasmid (transcription template) led to significantly higher HBsAg and HBeAg levels in HEK293 cells compared to HepG2 NTCP K7 cells (Fig. 3.27 A). Transfection of cells with 1 µg IVT mRNA (Fig. 3.27 B)

induced significantly lower but similar antigen levels in the supernatants of both HepG2 NTCP K7 and HEK293 cells compared to plasmid (transcription template) transfection (Fig. 3.27 A). No HBsAg and HBeAg secretion was observed in control cells.

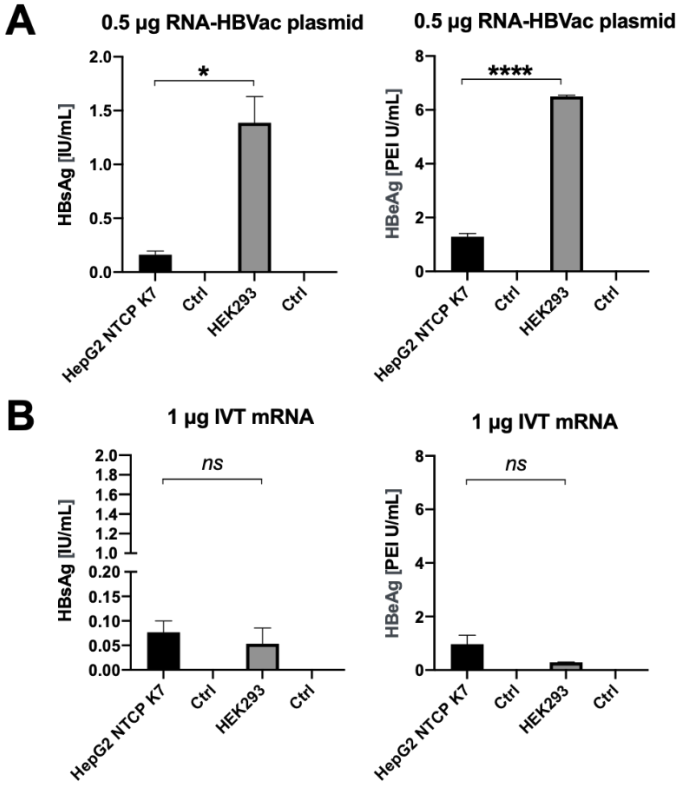

Figure 3.27 HBsAg and HBeAg levels in the supernatant of HepG2 NTCP K7 and HEK293 cells, 96h post-transfection with 0.5 µg *RNA-HBVac* (A) plasmid and 1 µg IVT mRNA (B)
HepG2 NTCP K7 and HEK293 cells were transfected with 0.5 *RNA-HBVac* plasmid and 1 µg IVT mRNA using Lipofectamine (A) or Lipofectamine MessengerMax™ (B) transfection reagent. Untransfected cells served as a control (Ctrl). HBsAg and HBeAg levels were measured in the supernatant using Architect™ platform. Statistical analysis was performed using an unpaired t-test with Welsh's correction (*p<0.05, ****p<0.0001, ns– not significant: p>0,05).

These findings demonstrate that both *RNA-HBVac* transcription template and *RNA-HBVac* IVT mRNA were successfully generated. For the establishment of highly functional *RNA-HBVac* IVT mRNA, chemically modified nucleotides can be introduced to increase protein expression, construct stability, and avoid the activation of the innate immune system by IVT mRNA (Karikó et al., 2005).

3.2.2 Implementation of chemical modifications to enhance the stability and protein expression of *RNA-HBVac* mRNA

RNA administration is known to activate the innate immune system through Toll-like receptors (TLR), Melanoma differentiation-associated gene 5 (MDA5), Retinoic acid-inducible gene I

(RIG-I), and Protein Kinase R (PKR) stimulation. To use mRNA as a therapeutic approach it is essential to inhibit its recognition by innate immune receptors (TLR3, TLR7, TLR8, MDA5, RIG-I, PKR, …) to prevent type I interferons release, stimulation of interferon-stimulated genes and thus translation inhibition (Karikó et al., 2005). Incorporation of chemically modified nucleotide analogs such as N^1 Methyl-pseudo(φ)-Uridine triphosphate (UTP), Pseudo(φ)-UTP, and 5-Methyl (^{5}m)-Cytidine triphosphate (CTP) has been shown to reduce or completely diminish the immunostimulatory effect of IVT mRNA (Karikó et al., 2005). Improved mRNA constructs represent promising therapeutic tools as they enhance mRNA stability and translation efficiency while downregulating innate immune system activation (Karikó et al., 2008). Therefore, mRNAs with two different modifications were generated. N^1 Methyl pseudo(φ)-UTP, and 5-Methyl (^{5}m)-CTP were incorporated in *RNA-HBVac* IVT mRNA 1 construct (Fig. 3.28 A) whereas Pseudo(φ)-UTP, and 5-Methyl (^{5}m)-CTP were used for *RNA-HBVac* IVT mRNA 2 construct (Fig. 3.28 B).

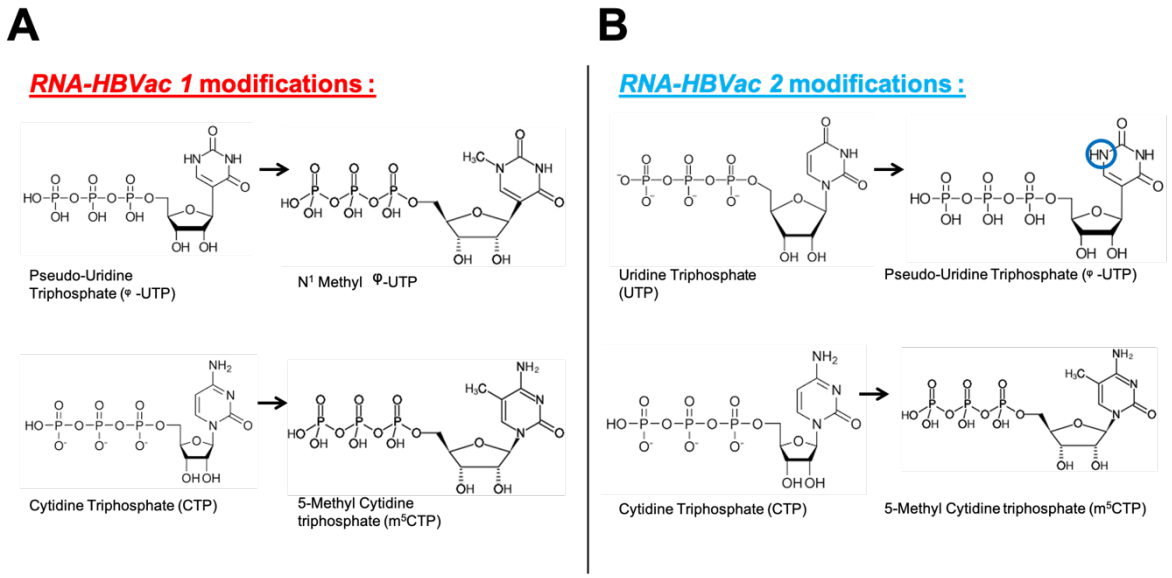

Figure 3.28 Structure of chemically modified nucleotide analogs implemented to *RNA-HBVac* 1 (A) and 2 constructs (B)
UTP analogs (upper panel): N^1 Methyl pseudo(φ)-UTP, Pseudo(φ)-UTP; CTP analog: 5-Methyl (^{5}m)-CTP.

To determine the expression of RNA1 and RNA2 and compare it to *RNA-HBVac* plasmid (P), HEK293 cells were transfected with 4, 2, and 1 µg of both modified RNA constructs. Cells transfected with 0.5 µg *RNA-HBVac* plasmid served as positive, untransfected cells as negative control. 96h post-transfection, the supernatant was collected, and proteins were isolated from cell lysate to perform WB analysis using HBsAg- and HBcAg-specific antibodies. Strong signals were observed in the cell lysates (Fig. 3.29 A) as well as in the supernatant

(Fig. 3.29 B) of samples transfected with 4 µg of both constructs. Signals were weaker in samples treated with 1 µg RNA1 and 2 constructs (Fig. 3.29 A and B).

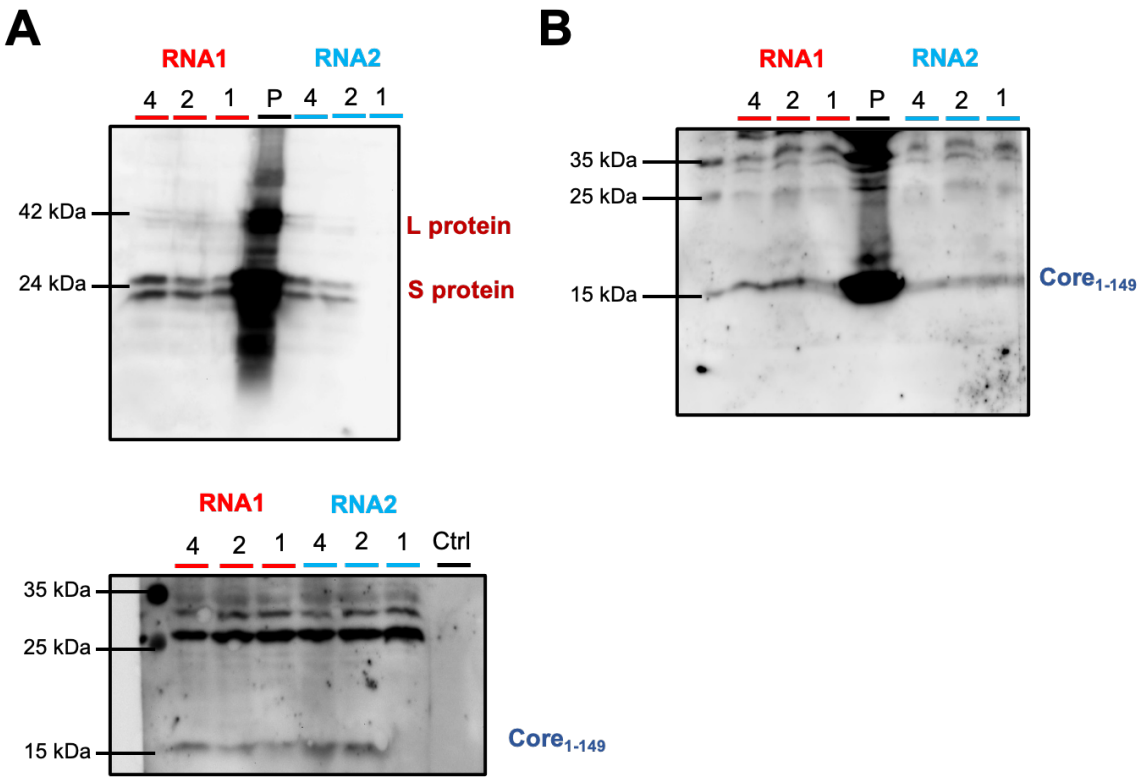

Figure 3.29 Expression of S, L and Core proteins in HEK293 cells 48h post-transfection with modified IVT mRNAs
HEK293 cells were transfected with 4, 2 and 1µg of *modified IVT mRNA (RNA-HBVac 1 or 2)* using Lipofectamine MessengerMax™ transfection reagent. Untransfected cells served as a control. Cell lysates (A) were separated, supernatants (B) were collected and WB analysis was performed using HBsAg- and HBcAg-specific antibodies. S and L proteins were detected around 24 kDa and 42 kDa respectively in naïve and glycosylated forms. Truncated Core protein was detected HBc at 19 kDa.

Taken together, these results indicate that S and Core proteins encoded by the HBVac insert are being correctly expressed in both modified RNA constructs.

3.2.3 Immunogenicity of priming immunization with *RNA-HBVac* in HBV-naïve mice

Based on the *in vitro* results, we investigated whether the mRNA-based therapeutic vaccine *RNA-HBVac* can induce significant HBV-specific humoral and cellular responses in HBV-naïve mice. Recent studies have shown that the incorporation of single modification N^1 Methyl φ-UTP or double N^1 Methyl φ-UTP/^{5}m-CTP modifications outperformed the properties of unmodified mRNA in mice (Andries et al., 2015). Further studies in cell culture reported that N^1 Methyl φ-UTP modification induced the most dramatic increase in protein expression in cells, whereas double modification resulted in similar expression levels. Therefore, optimal protein expression seemed to require only N^1 Methyl φ-UTP modification. Increased protein

expression may be induced by the increased ability of modified mRNA to escape endosomal TLR3 activation and thus downregulate innate immune sensing (Andries et al., 2015; Svitkin et al., 2017). Therefore, in collaboration with Ethris GmbH (Martinsried, Germany), large amounts of lipid nanoparticle (LNP) formulated single N^1 Methyl φ-UTP modified *RNA-HBVac* were produced for immunogenicity evaluation in mice. As shown in Fig. 3.30, HBV-naïve mice were i.m. immunized with a series of two prime immunizations, spaced two weeks apart consisting of LNP-formulated *RNA-HBVac* (100 µg, 50 µg, 25 µg or 12.5 µg), mixed adjuvanted recombinant proteins (10 µg HBsAg + 10 µg HBcAg + 15 µg CpG) or *DNA-HBVac* (50 µg or 100 µg dose) according to prime-boost immunization strategy. At week 4 booster immunization with MVA-HBVac (3×10^7 IFU/mouse) was administered. Mice receiving PBS injections served as controls. At week 5, mice were sacrificed and subjected to analysis.

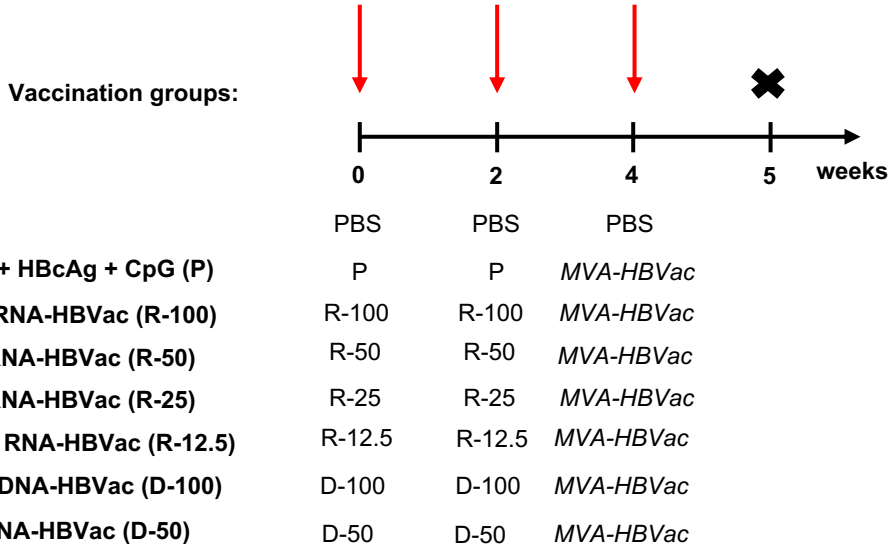

Figure 3.30 Vaccination scheme of prime immunization with *RNA-HBVac* in HBV-naïve mice
Nine-week-old male C57BL/6 mice were intramuscularly immunized three times (red arrows) in a two-week interval (week 0, week 2, and week 4 respectively). All animals received two prime immunizations consisting of either LNP-formulated *RNA-HBVac* (R) (100 µg, 50 µg, 25 µg or 12.5 µg), HBsAg + HBcAg + CpG-1018 (P), or *DNA-HBVac* (D) (50 µg or 100 µg) followed by a final boost immunization with *MVA-HBVac* (3×10^7 IFU/mouse) at week 4. Mice receiving PBS served as controls. Splenectomy and final analysis were performed in week 5.

a. Safety monitoring of immunization with *RNA-HBVac* compared to protein and DNA immunization

Immunization with D-50, D-100, and P resulted in similar and comparable weight increases after first immunization compared to control mice (Fig. 3.31 A). Moreover, weight monitoring remained comparable throughout the experiment (Fig. 3.31 B). No motoric dysfunctions or abscesses could be observed in those groups. In contrast, all mice immunized with *RNA-*

HBVac showed dose-dependent weight loss after the first immunization. The most dramatic weight loss occurred four days after the first priming immunization with *RNA-HBVac*. In mice immunized with R-100, weight loss of >10 % from the original weight at the onset of the experiment was measured at day 4 (Fig. 3.31 C). Motoric dysfunctions were observed in mice receiving R-50 and R-100. In addition, at day 4, abscesses could be observed at the site of injection on two animals immunized with R-100. As a result of these observations, two mice from the R-100 group had to be sacrificed and the two remaining animals did not receive a second prime immunization. Following the second prime immunization, RNA groups (R-50, R-25, and R-12.5) showed similar and comparable weight monitoring throughout the experiment compared to immunization with P or D-50 and D-100 (Fig. 3.31 B and D).

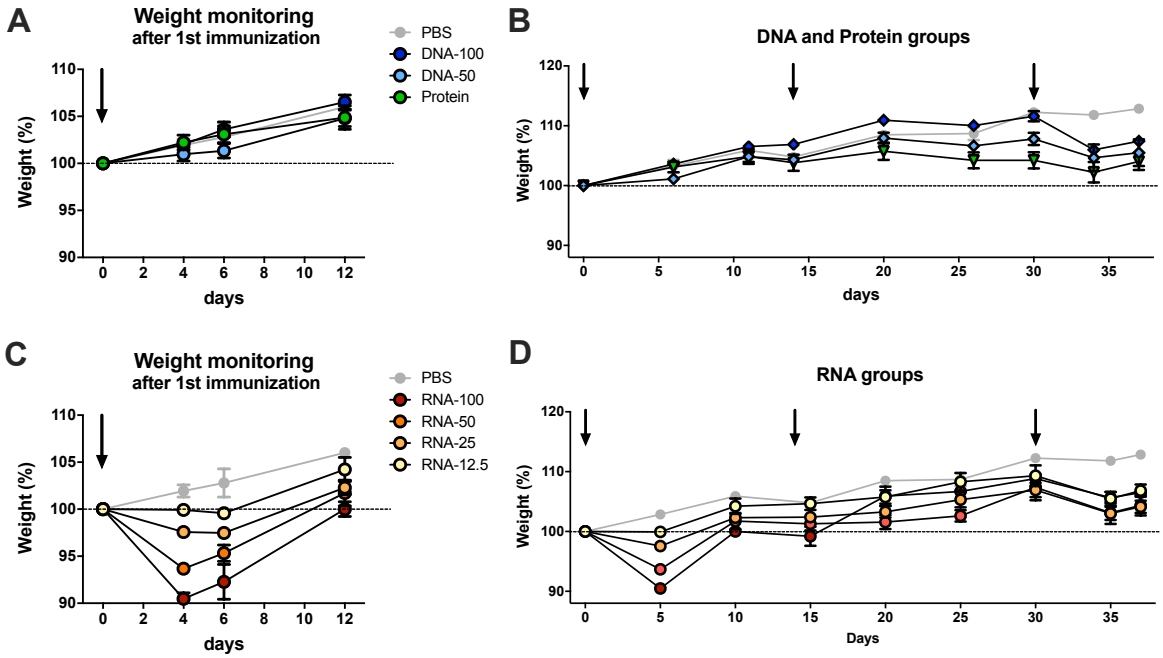

Figure 3.31 Weight monitoring of immunization with *RNA-HBVac* compared to mixed adjuvanted recombinant proteins and DNA
Weight monitoring after first immunization with DNA and mixed adjuvanted recombinant proteins groups (A) as well as RNA groups (C). Body weight monitoring throughout the experiment for DNA and mixed adjuvanted recombinant proteins groups (B) as well as RNA groups (D).

Next, hematoxylin/eosin (HE) staining of the thigh muscles of the hind limb region used for injection of *RNA-HBVac* (100 µg, 50 µg, 25 µg, and 12.5 µg) was performed. Muscle tissue of mice immunized with PBS served as control. Immunization with *RNA-HBVac* resulted in dose-dependent lymphocyte infiltration at the injection site. Immunization with R-100 induced significantly higher lymphocyte infiltration in muscle tissue compared to other *RNA-HBVac* groups and PBS control. Macroscopic purulent abscess was noticed in mice primed with R-100. Faint lymphocyte infiltration was observed in R-25 as well as R-12.5 groups (Fig. 3.32).

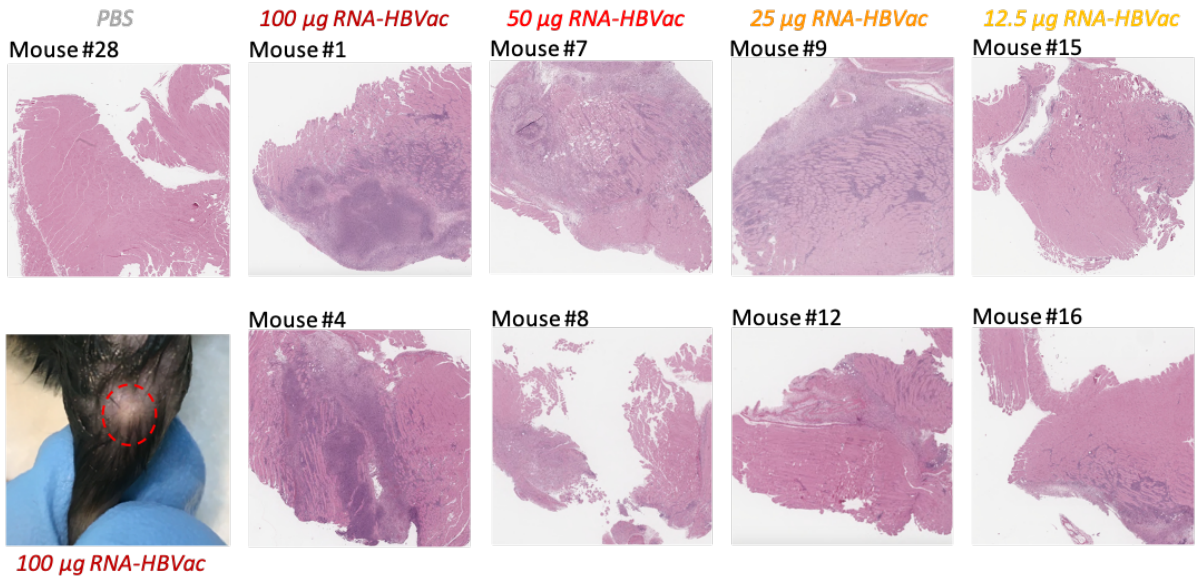

Figure 3.32 Dose-dependent lymphocyte infiltration at injection site after immunization with *RNA-HBVac*
Overview of hematoxylin/eosin staining of the thigh muscles of the hind limb region used for injection of *RNA-HBVac* (100 µg, 50 µg, 25 µg and 12.5 µg). Staining of mice receiving PBS served as controls. Purulent abscess observed at the injection site of one mouse immunized with 100 µg *RNA-HBVac* (lower panel left).

Taken together, these observations indicate that immunization with a high dose of *RNA-HBVac* (100 µg) resulted in highly concerning systemic side-effects. Therefore, considering the observed side effects, *RNA-HBVac* at a dose of 12.5 µg or 25 µg seemed to be the optimal dose for further investigation.

b. HBV-specific humoral and CD4$^+$ T-cell responses

To assess the humoral response, anti-HBc and anti-HBs titers were detected by ELISA in the serum of mice at week 5.

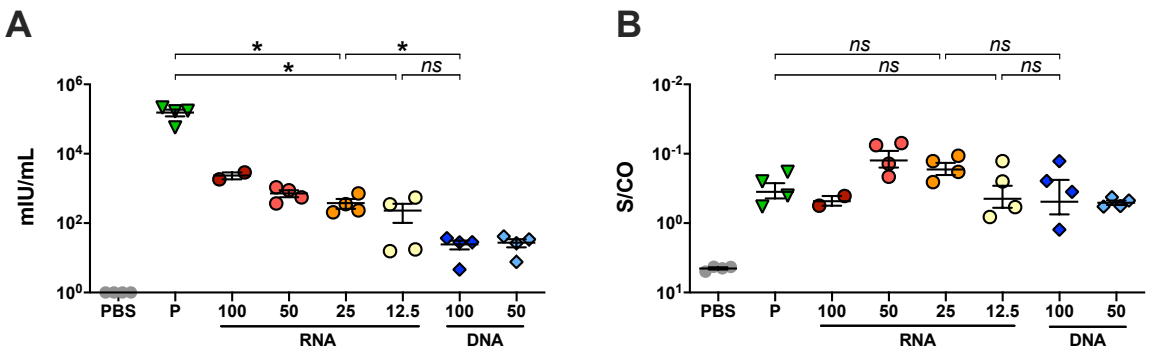

Figure 3.33 HBV-specific antibody responses

Serum levels of (A) anti-HBs and (B) anti-HBc titers detected at week 5. Mean±SEM is shown. Statistical analysis was performed using nonparametric One-Way ANOVA. Symbols represent individual mice. Values of individual mice are shown. Asterisks indicate statistically significant differences (*p<0.05, ns– not significant: p>0,05).

Immunization of mice with *RNA-HBVac* (all groups) showed to induce significantly lower antibody titers compared to immunization with mixed adjuvanted recombinant proteins (P). However, comparison of the anti-HBs antibody levels between the groups of mice vaccinated with *RNA-HBVac* showed that a higher dose of *RNA-HBVac* induced stronger anti-HBs titers. Immunization of mice with R-12.5 resulted in similar anti-HBs titers whereas immunization R-25 induced significantly higher anti-HBs titers compared to D-100 group (*p<0.05) (Fig. 3.33 A). Evaluation of anti-HBc response showed that immunization with *RNA-HBVac* (all groups) and D-100 induced similar anti-HBc titers compared to immunization with the mixed adjuvanted protein antigen group (P) (Fig. 3.33 B). Anti-HBs and anti-HBc titers from mice immunized with PBS remained at baseline level.

Next, the induction of HBV-specific $CD4^+$ T-cell responses after immunization with *RNA-HBVac* was analyzed by intracellular IFNγ-staining of HBV-peptide stimulated splenocytes at the timepoint of sacrifice. As shown in Fig. 3.34 A, vaccination with *RNA-HBVac* led to a lower S-specific $CD4^+$ T-cell response compared to prime immunization with mixed adjuvanted recombinant proteins (P). Low doses of *RNA-HBVac* (R-25 and R-12.5 groups) resulted in slightly higher S-specific $CD4^+$ T-cell responses. Similar core-specific $CD4^+$ T-cell responses were achieved in mice immunized with *RNA-HBVac* (50-12.5 µg) and 100 µg *DNA-HBVac* compared to vaccination with adjuvanted recombinant HBsAg + HBcAg (Fig. 3.34 B). In addition, immunization with *RNA-HBVac* (R-50 – R-12.5) led to comparable RT-specific $CD4^+$ T-cell responses compared to those detected in D-100 group (Fig. 3.34 C). Mice that received mixed adjuvanted protein antigens (P) as a prime did not show RT-specific $CD4^+$ T-cell responses in the spleen. In contrast, in mice primed with R-100 S-, core- and RT-specific $CD4^+$ T-cell responses remained at background level indicating the importance of two prime immunizations to elicit robust and multifunctional $CD4^+$ T-cell responses by RNA vaccination (Fig. 3.34 A-C). As expected, mice immunized with PBS did not show any S-, core- or RT-specific $CD4^+$ T-cell responses in the spleen.

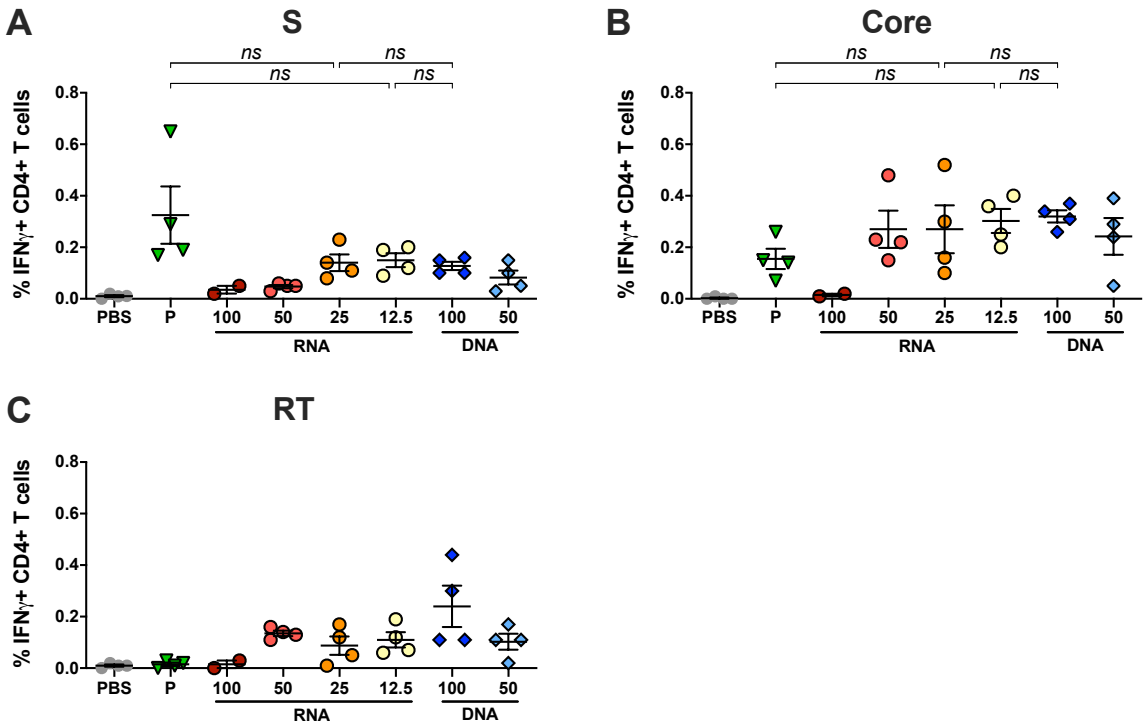

Figure 3.34 HBV-specific CD4⁺ T-cell responses
HBV S- (A), core- (B), and RT (C)-specific IFNγ responses of splenic CD4⁺ T cells after stimulation with overlapping HBV S-, core- and RT-specific peptide pools. Mean±SEM is shown. Statistical analysis was performed using nonparametric One-Way ANOVA. Symbols represent individual mice. Values of individual mice are shown. Asterisks indicate statistically significant differences (*p<0.05, ns– not significant: p>0,05).

Taken together, these results indicate that immunization with *RNA-HBVac* elicits low anti-HBs and comparable anti-HBc titers compared to mixed adjuvanted protein priming (P). The magnitude of core- and RT-specific CD4⁺ T-cell responses were higher in mice receiving *RNA-HBVac* for prime immunization compared to the mixed adjuvanted protein antigen group (P) group. Increasing the RNA dose for priming resulted in lower HBV-specific CD4⁺ T-cell responses. In addition, two prime immunizations were required to elicit robust and multifunctional CD4⁺ T-cell responses by RNA vaccination.

c. Evaluation of HBV-specific CD8⁺ T-cell response

At week 5, HBV-specific splenic CD8⁺ T-cell responses elicited by RNA vaccination with *RNA-HBVac* were analysed by intracellular IFNγ-staining of *ex vivo* stimulated splenocytes. Cells were stimulated with HBV S- and core-specific peptide pools as well as with HBV-specific single peptides S190, S208, RT86, and RT333. Splenocytes isolated from mice immunized with PBS served as negative controls.

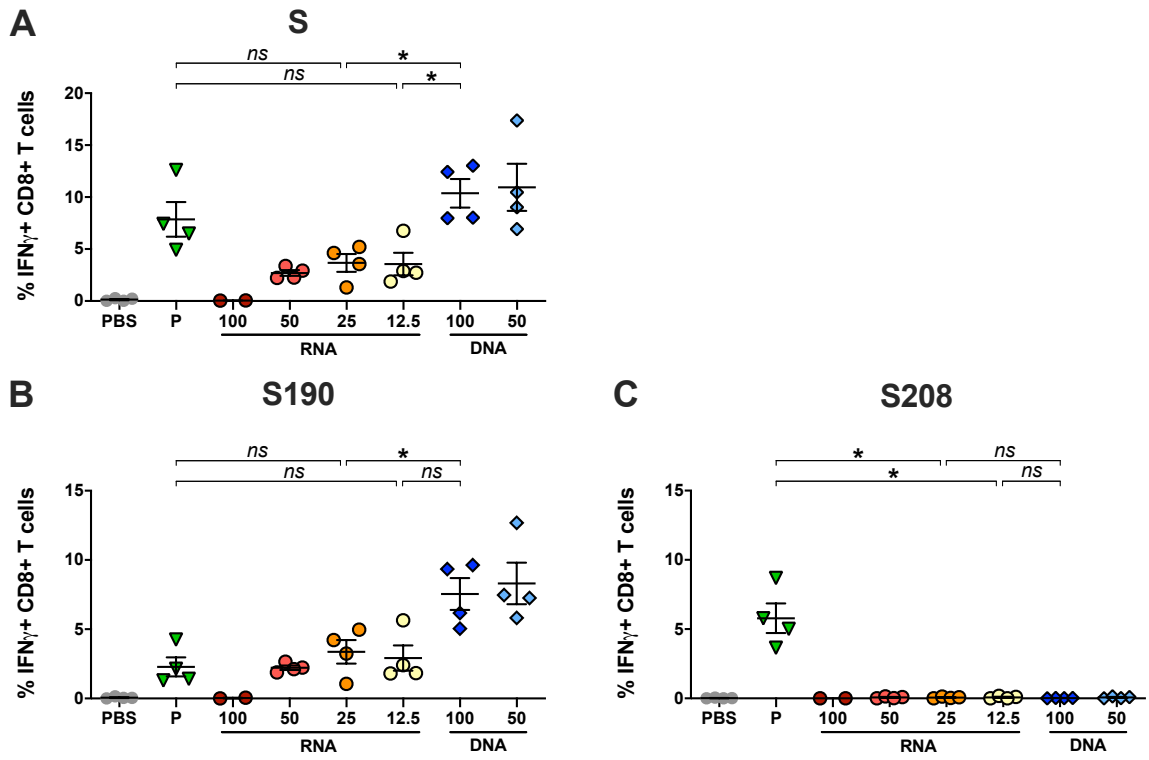

Figure 3.35 Splenic HBV S-specific CD8⁺ T-cell responses
(A) HBV S-specific IFNγ response of splenic CD8⁺ T cells determined by ICS following *ex vivo* stimulation with overlapping HBV S-specific peptide pool and with HBV peptides (B) S190 and (C) S208. Mean±SEM is shown. Statistical analysis was performed using nonparametric One-Way ANOVA. Symbols represent individual mice. Asterisks indicate statistically significant differences (*p<0.05, ns– not significant: p>0,05).

The frequency of S-specific CD8⁺ T cells detected in the spleens of mice immunized with *RNA-HBVac* was lower compared to P and DNA groups (D-50 and D-100). Two immunizations with a higher dose of *RNA-HBVac*, R-50, did not result in a dose-dependent increase of S-specific IFNγ^+ CD8⁺ T cells in spleens (Fig. 3.35 A). Next, IFNγ responses after stimulation of splenic CD8⁺ T cells with S-specific peptides S190 and S208 were further examined. Immunization with R-50 - R-12.5 mostly induced S190-specific CD8⁺ T-cell responses, implying that S-specific CD8⁺ T-cell responses elicited by immunization with *RNA-HBVac* are mostly S190-specific. However, the responses were lower than those elicited by immunization with DNA (Fig. 3.35 B). In addition, in contrary to S190-specific T cells, splenic S208-specific CD8⁺ T-cell responses were mainly detected in mice immunized with mixed adjuvanted protein antigens. Immunization with *RNA-HBVac* as well as *DNA-HBVac* resulted in baseline frequencies of S208-specific CD8⁺ T-cell responses (Fig. 3.35 C).

In addition, priming with *RNA-HBVac* induced lower percentages of core-specific IFNγ^+ CD8⁺ T cells in spleens compared to the mixed adjuvanted protein antigen group (P) or DNA groups. Frequencies of core-specific CD8⁺ T cells were similar in *RNA-HBVac* groups (R-50 – R-12.5)

(Fig. 3.36 A). Percentages of RT86-specific IFNγ$^+$ CD8$^+$ T cells in spleens of mice vaccinated with R-50 and R-25 were similar to those induced by the mixed adjuvanted protein antigen group (P) and therefore not RT86 peptide-specific. Splenic frequencies of RT86-specific IFNγ$^+$ CD8$^+$ T cells in mice vaccinated with R-12.5 as well as in mice receiving only one immunization with R-100, remained at baseline level (Fig. 3.36 B). In contrast, the magnitude of IFNγ$^+$ CD8$^+$ T cells stimulated with RT333 peptide resulted in similar responses in both R-25 and D-100 groups. Prime immunizations with R-25 elicited the strongest RT333-specific IFNγ$^+$ CD8$^+$ T cell responses within the spleens of all mice vaccinated with *RNA-HBVac* (Fig. 3.36 C).

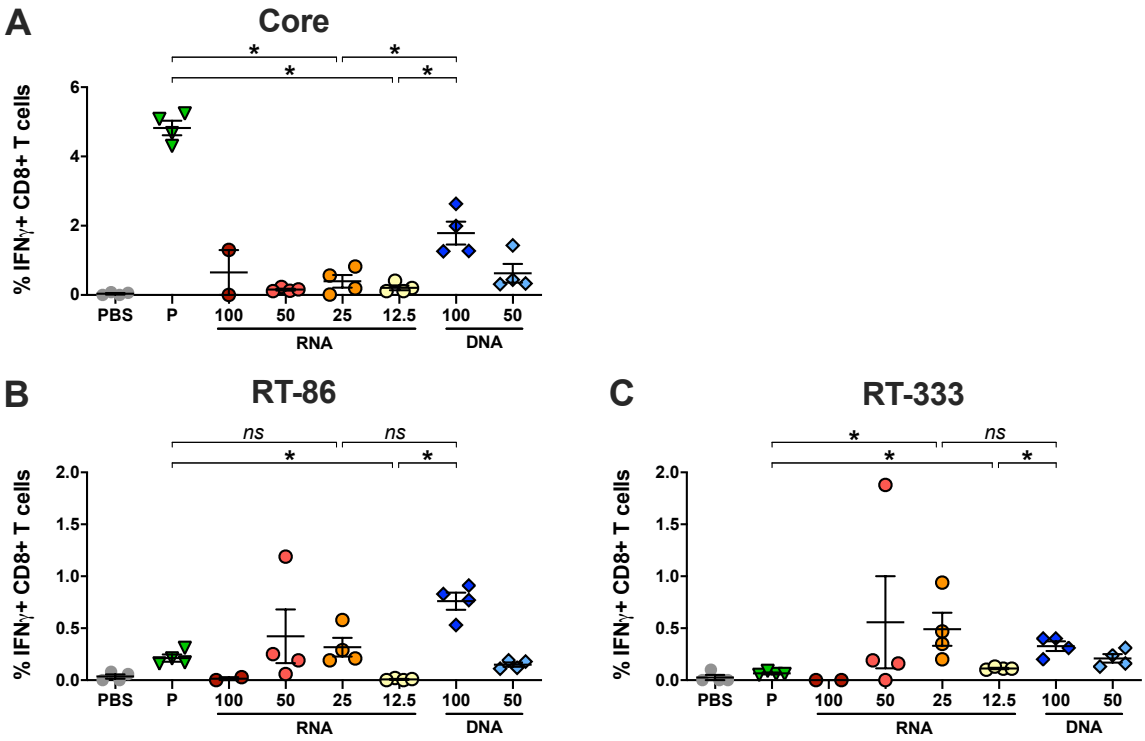

Figure 3.36 Splenic HBV Core- and RT-specific CD8$^+$ T-cell responses
(A) Core-specific IFNγ responses of splenic CD8$^+$ T cells determined by ICS following *ex vivo* stimulation with overlapping HBV core-specific peptide pool. Flow-cytometry analysis of ICS of CD8$^+$ T cells after *ex vivo* stimulation with HBV peptides (B) RT86 and (C) RT333. Mean±SEM is shown. Statistical analysis was performed using nonparametric One-Way ANOVA. Symbols represent individual mice. Asterisks indicate statistically significant differences (*p<0.05, ns– not significant: p>0,05).

These findings demonstrated that priming immunizations with *RNA-HBVac* induced higher anti-HBs titers compared to DNA priming. Two priming immunizations with *RNA-HBVac* were required to induce significant and polyfunctional T-cell responses in HBV-naïve mice. Immunization with *RNA-HBVac* elicited lower frequencies of S-, core- and RT-specific CD4$^+$ and CD8$^+$ T-cell responses compared to the protein antigen group (P) or DNA groups. For *RNA-HBVac*, the HBV S-specific CD8$^+$ T-cell response is mostly S190 peptide-specific. An increase of *RNA-HBVac* dose for priming resulted in dose-dependent systemic side effects and did not result in higher frequencies of HBV S-, Core- and RT-specific T-cell responses. R-

25 group elicited the strongest RT-specific $CD8^+$ T-cell response within RNA groups. Therefore, R-25 dose was selected to be used in further studies.

3.2.4 Evaluation of the long-term immunogenicity of RNA prime – MVA boost in HBV carrier mice

Following immunogenicity evaluation and optimal dose evaluation of *RNA-HBVac* for priming in HBV-naïve mice, immune responses elicited by *RNA-HBVac* in a persistent infection mouse model (AAV-HBV) were assessed. As shown in Fig. 3.37 nine-week-old C57BL/6 mice were i.v. transduced with AAV-HBV six weeks before the onset of the experiment to establish persistent HBV replication. Six weeks later, mice were i.m. immunized twice in two-week intervals with either adjuvanted recombinant proteins (10 µg HBsAg + 10 µg HBcAg + 15 µg CpG) (P), 100 µg *DNA-HBVac* (D-100) (D), 25 µg Lipid nanoparticle (LNP) formulated *RNA-HBVac* (LNP-25) or unformulated *RNA-HBVac* (25 µg or 100 µg dose, UF-25 and UF-100 respectively). At week 4, *MVA-HBVac* booster immunization ($3x10^7$ IFU *MVA-HBVac*/mouse) was administered. Mice receiving PBS injections served as controls. Nineteen weeks after the onset of the vaccination mice were sacrificed and analysed.

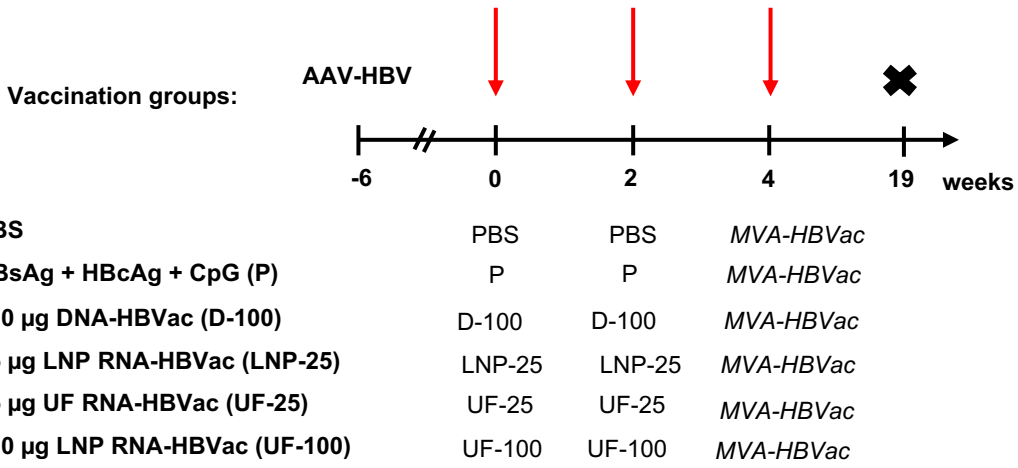

Figure 3.37 Vaccination scheme of prime immunizations with *RNA-HBVac* in HBV carrier mice
Nine weeks old C57BL/6 mice were i.v. transduced with AAV-HBV to establish persistent HBV replication. Six weeks later, mice were i.m. immunized three times (red arrows) in a two-week interval (week 0, week 2, and week 4 respectively). All animals received two prime immunizations consisting of either HBsAg + HBcAg + CpG (P), 100 µg *DNA-HBVac* (D-100) (D), 25 µg LNP formulated *RNA-HBVac* (LNP-25) or unformulated *RNA-HBVac* in 25 µg or 100 µg dose, named UF-25 and UF-100 respectively. At week 4 mice received a booster immunization with *MVA-HBVac* ($3×10^7$ IFU/mouse). Mice receiving PBS served as controls. The final analysis was performed at week 19.

a. HBV-specific humoral and $CD4^+$ T-cell responses induced by RNA prime – MVA boost immunization in HBV carrier mice

To determine the effect of prime immunizations with *RNA-HBVac* on HBsAg levels, and anti-HBs antibody generation in the sera of mice, HBsAg levels were assessed throughout the experiment, and anti-HBs titers were measured at the final analysis.

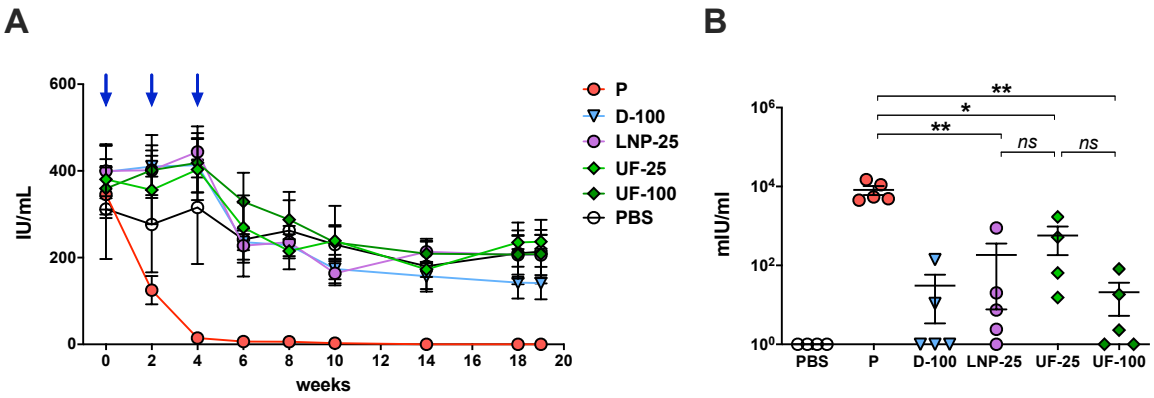

Figure 3.38 Serum HBsAg levels and anti-HBs titers induced by immunization with *RNA-HBVac* in HBV carrier mice
(A) Serum HBsAg levels throughout the experiment. (B) Serum levels of anti-HBs titers at week nineteen after priming. Mean±SEM is shown. Statistical analysis was performed using nonparametric One-Way ANOVA. Symbols represent individual mice. Values of individual mice are shown. Asterisks indicate statistically significant differences (*p<0.05, **p<0.005, ns– not significant: p>0,05).

While a profound decrease in HBsAg levels could be observed in the sera of mice vaccinated with recombinant proteins (P), a minor and comparable drop in HBsAg levels could be observed in all RNA groups. Immunization with LNP-25 as well as with UF-25 seemed to induce a slightly stronger drop in HBsAg levels compared to 100-UF. In addition, two doses of *RNA-HBVac* in combination with *MVA-HBVac* booster immunization were required to achieve HBsAg drop in the sera of vaccinated animals. In the control group, HBsAg levels remained stable throughout the whole experiment (Fig. 3.38 A). Next, the impact of priming with *RNA-HBVac* on anti-HBs generation was assessed by the detection of anti-HBs antibodies in the sera of mice at week 19. Mice primed with *RNA-HBVac* showed similar anti-HBs titers compared to DNA priming (D-100), however, those were significantly lower than detected in animals vaccinated with P (**p<0.005) (Fig. 3.38 B). LNP-formulated *RNA-HBVac* (LNP-25) did not induce higher anti-HBs titers in the sera of mice compared to unformulated RNA-*HBVac* groups (UF-25 and UF-100). UF-25 subgroup seemed to induce slightly stronger anti-HBs antibody titers within all RNA groups. Immunization of control mice with PBS did not induce any anti-HBs antibodies (Fig. 3.38 B). Taken together anti-HBs titers correlated with the minor drop in HBsAg levels observed in all mice vaccinated with *RNA-HBVac*.

To evaluate long-term CD4$^+$ T-cell responses elicited in livers and spleens by priming with *RNA-HBVac,* intracellular IFNγ staining of HBV peptide-stimulated splenocytes and LALs was performed at week 19.

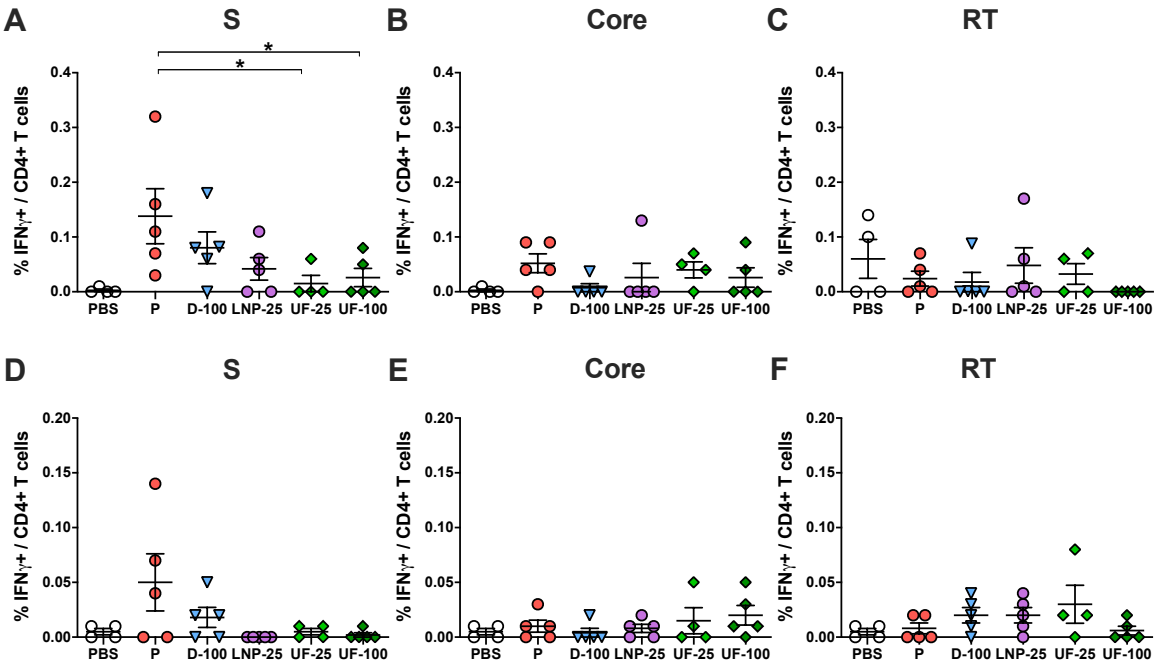

Figure 3.39 Hepatic and splenic CD4$^+$ T-cell responses induced by RNA prime – MVA boost immunization in HBV carrier mice
HBV-specific IFNγ responses of CD4$^+$ T cells determined by ICS following *ex vivo* stimulation with overlapping HBV S-, core- and RT-specific peptide pools in livers (A-C) and spleens (D-F). Mean±SEM is shown. Statistical analysis was performed using nonparametric One-Way ANOVA. Symbols represent individual mice. Values of individual mice are shown (*p<0.05).

All *RNA-HBVac* groups induced low S-specific CD4$^+$ T-cell responses in livers compared to priming with *DNA-HBVac* or mixed adjuvanted recombinant proteins (P). Within RNA groups, the strongest S-specific CD4$^+$ T-cell response was observed in the livers of mice immunized with LNP-25 (Fig. 3.39 A). In contrast, employing unformulated *RNA-HBVac* for priming (UF-25 and UF-100) induced slightly higher core-specific CD4$^+$ T-cell responses in the livers compared to formulated *RNA-HBVac* (LNP-25 group) which resulted in baseline responses (Fig. 3.39 B). In addition, using LNP-25 or UF-25 as a prime, resulted in low and comparable RT-specific CD4$^+$ T-cell responses in the livers of mice. UF-100 did not induce any RT-specific CD4$^+$ T-cell response (Fig. 3.39 C). In all RNA groups, barely detectable S-, core-and RT-specific CD4$^+$ T-cell responses could be detected in spleens of immunized mice (Fig. 3.39 D-F). As expected, vaccination of control mice with PBS did not induce S-, core, or RT-specific CD4$^+$ T-cell responses in livers and spleens.

b. HBV-specific CD8$^+$ T-cell responses induced by RNA prime – MVA boost immunization in HBV carrier mice

To determine whether heterologous formulated or unformulated *RNA-HBVac* vaccination can break immune tolerance against HBV antigens, HBV-specific CD8$^+$ T-cell responses were assessed at the endpoint. To analyze antigen-specific CD8$^+$ T cells generated by vaccination with *RNA-HBVac*, LALs, and splenocytes were stained *ex vivo* with S- and core-specific multimers S190 and C93, respectively.

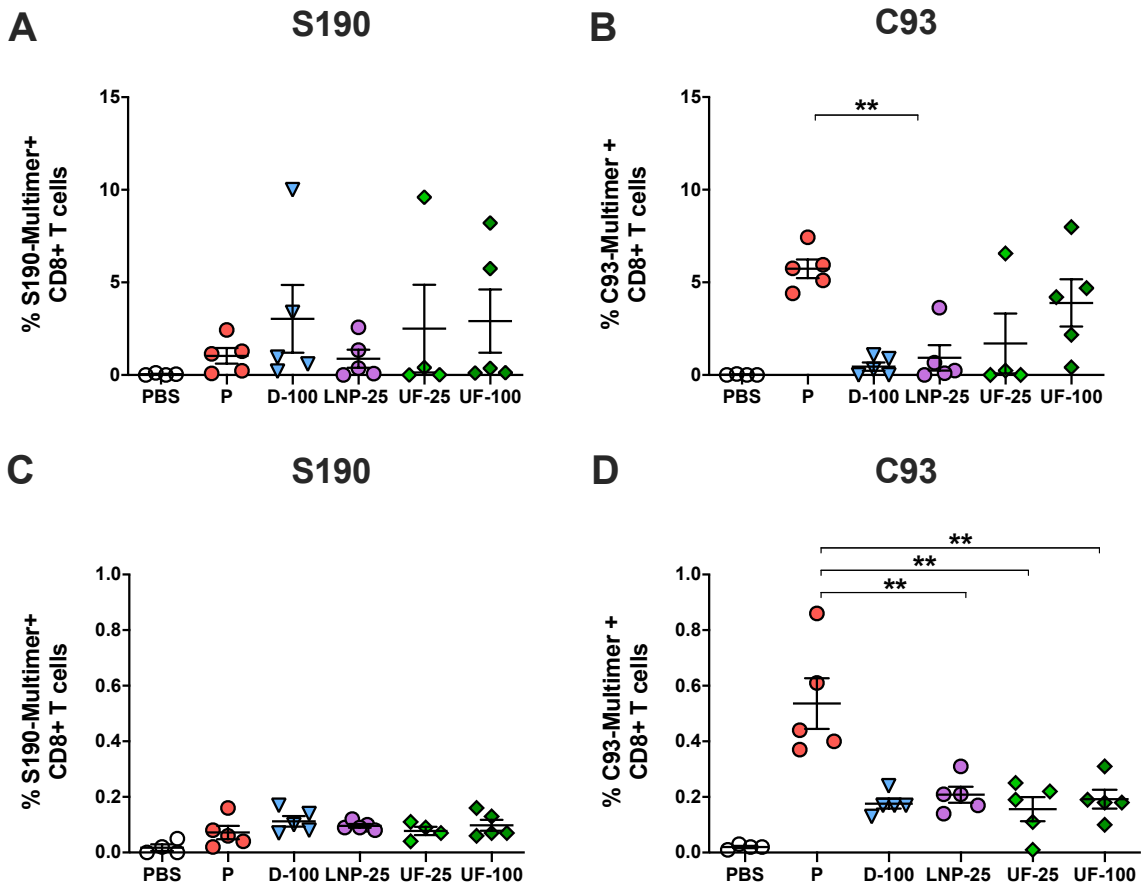

Figure 3.40 Induction of antigen-specific CD8$^+$ T cells by RNA prime – MVA boost immunization in HBV carrier mice
Frequencies of (A, C) S190- and (B, D) C93-antigen specific CD8$^+$ T cells in the (A-B) liver and (C-D) spleen determined by multimer staining of LALs and splenocytes. Mean±SEM is shown. Statistical analysis was performed using nonparametric One-Way ANOVA. Symbols represent individual mice. Values of individual mice are shown. Asterisks indicate statistically significant differences (**p<0.005).

Low and comparable frequencies of S190-specific CD8$^+$ T cells were detected in the livers (Fig. 3.40 A) and spleens (Fig. 3.40 C) of all experimental mice. Immunization with *RNA-HBVac* (all groups) resulted in low frequencies of C93-specific CD8$^+$ T cells compared to the mixed adjuvanted protein antigen group (P) in livers (Fig. 3.40 B) and spleens (Fig. 3.40 D). Immunization with LNP formulated as well as unformulated *RNA-HBVac* in dose 25 µg (LNP-

25 and UF-25 groups) induced barely detectable intrahepatic C93-specific CD8$^+$ T cells which were comparable to those elicited by D-100. Within RNA groups, a slight tendency of stronger induction of intrahepatic C93-specific CD8$^+$ T cells was observed in mice primed with UF-100 (Fig. 3.40 B). In contrast to the high frequencies of splenic C93-specific CD8$^+$ T cells induced by immunization with adjuvanted recombinant proteins (P), frequencies elicited by all RNA and DNA groups remained low and similar (Fig. 3.40 D).

Next, functional analysis of S-, core- and RT-specific CD8$^+$ T cells was performed by intracellular IFNγ staining of *ex vivo* stimulated LALs and splenocytes with overlapping HBV peptide pools as well as single HBV peptides.

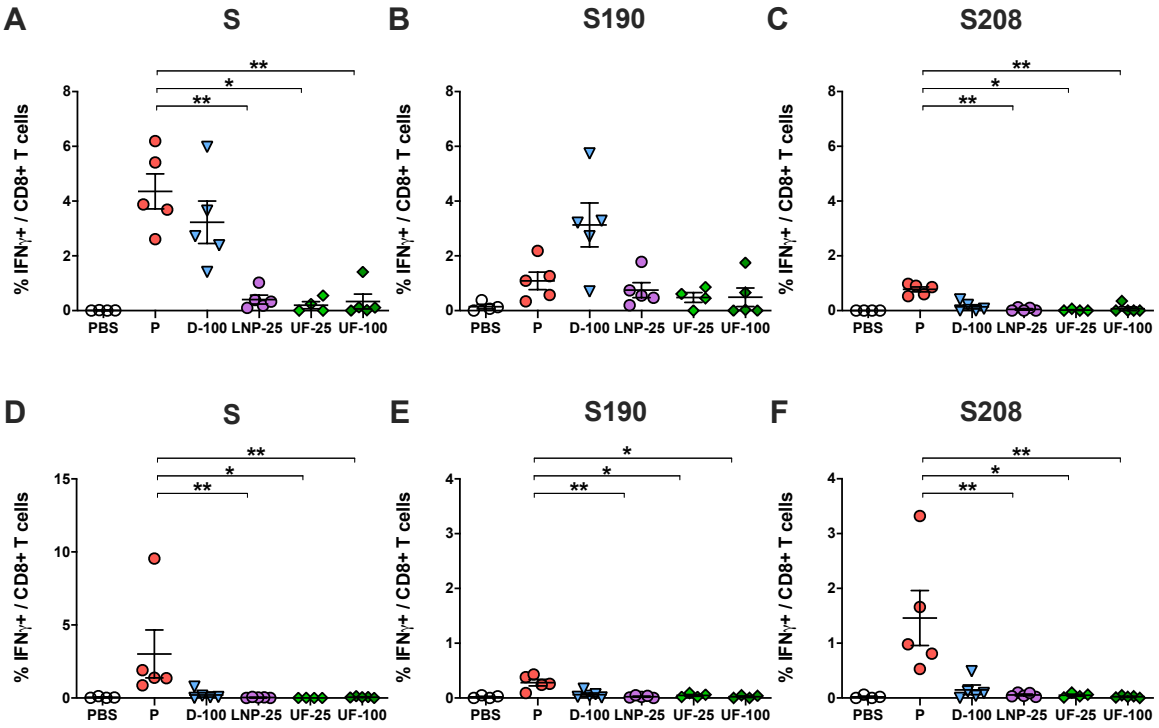

Figure 3.41 Functional analysis of hepatic and splenic S-specific CD8$^+$ T cells elicited by RNA prime – MVA boost vaccination in HBV carrier mice
Percentages of S-specific IFNγ^+ CD8$^+$ T cells in (A) livers and (D) spleens determined by intracellular IFNγ staining following *ex vivo* stimulation with overlapping S-specific peptide pool. Percentages of S190- and S208-specific IFNγ^+ CD8$^+$ T cells in (B-C) livers and (E-F) spleens determined by intracellular IFNγ staining following *ex vivo* stimulation with HBV peptides S190 and S208. Mean±SEM is shown. Statistical analysis was performed using nonparametric One-Way ANOVA. Symbols represent individual mice. Values of individual mice are shown. Asterisks indicate statistically significant differences (*p<0.05, **p<0.005).

As shown in Fig. 3.41, S-specific IFNγ^+ CD8$^+$ T cells were not detectable in (A) livers and (D) spleens of mice immunized with *RNA-HBVac* (LNP-25, UF-25 and UF-100 groups) compared to those receiving mixed adjuvanted recombinant proteins or D-100 as a prime. Priming

immunization with *RNA-HBVac*, stimulated long-term, in all subgroups, low and similar S190-specific IFNγ^+ CD8$^+$ T-cell responses in the liver compared to prime immunization with DNA (Fig. 3.41 B). Vaccination with *RNA-HBVac* resulted in barely detectable S208-specific IFNγ^+ CD8$^+$ T cells in the livers of mice from all RNA subgroups (Fig. 3.41 C). Splenic S190- as well as S208-specific IFNγ^+ CD8$^+$ T cell responses, remained at baseline level within all RNA groups (Fig. 3.41 E and F). As expected, in control mice no HBV S-, S190 and S208-specific IFNγ^+ CD8$^+$ T-cell responses were detected (Fig. 3.41 A-F).

Immunization with mixed adjuvanted protein antigens (P) resulted in high frequencies of core-specific IFNγ^+ CD8$^+$ T-cell responses in the livers (Fig. 3.42 A) and spleens (Fig. 3.42 B) of immunized mice. By contrast, the percentages of core-specific IFNγ^+ CD8$^+$ T-cell responses detected in the livers and spleens of mice immunized with *RNA-HBVac* (all subgroups) as well as with *DNA-HBVac* were low and comparable (Fig. 3.42 A and B). Within RNA groups slightly higher intrahepatic core-specific IFNγ^+ CD8$^+$ T-cell responses were assessed in LNP-25 and UF-100 subgroups (Fig. 3.42 A). In addition, almost undetectable RT-specific IFNγ^+ CD8$^+$ T-cell responses could be detected in the livers and spleens of mice receiving *RNA-HBVac* for prime immunization (Fig. 3.42 C and D).

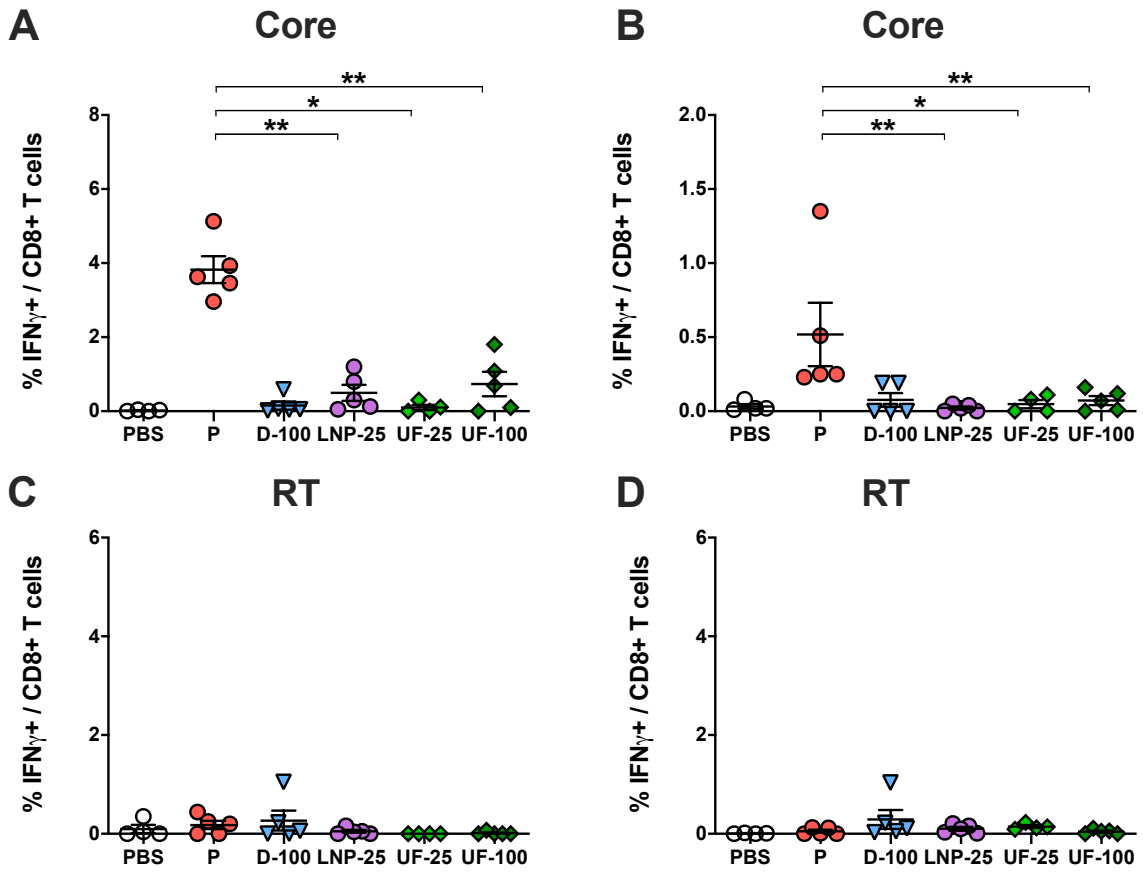

Figure 3.42 Functional analysis of core- and RT-specific CD8⁺ T cells elicited by RNA prime – MVA boost vaccination in HBV carrier mice
Percentages of (A-B) core- and (C-D) RT-specific IFNγ^+ CD8$^+$ T cells in the (A, C) liver and in the (B, D) spleen determined by intracellular IFNγ staining of LALs and splenocytes following *ex vivo* stimulation with overlapping core- and RT-specific peptide pools. Mean±SEM is shown. Statistical analysis was performed using nonparametric One-Way ANOVA. Symbols represent individual mice. Values of individual mice are shown. Asterisks indicate statistically significant differences (*p<0.05, **p<0.005).

To examine the impact of *RNA-HBVac*-based vaccination on long-term HBV replication in HBV carrier mice, HBeAg levels as well as ALT activity were monitored throughout the experiment. The quantification of HBeAg levels in the serum was performed by ELISA.

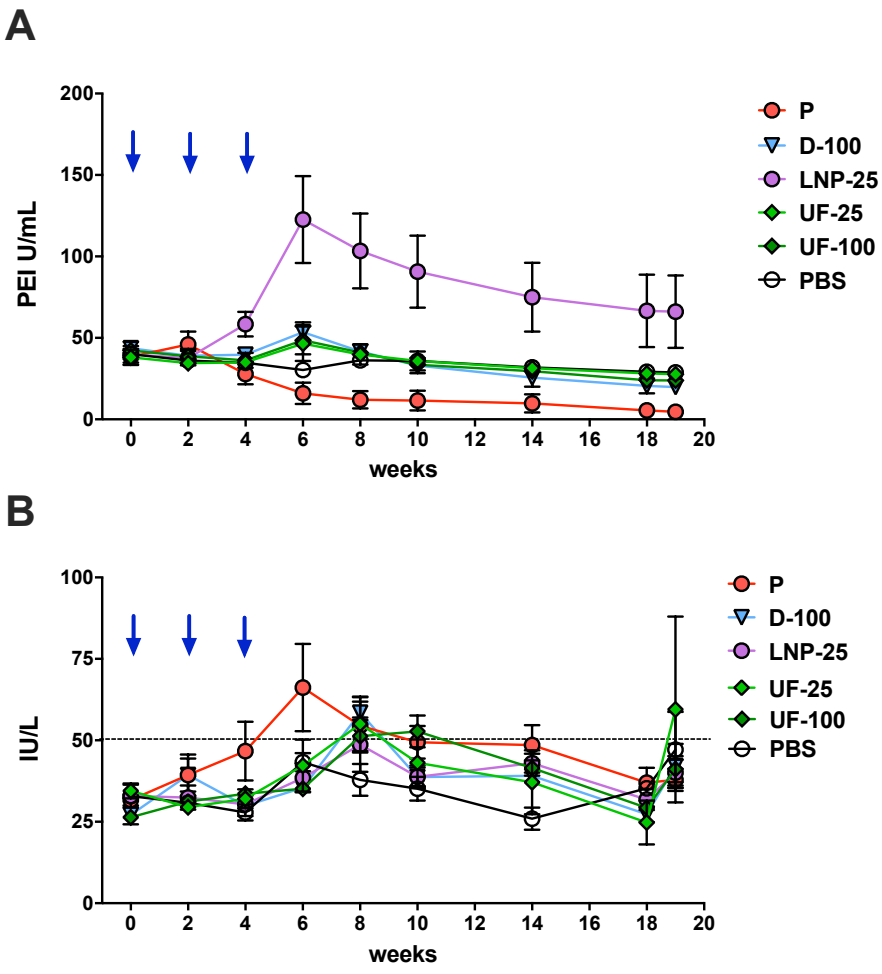

Figure 3.43 Evaluation of the antiviral effect induced by RNA prime – MVA boost immunization in HBV carrier mice
(A) HBeAg kinetics and (B) serum ALT activity throughout the experiment. Mean±SEM is shown. Values of individual mice are shown.

Compared to baseline HBeAg levels at week 0, the strongest decrease in HBeAg levels was observed in the sera of mice immunized with mixed adjuvanted protein antigens (P). In the groups of mice immunized with unformulated *RNA-HBVac* (UF-25 and UF-100) as well as with

D-100, similar and non-significant drops in HBeAg levels were detected in the sera. Unexpectedly, following the second prime immunization with LNP-25, a profound increase in HBeAg levels was observed in the sera. In those animals, peak HBeAg levels were detected at week 6, two weeks after booster immunization with *MVA-HBVac*. Even if a continuous drop in HBeAg levels was observed, at the final analysis, HBeAg levels did not show any reduction compared to HBeAg levels at the onset of the experiment (week 0) (Fig. 3.43 A). As depicted in Fig. 3.43 B, in mice immunized with mixed adjuvanted protein antigens (P), the highest ALT levels were detected two weeks after booster immunization (week 6) whereas *RNA-HBVac* primed animals showed an ALT-peak four weeks after booster immunization (week 8). As predicted, control mice injected with PBS mainly did not show any decrease in HBeAg levels throughout the experiment (Fig. 3.43 A) and ALT activity remained stable over time (Fig. 3.43 B).

Taken together, these findings demonstrated that the use of *DNA-HBVac* or mixed adjuvanted recombinant proteins as a prime, induced better long-term HBV-specific $CD8^+$ and $CD4^+$ T-cell responses in HBV carrier mice compared to *RNA-HBVac*. No significant increase in HBV-specific T-cell responses nor antiviral activity was detected in mice primed with LNP formulated instead of unformulated *RNA-HBVac.* Overall, the use of protein antigens for prime vaccination within the *TherVacB* regimen proved superior to either DNA or RNA vaccines.

4 Discussion

CHB represents a major health burden leading to approximately 820.000 deaths/year (WHO). Despite available treatment options that can suppress viral replication, the cure of CHB remains a challenge. In CHB HBV-specific B- and T-cell responses are insufficient and dysfunctional. Therefore, the induction of a strong HBV-specific immune response by therapeutic vaccination represents a promising strategy to achieve a functional cure. Recently, we developed a clinical candidate therapeutic vaccine, termed *TherVacB*, based on two protein prime immunizations and booster immunization with MVA expressing HBV antigens. In preclinical animal models of persistent HBV infection, we have shown that *TherVacB* was able to induce strong humoral and cellular immune response and led to long-term immune control of HBV (Backes et al., 2016; Kosinska et al., 2017). These encouraging results may initiate the translation of *TherVacB* into the clinics in the future. Nevertheless, we found that the success of therapeutic vaccination largely depended on the compatibility of the sequences between the vaccine and the endogenous HBV. In the present dissertation, the *TherVacB* priming strategy was improved using DNA- or mRNA-based vaccines to achieve a broader T-cell response covering the main HBV serotypes and genotypes, that commonly infect CHB patients.

4.1 Impact of the vaccination scheme on *DNA-HBVac* vaccine efficacy

The goal of vaccines is to establish immunogenicity against a pathogen potentially responsible for causing a life-threatening disease. It is known that potent vaccine-induced immunogenicity and efficacy largely depend on the appropriate prime-boost immunization strategy (Palgen et al., 2018). Therefore, the conducted studies focus on determining the appropriate priming immunization protocol of *DNA-HBVac* to further optimize the immunogenicity elicited by *TherVacB*.

According to the WHO, the objective of priming immunization is to sensitize the immune system to stimulate a protective immune response against the artificially administered antigens. The acquired long-term immune protection enables complete protection of the organism in case the individual may be exposed naturally to the pathogen (WHO, 2021). Previous studies have shown that using recombinant viral vector vaccines such as MVA as a single boost immunization can expand HBV-specific T-cell and humoral responses elicited by priming immunizations (Backes et al., 2016). MVA-based vectors can be easily designed according to one's individual needs thus enabling the expression of the antigens of interest to improve and broaden the immune responses achieved after priming. Therefore, prime-boost vaccination was employed to further improve the potential of therapeutic vaccines to cure

hepatitis B. Immunogenicity against the vector itself has to be taken into account, however, major concern arises mainly after repeated immunization (Kastenmuller et al., 2007).

4.2 Advantages, disadvantages, and improvements of DNA vaccines over protein or viral vector vaccines

Nucleic acid vaccines have numerous advantages over protein vaccines such as safety, the ability to induce cellular immune responses through MHC-I and MHC-II mediated antigen presentation, the capacity to simply adapt to emerging variants by cloning techniques as well as their easy and low-cost high-scale amplification and purification (Robinson & Pertmer, 2000; Sasaki et al., 2003; Sun et al., 2010). In addition, DNA vaccines can be combined with other DNA vaccines or various vaccine subtypes to enhance and broaden immune responses (Khan, 2009; Konishi et al., 2003). This immunization regimen is known as heterologous prime-boost vaccination. *In vivo,* expression of the encoded antigens mimics normal eukaryotic protein expression as their structure resembles more closely intracellular proteins including post-translational modifications (Alarcon et al., 1999). Furthermore, DNA vaccines are highly stable enabling their use in settings lacking a cold chain (Grunwald & Ulbert, 2015). Disadvantages of DNA vaccines are their limitation to protein-based immunogens, the potential induction of tolerance against the antigens expressed *in vivo*, their inability to induce potent humoral responses, and the risk of DNA integration into the host genome which may trigger cancer (Khan, 2009; Kindt et al., 2007). A variety of aspects must be considered while designing a DNA vaccine, such as the selection of the antigens, the vector, the immunization route, the interval between two immunizations, the selected adjuvants as well as boosting mechanism. All these factors are crucial for the magnitude, breadth, and quality of the immune responses elicited by vaccination. The plasmid backbone used for the expression of the antigens of interest can be optimized using promoters, enhancers, and introns which increase the expression levels of the desired antigens (Khan, 2013). It was shown that the implementation of the human T cell leukemia virus type 1 HTLV-1 sequence into the DNA vaccine backbone remarkably enhanced antigen expression as well as the immunogenicity against the encoded viral antigens (Barouch et al., 2005). Hence, within the *DNA-HBVac* plasmid backbone regulatory elements optimization was performed through the incorporation of a regulatory sequence from the R region of the HTLV-1 to the CMV promoter. An adjuvant is an additional component to the vaccine itself which significantly potentiates the immunogenicity of the vaccine. Adjuvants trigger the innate immune system to increase the magnitude of B and T cells to confer protective immunity (McKee et al., 2010; McKee et al., 2007). Reasons for incorporating adjuvants into a vaccine are numerous. Adjuvants are used to generate appropriate and broad functional immune responses against a specific pathogen, expand the

repertoire of memory T-cells, and increase the rapidity of humoral and cellular immunity against a pathogen in case of a pandemic outbreak (Galli et al., 2009; Huleatt et al., 2007; Khurana et al., 2010; Leroux-Roels et al., 2010). To mimic clinical application in the conducted studies, the adjuvant CpG, an oligonucleotide from Dynavax containing unmethylated CpG motifs and used as an adjuvant in the prophylactic protein vaccine against HBV (Heplisav-B^{TM}) was used (Campbell, 2017). CpG is known to stimulate the innate immune system through activation of TLR9 which stimulates antibody production, Th1 responses, and $CD8^+$ T cells (Coffman et al., 2010). In this study, it was shown that immunization with *DNA-HBVac*, HBsAg, and CpG led to the production of high titers of anti-HBs antibodies compared to immunization with *DNA-HBVac* + CpG or *DNA-HBVac* + HBsAg groups (Fig.3.14). In the *DNA-HBVac* + HBsAg + CpG group HBV-specific T-cell responses were moderate compared to *DNA-HBVac* + CpG or *DNA-HBVac* + HBsAg groups where frequencies remained at baseline level. Immunization with CpG adjuvanted HBsAg + HBcAg induced high levels of anti-HBs and high frequencies of HBV-specific T-cells indicating (Fig. 3.14, Fig. 3.15). These results support previous findings that CpG adjuvant potentiates humoral and cellular immune responses elicited by vaccination. Results also reveal that CpG adjuvant can activate and modulate different immune response profiles depending on which component is used for prime immunizations. It seems that the CpG adjuvant is more efficient at enhancing immune responses elicited by protein priming compared to DNA priming. Therefore, the importance of optimal Th1/Th2 balanced adjuvant for DNA priming needs to be considered as a determining factor for successful adaptive immune responses. To address this issue and increase *DNA-HBVac* vaccine potency, cytokines, chemokines, and co-stimulatory molecules can be considered. Previous studies have shown that DNA vaccine-induced immune response can be expanded by co-delivering additional plasmids encoding cytokines. Administration of plasmid encoding granulocyte-macrophage colony-stimulating factor (GM-CSF) alone stimulated both Th1/Th2 responses. Co-delivery of genetic adjuvants such as the cytokines GM-CSF and IL-2 or IL-4 proved to potentiate the immune responses to DNA vaccines. Co-delivery of plasmid GM-CSF with IL-2 proved to drive the Th1/Th2 balance towards Th2 whereas co-delivery of plasmid GM-CSF with IL-4 stimulated Th1 responses (Kusakabe et al., 2000; Scheerlinck, 2001). Therefore, adjuvant optimization should be further evaluated to enhance *DNA-HBVac* immunogenicity. Additional improvement to *DNA-HBVac* could be the expansion of CpG motifs which are present in the plasmid backbone. CpG motifs are known to significantly increase the immunogenicity of DNA vaccines by enhancing antigen-specific immune responses (Klinman et al., 1997). However, the bacterial plasmid DNA backbone does not have any therapeutic effect. This additional sequence lacking therapeutic benefit limits 1) the bioavailability of the plasmid because of its large size, 2) the expression of the encoded antigens and 3) the clinical application raising biosafety concerns (Mayrhofer et al., 2009).

Minicircles consist of supercoiled dsDNA derived from conventional bacterial plasmid DNA. Minicircles do not contain the conventional bacterial plasmid backbone composed of an antibiotic resistance gene, an origin of replication, and bacterial CpG motifs. Studies have reported that minicircle plasmid DNA resulted in persistent dramatically increased transgene expression levels compared to immunization with parental plasmid (Chen et al., 2003). Therefore, to improve gene transfer efficiency and safety, it would be of great interest to generate minicircle DNA out of *DNA-HBVac*.

Taken together, these findings indicate that DNA vaccines are promising candidates for therapeutic vaccination. Beyond vaccination, numerous factors such as construct optimization and adjuvant selection are decisive to use DNA vaccines to their full potential. In addition, DNA vaccine-induced immunogenicity largely relies on successful immunization. To this extent, appropriate delivery strategy and immunization protocol need to be investigated.

4.3 Determining the optimal immunization strategy of *DNA-HBVac*

Since the discovery of DNA vaccines, i.m. injection has been the predominant method used for vaccination. The WHO recommends i.m. administration of vaccines containing adjuvants to limit local side effects (WHO, 2021). The efficacy of i.m. immunization of *DNA-HBVac* was compared to co-administration of DNA and protein in both thigh muscles or to distinct contralateral administration sites of DNA (left thigh muscle) and adjuvanted recombinant HBsAg (right thigh muscle). Of note, experimental groups received the same series of immunizations in a two-week interval, the same doses of vaccine components, and the same number of anatomical sites for i.m. immunization. Immunization with *DNA-HBVac* in both muscles elicited significantly stronger HBV-specific antibody and T-cell responses than the co-administration of DNA and protein in the same muscles or the immunization of DNA and protein in contralateral administration sites. By contrast, mice in the co-administration group developed overall higher humoral and cellular responses compared to mice immunized with DNA and protein in contralateral thigh muscles (Fig. 3.17, Fig. 3.18). These observations imply that the uptake of the vaccine components (DNA, protein, and adjuvant) by the surrounding lymph nodes triggers qualitatively different primary immune responses whether components are co-administered or delivered in separate sites. Co-administration of DNA and protein most likely led to the simultaneous activation of B and T cells within the same follicles whereas separate immunization triggered either predominantly T-cell responses through endogenous peptide presentation following DNA administration or antibody responses through protein-induced B cell activation. Nevertheless, early priming-induced immunological processes taking place within the draining lymph nodes need to be further investigated to reveal bottlenecks of potent and successful priming (Felber et al., 2020; Havenar-Daughton et al., 2016; Liang et al., 2017). Therefore, successful DNA, protein, and adjuvant co-delivery targeting the same draining

lymph nodes may be a potent approach to induce balanced T and B cell responses thus increasing vaccine efficacy (Felber et al., 2020).

Besides the immunization route, the vaccine delivery method remarkably influences vaccine-induced immunogenicity. *In vivo,* cellular DNA uptake can be enhanced using physical or chemical delivery methods. Relative to conventional i.m. DNA immunization, gene gun DNA delivery, electroporation, sonoporation, liposomes, and nanoparticles have been shown to represent promising *in vivo* delivery methods to increase DNA vaccine efficacy (Castaldello et al., 2006; Escoffre et al., 2013; Larregina et al., 2001; Masotti et al., 2009; Patil et al., 2004; Widera et al., 2000). Therefore, the immunization route and delivery system of DNA vaccines should be carefully determined to ensure maximal vaccine efficacy.

4.4 High anti-HBs levels correlate with successful therapeutic vaccination

Strong anti-HBs titers in the serum of mice/infected patients correlate with long-term protective immunity either induced by resolved acute HBV infection or successful vaccination. HBsAg loss and anti-HBs seroconversion are referred to as functional cure (Lok et al., 2017). Anti-HBs antibodies confer protection through the binding of circulating HBV particles, by blocking viral entry into the hepatocytes as well as viral release from cells (Neumann et al., 2010; Schilling et al., 2003). However, even if functional cure is achieved, HBV cccDNA persists in the nucleus of the cells and acts as a reservoir for the potential reactivation of viral replication. A study in patients with resolved hepatitis B showed that using Rituximab, a B-cell depleting monoclonal chimeric antibody directed against the transmembraneous antigen CD20 present on the surface of B cells led to the reactivation of HBV in patients (Loomba & Liang, 2017). In CHB HBsAg-specific B-cell dysfunction can be observed. High anti-HBs levels are a prerequisite for successful therapeutic vaccination. Therefore, the question was raised whether immunization with *DNA-HBVac* in HBV-naïve and HBV carrier mice can elicit strong HBV-specific antibody responses that can induce HBsAg loss. AAV-HBV model has been reported to induce persistent HBV replication in mice and so mimics CHB infection in humans (Dion et al., 2013). Levels of anti-HBs and S-specific $CD4^+$ T-cell responses induced by 50 µg or 100 µg dose adjuvanted *DNA-HBVac* were low and comparable in both HBV-naïve and HBV carrier mice (Fig. 3.4, Fig. 3.7, Fig. 3.8). By contrast, prime immunization with adjuvanted recombinant proteins (HBsAg and HBcAg) elicited robust anti-HBs and S-specific $CD4^+$ T-cell responses in both models. These results emphasize the current knowledge about DNA vaccines, which are known to induce modest antibody responses as they are potent inducers of Th1-type T-cell responses whereas proteins effectively boost neutralizing antibodies and Th2-type T-cell responses. Thus, DNA vaccines are known to rarely achieve HBeAg or HBsAg seroconversion. Differences in the ability to generate antibodies may rather result from

interferences during the production, folding, or presentation of the antigens than from the selectivity of the immune system. Differences in expression levels as well as co-expression of the five proteins encoded by *DNA-HBVac* within the same cells may induce aggregation of misfolded proteins in the cells, thus being unable to favor a strong humoral immune response (Gašparić et al., 2007). To this end, this study aimed at increasing antibody and cellular immune responses elicited by *DNA-HBVAc* by using a priming-boosting regimen consisting of *DNA-HBVac* and adjuvanted recombinant HBsAg to broaden the spectrum of immune responses. This spectrum was not assessed with either DNA or protein alone (Cristillo et al., 2006; Otten et al., 2005; Pal et al., 2005). It was formerly reported that simultaneous immunization with DNA and protein vaccines synergistically increases the ability of each component to generate neutralizing antibodies in mice (Konishi et al., 2003). Therefore, immunization regimens consisting of either simultaneous immunization of *DNA-HBVac* and adjuvanted HBsAg or separated injection sites of *DNA-HBVac* and adjuvanted recombinant HBsAg were further evaluated. Results in HBV carrier mice demonstrated that even if simultaneous prime immunization with DNA and protein was able to induce robust anti-HBs response, HBV-specific T-cell responses were altered (Fig. 3.14, Fig. 3.15). Furthermore, in HBV-naïve mice, significant suppression of neutralizing anti-HBs antibody titers as well as abrogation of HBV-specific $CD8^+$ T-cell responses was observed when separating DNA and protein immunization sites (Fig. 3.17 and Fig. 3.18). These observations raise the question of how localized these immune responses are and to what extent potential interaction between both components can occur despite immunization in different legs. These, then, limit the ability of *DNA-HBVac* to induce broad and multispecific immune responses against the encoded antigens. In addition, these findings indicate that injection of the same amount of *DNA-HBVac*, in one instead of two injection sites as described above, may hinder efficient delivery for optimal transfection of cells *in situ*. Insufficient tissue distribution and cellular uptake are known to be determining factors for successful DNA immunogenicity (Dupuis et al., 2000). Previous studies have shown that sequential immunization with DNA and recombinant protein provided enhanced protective immunity (Epstein et al., 2004; Wang et al., 2004). In an attempt to generate antibodies and enhance T-cell responses, adjuvanted recombinant HBsAg or *DNA-HBVac* was administered to mice previously primed with either *DNA-HBVac* or adjuvanted HBsAg. Vaccination proved to be safe and well-tolerated. Sequential immunization starting with two injections of *DNA-HBVac* elicited higher HBV-specific antibody and T-cell responses compared to sequential immunization starting with adjuvanted recombinant HBsAg (Fig. 3.20, Fig. 3.23, Fig. 3.24). Thus, to fully investigate the potency of combined *DNA-HBVac* and adjuvanted recombinant HBsAg vaccination to induce robust B- and T-cell responses to break immune tolerance, sequential immunization proved to be a promising strategy to overcome this challenge and thus achieve strong and polyfunctional HBV-specific $CD4^+$ and $CD8^+$ T-cell

responses. These findings indicate that DNA vaccines can be sequentially combined with protein for vaccination to enhance and optimize vaccine-induced immune responses.

4.5 Exploring critical factors for strong *DNA-HBVac* induced immunogenicity in both HBV-naïve and AAV-HBV mice

To ensure equimolar expression of the proteins encoded on *DNA-HBVac*, HBV proteins were linked with P2A and T2A gene sequences (Luke et al., 2008; Szymczak & Vignali, 2005). However, within large polycistronic constructs, a variety of factors may affect the expression of the proteins located at the end of the sequence. For instance, ribosome binding efficiency or protein stability may be altered. These factors may influence protein expression levels, presentation, and thus recognition by the immune system. As a consequence, immune responses directed against HBV antigens located downstream of the HBVac insert may be less strong (Glick & Whitney, 1987). Supporting this knowledge, in both HBV-naïve and AAV-HBV mice, immunization with *DNA-HBVac* elicited strong S-specific T-cell responses but lower core- and RT-specific T-cell responses (Fig. 3.5, Fig. 3.10).

Cytotoxic S-specific T lymphocyte responses can be primed by immunization with recombinant HBs (exogenous) or by DNA vaccination (endogenous). Endogenous antigen processing occurs through antigen proteolysis in the cytosol of cells. This step forms peptides that subsequently bind to MHC class I molecules in the endoplasmic reticulum. Alternatively, exogenous antigens are degraded in the endolysosome of cells. Next, peptides are generated, processed, and then presented onto MHC class I molecules (Yewdell & Bennink, 1992). Therefore, the administration of endogenous or exogenous antigens results in distinct processing/presentation pathways. Previous studies have shown that S-specific K^b restricted S_{208} epitope is generated following immunization with exogenous HBsAg whereas K^b restricted S_{190} epitope is generated after processing of endogenous HBsAg (Schirmbeck & Reimann, 2002; Schirmbeck et al., 1998). To this extent this study aimed to evaluate and compare the MHC-class I restricted T-cell responses induced by recombinant protein (exogenous HBsAg) or DNA vaccination (endogenous HBsAg). Immunization of both HBV-naïve and HBV carrier mice with DNA vaccine *DNA-HBVac* induced profound S190-specific T-cell responses. By contrast, the frequency of S208-specific T-cell responses remained at the baseline level. On the contrary, immunization of both HBV-naïve and HBV carrier mice with recombinant protein elicited very strong S208-specific T-cell responses compared to S190-specific T-cell responses which remained unspecific and very low. The differences observed in S-specific T-cell responses whether mice received endogenous (*DNA-HBVac*) or exogenous HBsAg remained comparable throughout all experiments. Therefore, the results obtained in this study confirm the findings described above. Interestingly, when performing sequential immunization

with both DNA and adjuvanted recombinant protein, differences in the peptide specificity of S-specific T-cell responses could be observed. Sequential immunization of mice initiated with recombinant HBsAg (SSDD) stimulated very robust S208-specific IFNγ^+ CD8$^+$ T-cell responses in livers and spleens compared to baseline responses observed in mice primed with sequential immunization starting with *DNA-HBVac* (DDSS). Sequential immunization starting with *DNA-HBVac* elicited very profound S190-specific IFNγ^+ CD8$^+$ T-cell responses in livers and spleens compared to sequential immunization initiated with HBsAg (SSDD) (Fig. 3.23). These results suggest that sequential immunization starting with recombinant protein promotes Th2 immune skewing whereas immunization initiated with DNA promotes more likely Th1 immune responses. To further investigate these observations, one would need to analyze memory T-cell responses, phenotypes, and T-cell cytokine profiles more in detail.

Unlike in HBV-naïve mice, core-specific IFNγ^+ CD4$^+$ T-cell responses of HBV carrier mice immunized with any vaccine regimen could not be detected by ICS in livers and spleens at final analysis (Fig. 3.8, Fig. 3.21). These findings may indicate early apoptosis-induced killing of effector core-specific CD4$^+$ T cells (Dooms & Abbas, 2002; Wu et al., 2002). Thus, effector core-specific CD4$^+$ T cells would not be detectable by ICS at final analysis. To further investigate this phenomenon, it would be of high interest to analyze core-specific CD4$^+$ T cells early after vaccination as well as the induction of memory core-specific helper T cells.

As described above, previous studies have shown that DNA vaccines are able to induce strong T-cell responses but low B-cell responses. As protein vaccines are known to elicit potent antibody responses as well as Th2 responses. It was formerly reported that simultaneous immunization with DNA and protein vaccines synergistically increases the ability of each component to generate neutralizing antibodies in mice (Konishi et al., 2003). Anti-HBc antibodies lack neutralizing capacity. Therefore, only anti-HBs antibodies are neutralizing and thus confer protective immunity. Consequently, HBcAg was not combined with *DNA-HBVac* for vaccination.

Taken together, the results of this study showed that priming with *DNA-HBVac* induced broad HBV-specific CD8$^+$ T-cells directed against the various antigens. However, neither T-cell responses nor antiviral efficacy was superior to that achieved after a prime with combined adjuvanted protein antigens (HBsAg and HBcAg). To enhance antibody responses, *DNA-HBVac* can be combined with HBsAg for vaccination. Sequential immunization with first *DNA-HBVac* and then recombinant HBsAg resulted in strongest antibody and T-cell responses but again a protein prime using a combination of adjuvanted HBsAg and HBcAg was equally potent.

DNA-based therapeutic vaccines are potent tools to induce CD8$^+$ T-cell responses. However, a protein prime resulted in superior antibody responses and antiviral efficacy.

4.6 Advantages and disadvantages of RNA vaccines over viral vector or DNA vaccines

In 1993, Martinon and colleagues first showed that immunization with mRNA encoding influenza virus nucleoprotein was able to induce virus-specific immune responses in mice (Martinon et al., 1993). While in the 1990s and 2000s vaccine research focused on DNA vaccines, mRNA vaccines emerged as a prospective platform only a decade ago. In contrast to protein subunit vaccines, both DNA and mRNA vaccines can mimic intracellular pathogen infection therefore potentially promoting stronger and broader T-cell responses. In contrast to live attenuated vaccines, both mRNA and DNA vaccines carry no risk of potential conversion into disease-causing vaccines. This aspect may be of high concern, especially in immunocompromised individuals (Ljungman, 2012). An additional advantage of nucleic acid-based vaccines over conventional vaccines is their rapid scalable and low-cost manufacturing process (Tombacz et al., 2021). Moreover, once the manufacturing process is well established for either DNA or mRNA vaccines, any antigen encoding genetic vaccine can be easily generated. This versatile and easy-to-use production platform is of utmost importance in case of a pandemic as shown during the Covid-19 pandemic (Lurie et al., 2020). An additional benefit of both DNA and mRNA over subunit vaccines is their use of the host's own transcription/translation machinery, thus mimicking natural protein expression, folding, implementation of posttranslational modifications, and generation of aberrant proteins. Taken together, these increase the available T cell epitope repertoire compared to protein vaccines (Yewdell et al., 1996). In regard to transport, storage, and stability, mRNA vaccines have a clear disadvantage over DNA vaccines. While DNA vaccines are known to be highly stable, RNA vaccines are subjected to rapid degradation by omnipresent RNases leading to potential degradation of the construct within a short time frame. However, recent advances have addressed this issue. Through the incorporation of nucleoside modifications, untranslated regions, cap structure, and polyA tail, mRNA vaccines can be stabilized, and high levels of protein translation can be achieved. Furthermore, to protect mRNA from degradation, mRNA vaccines can be encapsulated using, for example, lipid nanoparticles (Kowalski et al., 2019). Transient expression, however, can be of advantage when controlled protein expression is desired. To this extent, immunization with RNA vaccines enables short-interval protein expression whereas the injection of plasmid DNA in mice results in the lifelong persistence of gene expression (Armengol et al., 2004). In contrary to DNA vaccines, RNA vaccines are known to be safe as RNA-based integration into the host's genome is highly improbable. While DNA vaccines first need to enter the nucleus before being processed further, RNA vaccines can be directly translated into proteins in the cytoplasm of the cells (Tombacz et al., 2021).

While the production and purification of plasmid DNA under Good Manufacturing Practice requirements is well-established, large-scale production of RNA vaccines requires additional processing steps (Tejeda-Mansir & Montesinos, 2008; Xenopoulos & Pattnaik, 2014). For successful mRNA vaccine amplification, a DNA template, an *in vitro* transcription reaction step, implementation of a cap structure and polyA tail sequence, as well as purification steps to remove dsRNA contaminants, are needed (Baiersdörfer et al., 2019; Kariko et al., 2011; Martin et al., 1975; STEPINSKI et al., 2001). Furthermore, compared to DNA vaccines, mRNA vaccines require additional appropriate delivery systems to the cytoplasm. Despite mRNA vaccines require further manufacturing steps compared to DNA vaccines, a minor amount of template DNA is sufficient to produce large amounts of mRNA through *in vitro* transcription (Tombacz et al., 2021).

Taken together, RNA-based vaccines represent a new era in vaccinology offering a promising and challenging alternative to conventional vaccines. Improvement of RNA vaccine design as well as delivery systems need to be addressed in the near future.

4.7 Incorporation of additional modifications to further upgrade *in vivo* mRNA immunogenicity

In the conducted studies, ARCA cap, polyA tail, and 100% N^1 Methyl-φ-UTP nucleoside modified mRNA were used to perform immunogenicity evaluation of *RNA-HBVac in vivo*. Andries and colleagues showed that upon immunization of mice, the alliance of these modifications proved to outperform protein expression and reduce intracellular innate immune activation through endosomal TLR-3 activation. Therefore, nucleoside modifications represent a hallmark in the field of future mRNA-based therapeutics (Andries et al., 2015; Karikó et al., 2008). Andries et al. showed that double N^1 Methyl-φ-UTP/^{5}m-CTP modified mRNA was able to induce up to 3-fold higher protein expression in mice compared to single N^1 Methyl-φ-UTP nucleoside modified mRNA (Andries et al., 2015). Therefore, additional optimization of chemical mRNA modifications as well as their *in vivo* immunogenicity should be investigated further. Capping of 5’ mRNA is known to regulate splicing, deterioration of mRNA through endonucleases as well as translation initiation. Through the incorporation of a cap structure, the mRNA can be recognized as a self-RNA by the innate immune system. The standard eukaryotic 5’ cap structure, known as cap 0, consists of a 7-methyl guanosine linked via a triphosphate bridge to the first nucleotide. Cap 1 results from the methylation of the 2’-hydroxyl group of the first nucleoside located proximal of the cap. In contrast to cap 0 analogs, ARCA cap analogs co-transcriptionally cap mRNAs and hinder the implementation of reversely orientated caps. Despite ARCA-capped mRNA proved to be greatly immunogenic, studies have shown that ARCA capping is inefficient (70%) and yields remain suboptimal. Therefore,

further optimization of mRNA capping strategies may be necessary. To this extent, a newly described co-translational mRNA capping technology named CleanCap (TriLink Biotechnologies) has shown superior efficacy compared to ARCA. While ARCA uses a dimer to initiate translation, CleanCap employs a trimer to initiate T7 transcription. T7 polymerase in combination with ARCA strongly limits initiation at 5'guanosine nucleotides, however combination of CleanCap and T7 polymerase do not show any nucleoside restriction allowing a variety of initiation sites. In addition, compared to ARCA, CleanCap was highly efficient and led to high yields of capped mRNAs (McCaffrey, 2019; Vaidyanathan et al., 2018). Nevertheless, other eukaryotic cap 1 and 2 variants should be investigated to improve mRNA capping. In addition, previous studies have shown that polyA tail plays a major role in mRNA stability and translation efficiency. Holtkamp et al. demonstrated that a polyA tail length of 120 nucleotides was the most optimal in terms of mRNA stability and protein expression (Holtkamp et al., 2006). Additionally, sequence optimization plays an important role in increasing protein expression. Replacing rare codons with commonly available ones, having abundant corresponding tRNAs in the cytosol, or increasing G:C ratio in the mRNA construct itself have been shown to increase protein expression (Gustafsson et al., 2004; Thess et al., 2015). Although all these modifications aim to increase the immunogenicity of in vivo mRNA, engineering may interfere with secondary mRNA structures, accurate translation and folding of proteins, and T-cell epitope generation (Buhr et al., 2016; Kudla et al., 2009; Mauro & Chappell, 2014; Yu et al., 2015). All these additional improvement steps could be further investigated in the context of *RNA-HBVac*.

4.8 Strategies for improvement of *in vivo* RNA vaccine delivery to enhance *RNA-HBVac* immunogenicity

Besides chemical modifications, an appropriate mRNA *in vivo* delivery system is crucial for successful therapeutic vaccination. To be translated into functionally active protein(s), mRNA needs to reach the cytoplasm of the cells. Cytoplasmic delivery can be achieved through the injection of dendritic cells previously loaded *ex-vivo* with mRNA or through direct immunization with formulated/unformulated mRNA (Benteyn et al., 2015). Although *ex-vivo* loading of dendritic cells allows controlled and highly efficient transfection of antigen-presenting cells, large-scale vaccination remains expensive and time-consuming. By contrast, injection of formulated/unformulated mRNA represents a feasible and cost-effective approach for worldwide vaccination strategies. In the conducted studies, injection of naked *RNA-HBVac*, especially in 25 µg dose (UF-25) led to higher anti-HBs levels compared to D-100 however those were lower than the mixed adjuvanted protein antigen group (P) (Fig. 3.38). In both UF-25 and UF-100 groups, HBV-specific T-cell responses remained scarce (Fig. 3.41 and Fig.

3.42). The results from the present study highlight the fact that i.m. immunization of naked mRNA might not be the most appropriate immunization route to target APCs and therefore induce adaptive immunity. In previous studies, it was observed that immunization with naked mRNA was particularly successful when injected intradermally or intranodally (Kreiter et al., 2010; Selmi et al., 2016). Therefore, alternative injection routes for naked mRNA immunization should be further investigated. To improve *in vivo* RNA vaccine delivery physical or chemical delivery systems can be used. Chemical delivery methods should be favored over gene guns or electroporation delivery, where limitations such as access to target tissues or increased local cell death play an important role (Pardi, Hogan, et al., 2018b). Recent studies have shown that LNP represents efficient *in vivo* delivery systems for mRNA (Pardi et al., 2015). Therefore, LNP-based delivery was used in the conducted studies. LNPs consist of four components: 1) an ionizable cationic lipid that stimulates the assembly in virus-like particles, 2) lipid-coupled polyethylene glycol, 3) cholesterol, and 4) phospholipids. Whereas polyethylene glycol enhances the half-life of the formulation, cholesterol works as a stabilizing agent. Despite LNP-based mRNA delivery represents a potent tool for *in vivo* mRNA delivery, efficient and safe delivery within target cells remains a major challenge. Immunization of wild-type mice with various doses of LNP-formulated *RNA-HBVac* therapeutic hepatitis B vaccine led to dose-dependent weight loss, motoric dysfunctions, and inflammation, especially in animals immunized with high doses of LNP-formulated *RNA-HBVac* (50 µg and 100 µg) (Fig. 3.31). Macroscopic purulent abscess was noticed in mice primed with 100 µg LNP formulated *RNA-HBVac.* In addition, HE staining of the thigh muscles of the hind limb region used for the injection of *RNA-HBVac* showed dose-dependent massive neutrophile infiltration at the injection site (Fig. 3.32). Inflammatory responses were rapid and robust, especially in mice receiving high doses of 100 µg LNP-formulated *RNA-HBVac*. Therefore, the used LNP components seem to be highly inflammatory conferring the vaccine an additional adjuvating effect (Pardi, Hogan, Naradikian, et al., 2018; Samaridou et al., 2020). Similar inflammatory side effects were observed in human clinical trials of Pfizer/BioNTech and Moderna LNP formulated mRNA vaccines against SARS-CoV-2 virus infection (Jackson et al., 2020; Walsh et al., 2020). To evaluate whether *RNA-HBVac* can break immune tolerance, HBV carrier mice were immunized with *RNA-HBVac.* Results indicate that even if LNP-formulated *RNA-HBVac* was able to induce both HBV-specific B- and T-cell responses, a protein prime showed superior efficacy (Fig. 3.39, Fig. 3.41, and Fig. 3.42). HBV carrier mice primed with *RNA-HBVac* showed only a minor antiviral effect, independently if the *RNA-HBVac* was formulated in LNPs or left unformulated (Fig. 3.43).

Nevertheless, *RNA-HBVac* proved to be immunogenic in both HBV-naïve and chronic hepatitis B mouse models, further studies need to be conducted to: 1) generate highly optimized LNP-based delivery systems for *RNA-HBVac* in the context of persistent HBV infection, 2) further

investigate the inflammatory responses induced by LNPs and 3) better understand the underlying mechanisms of endosomal mRNA escape into the cytoplasm.

4.9 Investigating critical factors for optimal mRNA priming of *TherVacB*

New measures to increase protein expression by *RNA-HBVac* and ways to induce balanced long-term humoral and cellular responses need to be investigated. Apart from *in vivo* delivery systems, *RNA-HBVac* immunogenicity can be enhanced by optimizing the priming strategy of *TherVacB*. Similarly, to the other vaccine regimens tested in this study, it could be beneficial to evaluate the immunogenicity elicited by co-administration of *RNA-HBVac* and an appropriate adjuvant. Previous findings have shown that protamine-complexed mRNA stimulates Th1 responses against the encoded antigens through TLR7/TLR8 activation (Carralot et al., 2004; Scheel et al., 2005). To this extent, CureVac GmbH recently developed a self-adjuvanted RNActive® vaccine, which consists of a modified unformulated mRNA co-administered with the same mRNA complexed with protamine. Results showed that RNActive® vaccine was able to induce balanced Th1/Th2 immune responses. The vaccine was not only able to induce strong effector T-cell responses but also strong memory T-cell responses upon repeated vaccine administration (Kallen et al., 2013). Therefore, adjuvanticity induced by mRNA/protamine complexes represents a promising approach to induce both strong humoral and cellular immune responses. Another promising alternative strategy for mRNA vaccination could be the simultaneous injection of unformulated mRNA with a mixture of 3 mRNAs encoding for the immunostimulatory molecules CD40 ligand, an active form TLR4 and the co-stimulatory molecule CD70 (TriMix). In the field of mRNA-based cancer immunotherapy, it was shown that TriMix was able to enhance effector T-cell responses and induce anti-tumor immunity compared to mRNA administration alone (Van Lint et al., 2012). As described above, the conducted studies have shown that mRNA, meaning ssRNA, is able to induce strong antibody levels but low T-cell responses. Previous findings have shown that dsRNA is able to expand cytolytic CD8+ T-cell responses when co-administered with recombinant protein (Jin et al., 2010). First, dsRNA is detected by PRR leading to the production of inflammatory cytokines which stimulate innate/adaptive immune responses. It is known that dsRNA is recognized by TLR3 in the endosome of dendritic cells leading to their activation into mature APCs. Mature APCs then present the processed antigen epitopes on MHC-I to naïve T cells. Therefore, dsRNA represents a promising potential adjuvant for *RNA-HBVac* to strengthen HBV-specific T-cell responses.

Taken together the results of this study demonstrated promising results using mRNA as a prime for therapeutic hepatitis B vaccination. Compared to conventional vaccines, mRNA vaccines are easy to produce, cost-effective, and allow to adapt to specific needs. Especially

in the case of an emerging pandemic, mRNA vaccines represent a potent and novel therapeutic approach that has shown great efficacy in the context of SARS-CoV-2 pandemic. 2020 for sure, represents a highlight in the bright future of mRNA vaccines. Nevertheless, in the context of CHB, *RNA-HBVac* needs to be optimized and further evaluated in different mouse models to successfully clear HBV infection.

5 Materials and Methods

5.1 Materials

5.1.1 Cell lines/bacterial strains

Table 5.1 Cell lines/bacterial strains

Cell line	Description
HEK293	Human embryonic kidney cells, transformed with adenovirus type 5 DNA fragments (Graham et al., 1977)
HepG2	Hepatocellular carcinoma cell line (Knowles et al., 1980)
HepG2-NTCP-K7	HepG2 derived cell line transduced with lentiviral expression cassette for NTCP (Ko et al., 2018)
E.coli stlb3 strain	Chemically competent *E. coli* strain (Invitrogen)
DF-1	Chicken embryo fibroblast cell line (Himly et al., 1998)

5.1.2 Media

Table 5.2 Cell culture media

Components	Standard	For differentiation
Dulbecco's Modified Eagle Medium (DMEM): Nutrient Mixture F-12	500 ml	500 ml
Heat-inactivated fetal calf serum (FCS)	10 %	10 %
Penicillin/streptomycin (P/S)	50 U/ml	50 U/ml
L-Glutamin 200mM	L-Glutamin 20mM	L-Glutamin 20mM
MEM NEA (100x)	MEM NEA (1x)	MEM NEA (1x)
Sodium pyruvate 100mM	Sodium pyruvate 1mM	Sodium pyruvate 1mM
DMSO		2.5 %

Table 5.3 Bacterial cell culture medium

Medium	Components
Lysogeny Broth (LB) medium pH 7.0 (in 1 L H_2O)	10 g Tryptone 5 g Yeast extract 10 g NaCl

Table 5.4 Media for mouse experiments

Medium	Components
DF-1 cell culture medium	DMEM GlutaMAX™ 10 % FCS 50 U/ml P/S
Full medium for murine primary lymphocyte culture	RPMI1640 medium 10 % FCS 50 U/ml P/S
Wash medium for murine primary lymphocyte culture	RPMI1640 medium 50 U/ml P/S
Medium for murine hepatocyte digestion	DMEM medium 10 % FCS 50 U/ml P/S

5.1.3 Plasmids

Table 5.5 Plasmids

Name	Source
pURVac	Prof. Ralf Wagner, Hospital Regensburg, Germany
DNA-HBVac	Prof. Dr. med U. Protzer's laboratory
RNA-HBVAc plasmid (transcription template)	Prof. Dr. med U. Protzer's laboratory

5.1.4 Primers

Primers were purchased from Microsynth AG (Balgach, Switzerland).

Table 5.6 Primers

Name	Sequence (5'-3')
HBVac_fw	CGGTACCGTCGACACGTGGGCGCGCCAGATCTGAGC
HBVac_rev	TCTAGATGATCACACGTGTTAATTAAAGATCTAAGCTTACGCG
FP1_T7ivt_PCRtemplate_fwd	TAGAGAACCCACTGCTTACTGGCTTATC
FP1_T7ivt_PCRtemplate_rev(120 polydT)	polydT(120)-AGAAGGCACAGTCGAGGCTGATCAG_rev

5.1.5 Enzymes

Table 5.7 Enzymes

Product	Supplier
Collagenase type IV	Worthington
FastDigest restriction enzymes (+ 10x FastDigest Green Buffer)	Thermo Fisher Scientific
RNaseA	Machery-Nagel
T4 DNA Ligase	Thermo Fisher Scientific
Trypsin	Thermo Fisher Scientific

5.1.6 Kits

Table 5.8 Kits

Product	Supplier
ARCHITECT anti-HBs Reagent Kit	Abbott
ARCHITECT HBsAg Reagent Kit	Abbott
ARCHITECT HBeAg Reagent Kit	Abbott
ECL Western Blotting Detection Kit	GE Healthcare
Enzygnost® Anti-HBc monoclonal Kit	Siemens Healthcare Diagnostics
Fixation/Permeabilization Kit	BD Biosciences
GeneJET Gel Extraction Kit	Thermo Fisher Scientific
GeneJET Plasmid Miniprep Kit	Thermo Fisher Scientific
HiScribe T7 ARCA	New England Biolabs
InFusion	Takara
NucleoBond® Xtra Midi Kit	Machery-Nagel
NucleoSpin RNA isolation Kit	Machery-Nagel
SuperScript III First-Strand Synthesis SuperMix for qRT-PCR I	Invitrogen

5.1.7 Vaccine components

a. Components of priming immunizations

Table 5.9 Antigens

Recombinant antigen	Organism used for amplification	Supplier
HBsAg (genotype A, adw)	Yeast	BioVac, Cape Town, South Africa
HBcAg (genotype D, ayw)	*E. coli*	APP Lativjjas Biomedicinas, Riga, Latvia

Table 5.10 *DNA-HBVac*

Product	Organism used for amplification	Source
DNA-HBVac	*E. coli* stlb3 strain	Dr. Martin Kächele/Hélène Kerth

Table 5.11 *RNA-HBVac*

Product	Source
RNA-HBVac (production for *in vitro* experiments)	Dr. Andreas Oswald/Hélène Kerth
RNA-HBVac LNP formulated & non formulated (large scale production)	Ethris GmbH

Table 5.12 Adjuvant

Product	Source
CpG	Dynavax

b. Component of boost immunization

Recombinant *MVA-HBVac* is an MVA viral vector that contains the *HBVac* expression cassette encoding for five HBV proteins (S(Small) serotype *adw*, genotype A2; C-terminally truncated $Core_{1-149}$ serotype *ayw*, genotype D; the consensus sequence of the RT domain of the viral polymerase RT(pol); L/S(Large) serotype *ayw*, genotype C and full-length $Core_{1-183}$ from genotype C). To allow equimolar expression, HBV proteins were linked via P2A and T2A sites. *MVA-HBVac* was generated in chicken embryo fibroblast cells (CEF) in the laboratory of Prof. Dr. Gerd Sutter (LMU) and amplified in DF-1 cells in the laboratory of Prof. Dr. med. Ulrike Protzer. *MVA-HBVac* was employed as a boost immunization in all vaccination regimens to enhance the immune responses elicited by priming.

5.1.8 Mouse models

a. Wild-type C57BL/6 mice

9 weeks old C57BL/6J mice of haplotype H-2^b were purchased from JANVIER LABS (Le Genest Saint-Isle, France) and maintained under specific pathogen-free conditions in the biosafety level 2 animal facility of the TUM Institute of Microbiology/Institute of virology (Munich, Germany).

b. HBV carrier mice

9 weeks old wild-type C57BL/6J mice of haplotype H-2^b were intravenously infected with a recombinant adeno-associated viral vector encoding for the 1.2 overlength HBV genome of genotype D, serotype *ayw* (AAV-HBV1.2). AAV-HBV1.2 stocks were kindly provided by research unity INSERM U1089 (Plateforme de Thérapie Génique, Nantes, France) or directly produced by Dr. Julia Festag in Prof. Dr. med. Ulrike Protzer's laboratory. In the present studies, the AAV-HBV mouse model was used to mimic chronic HBV infection in mice as it has shown to induce persistent HBV replication as well as antigen expression in mice (Dion et al., 2013). Again, mice were kept under specific pathogen-free conditions in the biosafety level 2 animal facility of the TUM Institute of Microbiology/Institute of Virology (Munich, Germany).

5.1.9 Peptides

All single peptides as well as peptide pools were produced by Peptides and Elephants GmbH, Hennigsdorf, Germany.

Table 5.13 Single peptides

Peptide	Specificity	Amino Acid Sequence	Haplotype
B8R	MVA	TSYKFESV	H-2 k^b
C93	HBcAg	MGLKFRQL	H-2 k^b
S190	HBsAg (adw)	VWLSAIWM	H-2 k^b
S208	HBsAg (adw)	IVSPFIPL	H-2 k^b
RT-86	RT(pol)	AAFYHIPL	H-2 k^b
RT-333	RT(pol)	KQYLNLYPV	H-2 d^b
OVA_{S8L}	ovalbumin	SIINFEKL	H-2 k^b

Table 5.14 Peptide pools

Peptide pool	Specificity	Genotype	Amino Acid sequence
HBV core pool	HBcAg	D	btw. aa 70-157
HBV S pool	HBsAg	D	btw. aa 145-226
HBV RT pool	RT(pol)	A-E	btw. aa 1-343

5.1.10 Multimers

Multimers were employed to stain antigen-specific TCRs on the surface of $CD8^+$ T cells. Streptamers belong to the family of multimers and consist of an MHC class I-peptide complex which binds non-covalently to Strep-Tactin. Streptamers were generously provided by Prof. Dirk Busch from the Institute of Microbiology (Technical University of Munich, Germany).

Table 5.15 Streptamers

Streptamer	Specificity	Amino acid sequence
B8R	MVA	TSYKFESV
C93	HBcAg	MGLKFRQL
S190	HBsAg	VWLSAIWM
OVA_{S8L}	ovalbumin	SIINFEKL

5.1.11 Antibodies

Table 5.16 Antibodies used for western blotting

Antibody	Dilution	Supplier
Mouse Anti-GAPDH	1: 1 000	Sigma-Aldrich
Mouse Anti-β Actin	1: 1 000	Sigma-Aldrich
Mouse Anti HBc (8C9)	1:1	E. Kremmer
Mouse Anti HBs (HB1)	1:1 000	A. Zyirbliene
Rabbit Anti-HBV polymerase RT domain aa 357-367 (IgG_{2c}) • **Clone 15D7** • **Clone 15C9**	1:1	Monoclonal Antibody Core Facility, Helmholtz Zentrum München, Germany
Goatαmouse	1: 10 000	Sigma-Aldrich
Mouseαrabbit IgG_{2C}	1: 1000	Sigma-Aldrich

Table 5.17 Antibodies used for flow cytometry

Antibody/Fluorochrome	Dilution	Article Number	Supplier
Dead/Live (eF780)	1: 3 000	65-0865-18	eBioscience
anti-mCD4 APC	1: 100	553051	BD Biosciences
anti-mCD4 PeCy7	1: 150	25-0042-82	eBioscience
anti-mCD8a V500	1: 150	560776	BD Biosciences
anti-mCD8a PB	1: 100	558106	BD Biosciences
anti-mCD44 FITC	1: 150	11-0441-85	eBioscience
anti-mGranzymeB PE	1: 100	GRB04	Invitrogen
anti-mIL-2 PE	1: 100	JES6-5H4	Invitrogen
anti-mIFNγ FITC	1: 300	554411	BD Biosciences
anti-mKLRG1 PB	1:200	753694	BD Biosciences
anti-mLAG3 PE	1: 200	12-2231-82	eBioscience
anti-mPD1 PerCp (eF710)	1: 200	46-9985-82	eBioscience
anti-mTNF-α PeCy7	1: 200	557644	BD Biosciences
Strep Tactin APC	1: 50	6-5010-001	IBA lifesciences
Strep Tactin PE	1: 50	6-5000-001	IBA lifesciences

5.1.12 Buffers and solutions

Table 5.18 Buffers and solutions

Buffer/solution	Ingredients
50x TAE Buffer	2 M Tris 2 M acetic acid 50 mM EDTA pH 8.0 H_2O
ACK lysis buffer	150 mM NH_4Cl 10 mM $KHCO_3$ 0.1 mM Na_2EDTA pH: 7.2-7.4 in H_2O
RIPA lysis buffer	50 mM Tris (pH 8.0) 100 mM NaCl 1 mM EDTA 0.5 % sodium deoxycholate 0.1% SDS 1 % NP-40 H_2O
6x Protein Loading Buffer	375 mM Tris-HCl (pH 6.8) 6 % SDS 4.8 % Glycerol 9 % Mercaptoethanol 0.03 % Bromophenol blue H_2O
Stacking gel 5 % for Western Blot, 2 ml	0.24 ml 40 % PAA/BisAA 0.5 ml 1 M Tris (pH 8.8) 20 µl SDS 10 % 1.25 ml sterile H_2O

	2 µl SDS 15 µl APS
Running gel 12.5 % for Western Blot, 8 ml	2.5 ml 40 % PAA/BisAA 3ml 1 M Tris (pH 8.8) 80 µl SDS 10 % 2.5 ml sterile H_2O 7 µl SDS 40 µl APS
Western Blot 10x Running buffer	25 mM Tris 192 mM glycine 0.1 % SDS H_2O
Western Blot 10x Transfer buffer (pH 8.3)	25 mM Tris 190 mM glycine 20 % methanol H_2O
Western Blot 10x TBST buffer (pH 7.4)	20 mM Tris 1.4 M NaCl 0.1 % Tween20 H_2O
Western Blot blocking solution	5 % skim milk powder PBS
10 mM Tris buffer (pH 9.0)	10 mM Tris H_2O
80 % Percoll (100 ml)	72 ml pure Percoll 8 ml 10x PBS 20 ml 1x PBS
40 % Percoll (100 ml)	50 ml 80 % Percoll 50 ml 1x PBS 100 IU/ml Heparin
FACS buffer	FCS 1% in PBS

5.1.13 Chemicals and reagents

Table 5.19 Chemicals and reagents

Chemical/Reagent	Supplier
2-Mercaptoethanol	Roth
2-Phenoxyethanol	Roth
Acetic acid	Roth
Agarose	Peqlab
Amersham ECL Prime Western Blotting Detection Reagent	GE Healthcare Life Sciences
Ammonium chloride (NH_4Cl)	Roth
Ammonium persulfate (APS)	Roth
Ampicillin	Roth
Bovine serum albumin (BSA)	Roth
Brefeldin A (BFA)	Sigma-Aldrich

Collagen R	Serva Electrophoresis
CountBright Absolute Counting Beads	ThermoFisher Scientific
CpG1018	Dynavax
Dead/Live staining eF780	eBioscience
Dimethyl sulfoxide (DMSO)	Sigma-Aldrich
DNA smart ladder 10 kb/1 kb/ 100 bp	Eurogentec
Dulbecco's Modified Eagle's Medium (DMEM)	Gibco/Invitrogen
EDTA	Roth
EDTA di-sodium salt (Na_2EDTA)	Roth
Ethanol	Roth
Fetal calf serum (FCS), heat inactivated	Gibco/Invitrogen
Glucose	Roth
Glycin	Roth
Heparin-Natrium 25 000	Ratiopharm
Hydrochloric acid (HCl)	Roth
Isoflurane	Henry Schein
Isopropanol	Roth
Kanamycin	Roth
L-Glutamine, 200 mM	Gibco
Lipofectamine 2000	Life Technologies
Lipofectamine MessengerMax	Life Technologies
Loading Dye 2x RNA	New England Biolabs
Lysogeny broth medium (LB)	Sigma-Aldrich
Mercaptoethanol, 50 mM	Gibco
Methanol (MeOH)	Roth
Milk powder	Roth
OptiMEM	Gibco/Invitrogen
Page Ruler Plus Prestained protein ladder	Thermo Fisher Scientific
Paraformaldehyde (PFA), 4 %	ChemCruz
Penicillin/streptomycin (P/S)	Gibco/Invitrogen
Percoll density gradient media	GE Healthcare
Phosphate Buffered Saline (PBS), pH 7.4	Gibco/Invitrogen
Phosphate Buffered Saline (PBS), pH 7.4, 10x	Gibco/Invitrogen
Pierce RIPA buffer	Thermo Fisher Scientific
Polyacrylamide (PAA)	Roth
Potassic hydrogenic carbonat ($KHCO_3$)	Roth
Protease Inhibitor	Roche
RNAlater RNA Stabilization Reagent	Qiagen
Roti®-Safe GelStain	Roth
RPMI 1640	Gibco
RPMI 1640 Dutch modified	Gibco
Sodium chloride (NaCl)	Roth
Sodium dodecyl sulfate (SDS)	Roth
ssRNA ladder	New England Biolabs
Tetramethylethylendiamin (TEMED)	Roth
Tris	Roth

Trypan blue	Gibco/Invitrogen
Trypsin	Gibco/Invitrogen
N1-Methylpseudo-UTP (φ)	Jena Bioscience
5-Methyl-CTP (m^5CTP)	Jena Bioscience

5.1.14 Laboratory devices

Table 5.20 Laboratory devices

Product	Supplier
Accu-jet® pro pipette	Brand
Agarose gel electrophoresis chambers	Peqlab
Amersham™ Hybond P Western blotting membranes, PVDF	GE Healthcare Life Sciences
Aperio AT2 slide scanner	Leica Biosystems
Architect™ platform	Abbott Laboratories
BEP III platform	Siemens Healthcare
Cell culture incubator HERAcell 150i	Thermo Fisher Scientific
Centrifuge 5417C/5417R/5920R	Eppendorf
CytoFLEX S	Beckman Coulter
ECL imaging system	Intas Science Imaging
Freezing device	Nalgene
Fusion Fx7 (luminescence detection, UV light system)	Peqlab
Heating Block	Eppendorf
Leica Bond MAX system	Leica Biosystems
Nanodrop One Photometer	Thermo Fisher Scientific
Neubauer improved hemocytometer	Brand
Ohmeda Tec4 Anesthetic Vaporizer	Datex-Ohmeda
Optima L-90K Ultracentrifuge	Beckman Coulter
PCR Thermal Cycler	Thermo Fisher Scientific
pHmeter	Mettler Toledo
Pipettes	Eppendorf
Reflotron® Reflovet Plus	Roche Diagnostics
SCN 400 slide scanner	Leica Biosystems
Shaker and incubator for bacteria	INFORS AG; Heraeus Holding GmbH
Sterile Hood	Heraeus Holding GmbH
ThermoMixer F1.5	Eppendorf
Ultracentrifuge SW 32 Ti Rotor	Beckman Coulter
Ultracentrifuge SW 41 Ti Rotor	Beckman Coulter
Ultrasonic homogenizer	Bandelin
Vi-CELL™ XR Cell Viability Analyzer	Beckman Coulter
Western Blotting chamber	Bio-Rad
Zeiss Axiovert 40C inverted microscope	Zeiss

5.1.15 Consumables

Table 5.21 Consumables

Product	Supplier
Cell culture flasks, dishes, plates	TPP
Cell strainers 70 µm/ 100 µm	Falcon
Centrifuge tubes SW32/SW41	Beckman Coulter
Costar® 50 ml/100 ml reagent reservoirs	Corning
Cryo tubes	Greiner Bio One
Falcon tubes 15 ml/ 50 ml	Greiner Bio One
Filter tips	Greiner Bio One
HistoBond® adhesive microscope slides	Marienfeld
Insulin syringes	Braun
Lancets for blood withdrawal	Marienfeld
Microvette 1.1 ml Z-gel tubes	Sarstedt
Mr. Frosty™ freezing container	Thermo Fisher Scientific
Needles 20, 23, 27 G	Braun
Non-tissue culture treated plates (6-well; 12-well; 24-well)	Falcon
Nunc-Immuno™ MicroWell™ 96-well plates (flat-bottom)	Sigma-Aldrich
PCR tubes	Thermo Fisher Scientific
Pipette tips 10 µl -1 ml	Biozym/Greiner Bio One/Gilson
Pipettes (disposable): 2, 5, 10, 25, 50 ml	Greiner Bio One
PVDF membrane	Bio-Rad
Reaction tubes 1.5 & 2 ml	Eppendorf
Reflotron Test Strips for ALT (GPT)	Roche
Surgical disposable scalpels	Braun
Syringes	Braun
V-bottom 96-well plates	Roth
Whatman paper	Bio-Rad

5.1.16 Software

Table 5.22 Software

Name	Supplier
Aperio eSlide Manager	Leica Biosystems
CytExpert	Beckman Coulter
FlowJo 10.4	BD Biosciences
Graph Pad Prism 9.1.0	Graph Pad
In-Fusion molar ratio calculator	Takara
Serial Cloner 2.6.1	Serial Basics
SnapGene	GSL Biotech LLC
Microsoft® Word version 16.47	Microsoft

5.2 Methods

5.2.1 Cell culture

Cells were cultured at 37°C, 5 % CO_2 and 95 % humidity, and all experiments were performed under sterile conditions.

5.2.1.1 Passaging of cell lines

HepG2 NTCP K7 and HEK293 cells were cultured in T75 flasks using DMEM 10% Medium (+ 10 % FCS; 50 U/ml P/S, 20mM L-Glut, 1x MEM NEAA, 1mM Sodium pyruvate). Adherent DF-1 cells were cultured in DMEM GlutaMAX™ (+ 10 % FCS; + 50 U/ml P/S). Cells were split twice a week in a ratio of 1:10. To do so, cells were first washed 3 times with 1x PBS before trypsin treatment to dissociate them from each other and the flask. For this, flasks were put in the incubator at 37°C for 4 minutes to activate trypsin. Once the cells were loose trypsin activity was stopped using 9 ml of culture medium, cells were split to the ratio needed and resuspended in 25 ml fresh cell culture medium.

5.2.1.2 Cell counting

a. Cell lines

Before each cell culture experiment, cells were counted manually to accurately determine the total amount of cells present in the cell suspension before performing the experiment. First, cells were thoroughly manually resuspended to obtain a homogenous cell suspension. Next, cells were counted using a Neubauer counting chamber. After cleaning the chamber with 70 % ethanol, it was covered with glass. Samples were diluted 1:1 with trypan blue to stain dead cells and thus facilitate counting. To this purpose, trypan blue staining solution was generated by diluting trypan blue 1 :3 with 1x PBS. In a 96-well plate, 10 µl of cell suspension and 10 µl of trypan blue were pipetted together. Following gentle and thorough homogenization of the solution, the chamber was loaded. Live cells were counted in four large squares of the counting chamber using a light microscope (Zeiss). In the event cells touched the perimeters of a large corner square, only the cells on the two outer sides were counted. Overall cell count was determined using the following formula:

$$\text{Cells/µl} = \frac{\text{Counted cells}}{\text{Counted surface (mm\^2)} * \text{chamber depth (mm)} * \text{dilution}}$$

Figure 5.1 : Overall cell count formula

b. Primary cells

Following the isolation of LALs and splenocytes from livers and spleens of treated C57BL/6 mice, primary cells were automatically counted on a Vi-Cell™ XR Cell Viability Analyser from

Beckman Coulter. For this cell suspension was diluted 1:20 with PBS in a Vi-CELL sample vial. Live cells present in each sample were determined using Vi-CELL X 203 Software from Beckman Coulter.

5.2.1.3 Transfection

a. Plasmid DNA transfection

On day 0, HepG2 NTCP K7 or HEK293 cells were seeded out in a 12 well-plate with $1{,}5*10^5$ cells/well to obtain a cell density for optimal transfection. On the following day, DNA transfection was performed according to the manufacturer's protocol with 2:1 Lipofectamine™ 2000 (Invitrogen™) using either 500 ng or 1 µg *DNA-HBVac* plasmid.

b. mRNA transfection using Lipofectamine Messenger Max

On day 0 HepG2 NTCP K7 or HEK293 cells were seeded out in a 12 well-plate with $1{,}2*10^6$ cells/well. On the next day, mRNA transfection was carried out by employing the transfection reagent Lipofectamine™ MessengerMAX™ (Invitrogen™). A ratio of 1:3, meaning 1 µg of mRNA and 3 µl transfection reagent was utilized throughout the experiments. First, Lipofectamine™ MessengerMAX™ was diluted in the appropriate volume of Opti-MEM® (Gibco™) according to the manufacturer's protocol. This master mix was incubated at room temperature for 10 minutes. Next, the appropriate amount of mRNA was diluted as well in Opti-MEM® (Gibco™) to form the mRNA master mix. The mRNA master mix was added to the Lipofectamine™ MessengerMAX™ master mix to allow lipoplex formation. Prior to mRNA transfection, a fresh cell culture medium was pipetted onto the cells. Cells were transfected with 50 µl /well of the final master mix.

5.2.1.4 Cell lysis

To collect the proteins generated by the cells after transfection with either mRNA or DNA, cell lysis was performed. Cell culture medium was withdrawn from the cells and the wells were washed once with 1x PBS. Next, lysis buffer was prepared using 1x Radio-Immunoprecipitation Assay (RIPA) Buffer (Sigma-Aldrich) as well as c0mplete™ proteinase inhibitor in a 1:25 ratio, to protect proteins from degradation. Cells were overlayed with 150 µl of the RIPA Proteinase Inhibitor Master Mix per well. Next, cell lysates were transferred into Eppendorf tubes. Cell lysates were incubated on ice for 10 minutes before being centrifugated for 10 minutes at 4°C, 20.000 g. Finally, supernatants were transferred into new Eppendorf tubes and stored at -20°C until further sample processing.

5.2.1.5 Western Blot analysis

Western Blot is a molecular biology method that allows the detection of specific proteins of interest present in a sample. For this purpose, samples first undergo protein denaturation

followed by gel electrophoresis to separate the proteins and finally, antibody recognition to identify specific target proteins. First, the medium was withdrawn from the cultivated cells and those were washed twice with 1x PBS solution. Next, cell lysis was performed as described in Methods section 1.1.1.4. Cell lysates were mixed 1:4 with a 4x Laemmli buffer containing SDS and β-Mercaptoethanol and incubated at 95°C for 10 min to remove secondary and tertiary structures of the proteins of interest. These denatured proteins were then loaded onto a gel. Here, proteins were separated according to their molecular mass. Once the electric voltage is applied for electrophoresis, proteins, which are anionic in the presence of sodium dodecyl buffer (SDS) containing laemmli buffer, therefore migrate towards the anode, the positive charged electrode. While migrating through the mesh of the gel, proteins are separated according to their molecular size (kDa). As the polyacrylamide gel meshes narrow down when getting closer to the anode, proteins of small size will migrate faster and further into the gel as compared to larger proteins. To estimate the molecular size of the analyzed protein, markers consisting of proteins with known molecular weight are used (PageRuler^{TM}, Prestained Protein Ladder, Thermo Fisher Scientific).

For each gel pocket of the stacking gel, 10 µl of the appropriate sample, 8,75 µl H_2O, and 6,25 µl SDS protein loading dye were pipetted into a reaction tube and incubated for 10 minutes at 95°C, 11 g for protein denaturation. Samples were briefly put on ice, centrifugated, and put on ice again. In the meantime, stacking gel as well as running gel were prepared for electrophoresis according to the instructions mentioned in Table 1.

Components	Stacking gel 5%	Running gel 12,5%
40% PAA/BisAA	0,24 ml	2,5 ml
1M Tris pH 8,8	0,5 ml	3 ml
10% SDS	20 µl	80 µl
MiliQ Water	1,25 ml	2,5 ml
TEMED	2 µl	7 µl
APS	15 µl	40 µl
Final volume	2 ml	8 ml

Table 5.23 : Description of collecting gel and running gel for electrophoresis

Next, gels were built up in the western blot chamber previously filled with running buffer. 20 µl sample or 5 µl marker were pipetted into each sample or marker gel pocket, respectively. Proteins were separated by Sodium Dodecyl Sulfate-polyacrylamide gel electrophoresis for approximately 30 minutes at 15 mA/gel (Bio-rad) until these proteins reached the running gel. Once the proteins got to the running gel; electrophoresis was pursued further for approximately 1 hour at 20 mA/gel. The proteins on the gel were blotted onto a methanol-activated polyvinylidene difluoride (PVDF) membrane to make them accessible for antibody recognition.

Next, electroblotting was performed. The western blot chamber was filled with transfer buffer and a 300-mA electric voltage was applied for 1,5-2 hours to enable the transfer of the proteins from the gel onto the membrane (Mini Trans-Blot® Cell device, Bio-Rad). Next, membranes were blocked with 50 ml 5 % milk powder resuspended in Tris-buffered saline solution supplemented with 1 % Tween-20 (TBST) for 1 hour on a shaker at room temperature (RT). Membranes were incubated in TBST solution supplemented with either HBsAg-specific monoclonal murine antibody HB1 (1:1000) or with HBcAg specific 8c9 murine in-house hybridoma supernatant (1:1 in 3 % milk powder diluted in TBST) overnight at 4°C. Following three washing steps of 10 minutes with TBST, membranes were incubated in the secondary antibody solution consisting of Horseradish Peroxidase (HRP) conjugated goat anti-mouse IgG (1:10.000 in TBST) for 2 hours at RT. ECL Prime Western Blotting Detection Reagent (Amersham) was overlayed onto the membranes prior to protein band detection by ECL Chemocam Detection System (Intas).

5.2.1.6 Cryoconservation of cells

For freezing the leftovers of LAL and splenocyte suspensions, cells were centrifugated for 5 minutes at 11 g, 4°C. The supernatant was withdrawn and the pellet was resuspended in 450 µl pure fetal calf serum (FCS) supplemented with 10 % dimethyl sulfoxide (DMSO). Next, cells were transferred into cryo vials and stored at -80°C for long-term storage.

5.2.1.7 Modified Vaccinia Ankara (MVA) amplification and purification

a. MVA amplification

For large-scale MVA (*MVA-HBVac*) amplification, a pre-culture stock of *MVA-HBVac* was generated. For this, approximately 95 % confluent DF-1 (chicken embryo fibroblast cell line) cells, cultured in one T175 flask, were infected with 10 µl of original purified *MVA-HBVac* stock (approximal concentration: $1*10^9$ IFU/ml) diluted in 5 ml of DMEM GlutaMAX™ full cell culture medium for 2 hours at 37°C, 5 % CO_2. Next, cell culture flasks were filled up with GlutaMAX™ full medium up to 20ml final volume and put for 2-3 days for incubation at 37°C, 5 % CO_2. Successful infection was observed when 90-100% of cells became round and were less adherent. Then, cells were scratched from the bottom of the flasks, transferred into a new 50 ml, and frozen at -80°C until further use (referred to as *MVA-HBVac* preculture). Next, large-scale MVA amplification was performed using approximately 30 T175 cell culture flasks of confluent DF-1 cells. For this purpose, MVA-precultures were thawed at 37°C in the water bath and diluted in the appropriate amount of GlutaMAX™ full medium needed to infect 30 T175 flasks. Original medium was withdrawn from the flasks and 5 ml diluted *MVA-HBVac* preculture was pipetted into each flask before incubation for 1 hour at 37°C, 5 % CO_2. One hour later each flask was filled up with 20 ml fresh GlutaMAX™ full medium. Upon successful infection

cells infected with *MVA-HBVac* were scratched using cell scrapers and centrifuged for 5 min at 1.968 g, 4°C. Finally, the cell pellet was resuspended in 30 ml Tris Buffer (10 mM; pH 9,0) and MVA suspension was stored at -80°C until further processing.

b. MVA purification

To rupture the cell membranes of *MVA-HBVac* infected DF-1 cells and release *MVA-HBVAc* particles in the supernatant, MVA suspension was alternately thawed at 37°C, frozen at -80°C and sonicated for three times each to collect viral supernatant. Sonication was performed on ice for 30 seconds each time with the ultrasonic homogenizer (Bandelin). Then the suspension was centrifuged for 5 minutes at 1.968 g, 4°C to pellet cell debris. The supernatant was transferred into a new 50 ml falcon tube and the cell debris pellet was resuspended into 20 ml 10 mM Tris buffer for the next sonication step. In the next step, MVA suspension was purified using two sucrose gradients. First, 6 Ultraclear tubes, previously cleaned with 70 % ethanol were filled with 25 ml 36 % sucrose and overlayed with 13 ml of the generated MVA suspension. UltraClear tubes were centrifuged for 1,5 hours at 22.413 g, 4°C using Ultracentrifuge and SW32 rotor (Beckman Coulter, SW32 Ti rotor). The supernatant was withdrawn and MVA pellets were dried at RT under sterile conditions. Once dried, the MVA pellet was resuspended in a final volume of 12 ml Tris Buffer (10 mM; pH 9,0) and stored at -80°C. Then, a second sucrose gradient was conducted. 6 Ultraclear tubes, previously cleaned with 70 % ethanol were filled with 10 ml 36 % sucrose and each tube was overlayed with 2 ml of the MVA-suspension. UltraClear tubes were centrifuged for 1,5 hours at 22.413 g, 4°C using Ultracentrifuge and SW41 Insert. MVA pellet was resuspended in 300 µl Tris Buffer (10 mM; pH 9,0), transferred into a cryotube, and stored at -80°C until titration of the generated MVA stock. MVA stock titration was performed by Dr. Julia Sacherl using a TCID50-based assay.

5.2.2 Molecular biology techniques

5.2.2.1 Culture of competent stlb3 Escherichia coli

In our studies, we used chemically competent Stlb3 *Escherichia coli* derived from the HB101 *E. coli* strain known for its high transformation efficiency. Bacterial culture was performed in large Erlenmeyer flasks filled with LB medium supplemented with the antibiotic kanamycin (1: 1000) or on kanamycin (100 µl /ml) treated agar plates, both incubating at 37°C for optimal bacteria growth.

5.2.2.2 Transformation of competent stlb3 Escherichia coli

Stlb3 *E. coli* aliquot, stored at -80°C, was thawed on ice. Once thawed, 1 µl plasmid DNA was added to the bacterial suspension. It was then incubated on ice for 15 minutes. Next, a heat shock was performed at 42°C for 45 seconds to allow the DNA to enter the bacterial cells. Afterward, the solution was put on ice for 2 minutes. 500 µl of LB medium were prewarmed at

37°C in the heating block. Following incubation, the bacterial suspension was transferred into the prewarmed LB medium. The suspension was gently but thoroughly mixed with a pipette for homogenization and the reaction tube was put for incubation, for one hour at 37°C, 31 g. Finally, to perform bacterial selection, the suspension was transferred onto LB agar plates containing 100 µg/ml kanamycin. The plates were put in the incubator overnight at 37°C for bacterial growth.

5.2.2.3 Amplification and isolation of plasmid DNA

One or two days after the transformation of bacteria, colonies were picked and transferred to a 15 ml falcon tube containing 5 ml of LB medium and 5 µl of kanamycin. The bacterial suspensions were cultured overnight at 37°C in the shaker. On the following day, bacterial precultures were used to amplify the bacterial suspension to a higher final yield volume. One to two days later, all bacterial cultures were harvested and centrifugated for 20 minutes at 500 g, 4°C. Plasmid purification and isolation were performed using Machery and Nagel DNA extraction Kit according to the manufacturer's protocol. The collected plasmid DNA was eluted in 500 µl 1x PBS. The concentration of the isolated DNA was determined by NanoDrop One (ThermoFisherScientific). Following plasmid amplification using the original stock, the presence of the right insert (*HBVac* insert) in the obtained plasmid was verified. To do so restriction digestion was conducted with two sets of previously optimally chosen restriction endonucleases that cleave DNA at specific sites.

Ingredients	**Reaction tube 1 (amplified stock)**	**Reaction tube 2 (original plasmid stock)**	**Reaction tube 3 (negative control)**
Set of restriction enzymes No. 1 (1µl/enzyme)	EcoRI PvuI	EcoRI PvuI	EcoRI PvuI
Set of restriction enzymes No. 2 (1µl/enzyme)	EcoRI KpnI	EcoRI KpnI	EcoRI KpnI
10xFast Digest Buffer (µl)	2	2	2
Plasmid volume (µl) containing 2,8 µg	0,98	0,67	0
H20 (up to 20µl)	15,02	15,33	16

Table 5.24 : Diagnostic enzymatic digestion of *DNA-HBVac*
Pipetting scheme to quickly control the identity of the amplified plasmid *DNA-HBVac* via diagnostic digestion. Reaction tubes were incubated for 1 hour at 37°C. Afterward the size of the obtained products was analyzed by 1% agarose gel electrophoresis using (50ml 1xTAE buffer, 0,5g Agarose, and 8 µl Ethidiumbromid for DNA intercalation) at 120 V for one hour. To determine the size of the products 10 µl of 10kB ladder was used. Gel interpretation was performed at UV light (320 nm wavelength).

5.2.3 Generation of *RNA-HBVac*: Molecular techniques and cloning

5.2.3.1 PCR

PCR enables the amplification of genes of interest. In this study, the gene fragments encoding for the *HBVac* insert were amplified by PCR to be used for further cloning procedures. Appropriate primer pairs for the amplification of the *HBVac* insert were designed using Takara InFusion Software.

The *HBVac* insert was amplified via PCR conditions described in table 3 and temperature settings shown in table 4.

Material	Concentration	Volume (µl)
Plasmid *RNA-HBVac*	100 ng/ µl	1
Primer forward	20 µM	0,75
Primer reverse	20 µM	0,75
Water for injection		Up to 50 µl

Table 5.25 : PCR mix to amplify the DNA sequence of the HBVac insert

Step	Temperature (°C)	Duration	Number of cycles
Step 1 : Initial denaturation	94	5 min	1
Step 2a : Denaturation	72	15 s	1
Step 2b : Annealing	70	30 s	40
Step 2c : Elongation	70	5 min	1
Step 3 : Final elongation	4	∞	-

Table 5.26 : Temperature conditions to amplify HBVac insert in PCR machine

5.2.3.2 Gel electrophoresis for PCR product analysis

Gel electrophoresis was performed to enable the estimation of the amount and the size of the amplified *HBVac* insert as well as the backbone plasmid. For this purpose, a 1 % agarose gel using 0,5 mg Agarose, 50 ml 1xTAE buffer, and 8 µl ethidium bromide for DNA intercalation was used. To determine the size of the obtained PCR products 5 µl of 10 kb DNA ladder was used. Electrophoresis was conducted at 100 V for 30 minutes. Finally, the gel was analyzed by UV light at a wavelength of 312 nm (Fusion Fx7 machine, Peqlab) to visualize bands.

5.2.3.3 DNA extraction from agarose gel

Following agarose gel electrophoresis, PCR products were purified from the template DNA using UV light to cut out of the gel the parts that contained the DNA fragments of interest. Those were cleaned up using a PCR Clean-up Kit (Hoffmann-La Roche AG) according to the manufacturer's protocol. The products were eluted in approximately 50 µl sterile H_2O miliQ. Concentrations of 30 ng/µl for *HBVac* insert and 60 ng/µl for *RNA-HBVac* target plasmid were obtained, respectively. Next, the target plasmid was digested with the restriction enzyme FastAP. For this, 13.5 µl of diluted target plasmid (~ 10 µg) were mixed with 1.5 µl FastAP, 2

µl 10x FastDigest Buffer and incubated for 1 h at 37°C. Plasmid clean-up was performed with the Gel extraction Kit from Qiagen according to the manufacturer's protocol.

5.2.3.4 Ligation

A molarity calculator from Takara Clontech was used to estimate the amounts of backbone plasmid and *HBVac* insert needed to ligate the insert into the target vector.

Insert/Vector ratio	Recommendation
Vector size (bp)	5 200
Insert size (bp)	4 200
Amount of vector	150 ng
Amount of insert	242.3 ng

Table 5.27 : Estimation of correct amounts of plasmid and insert for ligation

Component	Concentration	Amount
RNA-HBVac target plasmid	60 ng/µl	120 ng
HBVac insert	30 ng/µl	180 ng
5x InFusion HD Enzyme Premix (Takara)		2 µl
sterile H_2O miliQ		up to 20 µl

Table 5.28 : Reaction mix for InFusion ligation

To perform InFusion ligation, the reaction mixture was incubated for 15 minutes at 50°C and then frozen at -20°C.

5.2.3.5 Transformation in chemically competent Escherichia coli

Chemically competent *E. coli* were thawed for 30 min on ice. Following ligation, 5 µl of *RNA-HBVac* plasmid, which was generated by InFusion cloning, was incubated with 50 µl of chemically competent *E. coli* for 45 seconds at 42°C (heat shock). The reaction was stopped by putting the reaction tube on ice. 200 µl of SOC Medium (Super Optimal broth with catabolite repression) was added to the mixture to increase the transformation efficiency. Thereafter, the obtained mixture was incubated for 1 hour at 37°C. 200 µl of the transformed cells were plated out onto an agar plate containing 100 µg/ml ampicillin and incubated overnight at 37°C. This step was conducted to enable the selection of transformed bacteria. On the following day, single positive colonies were picked and transferred into reaction tubes containing 5 ml of LB Medium and 5 µl of ampicillin for inoculation overnight at 37°C with shaking. Mini preparation was performed using MiniPrep Kit from Qiagen following the manufacturer's instructions to purify the amplified plasmid. The obtained plasmid *RNA-HBVac* was eluted in 50 µl elution buffer. The concentration of isolated *RNA-HBVac* plasmid was assessed with Nanodrop™ One Photometer (Thermo Fisher Scientific).

5.2.3.6 Restriction enzyme digestion of RNA-HBVac plasmid

The purpose of restriction digestion was to check if our clones contained the desired insert, *HBVac*. Restriction enzyme digestion was performed using enzymes that cleave DNA at specific sequences. For each of the clones, we performed restriction enzyme digestion according to the following table.

Material	Component	Amount (µl)
Plasmid	*RNA-HBVac*	5
Restriction Enzyme 1	EcoRI	1,5
Restriction Enzyme 2	SacI	1,5
10x Green Fast Digest Buffer		2
Water for Injection		Up to 20

Table 5.29 : Reaction mixture for each clone for restriction enzyme digestion

The reaction tubes were incubated for 30 minutes at 37°C. Afterward, gel electrophoresis was performed as described in section 5.2.3.2. Using ApE software, the fragment lengths were checked following successful digestion. Restriction analysis was pursued to reveal that 2 fragments should be generated upon successful digestion: one fragment of 5.835 bp (from EcoRI to SacI) and another one of 3.729 bp (from SacI to EcoRI).

5.2.3.7 Sequencing of the plasmid construct

Gel Analysis was used to reveal if the clones showed a correct digestion profile. Next, the selected clones were sequenced to verify the forward as well as the reverse base sequence of the insert. Sequencing was performed by GATC Biotech (Germany).

5.2.3.8 RNA-synthesis

For messenger RNA (mRNA) synthesis, all materials were cleaned using RNaseZap™ (Invitrogen™) solution to prevent any degradation of the mRNA by RNases. In addition, only filter tips were used when pipetting to avoid any contamination. mRNA synthesis was performed using the T7 in vitro transcription method. First, the plasmid *RNA-HBVac* containing T7 promotor was linearized using the appropriate restriction enzyme, EcoRI, as it should be located right after the genomic sequence of the desired mRNA construct. 10 µl of plasmid were mixed with 2 µl 10x FastDigest Buffer, 5 µl EcoRI restriction enzyme, and 3 µl H2O. The mixture was incubated for 1 h at 37°C. 1% agarose gel analysis for proof of digestion efficiency was performed according to the protocol described in section 5.2.3.2. Next, the obtained linearized plasmid was cleaned up and precipitated using 1:20 volume of 0,5 M EDTA, 1:10 volume of 5 M NH_4 as well as 2 volumes of 100 % ethanol. For precipitation, the reaction mixture was incubated for 20 min at -20°C. To obtain a DNA pellet, the sample was centrifugated twice at 20.800 g for 15 min at 4°C. After two washing steps with 100 % ethanol

and removal of the residual fluid, the pellet was resuspended in 25 µl sterile nuclease-free H_2O MiliQ water. The final target concentration of the DNA template was ~ 0,3-1 µg/ µl. In the next step T7 in vitro transcription was performed using HiScribe T7 ARCA mRNA Kit (with PolyA tailing) from New England BioLabs, United Kingdom. First, all kit components were thawn at room temperature (RT). Then, the reaction mix was pipetted in PCR tubes strictly following the order described in Table 8.

Component	Concentration	Volume to pipette (µl)
Nuclease free water		up to 20 µl final volume
2x ARCA/NTP Mix		10
DNA Template	0,3-1 µg/ µl	1
T7 RNA polymerase mix		2
Final volume		20

Table 5.30 : Reaction mixture for mRNA synthesis

The reaction tube was incubated for 2 hours at 37°C (30 min synthesis and 25 min poly(A)-tailing steps). During this step, mRNA synthesis occurred by the T7 RNA polymerase, and an Anti-Reverse Cap Analog (ARCA cap) was cotranscriptionally introduced into the mRNA construct. To produce chemically modified mRNA constructs, N1-Methylpseudo-UTP (φ) and 5-Methyl-CTP (m^5CTP) analogous (Jena Bioscience) were added to the mRNA construct according to the manufacturer's protocol. Next, DNAse treatment of the samples was conducted to remove the template DNA. For this purpose, 2 µl of DNAse I was added to the reaction tube and incubated for 15 minutes at 37°C. In addition, 0,5 µl of the sample was collected and stored at -20°C for subsequent quality control of the untailed mRNA. Finally, a poly(A) tailing reaction was performed. For this purpose, the reaction mix was again pipetted in PCR tubes strictly following the order described in Table 9 and incubated for 25 minutes at 37°C.

Component	Concentration	Volume to pipette (µl)
Nuclease free water		65
In vitro synthesized mRNA		20
Poly(A) Polymerase rection buffer	10x	10
Poly(A) Polymerase		5
Final volume		100

Table 5.31 : Reaction mixture for poly(A) tailing of the synthesized mRNA

The capped and tailed mRNA was then cleaned up using an RNA Clean and Concentrator kit from Zymo Research, USA, following the manufacturer's instructions. The *in vitro* synthesized mRNA was eluted in 35 µl nuclease-free water. In addition, 0,5 µl of the sample was collected and stored at -20°C for subsequent quality control of the untailed mRNA.

5.2.3.9 Quality control of the in vitro synthesized mRNA

Quality check by gel analysis was used to check if the poly(A) tailing reaction was successful. Therefore, using the appropriate RNA ladder, it is assumed that the tailed mRNA construct should have a bigger molecular size than the untailed mRNA construct. To conduct quality control a 2 % agarose gel was prepared using fresh 1x TAE buffer to avoid RNase contamination and subsequent RNA degradation. RNA ladder was generated using 10 µl nuclease-free water and 12 µl 2x RNA loading dye. Quality control was achieved following the pipetting scheme described in Table 10.

Component	Concentration	Volume to pipette (µl)
Untailed or tailed mRNA		0,5
Nuclease free water		5,5
RNA loading dye	2x	6
Final volume		12

Table 5.32 : Quality control of in vitro transcribed mRNA

Samples were incubated for 10 minutes at 65°C and spun down after incubation. Those as well as the RNA ladder were loaded onto the agarose gel and electrophoresis was performed for 45 minutes at 80 V. Concentration of isolated mRNA construct *RNA-HBVac* was assessed with Nanodrop™ One Photometer (Thermo Fisher Scientific).

5.2.4 In vivo studies in C57BL/6 mice

Animals were kept in the biosafety level 2 pathogen-free animal facility of the Institute of Virology and Microbiology of the Technical University of Munich (TUM), Munich, Germany. All experiments were conducted following approval (approval number: ROB-55.2-2532.Vet_02-18-24) of the local animal care authorities of Upper Bavaria and in compliance with the regulations issued by the Federation of European Laboratory Animal Science Associations (FELASA) and the German Society for Animal Laboratory Science (GV-SOLAS). Animals were observed and scored once a week for description of behavior and appearance. Weight monitoring was performed once a week to assess potential drug-related side effects.

All *in vivo* experiments were performed with the kind support of Dr. Anna Kosinska.

5.2.4.1 Anesthesia

Before painful treatments were applied, mice were anesthetized with isoflurane. First, mice were put in an anesthetic induction chamber filled with 5 % isoflurane for 5 min to induce anesthesia. After induction, mice were transferred to a nose cone delivering isoflurane in a constant flow. Isoflurane was delivered with oxygen through an open circuit. Lubricant cream was used to cover the eyes of the animals to prevent dry eyes due to extended exposure to

isoflurane/O_2. Anaesthesia was monitored by observing chest wall and respiration movements. Body temperature was monitored and maintained constant with the help of infrared light. Pain and deepness of anesthesia were assessed via the lack of reaction to pain as well as to autonomous stimuli such as neurological reflexes (corneal reflex and paw reflex). Following vaccine administration, mice were observed and monitored until complete recovery.

5.2.4.2 Transduction of mice with AAV-HBV

In our studies, adenoviral-associated virus (AAV) vectors were used as a delivery system to establish persistent HBV replication and mimic chronic HBV infection in mice. Nine weeks old C57BL/6 male mice were intravenously infected with an adeno-associated virus encoding for 1.2 –overlength HBV genome (AAV-HBV 1.2) of genotype D (diluted in 100 µl PBS) which was previously established in our laboratory by Dr. Julia Festag. The infection was kindly performed by Dr. Anna Kosinska 6 weeks before the onset of prime-boost vaccination to ensure the establishment of sufficient persistent HBV replication in the livers of the mice.

5.2.4.3 Intravenous injection

Mice were put in a mechanical restrainer. Intravenous injection was administered into the veins of the tail of mice which were previously disinfected with 70 % ethanol. The tail was held under slight tension and AAV-HBV was slowly injected in a volume of 200 µl PBS in the vessel to prevent the rupture of the vein. Finally, pressure was applied on the injection site to prevent hematoma formation and stop the bleeding.

5.2.4.4 Immunization

a. Heterologous prime-MVA-HBVac boost therapeutic hepatitis B vaccine regimen

In the studies carried out, C57BL/6 mice were immunized with a heterologous prime-MVA-HBVac boost therapeutic hepatitis B vaccine according to the immunization scheme described by Backes and Jäger in 2016. Mice were primed twice in a 2–4-week interval with either *DNA-HBVac*, recombinant HBsAg, both, recombinant HBsAg and HBcAg, or with RNA-HBVac according to each experimental setup, 2-4 weeks after the second priming immunization, mice were boosted with $3*10^7$ IFU MVA-HBVac, a recombinant vector expressing HBV S, core as well as RT proteins. The vaccination scheme of each experiment can be looked up in the respective results section.

b. Subcutaneous injection

Before injection, mice were anesthetized with isoflurane as described in section 5.2.4.1. Injection sites were previously cleaned with disinfectant. The vaccine was diluted in PBS and injected subcutaneously in the interscapular space, located between the skin and the underlying muscles of the neck of C57BL/6 mice in a volume of 100 µl.

c. Intramuscular injection

Before injection, immunization sites were disinfected with a disinfectant solution. No anesthesia was used. The vaccine was diluted in sterile PBS to the given concentration and injected in a volume of 50 µl/leg. Vaccine formulations were carefully injected into the thigh muscles of the hind limb region using a 27-gauge needle to avoid damage to the sciatic nerve. After injection, mice were carefully monitored especially looking for potential motorical dysfunctions that may occur due to the injection.

5.2.4.5 Bleeding

Animals were bled from the submandibular vein using a lancet. Bleeding was performed for monitoring at several time points after AAV-HBV transduction and after immunization, mostly in a 2-week interval. Blood was collected in Microvette 1.1 ml Z-Gel tubes for HBV serological analyses. Following blood collection, serum tubes were centrifuged at RT for 5 minutes, 10.000 g to separate the serum from other blood components. Next, the isolated sera were transferred into fresh reaction tubes and stored at -20°C until further processing.

5.2.4.6 Analysis of HBV serum parameters

After the isolation of the serum from whole blood, serum analyses were conducted. First, immediately after blood collection and centrifugation alanine aminotransferase activity (ALT) was measured using the Reflotron® GPT/ALT test from Roche, Switzerland according to the manufacturer's protocol. For this purpose, serum was diluted 1:4 with PBS solution. Anti-HBc antibody titers were assessed with BEP III after 1:50 or 1:100 dilution in PBS using the Enzygnost® Anti-HBc monoclonal test from Siemens Healthcare. Furthermore, serum HBsAg as well as HBeAg levels were quantified on Architect™ platform (Abbott Laboratories) after 1:20 or 1:100 dilution with PBS. For this purpose, the quantitative HBsAg tests 6C36-44 (cut-off: 0.25 IU/ml) and the HBeAg reagent Kit 6C32-27 with quantitative calibrator 7P24-01 (cut-off: 0.20 PEI U/ml) were used.

5.2.4.7 Termination of mouse experiments

On the last day of the experiment, mice were sacrificed by neck dislocation, blood, spleen, and liver of the mice were collected and processed. A 23 G syringe was used to withdraw blood from the vena cava. The blood was transferred into a Microvette 1.1 ml Z-Gel tube for further serological analysis of the serum at killing timepoint. Following excision, the spleen was directly transferred into a 50 ml falcon tube containing RPMI 1640 medium (referred to as wash medium) and put on ice until proceeding with splenocyte isolation. Next, the liver was perfused with PBS through the portal vein to wash out any extrahepatic blood components and erythrocytes. Correct and sufficient perfusion of the liver was reached when liver tissue color got lighter. Before dissecting the liver, the gallbladder was excised. After excision, the liver was

put on a petri dish and kept on ice until further processing. Quadratic liver tissue pieces were cut out of the liver for later DNA and RNA extraction as well as histological analyses. Liver tissue for DNA extraction was transferred into a reaction tube containing T1 buffer (Nucleo Spin Tissue Kit) and directly frozen at -20°C until further processing. Liver tissue for RNA isolation was transferred into a reaction tube containing RNA later buffer and stored for 24 hours at 4°C before being frozen at -20°C until further processing. One slice of each liver sample was cut and transferred into a histological cassette for histological analysis. Cassettes were incubated in 4 % paraformaldehyde for 24 hours and then transferred to PBS to fix the tissue. Once fixed, paraffin embedding and further immunohistochemical analyses were kindly performed by the pathology department of the University Hospital Rechts der Isar, TUM, Munich, Germany. Next, livers were transferred to new 50 ml falcon tubes containing wash medium and put on ice until isolation of liver-associated lymphocytes.

5.2.4.8 Isolation of immune cells from the liver and spleen

a. Splenocyte isolation

Subsequently, the spleen was mashed through a 100 µm cell strainer using the plunger of a 2 ml syringe. To remove all the remaining cells on the strainer wash medium was used. Cells were collected in a 50 ml falcon tube with a final volume of 20 ml. Falcon tubes were spun for 5 minutes at 277 g, 4°C to pellet the cells. Next, the supernatant was withdrawn, and erythrocyte lysis was performed. To conduct erythrocyte lysis, the pellet was resuspended in 2 ml ammonium-chloride-potassium (ACK) lysis buffer and incubated for a maximum duration of 1 minute. Lysis was stopped by filling the falcon tube up to 45 ml with a wash medium. Cells were pelleted again (5 minutes, 277 g, 4°C) to wash out the lysis buffer. Cells were resuspended in 4-5 ml of RPMI 1640 medium supplemented with 10 % FCS and 50 IU/ml penicillin-streptomycin (referred to as full medium). Finally, the cell suspension was filtered through a fresh 100 µm cell strainer to remove potential cell clumps and obtain a single-cell suspension. Splenocytes were kept on ice until further processing.

b. Isolation of liver-associated lymphocytes

After liver perfusion with PBS to remove extrahepatic lymphocytes and erythrocytes, livers were mashed using the plunger of a 2 ml syringe through a 100 µm cell strainer to isolate liver-associated lymphocytes (LALs). To remove all the remaining cells from the strainer, wash medium was used. Cells were collected in a 50 ml falcon tube with a final volume of 30 ml. Samples were centrifuged for 5 minutes at 277 g, 4°C. Next, enzymatical digestion of the cell pellet was conducted by resuspending cells in collagenase-supplemented medium (200 µg/ml collagenase type IV diluted in full medium). Digestion was performed for 20 minutes at 37°C with vigorous sample shaking every 5 minutes. Next, cells were washed with a wash medium

to stop digestion and centrifuged again (5 minutes, 277 g, 4°C). Cells were resuspended in 3 ml PBS buffered 40 % percoll solution containing 100 IU/ml Heparin and layered on top of a fresh 15 ml falcon tube containing 3 ml 80% PBS buffered percoll to establish a percoll gradient. Samples were centrifuged for 20 minutes at 2.600 rpm without a break to isolate LALs. Finally, liver lymphocytes which were positioned between the erythrocyte and the hepatocyte layer were transferred into a new 50 ml falcon tube and resuspended in the appropriate volume of full medium needed.

5.2.4.9 Assessment of T-cell responses in liver-associated lymphocytes (LALs) and splenocytes

HBV-specific T-cell responses elicited by various prime-MVA-HBVac boost regimens were analyzed by MHC class I multimer staining as well as intra- and extracellular cytokine staining of cultured murine LALs and splenocytes by flow cytometry.

Flow Cytometry method is a single-cell analysis that aims to characterize cells by analyzing various surface or intracellular markers. For this purpose, a CytoFlex S flow cytometer from Beckman Coulter was used. First, cells were aspirated into a detection channel where each single cell was exposed to laser beams of different wavelengths. Sidelight scatter (SSC) and forward light scatter (FSC) generate information about the size and the granularity of cells. Next, fluorochrome-labelled antibodies were used to detect cell surface or intracellular markers. Each fluorochrome was selected to show a different emission wavelength to avoid signal overlap. The optical readout generated by the CytoFlex S flow cytometer was then converted into digital information analyzed using FlowJo software. Polyfunctionality and phenotype of $CD8^+$ and $CD4^+$ T-cells can be assessed in FlowJo using a proper gating strategy. First, the lymphocyte population was gated using FSC and SSC. Then, live cells were further analyzed by gating $CD8^+$ and $CD4^+$ T-cells. Finally, $CD8^+$ or $CD4^+$ T cells were gated according to their secretion of different markers such as IFNγ, TNF-α, IL-2, or Granzyme B.

a. Multimer Staining

Multimer staining aimed to stain antigen-specific TCRs on the surface of $CD8^+$ T cells. In the present studies, streptamers were used to identify HBV-specific TCRs on the surface of the cells. A streptamer, which is a multimer subtype, is an MHC class I peptide complex that binds non-covalently to Strep-Tactin. Strep-Tactin is labeled with a fluorescent agent (allophycocyanin, APC, or phycoerythrin, PE) and therefore enables the detection of specific TCRs by measuring its fluorescent signal. In the present studies, MHC class I multimers conjugated with H-$2K^b$-restricted MVA-specific B8R peptide or HBV-specific peptides S190, C93, and ovalbumin derived peptide (OVA_{S8L}) were used. All multimers were kindly generated by the TUM Institute of Microbiology (Prof. Dirk Busch's lab). For each sample 0,4 µg of the

appropriate streptamer was labeled with 0,4 µg APC- or PE-labeled Strep-Tactin in a total volume of 30 µl FACS buffer (sterile PBS supplemented with 1 % FCS). Streptamer/Strep-Tactin reaction mix was incubated for 20 minutes in the dark to enable non-covalent binding between Streptamer and Strep-Tactin to take place. In a V-bottom 96-well plate 150 µl/well splenocyte or LAL suspension were plated out and centrifuged for 3 min at 192 g, 4°C. After discarding the supernatant 30 µl of the appropriate Streptamer/Strep-Tactin mix were added to each well, gently mixed, and incubated on ice in the dark for 30 minutes. Next, 20 µl/ well of fluorescence-labeled antibody mix for cell surface staining (see Table 11), diluted in FACS buffer, was added to a final volume of 50 µl/well and incubated for half an hour. Dead-live staining of the cells was performed with fixable viability dye e780. Dead cells were excluded from the analysis. Following a washing step with FACS buffer, cells were spun down (192 g, 3 min, 4°C) and fixed with cytofix solution (70 µl/well) for 10-15 minutes. Thereafter, two washing steps were conducted, one with 150 µl/well Permwash Buffer and one with 150 µl/well FACS buffer. Finally, cells were resuspended in 200 µl/well FACS buffer. Samples were measured by flow cytometry on CytoFlex S from Beckman Coulter and analyzed using FlowJo software. CountBright™ absolute counting beads by Thermo Fisher were used to determine the absolute number of cells on flow cytometry. Counting bead solution was added to one sample well before measuring the absolute cell count of this sample on flow cytometry. The absolute number of cells obtained for one sample was extrapolated to the whole liver or spleen. Data of multimer analysis are shown as relative values after background subtraction of OVA_{SL8}.

Fluorochrome labeled antibody	Dilution
Dead-Live (eF780)	1:3 000
anti-mCD4 PeCy7	1:150
anti-mCD8a V500	1:150
anti-mCD44 FITC	1:150
anti-mPD1 PerCp (eF710)	1:200
anti-mLAG3 PE	1:200
anti-mKLRG1 PB	1:200

Table 5.33 : Fluorochrome labeled antibodies for cell surface staining

b. Intracellular cytokine staining

For analysis of intracellular cytokine production by splenocytes and LALs, cells were stimulated *ex-vivo* with different peptides or peptide pools. Those were thawed and a master mix of each peptide/peptide pool was prepared by diluting the peptide/s in full medium to a final concentration of 1 µg peptide/ml. 50 µl of the appropriate peptide was pipetted into the corresponding well of a flat-bottom 96-well plate. The ovalbumin-derived peptide OVA_{SL8} served as a negative control whereas the MVA-derived peptide B8R served as a positive control. Next, 200 µl of splenocytes or LAL's suspension (up to $2*10^6$ cells) were plated out in

each well and incubated for one hour at 37°C. Then, 20 µl/well of Brefeldin A (BFA), diluted in full medium to a final concentration of 5 mg/ml was pipetted into each well. Plates were put overnight in the incubator at 37°C for stimulation. On the next day, ICS was performed. After incubation cells were transferred to V-bottom 96-well plates and centrifuged for 2.5 minutes at 241 g, 4°C. Antibody mix for the staining of extracellular markers (CD4-APC 1: 100; CD8a-PB 1: 100; Dead-Live Staining (eF780) 1: 3 000 in FACS buffer) was prepared and 50 µl of the antibody mix was pipetted into each well. Plates were incubated for 15-20 minutes on ice in the dark. After a washing step with 150 µl/well FACS buffer, cells were fixed and permeabilized with 80 µl/well Cytofix/Cytoperm and incubated for 17 minutes on ice in the dark. Next, cells were washed using 150 µl/well 1x PermWash Buffer and ICS was initiated. Intracellular staining antibody mixture was prepared by diluting the antibodies in 1x PermWash Buffer (anti-IFN-γ-FITC: 1: 300; anti-TNF-α-PeCy7: 1: 200; Granzyme B-PE: 1: 100; anti-IL-2-PE: 1: 100). Cells were first pelleted by centrifugation and then 50 µl/well of intracellular staining antibody solution was added to each well. Plates were put for incubation for 25 minutes on ice, in the dark. Next, 150 µl/well of PermWash Buffer was added to wash the antibody solution. Finally, after two washing steps cells were resuspended in 200 µl/well of FACS buffer and prepared for measurement on the flow cytometer CytoFlex S. Sample analysis was performed using FlowJo software. Data of ICS are shown as relative values after background subtraction of the OVA_{SL8} peptide.

5.2.4.10 Histological analyses: Immunohistochemistry

After liver excision, tissue slices were incubated for 24 hours or more in 4 % paraformaldehyde (PFA) and thereafter transferred into PBS for later histological analysis. Next, paraffin embedding was performed, and liver slices were cut with the help of a rotary microtome (Thermo Fisher Scientific) into 2 µm-thin liver sections. Haematoxylin/eosin as well as core-specific immunohistochemical staining were conducted on the paraffin sections. Core-specific immunohistochemical staining was carried out using a Leica Bond MAX system with 1:50 core-specific rabbit polyclonal antibody coupled to an HRP-conjugated anti-rabbit secondary IgG antibody. Histological slides were scanned with Leica SCN 400 scanner (Leica Biosystems) and analyzed by a numerical count of $HBcAg^+$ hepatocytes in 10 random sample areas under 40x magnification. Immunohistochemical stainings was kindly performed by the Comparative experimental Pathology (CeP) division of the Pathology Department of the University Hospital Rechts der Isar from the Technical University Munich (TUM), Germany.

5.2.5 Statistical analysis

Data were statistically analyzed using GraphPad Prism software version 9.1.0 (GraphPad Software Inc.). Results are depicted as individual or mean values with standard error of the

mean (SEM). Statistical analysis was performed using nonparametric One-Way ANOVA. Asterisks were chosen to indicate statistical significance: *p<0.05, **p<0.005, ns– not significant: p>0,05.

6 List of tables

Table 5.1 Cell lines/bacterial strains....105
Table 5.2 Cell culture media....105
Table 5.3 Bacterial cell culture medium....105
Table 5.4 Media for mouse experiments....106
Table 5.5 Plasmids....106
Table 5.6 Primers....106
Table 5.7 Enzymes....106
Table 5.8 Kits....107
Table 5.9 Antigens....107
Table 5.10 *DNA-HBVac*....107
Table 5.11 *RNA-HBVac*....107
Table 5.12 Adjuvant....108
Table 5.13 Single peptides....109
Table 5.14 Peptide pools....109
Table 5.15 Streptamers....109
Table 5.16 Antibodies used for western blotting....109
Table 5.17 Antibodies used for flow cytometry....110
Table 5.18 Buffers and solutions....110
Table 5.19 Chemicals and reagents....111
Table 5.20 Laboratory devices....113
Table 5.21 Consumables....114
Table 5.22 Software....114
Table 5.23 : Description of collecting gel and running gel for electrophoresis....117
Table 5.24 : Diagnostic enzymatic digestion of *DNA-HBVac*....120
Table 5.25 : PCR mix to amplify the DNA sequence of the HBVac insert....121
Table 5.26 : Temperature conditions to amplify HBVac insert in PCR machine....121
Table 5.27 : Estimation of correct amounts of plasmid and insert for ligation....122
Table 5.28 : Reaction mix for InFusion ligation....122
Table 5.29 : Reaction mixture for each clone for restriction enzyme digestion....123
Table 5.30 : Reaction mixture for mRNA synthesis....124
Table 5.31 : Reaction mixture for poly(A) tailing of the synthesized mRNA....124
Table 5.32 : Quality control of in vitro transcribed mRNA....125
Table 5.33 : Fluorochrome labeled antibodies for cell surface staining....130

7 List of figures

Figure 1.1 Electron microscopy images of HBV viral (Dane particles) and noninfectious subviral particles (filaments and spheres) detected in the serum of highly viremic chronic HBV carrier 12
Figure 1.2 HBV virion structure and genome organization..... 13
Figure 1.3 Schematic representation of the HBV life cycle 17
Figure 1.4 Prevalence of viral hepatitis B in the world 18
Figure 1.5 Worldwide annual mortality from chronic HBV and HCV infection as compared to mortality from tuberculosis, Human Immunodeficiency Virus infection, and malaria 19
Figure 1.6 Contribution of genotypes to global chronic HBV infections 20
Figure 1.7 Distribution of HBV genotypes by country..... 21
Figure 1.8 Clinical and virological course of acute infection with HBV..... 22
Figure 1.9 Clinical and virological course of chronic infection with HBV through vertical transmission from mother to neonate..... 23
Figure 1.10 German guideline for chronic hepatitis B infection: algorithm for initiation of treatment 26
Figure 1.11 Comparison of antiviral drugs for chronic hepatitis B 27
Figure 1.12 Adoptive T-cell therapy for patients with CHB or HBV-induced HCC 31
Figure 1.13 Optimized prime-boost vaccination strategy for therapeutic vaccination against CHB..... 33
Figure 1.14 The dual mechanisms of action employed by HBV-specific $CD8^+$ T cells in eliminating HBV-infected hepatocytes..... 34
Figure 3.1 Gene expression cassette of the *HBVac* insert..... 43
Figure 3.2 Expression of HBsAg, HBcAg, and RT(pol) in HepG2 cells 24h after transfection with *DNA-HBVac* 44
Figure 3.3 Immunogenicity of *DNA-HBVac* prime – MVA boost in HBV-naïve mice..... 45
Figure 3.4 HBV-specific antibody and $CD4^+$ T-cell responses 46
Figure 3.5 HBV-specific $CD8^+$ T-cell responses..... 47
Figure 3.6 Immunogenicity of prime immunization with *DNA-HBVac* in AAV-HBV transduced mice..... 49
Figure 3.7 Serum HBsAg levels and anti-HBs titers induced by immunization with *DNA-HBVac* in HBV carrier mice 49
Figure 3.8 $CD4^+$ T-cell responses induced by immunization with *DNA-HBVac* in livers and spleens of HBV carrier mice..... 50
Figure 3.9 Induction of antigen-specific $CD8^+$ T cells by DNA-based therapeutic vaccination in HBV carrier mice 51

Figure 3.10 Functional analysis of S-specific CD8$^+$ T cells elicited by vaccination with *DNA-HBVac* in livers and spleens of HBV carrier mice 52
Figure 3.11 Functional analysis of Core- and RT-specific CD8$^+$ T cells elicited by immunization with *DNA-HBVac* in livers and spleens of HBV carrier mice 53
Figure 3.12 Evaluation of the antiviral effect induced by immunization with *DNA-HBVac* in the sera of HBV carrier mice 55
Figure 3.13 Vaccination scheme of simultaneous prime immunization with *DNA-HBVac* and recombinant HBsAg in HBV carrier mice 56
Figure 3.14 HBV-specific humoral and S-specific CD4 T-cell responses elicited by simultaneous DNA/HBsAg prime – MVA boost immunization in HBV carrier mice..... 57
Figure 3.15 Hepatic HBV-specific effector T-cell responses induced by DNA/HBsAg prime – MVA boost regimen in HBV carrier mice..... 58
Figure 3.16 Vaccination scheme of distinct prime immunization sites for *DNA-HBVac* and recombinant HBsAg in wild-type mice..... 60
Figure 3.17 HBV-specific humoral and CD4$^+$ T-cell responses elicited by distinct prime immunization sites for *DNA-HBVac* and recombinant HBsAg in HBV-naïve mice..... 61
Figure 3.18 Splenic HBV-specific CD8$^+$ T-cell responses elicited by distinct prime immunization sites for *DNA-HBVac* and recombinant HBsAg in HBV-naïve mice 62
Figure 3.19 Schedule of sequential prime immunization with *DNA-HBVac* and recombinant HBsAg in HBV carrier mice 63
Figure 3.20 HBV-specific humoral responses and serum HBV antigen kinetics at experiment onset and endpoint in HBV carrier mice receiving sequential DNA/HBsAg prime – MVA boost regimen 64
Figure 3.21 Hepatic and splenic HBV-specific CD4+ T cell responses in HBV carrier mice receiving sequential DNA/HBsAg prime – MVA boost regimen 66
Figure 3.22 Hepatic and splenic HBV-specific effector T-cell responses induced by sequential immunization with DNA/HBsAg prime – MVA boost regimen in HBV carrier mice 67
Figure 3.23 Functionality of HBV-specific CD8+ T cells isolated from livers and spleens of HBV carrier mice sequentially immunized with DNA and recombinant HBsAg 67
Figure 3.24 Core- and RT-specific CD8$^+$ T-cell responses induced by sequential immunization with DNA/HBsAg prime – MVA boost regimen in HBV carrier mice..... 69
Figure 3.25 Digestion profile of *RNA-HBVac* plasmid 71
Figure 3.26 Expression of S and Core proteins 72h post-transfection with *RNA-HBVac* plasmid 72
Figure 3.27 HBsAg and HBeAg levels in the supernatant of HepG2 NTCP K7 and HEK293 cells, 96h post-transfection with 0.5 µg *RNA-HBVac* (A) plasmid and 1 µg IVT mRNA (B)... 73

Figure 3.28 Structure of chemically modified nucleotide analogs implemented to *RNA-HBVac* 1 (A) and 2 constructs (B) 74
Figure 3.29 Expression of S, L and Core proteins in HEK293 cells 48h post-transfection with modified IVT mRNAs 75
Figure 3.30 Vaccination scheme of prime immunization with *RNA-HBVac* in HBV-naïve mice 76
Figure 3.31 Weight monitoring of immunization with *RNA-HBVac* compared to mixed adjuvanted recombinant proteins and DNA 77
Figure 3.32 Dose-dependent lymphocyte infiltration at injection site after immunization with *RNA-HBVac* 78
Figure 3.33 HBV-specific antibody responses 78
Figure 3.34 HBV-specific $CD4^+$ T-cell responses 80
Figure 3.35 Splenic HBV S-specific $CD8^+$ T-cell responses 81
Figure 3.36 Splenic HBV Core- and RT-specific $CD8^+$ T-cell responses 82
Figure 3.37 Vaccination scheme of prime immunizations with *RNA-HBVac* in HBV carrier mice 83
Figure 3.38 Serum HBsAg levels and anti-HBs titers induced by immunization with *RNA-HBVac* in HBV carrier mice 84
Figure 3.39 Hepatic and splenic $CD4^+$ T-cell responses induced by RNA prime – MVA boost immunization in HBV carrier mice 85
Figure 3.40 Induction of antigen-specific $CD8^+$ T cells by RNA prime – MVA boost immunization in HBV carrier mice 86
Figure 3.41 Functional analysis of hepatic and splenic S-specific $CD8^+$ T cells elicited by RNA prime – MVA boost vaccination in HBV carrier mice 87
Figure 3.42 Functional analysis of core- and RT-specific $CD8^+$ T cells elicited by RNA prime – MVA boost vaccination in HBV carrier mice 89
Figure 3.43 Evaluation of the antiviral effect induced by RNA prime – MVA boost immunization in HBV carrier mice 89
Figure 5.1 : Overall cell count formula 115

8 References

Ahmed, S. N. S., Tavan, D., Pichoud, C., Berby, F., Stuyver, L., Johnson, M., Merle, P., Abidi, H., TRepo, C., & Zoulim, F. (2000). Early detection of viral resistance by determination of hepatitis B virus polymerase mutations in patients treated by lamivudine for chronic hepatitis B. *Hepatology*, *32*(5), 1078-1088.

Akira, S., Uematsu, S., & Takeuchi, O. (2006). Pathogen recognition and innate immunity. *Cell*, *124*(4), 783-801.

Alarcon, J. B., Waine, G. W., & McManus, D. P. (1999). DNA vaccines: technology and application as anti-parasite and anti-microbial agents. *Advances in parasitology*, *42*, 343-410.

Amblard, F., Boucle, S., Bassit, L., Cox, B., Sari, O., Tao, S., Chen, Z., Ozturk, T., Verma, K., & Russell, O. (2020). Novel hepatitis B virus capsid assembly modulator induces potent antiviral responses in vitro and in humanized mice. *Antimicrobial agents and chemotherapy*, *64*(2).

Anastasiou, O. E., Theissen, M., Verheyen, J., Bleekmann, B., Wedemeyer, H., Widera, M., & Ciesek, S. (2019). Clinical and virological aspects of HBV reactivation: a focus on acute liver failure. *Viruses*, *11*(9), 863.

Andries, O., Mc Cafferty, S., De Smedt, S. C., Weiss, R., Sanders, N. N., & Kitada, T. (2015). N1-methylpseudouridine-incorporated mRNA outperforms pseudouridine-incorporated mRNA by providing enhanced protein expression and reduced immunogenicity in mammalian cell lines and mice. *Journal of Controlled Release*, *217*, 337-344.

Armengol, G., Ruiz, L. M., & Orduz, S. (2004). The injection of plasmid DNA in mouse muscle results in lifelong persistence of DNA, gene expression, and humoral response. *Molecular biotechnology*, *27*(2), 109-118.

Asbach, B., Kliche, A., Köstler, J., Perdiguero, B., Esteban, M., Jacobs, B. L., Montefiori, D. C., LaBranche, C. C., Yates, N. L., & Tomaras, G. D. (2016). Potential to streamline heterologous DNA prime and NYVAC/protein boost HIV vaccine regimens in rhesus macaques by employing improved antigens. *Journal of virology*, *90*(8), 4133-4149.

Backes, S., Jäger, C., Dembek, C. J., Kosinska, A. D., Bauer, T., Stephan, A.-S., Dišlers, A., Mutwiri, G., Busch, D. H., & Babiuk, L. A. (2016). Protein-prime/modified vaccinia virus Ankara vector-boost vaccination overcomes tolerance in high-antigenemic HBV-transgenic mice. *Vaccine*, *34*(7), 923-932.

Baiersdörfer, M., Boros, G., Muramatsu, H., Mahiny, A., Vlatkovic, I., Sahin, U., & Karikó, K. (2019). A facile method for the removal of dsRNA contaminant from in vitro-transcribed mRNA. *Molecular Therapy-Nucleic Acids*, *15*, 26-35.

Barnaba, V., Franco, A., Alberti, A., Benvenuto, R., & Balsano, F. (1990). Selective killing of hepatitis B envelope antigen-specific B cells by class I-restricted, exogenous antigen-specific T lymphocytes. *Nature*, *345*(6272), 258-260.

Barouch, D. H., Yang, Z.-y., Kong, W.-p., Korioth-Schmitz, B., Sumida, S. M., Truitt, D. M., Kishko, M. G., Arthur, J. C., Miura, A., & Mascola, J. R. (2005). A human T-cell leukemia virus type 1 regulatory element enhances the immunogenicity of human immunodeficiency virus type 1 DNA vaccines in mice and nonhuman primates. *Journal of virology*, *79*(14), 8828-8834.

Barry, M. E., Pinto-Gonzalez, D., Orson, F. M., McKenzie, G. J., Petry, G. R., & Barry, M. A. (1999). Role of endogenous endonucleases and tissue site in transfection and CpG-mediated immune activation after naked DNA injection. *Human gene therapy*, *10*(15), 2461-2480.

Beasley, R. P., & Hwang, L.-Y. (1983). Postnatal infectivity of hepatitis B surface antigen-carrier mothers. *Journal of Infectious Diseases*, *147*(2), 185-190.

Benn, J., & Schneider, R. J. (1995). Hepatitis B virus HBx protein deregulates cell cycle checkpoint controls. *Proceedings of the National Academy of Sciences*, *92*(24), 11215-11219.

Benteyn, D., Heirman, C., Bonehill, A., Thielemans, K., & Breckpot, K. (2015). mRNA-based dendritic cell vaccines. *Expert review of vaccines*, *14*(2), 161-176.

Bertoletti, A., & Ferrari, C. (2016). Adaptive immunity in HBV infection. *Journal of hepatology*, *64*(1), S71-S83.

Billioud, G., Kruse, R. L., Carrillo, M., Whitten-Bauer, C., Gao, D., Kim, A., Chen, L., McCaleb, M. L., Crosby, J. R., & Hamatake, R. (2016). In vivo reduction of hepatitis B virus antigenemia and viremia by antisense oligonucleotides. *Journal of hepatology*, *64*(4), 781-789.

Blumberg, B. S. (2002). *Hepatitis B: The hunt for a killer virus*. Princeton University Press.

Boag, F. (1991). Hepatitis B: heterosexual transmission and vaccination strategies. *International journal of STD & AIDS*, *2*(5), 318-324.

Bohne, F., Chmielewski, M., Ebert, G., Wiegmann, K., Kürschner, T., Schulze, A., Urban, S., Krönke, M., Abken, H., & Protzer, U. (2008). T cells redirected against hepatitis B virus surface proteins eliminate infected hepatocytes. *Gastroenterology*, *134*(1), 239-247.

Boni, C., Laccabue, D., Lampertico, P., Giuberti, T., Viganò, M., Schivazappa, S., Alfieri, A., Pesci, M., Gaeta, G. B., & Brancaccio, G. (2012). Restored function of HBV-specific T cells after long-term effective therapy with nucleos (t) ide analogues. *Gastroenterology*, *143*(4), 963-973. e969.

Bouchard, M. J., & Schneider, R. J. (2004). The enigmatic X gene of hepatitis B virus. *Journal of virology*, *78*(23), 12725-12734.

Bourgeois, C., & Tanchot, C. (2003). Mini-review CD4 T cells are required for CD8 T cell memory generation. *European journal of immunology*, *33*(12), 3225-3231.

Bourne, C. R., Finn, M., & Zlotnick, A. (2006). Global structural changes in hepatitis B virus capsids induced by the assembly effector HAP1. *Journal of virology*, *80*(22), 11055-11061.

Bruss, V., & Ganem, D. (1991). The role of envelope proteins in hepatitis B virus assembly. *Proceedings of the National Academy of Sciences*, *88*(3), 1059-1063.

Buchmann, P., Dembek, C., Kuklick, L., Jäger, C., Tedjokusumo, R., von Freyend, M. J., Drebber, U., Janowicz, Z., Melber, K., & Protzer, U. (2013). A novel therapeutic hepatitis B vaccine induces cellular and humoral immune responses and breaks tolerance in hepatitis B virus (HBV) transgenic mice. *Vaccine*, *31*(8), 1197-1203.

Buhr, F., Jha, S., Thommen, M., Mittelstaet, J., Kutz, F., Schwalbe, H., Rodnina, M. V., & Komar, A. A. (2016). Synonymous codons direct cotranslational folding toward different protein conformations. *Molecular cell*, *61*(3), 341-351.

Burrell, C., Mackay, P., Greenaway, P., Hofschneider, P., & Murray, K. (1979). Expression in Escherichia coli of hepatitis B virus DNA sequences cloned in plasmid pBR322. *Nature*, *279*(5708), 43-47.

Buynak, E. B., Roehm, R. R., Tytell, A. A., Bertland, A. U., Lampson, G. P., & Hilleman, M. R. (1976). Development and chimpanzee testing of a vaccine against human hepatitis B. *Proceedings of the Society for Experimental Biology and Medicine*, *151*(4), 694-700.

Cai, Y., & Yin, W. (2020). The Multiple Functions of B Cells in Chronic HBV Infection. *Frontiers in immunology*, *11*, 3272.

Campbell, J. D. (2017). Development of the CpG adjuvant 1018: a case study. *Vaccine Adjuvants*, 15-27.

Carralot, J.-P., Probst, J., Hoerr, I., Scheel, B., Teufel, R., Jung, G., Rammensee, H.-G., & Pascolo, S. (2004). Polarization of immunity induced by direct injection of naked sequence-stabilized mRNA vaccines. *Cellular and Molecular Life Sciences CMLS*, *61*(18), 2418-2424.

Casimiro, D. R., Chen, L., Fu, T.-M., Evans, R. K., Caulfield, M. J., Davies, M.-E., Tang, A., Chen, M., Huang, L., & Harris, V. (2003). Comparative immunogenicity in rhesus monkeys of DNA plasmid, recombinant vaccinia virus, and replication-defective adenovirus vectors expressing a human immunodeficiency virus type 1 gag gene. *Journal of virology*, *77*(11), 6305-6313.

Castaldello, A., Brocca-Cofano, E., Voltan, R., Triulzi, C., Altavilla, G., Laus, M., Sparnacci, K., Ballestri, M., Tondelli, L., & Fortini, C. (2006). DNA prime and protein boost

immunization with innovative polymeric cationic core-shell nanoparticles elicits broad immune responses and strongly enhance cellular responses of HIV-1 tat DNA vaccination. *Vaccine*, *24*(29-30), 5655-5669.

Cavenaugh, J. S., Awi, D., Mendy, M., Hill, A. V., Whittle, H., & McConkey, S. J. (2011). Partially randomized, non-blinded trial of DNA and MVA therapeutic vaccines based on hepatitis B virus surface protein for chronic HBV infection. *PLoS One*, *6*(2), e14626.

Cerino, A., Bremer, C. M., Glebe, D., & Mondelli, M. U. (2015). A human monoclonal antibody against hepatitis B surface antigen with potent neutralizing activity. *PLoS One*, *10*(4), e0125704.

Charnay, P., Pourcel, C., LouISE, A., Fritsch, A., & Tiollais, P. (1979). Cloning in Escherichia coli and physical structure of hepatitis B virion DNA. *Proceedings of the National Academy of Sciences*, *76*(5), 2222-2226.

Chen, P., Gan, Y., Han, N., Fang, W., Li, J., Zhao, F., Hu, K., & Rayner, S. (2013). Computational evolutionary analysis of the overlapped surface (S) and polymerase (P) region in hepatitis B virus indicates the spacer domain in P is crucial for survival. *PLoS One*, *8*(4), e60098.

Chen, Y., Cheng, G., & Mahato, R. I. (2008). RNAi for treating hepatitis B viral infection. *Pharmaceutical research*, *25*(1), 72-86.

Chen, Z.-Y., He, C.-Y., Ehrhardt, A., & Kay, M. A. (2003). Minicircle DNA vectors devoid of bacterial DNA result in persistent and high-level transgene expression in vivo. *Molecular therapy*, *8*(3), 495-500.

Chinnakannan, S. K., Cargill, T. N., Donnison, T. A., Ansari, M. A., Sebastian, S., Lee, L. N., Hutchings, C., Klenerman, P., Maini, M. K., & Evans, T. (2020). The design and development of a multi-HBV antigen encoded in chimpanzee adenoviral and modified vaccinia Ankara viral vectors; a novel therapeutic vaccine strategy against HBV. *Vaccines*, *8*(2), 184.

Chu, C.-M., & Liaw, Y.-F. (1987). Intrahepatic distribution of hepatitis B surface and core antigens in chronic hepatitis B virus infection: hepatocyte with cytoplasmic/membranous hepatitis B core antigen as a possible target for immune hepatocytolysis. *Gastroenterology*, *92*(1), 220-225.

Chuai, X., Chen, H., Wang, W., Deng, Y., Wen, B., Ruan, L., & Tan, W. (2013). Poly (I: C)/alum mixed adjuvant priming enhances HBV subunit vaccine-induced immunity in mice when combined with recombinant adenoviral-based HBV vaccine boosting. *PLoS One*, *8*(1), e54126.

Clark, D. N., & Hu, J. (2015). Unveiling the roles of HBV polymerase for new antiviral strategies. *Future virology*, *10*(3), 283-295.

Coffman, R. L., Sher, A., & Seder, R. A. (2010). Vaccine adjuvants: putting innate immunity to work. *Immunity*, *33*(4), 492-503.

Corcuera, A., Stolle, K., Hillmer, S., Seitz, S., Lee, J.-Y., Bartenschlager, R., Birkmann, A., & Urban, A. (2018). Novel non-heteroarylpyrimidine (HAP) capsid assembly modifiers have a different mode of action from HAPs in vitro. *Antiviral research*, *158*, 135-142.

Cornberg, M., Sandmann, L., Protzer, U., Niederau, C., Tacke, F., Berg, T., Glebe, D., Jilg, W., Wedemeyer, H., & Wirth, S. (2021). S3-Leitlinie der Deutschen Gesellschaft für Gastroenterologie, Verdauungs-und Stoffwechselkrankheiten (DGVS) zur Prophylaxe, Diagnostik und Therapie der Hepatitis-B-Virusinfektion–(AWMF-Register-Nr. 021-11). *Zeitschrift für Gastroenterologie*, *59*(07), 691-776.

Corona Gutierrez, C. M., Tinoco, A., Navarro, T., Contreras, M. L., Cortes, R. R., Calzado, P., Reyes, L., Posternak, R., Morosoli, G., & Verde, M. L. (2004). Therapeutic vaccination with MVA E2 can eliminate precancerous lesions (CIN 1, CIN 2, and CIN 3) associated with infection by oncogenic human papillomavirus. *Human gene therapy*, *15*(5), 421-431.

Cristillo, A. D., Wang, S., Caskey, M. S., Unangst, T., Hocker, L., He, L., Hudacik, L., Whitney, S., Keen, T., & Te-hui, W. C. (2006). Preclinical evaluation of cellular immune responses elicited by a polyvalent DNA prime/protein boost HIV-1 vaccine. *Virology*, *346*(1), 151-168.

Crotty, S. (2011). Follicular helper CD4 T cells (Tfh). *Annual review of immunology*, *29*, 621-663.

Crotty, S. (2015). A brief history of T cell help to B cells. *Nature Reviews Immunology*, *15*(3), 185-189.

Dane, D., Cameron, C., & Briggs, M. (1970). Virus-like particles in serum of patients with Australia-antigen-associated hepatitis. *The lancet*, *295*(7649), 695-698.

Darquet, A., Cameron, B., Wils, P., Scherman, D., & Crouzet, J. (1997). A new DNA vehicle for nonviral gene delivery: supercoiled minicircle. *Gene therapy*, *4*(12), 1341-1349.

Dion, S., Bourgine, M., Godon, O., Levillayer, F., & Michel, M.-L. (2013). Adeno-associated virus-mediated gene transfer leads to persistent hepatitis B virus replication in mice expressing HLA-A2 and HLA-DR1 molecules. *Journal of virology*, *87*(10), 5554-5563.

Donato, F., Tagger, A., Gelatti, U., Parrinello, G., Boffetta, P., Albertini, A., Decarli, A., Trevisi, P., Ribero, M., & Martelli, C. (2002). Alcohol and hepatocellular carcinoma: the effect of lifetime intake and hepatitis virus infections in men and women. *American journal of epidemiology*, *155*(4), 323-331.

Donnelly, J. J., Ulmer, J. B., Shiver, J. W., & Liu, M. A. (1997). DNA vaccines. *Annual review of immunology*, *15*(1), 617-648.

Dooms, H., & Abbas, A. K. (2002). Life and death in effector T cells. *Nature immunology*, *3*(9), 797-798.

Döring, B., Lütteke, T., Geyer, J., & Petzinger, E. (2012). The SLC10 carrier family: transport functions and molecular structure. *Current topics in membranes*, *70*, 105-168.

Du, W.-J., Liu, L., Sun, C., Yu, J.-H., Xiao, D., & Li, Q. (2017). Prodromal fever indicates a high risk of liver failure in acute hepatitis B. *International Journal of Infectious Diseases*, *57*, 98-103.

Dubois, M.-F., Pourcel, C., Rousset, S., Chany, C., & Tiollais, P. (1980). Excretion of hepatitis B surface antigen particles from mouse cells transformed with cloned viral DNA. *Proceedings of the National Academy of Sciences*, *77*(8), 4549-4553.

Duddy, M. E., Alter, A., & Bar-Or, A. (2004). Distinct profiles of human B cell effector cytokines: a role in immune regulation? *The journal of immunology*, *172*(6), 3422-3427.

Dupuis, M., Denis-Mize, K., Woo, C., Goldbeck, C., Selby, M. J., Chen, M., Otten, G. R., Ulmer, J. B., Donnelly, J. J., & Ott, G. (2000). Distribution of DNA vaccines determines their immunogenicity after intramuscular injection in mice. *The Journal of Immunology*, *165*(5), 2850-2858.

Eckhardt, S. G., Milich, D., & McLachlan, A. (1991). Hepatitis B virus core antigen has two nuclear localization sequences in the arginine-rich carboxyl terminus. *Journal of virology*, *65*(2), 575-582.

El–Serag, H. B., & Rudolph, K. L. (2007). Hepatocellular carcinoma: epidemiology and molecular carcinogenesis. *Gastroenterology*, *132*(7), 2557-2576.

Epstein, J. E., Charoenvit, Y., Kester, K. E., Wang, R., Newcomer, R., Fitzpatrick, S., Richie, T. L., Tornieporth, N., Heppner, D. G., & Ockenhouse, C. (2004). Safety, tolerability, and antibody responses in humans after sequential immunization with a PfCSP DNA vaccine followed by the recombinant protein vaccine RTS, S/AS02A. *Vaccine*, *22*(13-14), 1592-1603.

Erhardt, A., Blondin, D., Hauck, K., Sagir, A., Kohnle, T., Heintges, T., & Häussinger, D. (2005). Response to interferon alfa is hepatitis B virus genotype dependent: genotype A is more sensitive to interferon than genotype D. *Gut*, *54*(7), 1009-1013.

Escoffre, J.-M., Zeghimi, A., Novell, A., & Bouakaz, A. (2013). In-vivo gene delivery by sonoporation: recent progress and prospects. *Current gene therapy*, *13*(1), 2-14.

European Association For The Study Of The Liver (EASL). (2017). EASL 2017 Clinical Practice Guidelines on the management of hepatitis B virus infection. *Journal of hepatology*, *67*(2), 370-398.

Fattovich, G., Stroffolini, T., Zagni, I., & Donato, F. (2004). Hepatocellular carcinoma in cirrhosis: incidence and risk factors. *Gastroenterology*, *127*(5), S35-S50.

Faurez, F., Dory, D., Le Moigne, V., Gravier, R., & Jestin, A. (2010). Biosafety of DNA vaccines: New generation of DNA vectors and current knowledge on the fate of plasmids after injection. *Vaccine*, *28*(23), 3888-3895.

Felber, B. K., Lu, Z., Hu, X., Valentin, A., Rosati, M., Remmel, C. A., Weiner, J. A., Carpenter, M. C., Faircloth, K., & Stanfield-Oakley, S. (2020). Co-immunization of DNA and protein in the same anatomical sites induces superior protective immune responses against SHIV challenge. *Cell reports*, *31*(6), 107624.

Felberbaum, R. S. (2015). The baculovirus expression vector system: A commercial manufacturing platform for viral vaccines and gene therapy vectors. *Biotechnology journal*, *10*(5), 702-714.

Fire, A., Xu, S., Montgomery, M. K., Kostas, S. A., Driver, S. E., & Mello, C. C. (1998). Potent and specific genetic interference by double-stranded RNA in Caenorhabditis elegans. *Nature*, *391*(6669), 806-811.

Fisicaro, P., Valdatta, C., Boni, C., Massari, M., Mori, C., Zerbini, A., Orlandini, A., Sacchelli, L., Missale, G., & Ferrari, C. (2009). Early kinetics of innate and adaptive immune responses during hepatitis B virus infection. *Gut*, *58*(7), 974-982.

FRANCIS, D. P., HADLER, S. C., THOMPSON, S. E., MAYNARD, J. E., OSTROW, D. G., ALTMAN, N., BRAFF, E. H., O'MALLEY, P., HAWKINS, D., & JUDSON, F. N. (1982). The prevention of hepatitis B with vaccine: report of the Centers for Disease Control multi-center efficacy trial among homosexual men. *Annals of internal medicine*, *97*(3), 362-366.

Galli, G., Hancock, K., Hoschler, K., DeVos, J., Praus, M., Bardelli, M., Malzone, C., Castellino, F., Gentile, C., & McNally, T. (2009). Fast rise of broadly cross-reactive antibodies after boosting long-lived human memory B cells primed by an MF59 adjuvanted prepandemic vaccine. *Proceedings of the National Academy of Sciences*, *106*(19), 7962-7967.

Ganem, D., & Prince, A. M. (2004). Hepatitis B virus infection—natural history and clinical consequences. *New England Journal of Medicine*, *350*(11), 1118-1129.

Gašparić, M., Rubio, I., Thönes, N., Gissmann, L., & Müller, M. (2007). Prophylactic DNA immunization against multiple papillomavirus types. *Vaccine*, *25*(23), 4540-4553.

Geginat, J., Paroni, M., Maglie, S., Alfen, J. S., Kastirr, I., Gruarin, P., De Simone, M., Pagani, M., & Abrignani, S. (2014). Plasticity of human CD4 T cell subsets. *Frontiers in immunology*, *5*, 630.

Gehring, A. J., & Protzer, U. (2019). Targeting innate and adaptive immune responses to cure chronic HBV infection. *Gastroenterology*, *156*(2), 325-337.

Gerlich, W. H. (2013). Medical virology of hepatitis B: how it began and where we are now. *Virology journal*, *10*(1), 1-25.

Gerlich, W. H. (2015). Prophylactic vaccination against hepatitis B: achievements, challenges and perspectives. *Medical microbiology and immunology*, *204*(1), 39-55.

Gilbert, S. C. (2013). Clinical development of Modified Vaccinia virus Ankara vaccines. *Vaccine*, *31*(39), 4241-4246.

Gilbert, S. C., Moorthy, V. S., Andrews, L., Pathan, A. A., McConkey, S. J., Vuola, J. M., Keating, S. M., Berthoud, T., Webster, D., & McShane, H. (2006). Synergistic DNA–MVA prime-boost vaccination regimes for malaria and tuberculosis. *Vaccine*, *24*(21), 4554-4561.

Girard, M. P., Osmanov, S., Assossou, O. M., & Kieny, M.-P. (2011). Human immunodeficiency virus (HIV) immunopathogenesis and vaccine development: a review. *Vaccine*, *29*(37), 6191-6218.

Gish, R. G., Lok, A. S., Chang, T. T., Robert, A., Gadano, A., Sollano, J., Han, K. H., Chao, Y. C., Lee, S. D., & Harris, M. (2007). Entecavir therapy for up to 96 weeks in patients with HBeAg-positive chronic hepatitis B. *Gastroenterology*, *133*(5), 1437-1444.

Glebe, D., & Urban, S. (2007). Viral and cellular determinants involved in hepadnaviral entry. *World journal of gastroenterology: WJG*, *13*(1), 22.

Glebe, D., Urban, S., Knoop, E. V., Çağ, N., Krass, P., Grün, S., Bulavaite, A., Sasnauskas, K., & Gerlich, W. H. (2005). Mapping of the hepatitis B virus attachment site by use of

infection-inhibiting preS1 lipopeptides and tupaia hepatocytes. *Gastroenterology*, *129*(1), 234-245.
Glick, B. R., & Whitney, G. K. (1987). Factors affecting the expression of foreign proteins in Escherichia coli. *Journal of industrial microbiology and biotechnology*, *1*(5), 277-282.
Goepfert, P. A., Elizaga, M. L., Sato, A., Qin, L., Cardinali, M., Hay, C. M., Hural, J., DeRosa, S. C., DeFawe, O. D., & Tomaras, G. D. (2011). Phase 1 safety and immunogenicity testing of DNA and recombinant modified vaccinia Ankara vaccines expressing HIV-1 virus-like particles. *Journal of Infectious Diseases*, *203*(5), 610-619.
Graber-Stiehl, I. (2018). The silent epidemic killing more people than HIV, malaria or TB. *Nature*, *564*(7734), 24-27.
Graham, F. L., Smiley, J., Russell, W., & Nairn, R. (1977). Characteristics of a human cell line transformed by DNA from human adenovirus type 5. *Journal of general Virology*, *36*(1), 59-72.
Granstein, R. D., Ding, W., & Ozawa, H. (2000). Induction of anti-tumor immunity with epidermal cells pulsed with tumor-derived RNA or intradermal administration of RNA. *Journal of investigative dermatology*, *114*(4), 632-636.
Gripon, P., Rumin, S., Urban, S., Le Seyec, J., Glaise, D., Cannie, I., Guyomard, C., Lucas, J., Trepo, C., & Guguen-Guillouzo, C. (2002). Infection of a human hepatoma cell line by hepatitis B virus. *Proceedings of the National Academy of Sciences*, *99*(24), 15655-15660.
Gross, G., Waks, T., & Eshhar, Z. (1989). Expression of immunoglobulin-T-cell receptor chimeric molecules as functional receptors with antibody-type specificity. *Proceedings of the National Academy of Sciences*, *86*(24), 10024-10028.
Grunwald, T., & Ulbert, S. (2015). Improvement of DNA vaccination by adjuvants and sophisticated delivery devices: vaccine-platforms for the battle against infectious diseases. *Clinical and experimental vaccine research*, *4*(1), 1-10.
Guidotti, L. G., & Chisari, F. V. (2006). Immunobiology and pathogenesis of viral hepatitis. *Annu. Rev. Pathol. Mech. Dis.*, *1*, 23-61.
Guidotti, L. G., Ishikawa, T., Hobbs, M. V., Matzke, B., Schreiber, R., & Chisari, F. V. (1996). Intracellular inactivation of the hepatitis B virus by cytotoxic T lymphocytes. *Immunity*, *4*(1), 25-36.
Guidotti, L. G., Isogawa, M., & Chisari, F. V. (2015). Host–virus interactions in hepatitis B virus infection. *Current opinion in immunology*, *36*, 61-66.
Guidotti, L. G., Matzke, B., Schaller, H., & Chisari, F. V. (1995). High-level hepatitis B virus replication in transgenic mice. *Journal of virology*, *69*(10), 6158-6169.
Gust, I. (1996). Epidemiology of hepatitis B infection in the Western Pacific and South East Asia. *Gut*, *38*(Suppl 2), S18-S23.
Gustafsson, C., Govindarajan, S., & Minshull, J. (2004). Codon bias and heterologous protein expression. *Trends in biotechnology*, *22*(7), 346-353.
Hagenbuch, B., & Meier, P. J. (1994). Molecular cloning, chromosomal localization, and functional characterization of a human liver Na+/bile acid cotransporter. *The Journal of clinical investigation*, *93*(3), 1326-1331.
Harford, N., Cabezon, T., Crabeel, M., Simoen, E., Rutgers, A., & De Wilde, M. (1983). Expression of hepatitis B surface antigen in yeast. *Developments in biological standardization*, *54*, 125-130.
Harris, C. f. D. C. a. P.-A. (2023). *Hepatitis B CDC Yellow Book 2024*. CDC. Retrieved 22/11/2023 from https://wwwnc.cdc.gov/travel/yellowbook/2024/infections-diseases/hepatitis-b#map507
Harrop, R., Ryan, M. G., Myers, K. A., Redchenko, I., Kingsman, S. M., & Carroll, M. W. (2006). Active treatment of murine tumors with a highly attenuated vaccinia virus expressing the tumor associated antigen 5T4 (TroVax) is CD4+ T cell dependent and antibody mediated. *Cancer Immunology, Immunotherapy*, *55*(9), 1081-1090.
Harrop, R., Shingler, W., Kelleher, M., de Belin, J., & Treasure, P. (2010). Cross-trial analysis of immunologic and clinical data resulting from phase I and II trials of MVA-5T4

(TroVax) in colorectal, renal, and prostate cancer patients. *Journal of immunotherapy*, *33*(9), 999-1005.

Havenar-Daughton, C., Carnathan, D. G., de la Peña, A. T., Pauthner, M., Briney, B., Reiss, S. M., Wood, J. S., Kaushik, K., van Gils, M. J., & Rosales, S. L. (2016). Direct probing of germinal center responses reveals immunological features and bottlenecks for neutralizing antibody responses to HIV Env trimer. *Cell reports*, *17*(9), 2195-2209.

Heermann, K., Goldmann, U., Schwartz, W., Seyffarth, T., Baumgarten, H., & Gerlich, W. (1984). Large surface proteins of hepatitis B virus containing the pre-s sequence. *Journal of virology*, *52*(2), 396-402.

Hilleman, M., Buynak, E., Roehm, R., Tytell, A., Bertland, A., & Lampson, G. (1975). Purified and inactivated human hepatitis B vaccine: progress report. *The American journal of the medical sciences*, *270*(2), 401-404.

Himly, M., Foster, D. N., Bottoli, I., Iacovoni, J. S., & Vogt, P. K. (1998). The DF-1 chicken fibroblast cell line: transformation induced by diverse oncogenes and cell death resulting from infection by avian leukosis viruses. *Virology*, *248*(2), 295-304.

Hoebe, K., Du, X., Georgel, P., Janssen, E., Tabeta, K., Kim, S., Goode, J., Lin, P., Mann, N., & Mudd, S. (2003). Identification of Lps2 as a key transducer of MyD88-independent TIR signalling. *Nature*, *424*(6950), 743-748.

Holtkamp, S., Kreiter, S., Selmi, A., Simon, P., Koslowski, M., Huber, C., Türeci, O. z., & Sahin, U. (2006). Modification of antigen-encoding RNA increases stability, translational efficacy, and T-cell stimulatory capacity of dendritic cells. *Blood*, *108*(13), 4009-4017.

Hoofnagle, J. H., Doo, E., Liang, T. J., Fleischer, R., & Lok, A. S. (2007). Management of hepatitis B: summary of a clinical research workshop. *Hepatology*, *45*(4), 1056-1075.

Hu, T.-T., Song, X.-F., Lei, Y., Hu, H.-D., Ren, H., & Hu, P. (2014). Expansion of circulating TFH cells and their associated molecules: involvement in the immune landscape in patients with chronic HBV infection. *Virology journal*, *11*(1), 1-9.

Hui, C.-k., Lie, A., Au, W.-y., Leung, Y.-h., Ma, S.-y., Cheung, W. W., Zhang, H.-y., Chim, C.-s., Kwong, Y.-l., & Liang, R. (2005). A long-term follow-up study on hepatitis B surface antigen–positive patients undergoing allogeneic hematopoietic stem cell transplantation. *Blood*, *106*(2), 464-469.

Huleatt, J. W., Jacobs, A. R., Tang, J., Desai, P., Kopp, E. B., Huang, Y., Song, L., Nakaar, V., & Powell, T. (2007). Vaccination with recombinant fusion proteins incorporating Toll-like receptor ligands induces rapid cellular and humoral immunity. *Vaccine*, *25*(4), 763-775.

Hwang, E. W., & Cheung, R. (2011). Global epidemiology of hepatitis B virus (HBV) infection. *North American Journal of Medicine and Science*, *4*(1).

Isogawa, M., Robek, M. D., Furuichi, Y., & Chisari, F. V. (2005). Toll-like receptor signaling inhibits hepatitis B virus replication in vivo. *Journal of virology*, *79*(11), 7269-7272.

Jackson, L. A., Anderson, E. J., Rouphael, N. G., Roberts, P. C., Makhene, M., Coler, R. N., McCullough, M. P., Chappell, J. D., Denison, M. R., & Stevens, L. J. (2020). An mRNA vaccine against SARS-CoV-2—preliminary report. *New England Journal of Medicine*.

Janssen, H. L., van Zonneveld, M., Senturk, H., Zeuzem, S., Akarca, U. S., Cakaloglu, Y., Simon, C., So, T. M., Gerken, G., & de Man, R. A. (2005). Pegylated interferon alfa-2b alone or in combination with lamivudine for HBeAg-positive chronic hepatitis B: a randomised trial. *The lancet*, *365*(9454), 123-129.

Jiang, B. (2015). *Subviral Hepatitis B Virus Filaments are Released Like Infectious Viral Particles Via Multivesicular Bodies* Johann Wolfgang Goethe-Universität in Frankfurt am Main].

Jin, B., Sun, T., Yu, X.-H., Liu, C.-Q., Yang, Y.-X., Lu, P., Fu, S.-F., Qiu, H.-B., & Yeo, A. E. (2010). Immunomodulatory effects of dsRNA and its potential as vaccine adjuvant. *Journal of Biomedicine and Biotechnology*, *2010*.

June, C. H. (2007). Principles of adoptive T cell cancer therapy. *The Journal of clinical investigation*, *117*(5), 1204-1212.

Juszczyk, J. (2000). Clinical course and consequences of hepatitis B infection. *Vaccine*, *18*, S23-S25.

Kallen, K.-J., Heidenreich, R., Schnee, M., Petsch, B., Schlake, T., Thess, A., Baumhof, P., Scheel, B., Koch, S. D., & Fotin-Mleczek, M. (2013). A novel, disruptive vaccination technology: self-adjuvanted RNActive® vaccines. *Human vaccines & immunotherapeutics*, *9*(10), 2263-2276.

Kang, J.-A., Kim, S., Park, M., Park, H.-J., Kim, J.-H., Park, S., Hwang, J.-R., Kim, Y.-C., Kim, Y. J., & Cho, Y. (2019). Ciclopirox inhibits Hepatitis B Virus secretion by blocking capsid assembly. *Nature communications*, *10*(1), 1-14.

Kao, J.-H. (2008). Diagnosis of hepatitis B virus infection through serological and virological markers. *Expert review of gastroenterology & hepatology*, *2*(4), 553-562.

Kao, J.-H., Wu, N.-H., Chen, P.-J., Lai, M.-Y., & Chen, D.-S. (2000). Hepatitis B genotypes and the response to interferon therapy. *Journal of hepatology*, *33*(6), 998-1002.

Karikó, K., Buckstein, M., Ni, H., & Weissman, D. (2005). Suppression of RNA recognition by Toll-like receptors: the impact of nucleoside modification and the evolutionary origin of RNA. *Immunity*, *23*(2), 165-175.

Kariko, K., Muramatsu, H., Ludwig, J., & Weissman, D. (2011). Generating the optimal mRNA for therapy: HPLC purification eliminates immune activation and improves translation of nucleoside-modified, protein-encoding mRNA. *Nucleic acids research*, *39*(21), e142-e142.

Karikó, K., Muramatsu, H., Welsh, F. A., Ludwig, J., Kato, H., Akira, S., & Weissman, D. (2008). Incorporation of pseudouridine into mRNA yields superior nonimmunogenic vector with increased translational capacity and biological stability. *Molecular Therapy*, *16*(11), 1833-1840.

Karikó, K., Ni, H., Capodici, J., Lamphier, M., & Weissman, D. (2004). mRNA is an endogenous ligand for Toll-like receptor 3. *Journal of Biological Chemistry*, *279*(13), 12542-12550.

Kastenmuller, W., Gasteiger, G., Gronau, J. H., Baier, R., Ljapoci, R., Busch, D. H., & Drexler, I. (2007). Cross-competition of CD8+ T cells shapes the immunodominance hierarchy during boost vaccination. *The Journal of experimental medicine*, *204*(9), 2187-2198.

Kaul, R. (2013). Hepatitis. In *The Immunoassay Handbook* (pp. 901-911). Elsevier.

Khan, F. H. (2009). *The elements of immunology*. Pearson Education India.

Khan, K. H. (2013). DNA vaccines: roles against diseases. *Germs*, *3*(1), 26.

Khurana, S., Chearwae, W., Castellino, F., Manischewitz, J., King, L. R., Honorkiewicz, A., Rock, M. T., Edwards, K. M., Del Giudice, G., & Rappuoli, R. (2010). Vaccines with MF59 adjuvant expand the antibody repertoire to target protective sites of pandemic avian H5N1 influenza virus. *Science translational medicine*, *2*(15), 15ra15-15ra15.

Kindt, T. J., Goldsby, R. A., Osborne, B. A., & Kuby, J. (2007). *Kuby immunology*. Macmillan.

King, R. W., Ladner, S. K., Miller, T. J., Zaifert, K., Perni, R. B., Conway, S. C., & Otto, M. J. (1998). Inhibition of human hepatitis B virus replication by AT-61, a phenylpropenamide derivative, alone and in combination with (−) β-l-2′, 3′-dideoxy-3′-thiacytidine. *Antimicrobial agents and chemotherapy*, *42*(12), 3179-3186.

Klinman, D. M., Yamshchikov, G., & Ishigatsubo, Y. (1997). Contribution of CpG motifs to the immunogenicity of DNA vaccines. *The Journal of Immunology*, *158*(8), 3635-3639.

Knowles, B. B., Howe, C. C., & Aden, D. P. (1980). Human hepatocellular carcinoma cell lines secrete the major plasma proteins and hepatitis B surface antigen. *Science*, *209*(4455), 497-499.

Ko, C., Chakraborty, A., Chou, W.-M., Hasreiter, J., Wettengel, J. M., Stadler, D., Bester, R., Asen, T., Zhang, K., & Wisskirchen, K. (2018). Hepatitis B virus genome recycling and de novo secondary infection events maintain stable cccDNA levels. *Journal of hepatology*, *69*(6), 1231-1241.

Ko, C., Michler, T., & Protzer, U. (2017). Novel viral and host targets to cure hepatitis B. *Current opinion in virology*, *24*, 38-45.

Kondo, Y., Ueno, Y., & Shimosegawa, T. (2011). Toll-like receptors signaling contributes to immunopathogenesis of HBV infection. *Gastroenterology research and practice*, *2011*.

Konishi, E., Terazawa, A., & Imoto, J.-i. (2003). Simultaneous immunization with DNA and protein vaccines against Japanese encephalitis or dengue synergistically increases

their own abilities to induce neutralizing antibody in mice. *Vaccine*, *21*(17-18), 1826-1832.
Korn, T., Oukka, M., Kuchroo, V., & Bettelli, E. (2007). Th17 cells: effector T cells with inflammatory properties. Seminars in immunology,
Kosinska, A. D., Bauer, T., & Protzer, U. (2017). Therapeutic vaccination for chronic hepatitis B. *Current opinion in virology*, *23*, 75-81.
Kowalski, P. S., Rudra, A., Miao, L., & Anderson, D. G. (2019). Delivering the messenger: advances in technologies for therapeutic mRNA delivery. *Molecular Therapy*, *27*(4), 710-728.
Kramvis, A., Kew, M., & François, G. (2005). Hepatitis B virus genotypes. *Vaccine*, *23*(19), 2409-2423.
Krebs, K., Böttinger, N., Huang, L. R., Chmielewski, M., Arzberger, S., Gasteiger, G., Jäger, C., Schmitt, E., Bohne, F., & Aichler, M. (2013). T cells expressing a chimeric antigen receptor that binds hepatitis B virus envelope proteins control virus replication in mice. *Gastroenterology*, *145*(2), 456-465.
Kreiter, S., Selmi, A., Diken, M., Koslowski, M., Britten, C. M., Huber, C., Türeci, Ö., & Sahin, U. (2010). Intranodal vaccination with naked antigen-encoding RNA elicits potent prophylactic and therapeutic antitumoral immunity. *Cancer research*, *70*(22), 9031-9040.
Kudla, G., Murray, A. W., Tollervey, D., & Plotkin, J. B. (2009). Coding-sequence determinants of gene expression in Escherichia coli. *science*, *324*(5924), 255-258.
Kurt-Jones, E. A., Popova, L., Kwinn, L., Haynes, L. M., Jones, L. P., Tripp, R. A., Walsh, E. E., Freeman, M. W., Golenbock, D. T., & Anderson, L. J. (2000). Pattern recognition receptors TLR4 and CD14 mediate response to respiratory syncytial virus. *Nature immunology*, *1*(5), 398-401.
Kusakabe, K.-i., Xin, K.-Q., Katoh, H., Sumino, K., Hagiwara, E., Kawamoto, S., Okuda, K., Miyagi, Y., Aoki, I., & Nishioka, K. (2000). The timing of GM-CSF expression plasmid administration influences the Th1/Th2 response induced by an HIV-1-specific DNA vaccine. *The Journal of Immunology*, *164*(6), 3102-3111.
Kutzler, M. A., & Weiner, D. B. (2008). DNA vaccines: ready for prime time? *Nature Reviews Genetics*, *9*(10), 776-788.
Larregina, A., Watkins, S., Erdos, G., Spencer, L., Storkus, W., Stolz, D. B., & Falo Jr, L. (2001). Direct transfection and activation of human cutaneous dendritic cells. *Gene therapy*, *8*(8), 608-617.
Lau, G. K., Piratvisuth, T., Luo, K. X., Marcellin, P., Thongsawat, S., Cooksley, G., Gane, E., Fried, M. W., Chow, W. C., & Paik, S. W. (2005). Peginterferon Alfa-2a, lamivudine, and the combination for HBeAg-positive chronic hepatitis B. *New England Journal of Medicine*, *352*(26), 2682-2695.
Lazdina, U., Alheim, M., Nyström, J., Hultgren, C., Borisova, G., Sominskaya, I., Pumpens, P., Peterson, D. L., Milich, D. R., & Sällberg, M. (2003). Priming of cytotoxic T cell responses to exogenous hepatitis B virus core antigen is B cell dependent. *Journal of general Virology*, *84*(1), 139-146.
Leroux-Roels, I., Roman, F., Forgus, S., Maes, C., De Boever, F., Dramé, M., Gillard, P., van der Most, R., Van Mechelen, M., & Hanon, E. (2010). Priming with AS03A-adjuvanted H5N1 influenza vaccine improves the kinetics, magnitude and durability of the immune response after a heterologous booster vaccination: an open non-randomised extension of a double-blind randomised primary study. *Vaccine*, *28*(3), 849-857.
Levrero, M., & Zucman-Rossi, J. (2016). Mechanisms of HBV-induced hepatocellular carcinoma. *Journal of hepatology*, *64*(1), S84-S101.
Li, H.-C., Huang, E.-Y., Su, P.-Y., Wu, S.-Y., Yang, C.-C., Lin, Y.-S., Chang, W.-C., & Shih, C. (2010). Nuclear export and import of human hepatitis B virus capsid protein and particles. *PLoS Pathog*, *6*(10), e1001162.
Liang, F., Lindgren, G., Sandgren, K. J., Thompson, E. A., Francica, J. R., Seubert, A., De Gregorio, E., Barnett, S., O'Hagan, D. T., & Sullivan, N. J. (2017). Vaccine priming is

restricted to draining lymph nodes and controlled by adjuvant-mediated antigen uptake. *Science translational medicine*, *9*(393).
Liang, T. J. (2009). Hepatitis B: the virus and disease. *Hepatology*, *49*(S5), S13-S21.
Liang, X., Bi, S., Yang, W., Wang, L., Cui, G., Cui, F., Zhang, Y., Liu, J., Gong, X., & Chen, Y. (2013). Reprint of: Epidemiological serosurvey of Hepatitis B in China—declining HBV prevalence due to Hepatitis B vaccination. *Vaccine*, *31*, J21-J28.
Liljeqvist, S., & Ståhl, S. (1999). Production of recombinant subunit vaccines: protein immunogens, live delivery systems and nucleic acid vaccines. *Journal of biotechnology*, *73*(1), 1-33.
Ljungman, P. (2012). Vaccination of immunocompromised patients. *Clinical Microbiology and Infection*, *18*, 93-99.
Lok, A. S., & McMahon, B. J. (2009). Chronic hepatitis B: update 2009. *Hepatology*, *50*(3), 661-662.
Lok, A. S., Zoulim, F., Dusheiko, G., & Ghany, M. G. (2017). Hepatitis B cure: from discovery to regulatory approval. *Hepatology*, *66*(4), 1296-1313.
Loomba, R., & Liang, T. J. (2017). Hepatitis B reactivation associated with immune suppressive and biological modifier therapies: current concepts, management strategies, and future directions. *Gastroenterology*, *152*(6), 1297-1309.
Lorenz, C., Fotin-Mleczek, M., Roth, G., Becker, C., Dam, T. C., Verdurmen, W. P., Brock, R., Probst, J., & Schlake, T. (2011). Protein expression from exogenous mRNA: uptake by receptor-mediated endocytosis and trafficking via the lysosomal pathway. *RNA biology*, *8*(4), 627-636.
Lu, L. L., Suscovich, T. J., Fortune, S. M., & Alter, G. (2018). Beyond binding: antibody effector functions in infectious diseases. *Nature Reviews Immunology*, *18*(1), 46.
Lucifora, J., Arzberger, S., Durantel, D., Belloni, L., Strubin, M., Levrero, M., Zoulim, F., Hantz, O., & Protzer, U. (2011). Hepatitis B virus X protein is essential to initiate and maintain virus replication after infection. *Journal of hepatology*, *55*(5), 996-1003.
Lucifora, J., Xia, Y., Reisinger, F., Zhang, K., Stadler, D., Cheng, X., Sprinzl, M. F., Koppensteiner, H., Makowska, Z., & Volz, T. (2014). Specific and nonhepatotoxic degradation of nuclear hepatitis B virus cccDNA. *Science*, *343*(6176), 1221-1228.
Ludtke, J. J., Sebestyén, M. G., & Wolff, J. A. (2002). The effect of cell division on the cellular dynamics of microinjected DNA and dextran. *Molecular Therapy*, *5*(5), 579-588.
Luke, G. A., de Felipe, P., Lukashev, A., Kallioinen, S. E., Bruno, E. A., & Ryan, M. D. (2008). Occurrence, function and evolutionary origins of '2A-like'sequences in virus genomes. *The Journal of general virology*, *89*(Pt 4), 1036.
Lund, J. M., Alexopoulou, L., Sato, A., Karow, M., Adams, N. C., Gale, N. W., Iwasaki, A., & Flavell, R. A. (2004). Recognition of single-stranded RNA viruses by Toll-like receptor 7. *Proceedings of the National Academy of Sciences*, *101*(15), 5598-5603.
Lurie, N., Saville, M., Hatchett, R., & Halton, J. (2020). Developing Covid-19 vaccines at pandemic speed. *New England Journal of Medicine*, *382*(21), 1969-1973.
MacGregor, R. R., Boyer, J. D., Ugen, K. E., Lacy, K. E., Gluckman, S. J., Bagarazzi, M. L., Chattergoon, M. A., Baine, Y., Higgins, T. J., & Ciccarelli, R. B. (1998). First human trial of a DNA-based vaccine for treatment of human immunodeficiency virus type 1 infection: safety and host response. *Journal of Infectious Diseases*, *178*(1), 92-100.
MacLeod, M. K., Kappler, J. W., & Marrack, P. (2010). Memory CD4 T cells: generation, reactivation and re-assignment. *Immunology*, *130*(1), 10-15.
Maini, M. K., Boni, C., Ogg, G. S., King, A. S., Reignat, S., Lee, C. K., Larrubia, J. R., Webster, G. J., McMichael, A. J., & Ferrari, C. (1999). Direct ex vivo analysis of hepatitis B virus-specific CD8+ T cells associated with the control of infection. *Gastroenterology*, *117*(6), 1386-1396.
Maini, M. K., & Burton, A. R. (2019). Restoring, releasing or replacing adaptive immunity in chronic hepatitis B. *Nature Reviews Gastroenterology & Hepatology*, *16*(11), 662-675.
Maini, M. K., & Pallett, L. J. (2018). Defective T-cell immunity in hepatitis B virus infection: why therapeutic vaccination needs a helping hand. *The Lancet Gastroenterology & Hepatology*, *3*(3), 192-202.

Marchetti, A. L., & Guo, H. (2020). New insights on molecular mechanism of hepatitis B virus covalently closed circular DNA formation. *Cells*, *9*(11), 2430.

Margolis, H. S., Alter, M. J., & Hadler, S. C. (1991). Hepatitis B: evolving epidemiology and implications for control. Seminars in liver disease,

Martin, S., Paoletti, E., & Moss, B. (1975). Purification of mRNA guanylyltransferase and mRNA (guanine-7-) methyltransferase from vaccinia virions. *Journal of Biological Chemistry*, *250*(24), 9322-9329.

Martinon, F., Krishnan, S., Lenzen, G., Magné, R., Gomard, E., Guillet, J. G., Lévy, J. P., & Meulien, P. (1993). Induction of virus-specific cytotoxic T lymphocytes in vivo by liposome-entrapped mRNA. *European journal of immunology*, *23*(7), 1719-1722.

Mascola, J. R., Sambor, A., Beaudry, K., Santra, S., Welcher, B., Louder, M. K., VanCott, T. C., Huang, Y., Chakrabarti, B. K., & Kong, W.-P. (2005). Neutralizing antibodies elicited by immunization of monkeys with DNA plasmids and recombinant adenoviral vectors expressing human immunodeficiency virus type 1 proteins. *Journal of virology*, *79*(2), 771-779.

Masotti, A., Mossa, G., Cametti, C., Ortaggi, G., Bianco, A., Del Grosso, N., Malizia, D., & Esposito, C. (2009). Comparison of different commercially available cationic liposome–DNA lipoplexes: Parameters influencing toxicity and transfection efficiency. *Colloids and Surfaces B: Biointerfaces*, *68*(2), 136-144.

Mauro, V. P., & Chappell, S. A. (2014). A critical analysis of codon optimization in human therapeutics. *Trends in molecular medicine*, *20*(11), 604-613.

Mayrhofer, P., Schleef, M., & Jechlinger, W. (2009). Use of minicircle plasmids for gene therapy. *Gene Therapy of Cancer*, 87-104.

McCaffrey, A. P. (2019). RNA Epitranscriptome: Role of the 5'Cap: Producing superior mRNA therapeutics through optimized capping. *Genetic Engineering & Biotechnology News*, *39*(5), 59, 61.

McKee, A. S., MacLeod, M. K., Kappler, J. W., & Marrack, P. (2010). Immune mechanisms of protection: can adjuvants rise to the challenge? *BMC biology*, *8*(1), 1-10.

McKee, A. S., Munks, M. W., & Marrack, P. (2007). How do adjuvants work? Important considerations for new generation adjuvants. *Immunity*, *27*(5), 687-690.

McShane, H., Pathan, A. A., Sander, C. R., Keating, S. M., Gilbert, S. C., Huygen, K., Fletcher, H. A., & Hill, A. V. (2004). Recombinant modified vaccinia virus Ankara expressing antigen 85A boosts BCG-primed and naturally acquired antimycobacterial immunity in humans. *Nature medicine*, *10*(11), 1240-1244.

Medzhitov, R., & Janeway Jr, C. (2000). Innate immune recognition: mechanisms and pathways. *Immunological reviews*, *173*, 89-97.

Meier, A., Mehrle, S., Weiss, T. S., Mier, W., & Urban, S. (2013). Myristoylated PreS1-domain of the hepatitis B virus L-protein mediates specific binding to differentiated hepatocytes. *Hepatology*, *58*(1), 31-42.

Michler, T., Kosinska, A. D., Festag, J., Bunse, T., Su, J., Ringelhan, M., Imhof, H., Grimm, D., Steiger, K., & Mogler, C. (2020). Knockdown of virus antigen expression increases therapeutic vaccine efficacy in high-titer hepatitis B virus carrier mice. *Gastroenterology*, *158*(6), 1762-1775. e1769.

Milich, D. R., & McLachlan, A. (1986). The nucleocapsid of hepatitis B virus is both a T-cell-independent and a T-cell-dependent antigen. *Science*, *234*(4782), 1398-1401.

Miller, R. H., Kaneko, S., Chung, C. T., Girones, R., & Purcell, R. H. (1989). Compact organization of the hepatitis B virus genome. *Hepatology*, *9*(2), 322-327.

Ming, L., Thorgeirsson, S. S., Gail, M. H., Lu, P., Harris, C. C., Wang, N., Shao, Y., Wu, Z., Liu, G., & Wang, X. (2002). Dominant role of hepatitis B virus and cofactor role of aflatoxin in hepatocarcinogenesis in Qidong, China. *Hepatology*, *36*(5), 1214-1220.

Moriarty, A. M., Hoyer, B. H., Shih, J. W.-K., Gerin, J. L., & Hamer, D. H. (1981). Expression of the hepatitis B virus surface antigen gene in cell culture by using a simian virus 40 vector. *Proceedings of the National Academy of Sciences*, *78*(4), 2606-2610.

Mosmann, T., & Coffman, R. (1989). TH1 and TH2 cells: different patterns of lymphokine secretion lead to different functional properties. *Annual review of immunology*, *7*(1), 145-173.

Nassal, M. (2008). Hepatitis B viruses: reverse transcription a different way. *Virus research*, *134*(1-2), 235-249.

Nassal, M. (2015). HBV cccDNA: viral persistence reservoir and key obstacle for a cure of chronic hepatitis B. *Gut*, *64*(12), 1972-1984.

Neumann, A. U., Phillips, S., Levine, I., Ijaz, S., Dahari, H., Eren, R., Dagan, S., & Naoumov, N. V. (2010). Novel mechanism of antibodies to hepatitis B virus in blocking viral particle release from cells. *Hepatology*, *52*(3), 875-885.

Nizzoli, G., Krietsch, J., Weick, A., Steinfelder, S., Facciotti, F., Gruarin, P., Bianco, A., Steckel, B., Moro, M., & Crosti, M. (2013). Human CD1c+ dendritic cells secrete high levels of IL-12 and potently prime cytotoxic T-cell responses. *Blood, The Journal of the American Society of Hematology*, *122*(6), 932-942.

Okamoto, H., Tsuda, F., Sakugawa, H., Sastrosoewignjo, R. I., Imai, M., Miyakawa, Y., & Mayumi, M. (1988). Typing hepatitis B virus by homology in nucleotide sequence: comparison of surface antigen subtypes. *Journal of general Virology*, *69*(10), 2575-2583.

Otten, G. R., Schaefer, M., Doe, B., Liu, H., Srivastava, I., zur Megede, J., Kazzaz, J., Lian, Y., Singh, M., & Ugozzoli, M. (2005). Enhanced potency of plasmid DNA microparticle human immunodeficiency virus vaccines in rhesus macaques by using a priming-boosting regimen with recombinant proteins. *Journal of virology*, *79*(13), 8189-8200.

Overton, E. T., Stapleton, J., Frank, I., Hassler, S., Goepfert, P. A., Barker, D., Wagner, E., von Krempelhuber, A., Virgin, G., & Meyer, T. P. (2015). Safety and immunogenicity of modified vaccinia Ankara-Bavarian Nordic smallpox vaccine in vaccinia-naive and experienced human immunodeficiency virus-infected individuals: an open-label, controlled clinical phase II trial. Open forum infectious diseases,

Pal, R., Wang, S., Kalyanaraman, V., Nair, B., Whitney, S., Keen, T., Hocker, L., Hudacik, L., Rose, N., & Cristillo, A. (2005). Polyvalent DNA prime and envelope protein boost HIV-1 vaccine elicits humoral and cellular responses and controls plasma viremia in rhesus macaques following rectal challenge with an R5 SHIV isolate. *Journal of medical primatology*, *34*(5-6), 226-236.

Palgen, J.-L., Tchitchek, N., Elhmouzi-Younes, J., Delandre, S., Namet, I., Rosenbaum, P., Dereuddre-Bosquet, N., Martinon, F., Cosma, A., & Lévy, Y. (2018). Prime and boost vaccination elicit a distinct innate myeloid cell immune response. *Scientific reports*, *8*(1), 1-18.

Palumbo, G. A., Scisciani, C., Pediconi, N., Lupacchini, L., Alfalate, D., Guerrieri, F., Calvo, L., Salerno, D., Di Cocco, S., & Levrero, M. (2015). IL6 inhibits HBV transcription by targeting the epigenetic control of the nuclear cccDNA minichromosome. *PLoS One*, *10*(11), e0142599.

Pancholi, P., Lee, D.-H., Liu, Q., Tackney, C., Taylor, P., Perkus, M., Andrus, L., Brotman, B., & Prince, A. M. (2001). DNA prime/canarypox boost—based immunotherapy of chronic hepatitis B virus infection in a chimpanzee. *Hepatology*, *33*(2), 448-454.

Pardi, N., Hogan, M. J., Naradikian, M. S., Parkhouse, K., Cain, D. W., Jones, L., Moody, M. A., Verkerke, H. P., Myles, A., & Willis, E. (2018). Nucleoside-modified mRNA vaccines induce potent T follicular helper and germinal center B cell responses. *Journal of Experimental Medicine*, *215*(6), 1571-1588.

Pardi, N., Hogan, M. J., Porter, F. W., & Weissman, D. (2018a). mRNA vaccines—a new era in vaccinology. *Nature reviews Drug discovery*, *17*(4), 261.

Pardi, N., Hogan, M. J., Porter, F. W., & Weissman, D. (2018b). mRNA vaccines—a new era in vaccinology. *Nature reviews Drug discovery*, *17*(4), 261-279.

Pardi, N., Tuyishime, S., Muramatsu, H., Kariko, K., Mui, B. L., Tam, Y. K., Madden, T. D., Hope, M. J., & Weissman, D. (2015). Expression kinetics of nucleoside-modified mRNA delivered in lipid nanoparticles to mice by various routes. *Journal of Controlled Release*, *217*, 345-351.

Park, S. G., Kim, Y., Park, E., Ryu, H. M., & Jung, G. (2003). Fidelity of hepatitis B virus polymerase. *European journal of biochemistry*, *270*(14), 2929-2936.

Pascolo, S. (2008). Vaccination with messenger RNA (mRNA). *Toll-like receptors (TLRs) and innate immunity*, 221-235.

Pasek, M., Goto, T., Gilbert, W., Zink, B., Schaller, H., MacKay, P., Leadbetter, G., & Murray, K. (1979). Hepatitis B virus genes and their expression in E. coli. *Nature*, *282*(5739), 575-579.

Patil, S. D., Rhodes, D. G., & Burgess, D. J. (2004). Anionic liposomal delivery system for DNA transfection. *The AAPS journal*, *6*(4), 13-22.

Pavot, V., Sebastian, S., Turner, A. V., Matthews, J., & Gilbert, S. C. (2017). Generation and production of modified vaccinia virus Ankara (MVA) as a vaccine vector. In *Recombinant Virus Vaccines* (pp. 97-119). Springer.

Penna, A., Chisari, F. V., Bertoletti, A., Missale, G., Fowler, P., Giuberti, T., Fiaccadori, F., & Ferrari, C. (1991). Cytotoxic T lymphocytes recognize an HLA-A2-restricted epitope within the hepatitis B virus nucleocapsid antigen. *The Journal of experimental medicine*, *174*(6), 1565-1570.

Peto, T. J., Mendy, M. E., Lowe, Y., Webb, E. L., Whittle, H. C., & Hall, A. J. (2014). Efficacy and effectiveness of infant vaccination against chronic hepatitis B in the Gambia Hepatitis Intervention Study (1986–90) and in the nationwide immunisation program. *BMC infectious diseases*, *14*(1), 1-8.

Phillips, S., Chokshi, S., Riva, A., Evans, A., Williams, R., & Naoumov, N. V. (2010). CD8+ T cell control of hepatitis B virus replication: direct comparison between cytolytic and noncytolytic functions. *The journal of immunology*, *184*(1), 287-295.

Pichoud, C., Seignères, B., Wang, Z., Trépo, C., & Zoulim, F. (1999). Transient selection of a hepatitis B virus polymerase gene mutant associated with a decreased replication capacity and famciclovir resistance. *Hepatology*, *29*(1), 230-237.

Pipili, C., Cholongitas, E., & Papatheodoridis, G. (2014). nucleos (t) ide analogues in patients with chronic hepatitis B virus infection and chronic kidney disease. *Alimentary pharmacology & therapeutics*, *39*(1), 35-46.

Pol, S., Nalpas, B., Driss, F., Michel, M.-L., Tiollais, P., Denis, J., & Bréchot, C. (2001). Efficacy and limitations of a specific immunotherapy in chronic hepatitis B. *Journal of hepatology*, *34*(6), 917-921.

Polack, F. P., Thomas, S. J., Kitchin, N., Absalon, J., Gurtman, A., Lockhart, S., Perez, J. L., Pérez Marc, G., Moreira, E. D., & Zerbini, C. (2020). Safety and efficacy of the BNT162b2 mRNA Covid-19 vaccine. *New England Journal of Medicine*, *383*(27), 2603-2615.

Pollicino, T., Vegetti, A., Saitta, C., Ferrara, F., Corradini, E., Raffa, G., Pietrangelo, A., & Raimondo, G. (2013). Hepatitis B virus DNA integration in tumour tissue of a non-cirrhotic HFE-haemochromatosis patient with hepatocellular carcinoma. *Journal of hepatology*, *58*(1), 190-193.

Probst, J., Brechtel, S., Scheel, B., Hoerr, I., Jung, G., Rammensee, H.-G., & Pascolo, S. (2006). Characterization of the ribonuclease activity on the skin surface. *Genetic vaccines and therapy*, *4*(1), 1-9.

Probst, J., Weide, B., Scheel, B., Pichler, B., Hoerr, I., Rammensee, H., & Pascolo, S. (2007). Spontaneous cellular uptake of exogenous messenger RNA in vivo is nucleic acid-specific, saturable and ion dependent. *Gene therapy*, *14*(15), 1175-1180.

Protzer, U., & Knolle, P. (2016). “To be or not to be”: immune tolerance in chronic hepatitis B. *Gastroenterology*, *151*(5), 805-806.

Purcell, R., & Gerin, J. (1975). Hepatitis B subunit vaccine: a preliminary report of safety and efficacy tests in chimpanzees. *The American journal of the medical sciences*, *270*(2), 395-399.

Qiu, P., Ziegelhoffer, P., Sun, J., & Yang, N. (1996). Gene gun delivery of mRNA in situ results in efficient transgene expression and genetic immunization. *Gene therapy*, *3*(3), 262-268.

Rabe, B., Glebe, D., & Kann, M. (2006). Lipid-mediated introduction of hepatitis B virus capsids into nonsusceptible cells allows highly efficient replication and facilitates the study of early infection events. *Journal of virology*, *80*(11), 5465-5473.

Rabe, B., Vlachou, A., Panté, N., Helenius, A., & Kann, M. (2003). Nuclear import of hepatitis B virus capsids and release of the viral genome. *Proceedings of the National Academy of Sciences*, *100*(17), 9849-9854.

Radziwill, G., Tucker, W., & Schaller, H. (1990). Mutational analysis of the hepatitis B virus P gene product: domain structure and RNase H activity. *Journal of virology*, *64*(2), 613-620.

Ray, M., Desmet, V., Fevery, J., De Groote, J., Bradburne, A., & Desmyter, J. (1976). Distribution patterns of hepatitis B surface antigen (HBsAg) in the liver of hepatitis patients. *Journal of clinical pathology*, *29*(2), 94-100.

Raziorrouh, B., Heeg, M., Kurktschiev, P., Schraut, W., Zachoval, R., Wendtner, C., Wächtler, M., Spannagl, M., Denk, G., & Ulsenheimer, A. (2014). Inhibitory phenotype of HBV-specific CD4+ T-cells is characterized by high PD-1 expression but absent coregulation of multiple inhibitory molecules. *PLoS One*, *9*(8), e105703.

Rehermann, B., Fowler, P., Sidney, J., Person, J., Redeker, A., Brown, M., Moss, B., Sette, A., & Chisari, F. V. (1995). The cytotoxic T lymphocyte response to multiple hepatitis B virus polymerase epitopes during and after acute viral hepatitis. *The Journal of experimental medicine*, *181*(3), 1047-1058.

Rehermann, B., & Nascimbeni, M. (2005). Immunology of hepatitis B virus and hepatitis C virus infection. *Nature Reviews Immunology*, *5*(3), 215-229.

Ringehan, M., McKeating, J. A., & Protzer, U. (2017). Viral hepatitis and liver cancer. *Philosophical Transactions of the Royal Society B: Biological Sciences*, *372*(1732), 20160274.

Robert Koch Institute. (2016). *RKI-Ratgeber Hepatitis B und D*. Retrieved 21/06/2021 from https://www.rki.de/DE/Content/Infekt/EpidBull/Merkblaetter/Ratgeber_HepatitisB.html;jsessionid=66AE610903CC4B90C6D1B416874B9643.internet051#doc2390050bodyText3

Robinson, D. S., Hamid, Q., Ying, S., Tsicopoulos, A., Barkans, J., Bentley, A. M., Corrigan, C., Durham, S. R., & Kay, A. B. (1992). Predominant TH2-like bronchoalveolar T-lymphocyte population in atopic asthma. *New England Journal of Medicine*, *326*(5), 298-304.

Robinson, H. L., & Pertmer, T. M. (2000). DNA vaccines for viral infections: basic studies and applications.

Rollier, C., Sunyach, C., Barraud, L., Madani, N., Jamard, C., Trepo, C., & Cova, L. (1999). Protective and therapeutic effect of DNA-based immunization against hepadnavirus large envelope protein. *Gastroenterology*, *116*(3), 658-665.

Romagnani, S. (1997). The th1/th2 paradigm. *Immunology today*, *18*(6), 263-266.

Rong, M., He, B., McAllister, W. T., & Durbin, R. K. (1998). Promoter specificity determinants of T7 RNA polymerase. *Proceedings of the National Academy of Sciences*, *95*(2), 515-519.

Sakaguchi, S. (2005). Naturally arising Foxp3-expressing CD25+ CD4+ regulatory T cells in immunological tolerance to self and non-self. *Nature immunology*, *6*(4), 345-352.

Samaridou, E., Heyes, J., & Lutwyche, P. (2020). Lipid nanoparticles for nucleic acid delivery: Current perspectives. *Advanced Drug Delivery Reviews*, *154*, 37-63.

Sasaki, S., Takeshita, F., Xin, K.-Q., Ishii, N., & Okuda, K. (2003). Adjuvant formulations and delivery systems for DNA vaccines. *Methods*, *31*(3), 243-254.

Sato, Y., Roman, M., Tighe, H., Lee, D., Corr, M., Nguyen, M.-D., Silverman, G. J., Lotz, M., Carson, D. A., & Raz, E. (1996). Immunostimulatory DNA sequences necessary for effective intradermal gene immunization. *Science*, *273*(5273), 352-354.

Schaefer, S. (2007). Hepatitis B virus taxonomy and hepatitis B virus genotypes. *World journal of gastroenterology: WJG*, *13*(1), 14.

Scheel, B., Teufel, R., Probst, J., Carralot, J. P., Geginat, J., Radsak, M., Jarrossay, D., Wagner, H., Jung, G., & Rammensee, H. G. (2005). Toll-like receptor-dependent

activation of several human blood cell types by protamine-condensed mRNA. *European journal of immunology*, *35*(5), 1557-1566.
Scheerlinck, J.-P. Y. (2001). Genetic adjuvants for DNA vaccines. *Vaccine*, *19*(17-19), 2647-2656.
Schiller, J. T., & Lowy, D. R. (2015). Raising expectations for subunit vaccine. *The Journal of infectious diseases*, *211*(9), 1373-1375.
Schilling, R., Ijaz, S., Davidoff, M., Lee, J. Y., Locarnini, S., Williams, R., & Naoumov, N. V. (2003). Endocytosis of hepatitis B immune globulin into hepatocytes inhibits the secretion of hepatitis B virus surface antigen and virions. *Journal of virology*, *77*(16), 8882-8892.
Schirmbeck, R., Dikopoulos, N., Kwissa, M., Leithäuser, F., Lamberth, K., Buus, S., Melber, K., & Reimann, J. (2003). Breaking tolerance in hepatitis B surface antigen (HBsAg) transgenic mice by vaccination with cross-reactive, natural HBsAg variants. *European journal of immunology*, *33*(12), 3342-3352.
Schirmbeck, R., & Reimann, J. (2002). Alternative processing of endogenous or exogenous antigens extends the immunogenic, H-2 class I-restricted peptide repertoire. *Molecular immunology*, *39*(3-4), 249-259.
Schirmbeck, R., Wild, J., & Reimann, J. (1998). Similar as well as distinct MHC class I-binding peptides are generated by exogenous and endogenous processing of hepatitis B virus surface antigen. *European journal of immunology*, *28*(12), 4149-4161.
Schmitz, A., Schwarz, A., Foss, M., Zhou, L., Rabe, B., Hoellenriegel, J., Stoeber, M., Panté, N., & Kann, M. (2010). Nucleoporin 153 arrests the nuclear import of hepatitis B virus capsids in the nuclear basket. *PLoS Pathog*, *6*(1), e1000741.
Schulze, A., Gripon, P., & Urban, S. (2007). Hepatitis B virus infection initiates with a large surface protein–dependent binding to heparan sulfate proteoglycans. *Hepatology*, *46*(6), 1759-1768.
Scott, L. J., & Chan, H. L. (2017). Tenofovir alafenamide: a review in chronic hepatitis B. *Drugs*, *77*(9), 1017-1028.
Seeger, C., & Mason, W. S. (2000). Hepatitis B virus biology. *Microbiology and molecular biology reviews*, *64*(1), 51-68.
Seignères, B., Pichoud, C., Ahmed, S. S., Hantz, O., Trépo, C., & Zoulim, F. (2000). Evolution of hepatitis B virus polymerase gene sequence during famciclovir therapy for chronic hepatitis B. *The Journal of infectious diseases*, *181*(4), 1221-1233.
Selmi, A., Vascotto, F., Kautz-Neu, K., Türeci, Ö., Sahin, U., von Stebut, E., Diken, M., & Kreiter, S. (2016). Uptake of synthetic naked RNA by skin-resident dendritic cells via macropinocytosis allows antigen expression and induction of T-cell responses in mice. *Cancer Immunology, Immunotherapy*, *65*(9), 1075-1083.
Sheets, R. L., Stein, J., Manetz, T. S., Duffy, C., Nason, M., Andrews, C., Kong, W.-P., Nabel, G. J., & Gomez, P. L. (2006). Biodistribution of DNA plasmid vaccines against HIV-1, Ebola, Severe Acute Respiratory Syndrome, or West Nile virus is similar, without integration, despite differing plasmid backbones or gene inserts. *Toxicological Sciences*, *91*(2), 610-619.
Shen, P., & Fillatreau, S. (2015). Antibody-independent functions of B cells: a focus on cytokines. *Nature Reviews Immunology*, *15*(7), 441-451.
Sherman, M. (2009). Risk of hepatocellular carcinoma in hepatitis B and prevention through treatment. *Cleveland Clinic journal of medicine*, *76*, S6-9.
Shin, E.-C., Sung, P. S., & Park, S.-H. (2016). Immune responses and immunopathology in acute and chronic viral hepatitis. *Nature Reviews Immunology*, *16*(8), 509.
Shortman, K., & Heath, W. R. (2010). The CD8+ dendritic cell subset. *Immunological reviews*, *234*(1), 18-31.
Sin, J.-I., Bagarazzi, M., Pachuk, C., & Weiner, D. B. (1999). DNA priming-protein boosting enhances both antigen-specific antibody and Th1-type cellular immune responses in a murine herpes simplex virus-2 gD vaccine model. *DNA and cell biology*, *18*(10), 771-779.

Soema, P. C., Kompier, R., Amorij, J.-P., & Kersten, G. F. (2015). Current and next generation influenza vaccines: Formulation and production strategies. *European Journal of Pharmaceutics and Biopharmaceutics*, *94*, 251-263.

STEPINSKI, J., WADDELL, C., STOLARSKI, R., DARZYNKIEWICZ, E., & RHOADS, R. E. (2001). Synthesis and properties of mRNAs containing the novel “anti-reverse” cap analogs 7-methyl (3′-O-methyl) GpppG and 7-methyl (3′-deoxy) GpppG. *Rna*, *7*(10), 1486-1495.

Stevens, C. E., Beasley, R. P., Tsui, J., & Lee, W.-C. (1975). Vertical transmission of hepatitis B antigen in Taiwan. *New England Journal of Medicine*, *292*(15), 771-774.

Stibbe, W., & Gerlich, W. H. (1983). Structural relationships between minor and major proteins of hepatitis B surface antigen. *Journal of virology*, *46*(2), 626-628.

Stieger, B. (2011). The role of the sodium-taurocholate cotransporting polypeptide (NTCP) and of the bile salt export pump (BSEP) in physiology and pathophysiology of bile formation. *Drug transporters*, 205-259.

Stray, S. J., Bourne, C. R., Punna, S., Lewis, W. G., Finn, M., & Zlotnick, A. (2005). A heteroaryldihydropyrimidine activates and can misdirect hepatitis B virus capsid assembly. *Proceedings of the National Academy of Sciences*, *102*(23), 8138-8143.

Stray, S. J., & Zlotnick, A. (2006). BAY 41-4109 has multiple effects on hepatitis B virus capsid assembly. *Journal of Molecular Recognition: An Interdisciplinary Journal*, *19*(6), 542-548.

Summers, J., O'Connell, A., & Millman, I. (1975). Genome of hepatitis B virus: restriction enzyme cleavage and structure of DNA extracted from Dane particles. *Proceedings of the National Academy of Sciences*, *72*(11), 4597-4601.

Sun, Y., Hu, Y.-h., Liu, C.-s., & Sun, L. (2010). Construction and analysis of an experimental Streptococcus iniae DNA vaccine. *Vaccine*, *28*(23), 3905-3912.

Sung, H., Ferlay, J., Siegel, R. L., Laversanne, M., Soerjomataram, I., Jemal, A., & Bray, F. (2021). Global cancer statistics 2020: GLOBOCAN estimates of incidence and mortality worldwide for 36 cancers in 185 countries. *CA: a cancer journal for clinicians*, *71*(3), 209-249.

Suslov, A., Wieland, S., & Menne, S. (2018). Modulators of innate immunity as novel therapeutics for treatment of chronic hepatitis B. *Current opinion in virology*, *30*, 9-17.

Svitkin, Y. V., Cheng, Y. M., Chakraborty, T., Presnyak, V., John, M., & Sonenberg, N. (2017). N1-methyl-pseudouridine in mRNA enhances translation through eIF2α-dependent and independent mechanisms by increasing ribosome density. *Nucleic acids research*, *45*(10), 6023-6036.

Szmuness, W., Stevens, C. E., Harley, E. J., Zang, E. A., Oleszko, W. R., William, D. C., Sadovsky, R., Morrison, J. M., & Kellner, A. (1980). Hepatitis B vaccine: demonstration of efficacy in a controlled clinical trial in a high-risk population in the United States. *New England Journal of Medicine*, *303*(15), 833-841.

Szymczak, A. L., & Vignali, D. A. (2005). Development of 2A peptide-based strategies in the design of multicistronic vectors. *Expert opinion on biological therapy*, *5*(5), 627-638.

Takebe, Y., Seiki, M., Fujisawa, J.-I., Hoy, P., Yokota, K., Arai, K.-L., Yoshida, M., & Arai, N. (1988). SR alpha promoter: an efficient and versatile mammalian cDNA expression system composed of the simian virus 40 early promoter and the R-U5 segment of human T-cell leukemia virus type 1 long terminal repeat. *Molecular and cellular biology*, *8*(1), 466-472.

Tan, A. T., & Schreiber, S. (2020). Adoptive T-cell therapy for HBV-associated HCC and HBV infection. *Antiviral research*, *176*, 104748.

Tang, C.-M., Yau, T. O., & Yu, J. (2014). Management of chronic hepatitis B infection: current treatment guidelines, challenges, and new developments. *World journal of gastroenterology: WJG*, *20*(20), 6262.

Tang, D.-c., DeVit, M., & Johnston, S. A. (1992). Genetic immunization is a simple method for eliciting an immune response. *Nature*, *356*(6365), 152-154.

Tang, L., Zhao, Q., Wu, S., Cheng, J., Chang, J., & Guo, J.-T. (2017). The current status and future directions of hepatitis B antiviral drug discovery. *Expert opinion on drug discovery*, *12*(1), 5-15.

Tatsis, N., & Ertl, H. C. (2004). Adenoviruses as vaccine vectors. *Molecular Therapy*, *10*(4), 616-629.

Tejeda-Mansir, A., & Montesinos, R. M. (2008). Upstream processing of plasmid DNA for vaccine and gene therapy applications. *Recent patents on biotechnology*, *2*(3), 156-172.

Tenney, D. J., Rose, R. E., Baldick, C. J., Pokornowski, K. A., Eggers, B. J., Fang, J., Wichroski, M. J., Xu, D., Yang, J., & Wilber, R. B. (2009). Long-term monitoring shows hepatitis B virus resistance to entecavir in nucleoside-naive patients is rare through 5 years of therapy. *Hepatology*, *49*(5), 1503-1514.

Terrault, N. A., Bzowej, N. H., Chang, K. M., Hwang, J. P., Jonas, M. M., & Murad, M. H. (2016). A ASLD guidelines for treatment of chronic hepatitis B. *Hepatology*, *63*(1), 261-283.

Thess, A., Grund, S., Mui, B. L., Hope, M. J., Baumhof, P., Fotin-Mleczek, M., & Schlake, T. (2015). Sequence-engineered mRNA without chemical nucleoside modifications enables an effective protein therapy in large animals. *Molecular Therapy*, *23*(9), 1456-1464.

Thimme, R., Wieland, S., Steiger, C., Ghrayeb, J., Reimann, K. A., Purcell, R. H., & Chisari, F. V. (2003). CD8+ T cells mediate viral clearance and disease pathogenesis during acute hepatitis B virus infection. *Journal of virology*, *77*(1), 68-76.

Thomas, D. L. (2019). Global elimination of chronic hepatitis. *New England Journal of Medicine*, *380*(21), 2041-2050.

Tiollais, P., Pourcel, C., & Dejean, A. (1985). The hepatitis B virus. *Nature*, *317*(6037), 489-495.

Tombacz, I., Weissman, D., & Pardi, N. (2021). Vaccination with messenger RNA: a promising alternative to DNA vaccination. In *DNA Vaccines* (pp. 13-31). Springer.

Ulmer, J. B., Donnelly, J. J., Parker, S. E., Rhodes, G. H., Felgner, P. L., Dwarki, V., Gromkowski, S. H., Deck, R. R., DeWitt, C. M., & Friedman, A. (1993). Heterologous protection against influenza by injection of DNA encoding a viral protein. *Science*, *259*(5102), 1745-1749.

Ulmer, J. B., Mason, P. W., Geall, A., & Mandl, C. W. (2012). RNA-based vaccines. *Vaccine*, *30*(30), 4414-4418.

Vaidyanathan, S., Azizian, K. T., Haque, A. A., Henderson, J. M., Hendel, A., Shore, S., Antony, J. S., Hogrefe, R. I., Kormann, M. S., & Porteus, M. H. (2018). Uridine depletion and chemical modification increase Cas9 mRNA activity and reduce immunogenicity without HPLC purification. *Molecular Therapy-Nucleic Acids*, *12*, 530-542.

Valaydon, Z. S., & Locarnini, S. A. (2017). The virological aspects of hepatitis B. *Best practice & research clinical gastroenterology*, *31*(3), 257-264.

Valenzuela, P., Medina, A., Rutter, W. J., Ammerer, G., & Hall, B. D. (1982). Synthesis and assembly of hepatitis B virus surface antigen particles in yeast. *Nature*, *298*(5872), 347-350.

Valera, A., Perales, J. C., Hatzoglou, M., & Bosch, F. (1994). Expression of the neomycin-resistance (neo) gene induces alterations in gene expression and metabolism. *Human gene therapy*, *5*(4), 449-456.

Van Lint, S., Goyvaerts, C., Maenhout, S., Goethals, L., Disy, A., Benteyn, D., Pen, J., Bonehill, A., Heirman, C., & Breckpot, K. (2012). Preclinical evaluation of TriMix and antigen mRNA-based antitumor therapy. *Cancer research*, *72*(7), 1661-1671.

Vandepapelière, P., Lau, G. K., Leroux-Roels, G., Horsmans, Y., Gane, E., Tawandee, T., bin Merican, M. I., Win, K. M., Trepo, C., & Cooksley, G. (2007). Therapeutic vaccination of chronic hepatitis B patients with virus suppression by antiviral therapy: a randomized, controlled study of co-administration of HBsAg/AS02 candidate vaccine and lamivudine. *Vaccine*, *25*(51), 8585-8597.

Velkov, S., Ott, J. J., Protzer, U., & Michler, T. (2018). The global hepatitis B virus genotype distribution approximated from available genotyping data. *Genes*, *9*(10), 495.

Venook, A. P., Papandreou, C., Furuse, J., & Ladron de Guevara, L. (2010). The incidence and epidemiology of hepatocellular carcinoma: a global and regional perspective. *The oncologist*, *15*, 5-13.

Viswanathan, U., Mani, N., Hu, Z., Ban, H., Du, Y., Hu, J., Chang, J., & Guo, J.-T. (2020). Targeting the multifunctional HBV core protein as a potential cure for chronic hepatitis B. *Antiviral research*, 104917.

Wai, C. T., Chu, C. J., Hussain, M., & Lok, A. S. (2002). HBV genotype B is associated with better response to interferon therapy in HBeAg (+) chronic hepatitis than genotype C. *Hepatology*, *36*(6), 1425-1430.

Walsh, E. E., Frenck Jr, R. W., Falsey, A. R., Kitchin, N., Absalon, J., Gurtman, A., Lockhart, S., Neuzil, K., Mulligan, M. J., & Bailey, R. (2020). Safety and immunogenicity of two RNA-based Covid-19 vaccine candidates. *New England Journal of Medicine*, *383*(25), 2439-2450.

Wang, R., Doolan, D. L., Le, T. P., Hedstrom, R. C., Coonan, K. M., Charoenvit, Y., Jones, T. R., Hobart, P., Margalith, M., & Ng, J. (1998). Induction of antigen-specific cytotoxic T lymphocytes in humans by a malaria DNA vaccine. *Science*, *282*(5388), 476-480.

Wang, R., Epstein, J., Charoenvit, Y., Baraceros, F. M., Rahardjo, N., Gay, T., Banania, J.-G., Chattopadhyay, R., de la Vega, P., & Richie, T. L. (2004). Induction in humans of CD8+ and CD4+ T cell and antibody responses by sequential immunization with malaria DNA and recombinant protein. *The Journal of Immunology*, *172*(9), 5561-5569.

Wang, Y.-J., Lu, D., Xu, Y.-B., Xing, W.-Q., Tong, X.-K., Wang, G.-F., Feng, C.-L., He, P.-L., Yang, L., & Tang, W. (2015). A novel pyridazinone derivative inhibits hepatitis B virus replication by inducing genome-free capsid formation. *Antimicrobial agents and chemotherapy*, *59*(11), 7061-7072.

Webster, D. P., Dunachie, S., Vuola, J. M., Berthoud, T., Keating, S., Laidlaw, S. M., McConkey, S. J., Poulton, I., Andrews, L., & Andersen, R. F. (2005). Enhanced T cell-mediated protection against malaria in human challenges by using the recombinant poxviruses FP9 and modified vaccinia virus Ankara. *Proceedings of the National Academy of Sciences*, *102*(13), 4836-4841.

Westland, C. E., Yang, H., Delaney IV, W. E., Gibbs, C. S., Miller, M. D., Wulfsohn, M., Fry, J., Brosgart, C. L., & Xiong, S. (2003). Week 48 resistance surveillance in two phase 3 clinical studies of adefovir dipivoxil for chronic hepatitis B. *Hepatology*, *38*(1), 96-103.

WHO. (2017a). *Global Hepatitis Report*. https://www.who.int/publications/i/item/global-hepatitis-report-2017

WHO. (2017b). Hepatitis B vaccines: WHO position paper-July 2017. *Weekly epidemiological record*, *92*(27), 369-392.

WHO. (2020). *Hepatitis B Fact Sheets*. Retrieved 21/06/2021 from https://www.who.int/news-room/fact-sheets/detail/hepatitis-b

WHO. (2021). *Vaccine safety basics e-learning course*. Retrieved 04.07.2021 from https://vaccine-safety-training.org/how-vaccines-work.html

WHO. (2023, 18 July 2023). *Hepatitis B Fact Sheet*. WHO. Retrieved 14/09/2023 from https://www.who.int/news-room/fact-sheets/detail/hepatitis-b

Widera, G., Austin, M., Rabussay, D., Goldbeck, C., Barnett, S. W., Chen, M., Leung, L., Otten, G. R., Thudium, K., & Selby, M. J. (2000). Increased DNA vaccine delivery and immunogenicity by electroporation in vivo. *The journal of immunology*, *164*(9), 4635-4640.

Wieland, S. F., Spangenberg, H. C., Thimme, R., Purcell, R. H., & Chisari, F. V. (2004). Expansion and contraction of the hepatitis B virus transcriptional template in infected chimpanzees. *Proceedings of the National Academy of Sciences*, *101*(7), 2129-2134.

Wolff, J. A., Malone, R. W., Williams, P., Chong, W., Acsadi, G., Jani, A., & Felgner, P. L. (1990). Direct gene transfer into mouse muscle in vivo. *Science*, *247*(4949), 1465-1468.

Woo, G., Tomlinson, G., Nishikawa, Y., Kowgier, M., Sherman, M., Wong, D. K., Pham, B., Ungar, W. J., Einarson, T. R., & Heathcote, E. J. (2010). Tenofovir and entecavir are the most effective antiviral agents for chronic hepatitis B: a systematic review and Bayesian meta-analyses. *Gastroenterology*, *139*(4), 1218-1229. e1215.

Wu, C.-y., Kirman, J. R., Rotte, M. J., Davey, D. F., Perfetto, S. P., Rhee, E. G., Freidag, B. L., Hill, B. J., Douek, D. C., & Seder, R. A. (2002). Distinct lineages of Th 1 cells have differential capacities for memory cell generation in vivo. *Nature immunology*, *3*(9), 852-858.

Wu, G., Liu, B., Zhang, Y., Li, J., Arzumanyan, A., Clayton, M. M., Schinazi, R. F., Wang, Z., Goldmann, S., & Ren, Q. (2013). Preclinical characterization of GLS4, an inhibitor of hepatitis B virus core particle assembly. *Antimicrobial agents and chemotherapy*, *57*(11), 5344-5354.

Xenopoulos, A., & Pattnaik, P. (2014). Production and purification of plasmid DNA vaccines: is there scope for further innovation? *Expert review of vaccines*, *13*(12), 1537-1551.

Xia, Y., Stadler, D., Lucifora, J., Reisinger, F., Webb, D., Hösel, M., Michler, T., Wisskirchen, K., Cheng, X., & Zhang, K. (2016). Interferon-γ and tumor necrosis factor-α produced by T cells reduce the HBV persistence form, cccDNA, without cytolysis. *Gastroenterology*, *150*(1), 194-205.

Xu, L., Sanchez, A., Yang, Z.-Y., Zaki, S. R., Nabel, E. G., Nichol, S. T., & Nabel, G. J. (1998). Immunization for Ebola virus infection. *Nature medicine*, *4*(1), 37-42.

Yan, H., Liu, Y., Sui, J., & Li, W. (2015). NTCP opens the door for hepatitis B virus infection. *Antiviral research*, *121*, 24-30.

Yan, H., Zhong, G., Xu, G., He, W., Jing, Z., Gao, Z., Huang, Y., Qi, Y., Peng, B., & Wang, H. (2012). Sodium taurocholate cotransporting polypeptide is a functional receptor for human hepatitis B and D virus. *elife*, *1*, e00049.

Yang, L., Wang, Y.-J., Chen, H.-J., Shi, L.-P., Tong, X.-K., Zhang, Y.-M., Wang, G.-F., Wang, W.-L., Feng, C.-L., & He, P.-L. (2016). Effect of a hepatitis B virus inhibitor, NZ-4, on capsid formation. *Antiviral research*, *125*, 25-33.

Yang, Y., Liu, Y., Hua, H., & Li, L. (2010). Effect of Sanhuangyinchi decoction on liver damage and caspase-3 in rats with acute hepatic failure. *Nan fang yi ke da xue xue bao= Journal of Southern Medical University*, *30*(11), 2443-2445.

Ye, B., Liu, X., Li, X., Kong, H., Tian, L., & Chen, Y. (2015). T-cell exhaustion in chronic hepatitis B infection: current knowledge and clinical significance. *Cell death & disease*, *6*(3), e1694-e1694.

Yeh, C.-T., Liaw, Y., & Ou, J.-H. (1990). The arginine-rich domain of hepatitis B virus precore and core proteins contains a signal for nuclear transport. *Journal of virology*, *64*(12), 6141-6147.

Yewdell, J. W., Antón, L. C., & Bennink, J. R. (1996). Defective ribosomal products (DRiPs): a major source of antigenic peptides for MHC class I molecules? *The Journal of Immunology*, *157*(5), 1823-1826.

Yewdell, J. W., & Bennink, J. R. (1992). Cell biology of antigen processing and presentation to major histocompatibility complex class I molecule-restricted T lymphocytes. *Advances in immunology*, *52*, 1-123.

Yotsuyanagi, H., Yasuda, K., Iino, S., Moriya, K., Shintani, Y., Fujie, H., Tsutsumi, T., Kimura, S., & Koike, K. (1998). Persistent viremia after recovery from self-limited acute hepatitis B. *Hepatology*, *27*(5), 1377-1382.

Yu, C.-H., Dang, Y., Zhou, Z., Wu, C., Zhao, F., Sachs, M. S., & Liu, Y. (2015). Codon usage influences the local rate of translation elongation to regulate co-translational protein folding. *Molecular cell*, *59*(5), 744-754.

Yu, H., Yuan, Q., Ge, S.-X., Wang, H.-Y., Zhang, Y.-L., Chen, Q.-R., Zhang, J., Chen, P.-J., & Xia, N.-S. (2010). Molecular and phylogenetic analyses suggest an additional hepatitis B virus genotype "I". *PLoS One*, *5*(2), e9297.

Yuen, M.-F., Heo, J., Jang, J.-W., Yoon, J.-H., Kweon, Y.-O., Park, S.-J., Tami, Y., You, S., Yates, P., & Tao, Y. (2021). Safety, tolerability and antiviral activity of the antisense

oligonucleotide bepirovirsen in patients with chronic hepatitis B: a phase 2 randomized controlled trial. *Nature medicine*, *27*(10), 1725-1734.

Zeng, Y., & Cullen, B. R. (2002). RNA interference in human cells is restricted to the cytoplasm. *Rna*, *8*(7), 855-860.

Zhang, C., Maruggi, G., Shan, H., & Li, J. (2019). Advances in mRNA vaccines for infectious diseases. *Frontiers in immunology*, *10*, 594.

Zhang, H., Kolb, F. A., Jaskiewicz, L., Westhof, E., & Filipowicz, W. (2004). Single processing center models for human Dicer and bacterial RNase III. *Cell*, *118*(1), 57-68.

Zhang, S., Zhang, H., & Zhao, J. (2009). The role of CD4 T cell help for CD8 CTL activation. *Biochemical and biophysical research communications*, *384*(4), 405-408.

Zhao, L., Chen, F., Quitt, O., Festag, M., Ringelhan, M., Wisskirchen, K., Festag, J., Yakovleva, L., Sureau, C., & Bohne, F. (2021). Hepatitis B virus envelope proteins can serve as therapeutic targets embedded in the host cell plasma membrane. *Cellular Microbiology*, *23*(12), e13399.

Zlotnick, A., Venkatakrishnan, B., Tan, Z., Lewellyn, E., Turner, W., & Francis, S. (2015). Core protein: a pleiotropic keystone in the HBV lifecycle. *Antiviral research*, *121*, 82-93.

Zoulim, F., Saputelli, J., & Seeger, C. (1994). Woodchuck hepatitis virus X protein is required for viral infection in vivo. *Journal of virology*, *68*(3), 2026-2030.

Zoutendijk, R., Reijnders, J. G., Zoulim, F., Brown, A., Mutimer, D. J., Deterding, K., Hofmann, W. P., Petersen, J., Fasano, M., & Buti, M. (2013). Virological response to entecavir is associated with a better clinical outcome in chronic hepatitis B patients with cirrhosis. *Gut*, *62*(5), 760-765.

Zuckerman, A. (1999). More than third of world's population has been infected with hepatitis B virus. *Bmj*, *318*(7192), 1213.

Publications and Meetings

a) Articles in peer-reviewed journals

Sacherl*, J., Kosinska*, A. D., Kemter, K., Kächele, M., Laumen, S. C., **Kerth, H. A.**, Öz, E. A.,Wolff, L. S., Su, J., & Essbauer, S. (2023). Efficient stabilization of therapeutic hepatitis B vaccine components by amino-acid formulation maintains its potential to break immune tolerance. ***JHEP Reports***, *5*(2), 100603.

Su, J., Brunner, L., Oz, E. A., Sacherl, J., Frank, G., **Kerth, H. A.**, Thiele, F., Wiegand, M., Mogler, C., & Aguilar, J. C. (2023). Activation of CD4 T cells during prime immunization determines the success of a therapeutic hepatitis B vaccine in HBV-carrier mouse models. ***Journal of hepatology***, 78(4), 717-730.

(* authors contributed equally to the study)

b) Conference proceedings

Kerth H, Kosinska AD, Kächele M, Oswald A, Su J, Knolle PA, Protzer U. Multicistronic DNA-based therapeutic vaccine as a promising candidate to treat chronic hepatitis B virus (HBV) infection. **Journal of Hepatology 2020** vol. 73 | S653-S915

c) Conferences

2019 IRTG Immunovirology Retreat, May 27-29, 2019, St. Peter, Germany.
Oral presentation: Generation of multicistronic mRNA- and DNA-based therapeutic vaccines.

The International Liver Congress 2020, August 27-29, held digitally due to Covid-19 pandemic
Poster presentation: ‘Multicistronic DNA-based therapeutic vaccine as a promising candidate to treat chronic hepatitis B virus (HBV) infection.’

2021 International HBV meeting, September 26-30, 2021, Toronto, Canada.
Oral presentation (5 min + 5 min Q&A) + poster presentation : ‘Particulate protein is superior to DNA and mRNA for priming antiviral T-cell responses in a therapeutic hepatitis B vaccine.’

d) Workshops

“Steppingstone to an academic career in Virology”, April 15-June 3rd, 2021, held digitally due to Covid-19 pandemic

Acknowledgments

Pursuing an experimental thesis as a medical student, in a research laboratory in a foreign country, can be challenging. I would like to express my deepest gratitude to everyone who helped me find my path and achieve my goals. Once you start this long journey, not only motivation and intensive work are required to fulfil your goals but also support and advice.

I am deeply thankful to my M.D. project supervisor Prof. Dr. Ulrike Protzer for giving me the opportunity to carry out this project and believing in me from the beginning on. You always encouraged me and pushed me to go beyond my limits. I am deeply grateful for your intellectual guidance as well as the inspiring personal and work-related discussions. In addition, I would like to express my sincere gratitude to you for the continuous financial support of the project and my dissertation.

I am very thankful to Prof. Dr. Percy Knolle not only for being my mentor but also for his constructive discussions, time and support throughout the project.

I am beyond thankful to Dr. Anna Kosinska for her excellent and intense supervision of the project, for teaching as well as supporting me throughout all the animal experiments. Without her the project would not have been possible. I am very grateful not only for her guidance and constructive discussions but also for all the great time we spent together outside of the lab, getting to know each other better.

I am thankful to Dr. Christian Plank and Dr. Yolanda Sanchez from Ethris GmbH for the great collaboration within the mRNA project.

I would like to express widespread praise for my colleagues Dr. Martin Kächele, Dr. Julia Sacherl and Dr. Andreas Oswald for supporting me continuously technically, mentally and editorially throughout the dissertation. You were great – thank you so much!

I would like to express gratitude to Dr. Jinpeng Su and Edanur Ates-Öz for helping me with the termination of the animal experiments as well as for all the good times we spent together.

I am deeply thankful to Theresa Asen, Ana-Marija Jetzelsperger, Philipp Hagen and Susanne Bartsch for helping me not only in the lab in general, but also with the serological measurements.

I would like to say thank you to Daniela Rizzi, Doris Pelz, Halid Musanovic, Dr. Marian Wiegand, Rita Pflieger-Kerle and Dr. Frank Thiele for the administrative support and the great discussions which encouraged me in difficult times.

I would like to express my deepest gratitude for the financial support offered by the TRR179 as well as by the German Center for Infectious Research (DZIF).

I am truly thankful to have met my friends Jakob Zillinger and Alexandre Klopp. Thank you for all the laughs, storytelling and coffees we had together – it was great!

Special thanks to my forever friends Charlotte, Floriane, Léa and Camille for all the love and continuous support throughout this journey.

I am deeply grateful to my family, especially my sister Sophie, my parents Valérie and Paul and my grandma mamie Marlyse for the tremendous support, motivation and love during all these years – you always believed in me and provided incredible support when times were difficult. I love you all so much and I am so grateful to have you in my life.

Last but not least I would like to thank Julien for all the love, motivation and support. You always helped me keep my spirits up!